IMPROVING ONCOLYTIC VESICULAR STOMATITIS VIRUS

IMPROVING ONCOLYTIC VESICULAR STOMATITIS VIRUS THROUGH MODULATION OF THE ANTI-TUMOUR IMMUNE RESPONSE

BY

KYLE B STEPHENSON, B.Sc.

A Thesis

Submitted to the School of Graduate Studies

in Partial Fulfillment of the Requirements

of the Degree

Doctor of Philosophy

McMaster University

© Copyright by Kyle B Stephenson, November 2012

McMaster University Hamilton, ON

DOCTOR OF PHILOSOPHY (2012)

TITLE:	Improving Oncolytic Vesicular Stomatitis Virus Through Modulation of the Anti-Tumour Immune Response
AUTHOR:	Kyle B Stephenson, B.Sc. (University of Waterloo)
SUPERVISOR:	Dr. Brian Lichty
NUMBER OF PAGES:	xviii, 231

ABSTRACT

Despite improvements in detection and treatment, cancer is the leading cause of death worldwide. Current treatment modalities have not been able to improve the mortality rates and significant toxicities limit efficacy. Therefore there is a need for development of novel therapeutics.

Oncolytic viruses have the ability to efficiently replicate in and destroy tumours while leaving normal tissues unharmed. These treatment platforms have been gaining momentum in recent years due to pre-clinical and clinical successes. Oncolytic viruses are extremely safe with limited toxicity observed in phase I/II clinical trials, and objective responses have been observed in some patients treated with oncolytic viruses. However, there is still room to improve on these therapeutic platforms.

Recently, the importance of the induction of anti-tumour immunity during oncolytic virotherapy has been realized and harnessing this immune response can be used to improve current oncolytic virus platforms. To this end we have conducted numerous studies assessing our ability to improve oncolytic VSV through the addition of transgenes to enhance the immunostimulatory properties of oncolytic VSV treatment. These studies showed that only the addition of a highly secreted form of human IL-15 was able to improve VSV therapy through enhanced anti-tumour immunity. However, expressing cell-autonomous transgenes from oncolytic VSV was unable to modify the therapeutic efficacy of

VSV due to limited replication, both temporally and geographically within the tumour, and the indirect vascular shutdown induced by VSV infection of tumours. We believe that the drastic vascular shutdown observed following VSV therapy is an important component to the success of VSV and we have investigated which steps in this process are critical for induction of anti-tumour immunity.

The research presented in this thesis further enforces the requirement for induction of anti-tumour immune responses in the success of OV therapy. Our findings also indicate that manipulating the tumour as a whole, rather than the virus, will lead to improved oncolytic therapeutics.

ACKNOWLEDGEMENTS

I would first like to thank my supervisor Dr. Brian Lichty for taking a chance on me considering that i had an “unusual” undergraduate career. Brian’s been an incredible supervisor who’s door was always open at any time for a discussion about science or career. The knowledge he has imparted is invaluable and I have learned a great deal about how to conduct scientific exploration as well as many other aspects of working in academia which will help shape my future career.

My committee members, Dr. Karen Mossman and Dr. Yonghong Wan, were a fantastic resource and always kept me on track. The criticisms and suggestions during committee meetings were always helpful and insightful. They always kept me reeled in if I began to spread my interests and experimentation too wide keeping me focused and on a path towards a specific goal. I would also like to thank Dr. Ali Ashkar, whose experience and expertise with IL-15 were instrumental in completing my second manuscript.

The scientific environment in MiRC has been nothing but amazing. I would not have been able to advance as far as i have without the amazing collaborations that this research setting allows to happen. The ability to share techniques and reagents and everyone always willing to lend a hand has made a huge difference in completing my studies.

Mary Jo Smith and Mary Bruni, without your assistance very little histology would have been accomplished. Everything I have learned about histology I have learned from the two of you and i can’t thank you enough for all the times I have come up asking questions 4 or 5 times a day. You were always willing to help me work up and troubleshoot new protocols, and I am deeply indebted.

My friends, neighbors and colleagues throughout MiRC have always been there to lend an ear or have a coffee and there are so many memories and great times throughout my time at McMaster. Frances, Amy, Nicole, Amanda, Tamara, Marianne, Sarah Reid, Sarah McCormick, Ryan, Anne, Steve and Jo, you have all made this such a positive experience throughout my degree and I thank each of you for helping me get through to the end. Oh, and of course lots of help with scientific discussion and numerous animal experiments. I must specifically thank Jo for all his help with animal experiments, taking over while i was away. He has never once said no to helping out, even if its a late night flow experiment that needs to be run. As well, Frances has helped out too many times to count with many experiments and tissue culture, or when i forgot to do something and realized after leaving, she was always willing to help out.

To my family, thank you for all your support over the years. My Mom, her husband Brian and Tyler, you have been nothing but supportive during this journey. My in-laws, Jim and Kathy Woodworth, have always been there to lend a

hand, even if it meant a three hour drive, and have been extremely supportive and motivational throughout my degree.

The last and most important person to thank is my wife Laura. Without your unwavering support and patience I never would have made it through this incredible journey. You followed me to McMaster so i could pursue my graduate work with Brian and I am forever grateful. You kept me motivated and on track throughout my degree and even through the low times you always found a way to turn everything into a positive experience. I also have to thank our beautiful baby boy Duncan who joined our family as I finished my degree. Being able to be home with the two of you working on my thesis has been the most amazing experience, especially being able to watch him grow up so quickly. Something I will always cherish. This small paragraph can never convey how much you mean to me and have helped me through my PhD. I Love You!

TABLE OF CONTENTS

Title Page…….. i

Descriptive Note …… ii

Abstract ……... iii

Acknowledgments …… v

Table of Contents …….. viii

List of Figures …… xii

List of Abbreviations and Symbols …….. xvi

Chapter 1 - Introduction 1

1.0 Cancer 2

1.1 Cancer 2

1.2 The impact of tumorigenesis on type 1 IFN pathway.....3

1.3 Conventional cancer therapy 4

2.0 Cancer and the Immune System 6

2.1 Overview of the immune system 6

2.2 Generating adaptive CTL immune responses 8

3.0 Oncolytic Viruses 15

3.1 History of oncolytic viruses 15

3.2 Types of oncolytic viruses 16

3.3 Oncolytic viruses in the clinic.....20

3.4 Immunostimulatory oncolytic viruses 24

4.0 Vesicular Stomatitis Virus 27

4.1 Overview.....27

4.2 VSV life cycle 27

4.3 VSV and type I IFN 29

4.4 VSV as an oncolytic virus 32

5.0 Scope of Thesis Research 33

5.1 Research Objectives 35

Chapter 2: Materials and Methods 37

Chapter 3: Modifying oncolytic VSV through the addition of cell-autonomous transgenes: 51

1.0 Introduction 52

1.1 Immunogenic cell death 52

1.3 Apoptosis in VSV infected cells 55

1.4 Anti-apoptotic poxviral proteins 56

1.5 Cell death in cancer therapies 57

2.0 Results 58

2.1 Characterization and assessment of the oncolytic potential of ΔM51 VSV/FAST 58

2.2 Characterization and assessment of the oncolytic potential of anti-apoptotic VSV vectors ΔM51 VSV/Flag-F1L and ΔM51 VSV/GFP-FPV039 69

3.0 Discussion 81

Chapter 4: Express human Interleukin-15 from oncolytic VSV improves survival in a murine metastatic colon adenocarcinoma model through the enhancement of anti-tumour immunity 87

Preface: 88

1.0 Introduction 89

2.0 Results 91

3.0 Discussion 101

Chapter 5: Investigating the role of vascular shutdown and apoptotic cell death in the core of VSV treated tumours on induction of anti-tumour immunity and overall therapeutic outcome 105

1.0 Introduction 106

2.0 Results 109

2.1 Pharmacological inhibition of apoptosis was not achieved using either pan caspase inhibitor or more specific caspase3/7 inhibitor. 109

2.2 Creation of stable CT26 cell line over expressing BCL-2 116

2.3 Heparin treatment during VSV oncolysis proved unable to prevent vascular shut-down. 124

2.4 Depletion of neutrophils impairs vascular shutdown 127

3.0 Discussion 138

Chapter 6: Summary and Conclusions 149

1.0 Summary of findings 150

2.0 Considerations for future VSV oncolytic studies. 154

3.0 Concluding remarks 158

References 161

Appendix 1 185

Preface: 186

ABSTRACT 187

INTRODUCTION 188

MATERIALS AND METHODS 191

RESULTS 195

DISCUSSION 204

REFERENCES.....209
FIGURE LEGENDS 212
FIGURES 217
TABLE LEGENDS.....225
TABLES.....226
Appendix 2 - Permission to reprint published manuscripts 227

List of Tables and Figures

Chapter 1

Table 1 - Oncolytic Virus monotherapy clinical trials 22

Table 2 - Phase II and III clinical trials combining oncolytic viruses with chemotherapy 24

Figure 1 - Recognition of VSV infection and VSV control of interferon and ISG production 30

Figure 2 - Requirement for adaptive immune response during VSV therapy 34

Chapter 2

Figure 3 - VSV Genome organization 40

Table 3 - Primers for construction of anti-apoptotic viruses 40

Table 4 - Western blot antibody conditions 42

Chapter 3

Figure 4 - Characterization of ΔM51 VSV/FAST 59

Figure 5 - Replication of VSV is not impaired by the expression of p14 FAST 60

Figure 6 - Vascular perfusion and viral spread in ΔM51 VSV/FAST treated tumours 61

Figure 7 - Titers in ΔM51 VSV/FAST treated tumours is lower than ΔM51 VSV/GFP treated tumours 62

Figure 8 - Δ51 VSV/FAST treatment of CT26 in CD-1 nude mice …… 63

Figure 9 - ΔM51 VSV/FAST treatment of subcutaneous CT26 tumours …..64

Figure 10 - Expression of FAST from VSV does not improve efficacy ……. 66

Figure 11 - FAST expression does not improve on VSV oncolytic efficacy in a CT26 lung metastases model …….. 68

Figure 12 - Characterization of anti-apoptotic VSV ……. 70

Figure 13 - Apoptosis induction is delayed in Δ51 VSV/Flag-F1L and ΔM51 VSV/GFP-FPV039 infected cells ……. 72

Figure 14 - Infection of CT26 *in vitro* with anti-apoptotic VSV viruses modifies cell death ……. 74

Figure 15 - Replication of anti-apoptotic VSV vectors is not impaired *in vivo* ……... *76*

Figure 16 - ΔM51 VSV/Flag-F1L and ΔM51 VSV/GFP-FPV039 treatment of subcutaneous CT26 tumours ……...78

Figure 17 - FAST expression does not improve on VSV oncolytic efficacy in a CT26 lung metastases model …….. 80

Chapter 4

Figure 18 - Construction of ΔM51 VSV/opt.hIL-15 …….. 92

Figure 19 - Expression of hIL-15 from ΔM51 VSV/opt.hIL-15 *in vitro* and *in vivo* …….. 93

Figure 20 - Treatment of sub-cutaneous CT26 tumors with ΔM51 VSV/opt.hIL-15 ……... 94

Figure 21 - Expression of human interleukin-15 (hIL-15) from vesicular stomatitis virus (VSV) significantly improves oncolytic virus (OV) therapy .. 96

Figure 22 - Pretreatment of CT26 lung metastases with hIL-15/Rα increases peripheral NK cell frequencies ……98

Figure 23 - Pretreatment with hIL-15/Rα does not improve on treatment with either virus alone ……..…. 100

Figure 24 - Survival correlates with anti-tumor immune response …… 101

Chapter 5

Table 5 - Approaches to determine what makes oncolytic VSV successful..108

Figure 25 - Inhibiting caspase-3 mediated apoptosis in tumour core did not improve oncolytic VSV therapy …… 111

Figure 26 - Z-VAD-FMK does not impair apoptosis in tumours during oncolytic VSV treatment ……... 113

Figure 27 - DEVD treatment is unable to prevent apoptosis in CT26 tumours during VSV oncolysis …… 115

Figure 28 - Testing CT26.Bcl-2 clones for stable expression of FLAG-Bcl-2 ……....117

Figure 29 - Staurosporine selection of CT26.Bcl-2 increased the percent of Flag-Bcl-2 positive stable cells …… 119

Figure 30 - CT26.Bcl-2 clones have normal response to IFN-β and VSV infection …….. 120

Figure 31 - Stable Bcl-2 expression delays onset of apoptosis …… 121

Figure 32 - VSV replication is not modified in CT26.Bcl-2 *in vivo* ……123

Figure 33 - Preventing apoptosis in CT26.BCL-2 tumours does not modify immunological or survival outcomes …….. 124

Figure 34 - Heparin treatment during VSV oncolysis does not completely prevent vascular shutdown …….. 126

Figure 35 - Neutrophil depletion led to >95% reduction in neutrophils …….129

Figure 36 - Immunohistochemistry following neutrophil depletion during VSV treatment ……. 130

Figure 37 - Neutrophil depletion increases and extends VSV replication in CT26 …….131

Figure 38 - Depletion of neutrophils during VSV oncolysis has no significant treatment effect …….. 135

Figure 39 - Inhibiting vasculature shutdown through neutrophil depletion significantly improves the percentage of anti-tumour $CD8^+$ T cells ..……. 136

Figure 40 - Neutrophil depletion also depletes $CD8^+$ T cells ……... 137

Table 6 - Survival and immunological outcomes from interventions presented in chapter 5 ……. 148

Chapter 6

Table 7 - Power associated with group numbers and overall survival assuming 30% survival of control animals …… 157

LIST OF ABBREVIATIONS AND SYMBOLS

α	alpha
β	beta
Δ	delta
γ	gamma
µg	microgram
mg	milligram
kg	kilogram
µm	micrometer
µL	microliter
kDa	kilodalton
mM	millimolar
M	molar
2’5’-OAS	2’,5’ oligoadenylate synthetase
AnV	annexin V
APC	antigen presenting cell
ATP	adenosine tri-phosphate
BCR	B cell receptor
CNS	central nervous system
CR	complete response (RECIST criteria)
CRT	calreticulin
CTL	cytotoxic T lymphocytes
CTLA-4	cytotoxic T lymphocyte associated protein-4
DAMP	damage-associated molecular pattern
DC	dendritic cell
DNA	deoxy-ribonucleic acid
dsRNA	double stranded ribonucleic acid
EBV	Epstein-Barr virus
EDTA	Ethylenediaminetetraacetic acid
ELISA	enzyme linked immunosorbant assay
ER	endoplasmic reticulum
FAST	fusion-associated small transmembrane protein
FACS	fluorescence activated cell sorting
GFP	green fluorescent protein
GM-CSF	granulocyte macrophage colony stimulating factor
hIL-15	human IL-15
HMGB-1	high mobility group box 1
h.p.i.	hours post infection
HBV	hepatitis B virus
HCC	hepatocellular carcinoma
HCV	hepatitis C virus
HHV-8	human herpes virus 8

HPV	human papilloma virus
HSV	herpes simplex virus
HTLV-1	human T-cell leukemia virus
ICCS	intracellular cytokine staining
IFN	interferon
IFNAR	interferon α/β receptor
IHC	immunohistochemistry
ISG	interferon stimulated gene
ISGF3	interferon stimulated gene factor 3
ISRE	interferon stimulated response element
IRES	internal ribosomal entry site
IL-	Interleukin-
i.n.	intranasal
i.v.	intravenous
i.p.	intraperitoneal
IVIS	*In Vivo* Imaging System
MART-1	melanoma associated antigen recognized by T cells 1
MIIC	MHC class II rich compartments
MHC	major histocompatibility complex
MOI	multiplicity of infection
MPM	malignant pleural mesothelioma
mRNA	messenger ribonucleic acid
NDV	Newcastle disease virus
NFκB	nuclear factor κ B
NK	natural killer cell
NLR	NOD-like receptor
ns	not significant
OV	oncolytic virus
opt.hIL15	optimized human interleukin 15
PAMP	pathogen associated molecular pattern
PARP	poly ADP ribose polymerase
PBS	phosphate buffered saline
PD	progressive disease
PD-L1	programmed death ligand-1
PE	Phycoerythrin
PFU	plaque forming unit
PI	propidium iodide
PKR	protein kinase R
PR	partial response (RECIST criteria)
PRR	pattern recognition receptor
PS	phosphatidylserine
RECIST	response evaluation criteria in solid tumours
REN	restriction endonuclease sites

RIPA	radioimmunoprecipitation assay buffer
RIG-I	retinoic-acid inducible gene I
RNA	ribonucleic acid
RPM	revolutions per minute
RT	room temperature
SCC	squamous cell carcinoma
SDS	sodium dodecyl sulfate
SDS-PAGE	SDS - polyacrylamide gel electrophoresis
s.e.m.	standard error mean
ssRNA	single stranded ribonucleic acid
STS	staurosporine
s.q.	subcutaneous
TBS	tris buffered saline
Th	T helper cell
TLR	Toll-like receptor
TK	thymidine kinase
VSV	vesicular stomatitis virus
VSV-N	vesicular stomatitis virus nucleoprotein
VSV-P	vesicular stomatitis virus phosphoprotein
VSV-M	vesicular stomatitis virus matrix protein
VSV-L	vesicular stomatitis virus polymerase
VSV-G	vesicular stomatitis virus glycoprotein
WT	wild type

~ Chapter 1 ~

Introduction

1.0 Cancer

1.1 Cancer

Cancer is the significant health issue as it is the leading cause of death worldwide and in 2008 13% of all deaths were attributed to cancer[1]. Cancer occurs when normal cells gain the ability to continuously grow and divide due to loss of regulatory mechanisms that control cell cycle and homeostasis. These defects can be caused by mutations in the germline[2-6], environmental exposure to cigarette smoke and other chemicals/pollutants[7,8] and viral infections such as EBV, HPV, HHV-8, HCV, HBV and HTLV-1[9]. One of the issues surrounding cancer research and treatment is that cancer can be thought of as a collection of over 100 distinct diseases[10], as cancer can develop in any cell type through various processes including a variety of mutations or viral infections. Although each cancer may be a distinct disease there are certain characteristics that are required for cancer to develop. These hallmarks of cancer were proposed by Hanahan and Weinberg in 2000[10] and include: 1) resisting cell death; 2) sustaining proliferative signaling; 3) evasion of growth suppressors; 4) inducing angiogenesis; 5) replicative immortality; 6) invasion and metastases. More recently, the importance of the immune system in not only control of cancer, but also in tumour development has been realized[11]. This has led to the addition of immune evasion as an emerging hallmark in addition to those discussed above[11].

1.2 The impact of tumorigenesis on type 1 IFN pathway

Whether through the mutations[12] that lead to the formation of cancer, or the subsequent genomic instability[11] that leads to further mutations, numerous cellular genes and pathways are modified during the process of tumorigenesis, including the type I interferon pathway[13]. This is an important pathway for tumours to down-regulate due type I IFN's ability to impact tumour growth through modulation of proliferation, angiogenesis and the generation of immune responses[14,15]. Multiple genes involved in interferon signaling have been found to be mutated/deleted in a variety of cancers leading to their inability to respond properly to interferon[16]. This can be seen in the NCI-60 panel, a collection of human cancers cell lines, with approximately 80% cell lines showing hypo-responsiveness to IFN[13].

Upon ligation of the type I IFN receptor (IFNAR) the Jak/STAT signaling pathway is initiated leading to phosphorylation of STAT1/2. IRF-9 subsequently joins phospho-STAT 1 and 2 forming the ISGF3 complex[17]. This complex then translocates to the nucleus, binds to the ISRE leading to the transcription of ISGs including PKR, ISG-15 and 2'5'-OAS[17] (See the right side of figure A). Numerous aspects of this pathway have been found to be mutated or down-regulated in different cancers. For example in high-grade bladder cancers the IFNAR has been found to be down-regulated[18]. Mutations have also been observed in the components making up the ISGF3 complex in melanoma, leukemia, human sarcoma, breast and gastric cancers[19-24]. These mutations lead to a lack of ISG

expression due to the fact that the ISGF3 complex is unable to form and bind to ISRE regions of the DNA to induce expression of ISGs including 2'5' OAS[21,22]. The lack of interferon response in tumour cells has been exploited in the creation of tumour specific oncolytic viruses including VSV[13,25] (discussed below)

1.3 Conventional cancer therapy

Primary treatments following cancer diagnosis are generally surgery, to remove or debulk accessible primary tumours, alone or in combination with chemo- and radiotherapy. While surgery is an excellent option when the cancer is localized and accessible, further treatment is required for cancer that has metastasized[26,27].

When surgery alone is not enough chemotherapy can be used in an attempt to kill any tumour cells, or metastases, that remain. Chemotherapeutics are a class of drugs that target actively dividing cells. There are numerous chemotherapy drugs currently available and these drugs can be classified into different families based on their mode of action. One class of chemotherapeutics are the alkylating agents, including nitrogen and platinum containing compounds. These drugs rely on cell proliferation and cause alkylation of DNA, RNA and proteins, however their cytotoxic effects are due to the alkylation of guanine in DNA[28]. A second category of chemotherapy drugs are the anti-metabolites, including purine, pyrimidine adenosine and folate analogues[28]. These compounds are most effective with tumours that are highly replicative and impact on

cancerous cells that are in S phase. These compounds act as analogues to important molecules in DNA and RNA synthesis preventing proper replication[28]. A final example of chemotherapeutic agents is a group of molecules that block cell division at mitosis through stabilization of of microtubule assembly. Paclitaxel and docetaxel are examples of these compounds that contain taxane, a 14-member ring structure[28].

Chemotherapy can kill a large portion of tumour cells, however at some frequency cells can become resistant to the chemotherapeutic agent used to treat the tumour. This resistance may also lead to multi-drug resistant tumour cells that are resistant to drugs of similar structure or modes of action[28,29]. Along with drug resistance, another disadvantage to chemotherapy is that it can be quite toxic leading to significant side effects[27,28]. Some chemotherapy combinations can lead to Grade 3/4 adverse events in almost half of patients[27].

Another standard treatment modality is radiotherapy, where primary tumours and metastases are treated with radiation. The radiation causes toxic DNA damage in tumour cells leading to their death[30]. Improvements in imaging techniques have aided radiotherapy allowing for improved targeting of the radiation to tumour sites[31,32]. However, radiotherapy still has off target toxicity and overall survival in patients treated with radiotherapy leaves much room for improvement[30].

While surgery, chemotherapy and radiotherapy can be successful in treating cancer, there is room for improvement. Issues surrounding resistance to

chemo- and radio- therapy and toxicity could be answered with the advent of new biological therapeutics, including oncolytic viruses. These novel therapeutics show little toxicity and have been shown to be effective in treating a number of different cancer types.

2.0 Cancer and the Immune System

2.1 Overview of the immune system

Our bodies are constantly assaulted by microorganisms and therefore need to have defenses in place to deal with the many bacteria, viruses and fungi that we contract. The primary defenses preventing entry of pathogenic organisms are skin and mucosal membranes, which form a physical barrier keeping out unwanted microorganisms. However, if a pathogen is able to gain entry into the human body, we have a multitude of defenses, that make up the innate and adaptive immune response, to deal with the invading organism[33-35].

Once inside the body the invading organism is first recognized by the innate immune system. Cells of the innate immune system express receptors that have the ability to detect specific molecular patterns unique to microorganisms (PAMP)[33]. Numerous pattern recognition receptors (PRR) are present on both the cell surface (TLRs) and inside the cell (TLRs, NLRs, PKR, OAS) and recognize different PAMPs from various organisms[33]. These PRRs are involved in opsonization, activation of coagulation cascades and phagocytosis. As well, once the invading organism is sensed the activated receptors begin a signaling

cascade resulting in the activation of NFκB[33]. This then leads to the expression of numerous genes involved in host defense, including inflammatory cytokines and chemokines[33,36]. The signals received by the innate immune cells upon recognition of a pathogen also lead to the expression of MHC and co-stimulatory molecules, as well as induction of antigen processing. These are important steps that occur in antigen presenting cells leading to dendritic cell maturation and priming of the adaptive immune response[37].

The innate immune response, which responds quickly to a broad range of pathogens, is able to hold invading pathogens in check while the adaptive immune response is activated[34,35]. The adaptive response is characterized by the antigen specificity of T and B cells, along with the generation of antigenic memory, allowing for rapid recognition and clearance of subsequent infections with the same pathogen[34,35]. The specificity of the adaptive response is conferred by T cell and B cell receptors, which are constructed through recombination and hyper-mutation of gene segments encoding the three regions of the receptors. This leads to the ability to generate a vast repertoire of TCRs with the ability to recognize virtually any antigen or pathogen that will be encountered[33,35]. However, each clonal T cell will only recognize one specific molecular structure[33]. To minimize reaction with self antigens, T cells go through a selection process leading to the release of naive $CD4^+$ and $CD8^+$ T cells from the thymus that do not recognize self antigens. This is a critical process as any T cells that are able to recognize a self antigen may lead to autoimmune disorders[34].

2.2 Generating adaptive CTL immune responses

There are numerous steps that are required for the induction of cytotoxic T cells to deal with infections and malignancies. This section will introduce the various processes that have to occur leading to the induction of adaptive immunity.

Antigen uptake and processing

When an invading pathogen is recognized there are a number of phagocytic cells that reside in tissues, ready and able to ingest the pathogen or infected cells. Macrophages and granulocytes are highly phagocytic and generally take up microorganisms and destroy them[38]. DCs on the other hand, reside in the tissue in an immature state and are less phagocytic, but their uptake of antigens from pathogens and dying cells is a critical step in the induction of an adaptive immune response[38].

Once the DC encounters and takes up the pathogen or dying cell, the presence of PAMPs and DAMPs cause the DC to undergo maturation. This maturation leads to a decrease in phagocytic capacity but increases antigen processing and presentation. The antigen is then processed and presented on MHC II to $CD4^+$ T cells. In immature DCs there are lysosomal compartments that constantly accumulate MHC II molecules (MIIC)[39,40]. When the DC takes up antigen it is processed and small peptides are loaded onto MHC II in the MIIC. These MHC II complexes are then trafficked to the cell surface and are available

to be presented to $CD4^+$ T cells[41]. As DCs mature the production and translocation of MHC II increases, and the MHC II/peptide complexes become more stable at the cell surface allowing for increased availability to $CD4^+$ T cells[40,42,43].

Alternatively, DCs are able to present antigen to naive $CD8^+$ T cells directly through a process known as cross-presentation, generating cytotoxic T cells[44,45]. The DCs are able to take up extracellular antigen, which is processed in phagosomes and endosomes and loaded onto MHC I and presented to $CD8^+$ T cells[44,46-48]. This pathway has been shown to prime $CD8^+$ CTL in response to both viral infections[49] and tumour cells[50,51]. The cross-presentation pathway is important, especially in generating anti-tumour immune responses, but DCs can also be infected by some viruses leading directly to endogenous antigen processing and presentation on MHC I. Indeed, DCs infected with HSV or influenza present viral antigen on both MHC I and II[52]. To combat the induction of anti-viral immunity, viruses have evolved numerous mechanisms to prevent proper antigen presentation[53].

Activation of naive T cells

The presentation of antigen in the context of MHC to a T cell is not sufficient to activate the T cell. This presentation represents “signal one” and in the absence of a second signal will lead to T cell anergy[34]. In order to get

activation of antigen specific T cells, a second signal is required in the form of co-stimulatory molecules on the DC.

After DCs mature they up-regulate co-stimulatory molecules such as CD80 and CD86. When antigen-specific T cells encounter an activated APC an immunological synapse forms leading to clustering of TCR, MHC/peptide complex, CD4 or CD8, CD3, along with co-stimulatory and adhesion molecules[35]. This results in a signaling cascade leading to the expression of genes involved in cell proliferation and differentiation[34]. The generation of cytotoxic $CD8^+$ T cell responses can be either T helper dependent or independent. In circumstances where the DC is unable to fully activate, T cell help is required. Peptide presented by DCs on MHC II to $CD4^+$ T cells in the presence of co-stimulation and IL-12 (produced from DCs) causes the $CD4^+$ T cells to activate and produce IFNγ and IL-2 (this cytokine production indicates the Th1 phenotype)[35]. The Th1 cells are then able to condition the DC, through CD40/CD40L interaction, enabling the DC to stimulate the $CD8^+$ T cell, inducing CTL killer cells[54-56]. Alternatively, in certain contexts the DC is able to directly activate the $CD8^+$ T cell in the absence of $CD4^+$ T cell help. The generation of CTL in the absence of T cell help can also occur in the presence of viral antigens, which condition the DC presenting antigen on MHC I to $CD8^+$ T cells[54,57-59].

CTL activity

The CTLs generated during the induction of an immune response can now circulate through the lymphatics searching for virally infected cells or tumour cells. Infected cells will present antigens on MHC I and are recognized by the surrounding CTLs. Upon recognition of the peptide/MHC complex, the CTL forms an immunological synapse and kills the infected or malignant cell[60,61].

There are two pathways that are able to accomplish this killing, the perforin/granzyme pathway and Fas/FasL pathway[62]. Target cell killing utilizing perforin and granzyme occurs when the CTL recognizes the infected/malignant cell and a synapse is formed leading to directional release of perforin and granzyme[62]. The granzyme gains entry into the target through perforin pores[62] causing cleavage of effector caspases, including caspase 3, leading to DNA fragmentation and apoptotic cell death[63]. More recently it has been recognized that granzyme also gains entry into the target cell through endocytic pathways. The release of perforin from the CTL leads to a loss of Ca^{++} from the target cell, activating cell membrane repair allowing granzyme access to the endosomal compartment[64]. The perforin then forms a pore in the endosomal membrane allowing access to the cytosol for the granzyme to mediate apoptosis[64-66].

Alternatively CTLs can kill cells through a separate process that does not require Ca^{++} or degranulation[67]. The Fas/FasL pathway is an extrinsic pathway that is able to induce apoptosis in cells where Fas is ligated by FasL. Following ligation of Fas, caspase-8 is activated leading to direct and indirect caspase-3

activation causing apoptotic cell death[63]. During activation of $CD8^+$ T cells FasL is up-regulated and expressed on the surface of the CTL or is readily available in the golgi for transport to the cell surface[68]. Upon recognition of target cells through MHC I/peptide complexes, the CTL is able to induce target cell death through ligation of the Fas receptor, which has been shown to be induced by DNA damaging agents and cytokines, including TNFα and IFNγ[69-72].

2.3 Immunological control of cancer

Throughout tumourigenesis the immune system plays an important role in control and removal of cancerous cells. The idea of cancer immunosurveillance was proposed in the early 1900s, but it was not until the 1990s when the hypothesis gained increased acceptance[73]. The importance of an intact immune response in cancer development can be seen by observing the cancer incidence in both mice and humans who have defects in their immune systems[74]. As well, detection of immunological markers in a tumour indicating the presence of T cells, particularly those of a Th1 or cytotoxic nature, are favorable prognostic indicators[75].

While immune surveillance and control of tumours is important, recent studies have shown that the immune system also has the ability to shape the immunogenicity of tumours[76-78]. These observations have led to an updated view on cancer immunosurveillance coined “cancer immunoediting”[73,76,79]. The

immunoediting of tumours can be broken down into three stages: 1) immune clearance, 2) immune equilibrium and 3) immune escape[73,80].

When cells lose their internal checkpoints and gain the ability to continually proliferate the immune system still has the ability to prevent the outgrowth of a tumour. Through studies of immunodeficient mice and mice with genetic predispositions to cancer, there is evidence that aspects of both innate and adaptive immunity are required to prevent the generation of cancer[74]. Similarly, there is evidence of immunological clearance of cancer in humans. Immunodeficiency and immunosuppression during organ transplantation in human patients increases cancer risk to cancer of both viral and non-viral etiologies[81-83]. Antibody and T cell responses recognizing tumour associated antigens have also been observed in cancer patients[73,74]. While these responses can be observed in patients with growing tumours, in some cases clonal T cell expansion has been found to recognize neo-antigens in spontaneously regressing malignant melanoma[73,84]. The presence of T cells, especially $CD8^+$ T cells, infiltrating the tumour is also a positive prognostic indicator[73]. Taken together, the murine and human data point to an important control mechanism preventing, or slowing, the formation of tumours. If a tumour is able to make it through this immunological control it may persist in equilibrium or completely escape immune control leading to further tumour growth.

Malignant cells that are not cleared by the mechanisms discussed above have the ability to continue to proliferate and form a tumour. However, there are

still barriers that the need to be overcome including requirements for further mutations, angiogenesis and escape from adaptive anti-tumour responses[74,85]. Unlike clearance of early transformed cells, only the adaptive immune system is required to hold the malignant cells in equilibrium, specifically T cells, IFNγ and IL-12[73,86]. In mouse models of MCA induced cancers, the T cell compartment can hold tumour growth in check. However, as soon as these cells and related cytokines were removed, immunogenic tumours were able to grow due to a lack of immunity and immunoediting[86]. In order for the cancerous cells to continue to grow uncontrolled and form a malignant tumour they must escape from this immune control.

There are a variety of mechanisms tumours can utilize in order to evade the immune system. Since the tumour is being held in check mainly by $CD8^+$ T cells, the antigen specific T cells need to be able to recognize antigen in the context of MHC I on the surface of the tumour cell. Therefore if the tumour loses MHC I expression, antigen processing components are mutated or if antigen expression is lost, there will be no antigen available on the surface of the cell for recognition by the immune system[73,74]. This can be seen in human tumours through the generation of antigen loss variants that are no longer presenting TAAs on the surface of the cell[87-90]. Alternatively, tumour cells have the ability to modulate T cell activation and anergy through expression of inhibitory molecules such as PD-L1[91]. When the T cell encounters such ligands, TCR signaling is decreased inhibiting proliferation and cytokine production[92]. The inhibitory

molecules may also cause the T cell to undergo cell cycle arrest and apoptosis[93]. Lastly, tumour cells can resist killing by CTLs due to mutations in death receptors (CD95/Fas) and prevention of apoptotic signaling[94-97].

Along with these tumour cell autonomous mechanisms, there are other molecules, cytokines and cells that shape the immunosuppressive tumour microenvironment. The presence of effector molecule ligands and cellular metabolites within the tumour lead to impairment of NK and T cell killing, as well as DC migration, preventing $CD8^+$ T cell priming in the draining lymph nodes[98-100]. Tumour cells also secrete a number of cytokines, including TGFβ and VEGF, that recruit, or induce, regulatory cells such as Tregs and MDSCs[101-103]. These cells further impair lymphocyte function in part by further production of cytokines such as TGFβ[101,104]. Whatever the mechanism, the immune system plays an important role in early control of malignant tissue and ultimately shape the immunosuppressive landscape in the growing tumour. Therefore, successful biological and immunotherapeutic treatment of cancer will need to overcome this barrier in order to create a successful therapeutic. One such treatment strategy is the use of oncolytic viruses (OV).

3.0 Oncolytic Viruses

3.1 History of oncolytic viruses

Viruses that have a propensity to replicate in and kill tumour cells have been coined oncolytic viruses. Anecdotal evidence from the early to mid 20th

century indicated that viruses may be able to impair tumour growth. Case reports have shown that there was improved control of hematological malignancies during bouts of viral infection in patients, including measles, varicella zoster, influenza and Epstein-Barr virus[105-112]. In the majority of these cases the patients relapsed shortly after clearance of the viral infection.

While viruses appeared to control cancer in these anecdotal cases, it took numerous advancements in cell culture and animal models of cancer before the potential of viruses as therapeutics could be fully realized[113]. As early as the 1970's, cancer patients were being treated with a number of viruses including Adenovirus, measles, mumps, and Newcastle disease virus[109,114-118]. More recently with the advent of genetic engineering, viruses can be manipulated as needed. Modifications to the viral genome can attenuate or target the virus for use as an oncolytic agent. Alternatively genes can be added to improve targeting of the virus or manipulation of the immune system[113,119].

3.2 Types of oncolytic viruses

Examples of oncolytic viruses can be found in a variety of viral classes, everything from small RNA viruses to large DNA viruses[120]. As long as the virus is able to replicate in malignant tissue while sparing any normal cells that are encountered it has the potential to be a successful oncolytic virus. While some viruses are naturally oncolytic, others have required modification to ensure selective replication in the tumour. Some examples of the viruses currently being

studied will be presented. See references[119,120] for a more extensive review of the numerous viruses being studied as potential oncolytic therapeutics.

In a sense all cytolytic viruses likely have the ability to kill tumour cells. What differentiates an oncolytic virus is the innate or engineered inability to replicate in normal cells and tissues. Viruses that have a natural propensity to be good candidate oncolytic therapeutics are viruses that don't infect humans or at the bare minimum are non-pathogenic. Two viruses that are currently in clinical trials and fit this description are Newcastle disease virus and reovirus[121]. NDV's natural ability to replicate in tumours rather than normal human cells is due to the virus' inability to deal with human interferon[20]. The virus' interferon antagonist is very species specific and only able to modulate avian interferon responses[122]. Therefore NDV is able to replicate in interferon hypo-responsive tumour cells and the interferon produced during NDV infection minimizes infection of normal tissues. Reovirus on the other hand is a human virus, however has not been linked to any specific disease[123]. The selective replication of reovirus has been proposed to occur through a PKR dependent mechanism. In normal cells PKR is able to sense infection and induce apoptosis of the infected cells; however, in tumours with Ras activation, the PKR pathway is impaired allowing reovirus to replicate in the tumour cells[124]. RNA viruses are not the only examples of "naturally" occurring oncolytic viruses. Two large DNA viruses in the *poxviridae* family have been shown to be naturally oncolytic. Unable to infect and cause

disease in humans, myxoma virus and ORFV have been found to be novel candidate oncolytic viruses with immunostimulatory properties[125-127].

For viruses that are not naturally attenuated in normal tissues, genetic engineering has been utilized to modify the viral genomes in an effort to attenuate the viruses, leading to tumour selective replication. DNA viruses have evolved numerous ways to control cell replication and the immune system. By removing some of these controls from the virus it is possible to prevent replication in normal cells and tissues, but due to changes in tumour cells during tumourigenesis the oncolytic DNA virus is still capable of killing the cancerous cells. There are many examples of how DNA viruses can be attenuated for use as an oncolytic agent[119,120]. For example, HSV has been modified by removing or destroying genes required for replication in the CNS and non-dividing cells, or genes involved in the control of the type I IFN pathway[128,129]. In both cases this restricts the replication of the attenuated HSV vectors to actively dividing tumour cells. Poxviruses have also been modified for tumour selective replication by removing thymidine kinase, a critical enzyme in DNA replication, thereby only permitting replication in highly active tumour cells[130,131].

Similarly, RNA viruses have been modified to prevent replication in normal tissue[120]. Unlike large DNA viruses, RNA viruses generally do not encode accessory proteins to control host immune responses or cell cycle. Therefore rather than removing genetic components of the virus the genes or regulatory factors can be modified without completely impairing the function of the gene.

VSV has been modified in this way by deleting a single amino acid in the matrix protein. This modification prevents the virus from shutting down innate anti-viral cytokines but does not impair the viral growth allowing replication in interferon hypo-responsive tumours[132,133]. Another example of an engineered RNA virus is poliovirus, which is naturally neurotropic. To attenuate this neurovirulence, the poliovirus IRES was replaced with an IRES from a related rhinovirus. This attenuated poliovirus showed potential as an oncolytic therapy for glioma[134].

While attenuating viruses may improve their oncolytic potential, the tumours being treated still need to express the receptor for the virus to allow for infection and lytic destruction of cancer cells. Therefore, while poliovirus can be attenuated by modifying the IRES, there is still the issue of having tumour cells expressing its receptor, CD155[134,135]. A number of human gliomas express the poliovirus receptor, however not all do, thereby limiting the use of poliovirus as an oncolytic virus[134]. In some cases it is possible to modify a virus in order to target it to a specific cell type. For example, it has been shown that measles virus, which naturally infects cells expressing CD46 or SLAM, can be retargeted by engineering a chimeric viral glycoprotein that contains a single chain antibody that recognizes cell surface proteins expressed by tumours[136]. Although it is possible to retarget a virus for use in certain tumours, the ideal oncolytic virus would be one which is able to infect different cancer types rather than having to develop a specific virus for a single malignancy.

3.3 Oncolytic viruses in the clinic

With the success of oncolytic viruses in pre-clinical testing a number of viruses have moved forward into clinical testing[137-140]. Table 1 outlines some of the recent and ongoing clinical trials involving oncolytic viral therapy. Since the majority of these clinical studies are in early Phase I/II trials, the primary objective has been testing the safety of the viruses in human patients. In all cases the viruses have been well tolerated with only minor adverse events such as flu like symptoms.

In these early studies the primary endpoint has been toxicity, however the studies were also able to assess efficacy, at least during the short followup period. The trials conducted to date have shown promising results, with complete responses observed in a few patients. In a phase II study of HSV expressing GM-CSF, intratumoural injection of the oncolytic virus was found to have significant impact on the injected and distant tumours. This treatment resulted in complete responses, as defined by RECIST, in approximately 20% of patients with stage III/IV melanoma. When stratified by response, patients with complete responses, combined with partial responses and surgical complete responses, had approximately 80% survival rate at 4 years (n=15). This is a significant improvement compared to survival of all patients in the trial which was around 40% (n=50, the 15 patients described above are also included in this value).

The viruses furthest along in the clinic have been armed with an immunostimulatory transgene (GM-CSF)[141,142]. Therefore in patients treated with

these viruses, not only does oncolytic destruction play an important role in the efficacy, but the addition of GM-CSF has the potential to stimulate the immune system leading to anti-tumour immune responses. Indeed, some of the studies have observed effects in uninjected tumours both near the injection site and in distant metastases[141-143]. Although it is possible that the responses observed in uninjected tumours may be the result of anti-tumour immunity being induced, viral dissemination to uninjected tumours may also account for some of the responses observed[141]. Unfortunately few studies have directly assessed the anti-tumour immune response during oncolytic therapy. However in one clinical study assessing HSV expressing GM-CSF(Oncovex®), tumour biopsies revealed the presence of tumour specific T cells and a decrease in suppressive immune cells in treated tumours[144]. Therefore it is important moving forward that along with safety and efficacy endpoints, immunological endpoints are incorporated into oncolytic virus studies.

Table 1 - Oncolytic Virus monotherapy clinical trials. This is not a comprehensive list, for further review see[137,138]

Virus	Phase	Cancer - route of delivery	Response	Immune	Ref
HSV (OncoVex^{GM-CSF})	I	various - i.t.	SD 3 patients*	ND	142 †
	II	Stage III/IV Melanoma - i.t.	Overall 26% (CR+PR)	ND	143 †
	II	Stage III/IV Melanoma (subset of above trial assessed [143]) - i.t.	Subset of patients from[143]	↑ MART-1 specific T cells ↓Suppressive immune cells	144
	III	Stage III/IV Melanoma - i.t. recruitment complete			145
Vaccinia (Wyeth) JX-594	I	Various - i.t.	3/10 PR† 6/10 SD† 1/10 PD	ND	141
	I	Stage IV Melanoma - i.t.	5 SD†	ND	146††
	I	Various - i.v.	Not assessed - IV delivery of virus primary objective	ND	147
Reovirus (Reolysin®)	I	Glioma - i.t.	1/12 SD 10/12 PD	ND	148
	I	various - i.v.	8/10 SD	ND	149
	I	sarcoma w/ lung metastases - i.v.	14% SD > 24 weeks	ND	150
	I	Various - i.v.	8/18 (PR+SD)	ND	151

Virus	Phase	Cancer - route of delivery	Response	Immune	Ref
	II	Metastatic Melanoma - i.v.	No objective responses	ND	152
MV-CEA	I	Glioblastoma - i.t.			recruiting
MV-NIS	I	MPM			recruiting
VSV-IFNβ	I	HCC			recruiting

ND - Not determined; HCC - Hepatocellular carcinoma; SCC - squamous cell carcinoma; MPM - malignant pleural mesothelioma
*Safety study - only 6 week followup therefore long-term effects not properly assessed - along with 3 stable disease had a number of patients who showed some response in injected and local tumours
† Responses observed in non-injected tumours
†† Primarily phase I safety study - short follow up makes it difficult to assess long term tumour responses

With oncolytic viruses moving into phase III testing as a stand-alone therapy[145], there have also been promising results observed with oncolytic viruses in combination with standard chemotherapy in phase I studies[153-155]. There are currently phase II and III trials in progress to further study oncolytic viruses in combination with chemotherapy (see Table 2).

Table 2 - Phase II and III clinical trials combining oncolytic viruses with chemotherapy

Virus	Phase	Chemotherapy	Cancer - route of delivery	Status
Reolysin (clinicaltrials.gov ID:NCT01166542)	III	carboplatin, paclitaxel	SCC - Head and Neck	active
JX-594 (clinicaltrials.gov ID:NCT01171651)	II	sorafenib	HCC - i.v.	recruiting

3.4 Immunostimulatory oncolytic viruses[a]

With indications that the use of oncolytic viruses in the clinic have led to the generation of anti-tumour immune responses (see Section 3.2), and the requirement of $CD8^+$ T cells for successful VSV oncolytic therapy (FIgure 2), harnessing the immune response during oncolytic virus therapy is a useful strategy towards improving oncolytic viruses. A number of groups have begun investigating the utility of expressing immunostimulatory transgenes from oncolytic viruses. By incorporating cytokines and chemokines as transgenes into oncolytic viruses, it is possible to increase immune stimulation through the local and systemic expression of these molecules leading to improved oncolytic virus therapeutics.

[a] Reprinted, with kind permission from Springer Science and Business, in part from: Experimental and Applied immunotherapy, 2011, pages 344-345, Chapter 16: Combining Oncolytic Viruses with Cancer Immunotherapy, Stephenson KB, Bell J, Lichty B, © Springer Science+Business Media, LLC, 2011.

Various immune cells can be targeted to increase anti-tumour immune responses following oncolytic virus treatment. Both innate and adaptive cells can be manipulated, with the ultimate end goal to induce cytotoxic effector cells that can be either nonspecific NK cells or tumor antigen-specific T cells. The activation of APCs, including DCs, is important in both of these processes. DCs have an exquisite ability to take up released tumor antigens and cross-present them to $CD8^+$ T cells as well as activate $CD4^+$ T cells through MHC-II molecules. As the DCs take up this antigen they will mature as they travel to lymph nodes, and subsequently secrete cytokines that will impact both innate effector cells (NK) as well as adaptive immune cells ($CD4^+$ and $CD8^+$ T cells)[156,157]. In an effort to recruit and activate APCs, a variety of cytokines, chemokines, and co-stimulatory molecules have been added to oncolytic viruses in the preclinical setting[158-169] and the clinical setting[141,170,171]. RANTES is one such chemokine that is able to recruit numerous immune cell populations. Expression of RANTES leads to higher numbers of activated DCs within the tumor, thereby increasing tumor-specific T cells[172]. Alternatively, other groups have added GM-CSF to HSV and adenovirus to enhance maturation and activation of APCs[158,173]. Treatment with these modified viruses led to increased efficacy with evidence of tumor-specific immune responses. Vaccinia virus expressing GM-CSF has also been show to increase vaccinia efficacy in preclinical models[130] and has shown efficacy in phase I clinical trials. Of the ten treated patients, one showed progressive

disease while three patients had a partial response and six had stable disease according to RECIST criteria[141].

There are numerous examples of tumor cells that have decreased expression of both MHC-I and co-stimulatory molecules and therefore do not efficiently present antigen directly to T cells[174]. The expression of co-stimulatory molecules, including B7-1, can help induce activation of T cells that otherwise may be anergic[175]. Expression of soluble B7-1 (CD80) from oncolytic viruses slightly increased vaccine efficacy with concomitant induction of a systemic anti-tumour immune response[176]. The use of B7-1 expressing oncolytic viruses can also be enhanced by co-expression of other cytokines such as IL-12, which is up-regulated in activated DCs. IL-12 promotes cellular proliferation and induction of IFN-g from both T cells and NK cells, thereby inducing Th1 responses[177,178]; IL-12 has been shown to have a significant impact on tumor growth when expressed from the liver following hydrodynamic injection of DNA[179]. However, IL-12 has been associated with substantial toxicity when given systemically; therefore, the use of viruses to restrict IL-12 expression may reduce toxicity associated with this cytokine[180,181]. Importantly, the combination of IL-12 and B7-1 was shown to further enhance the efficacy of oncolytic viral therapy[176,182].

4.0 Vesicular Stomatitis Virus

4.1 Overview

VSV is a bullet shaped, single-stranded negative sense RNA virus and is the prototypical virus in the *vesiculovirus* genus within the *Rhabdoviridae* family[183-185]. The Indiana and New Jersey serotypes of VSV were originally isolated in the 1920s[186,187] and are important agricultural pathogens[184]. VSV naturally infects cattle, horses and swine causing lesions in the mouth of animals and clinical symptoms similar to that of foot-and-mouth disease[184]. While the natural host for VSV has not been determined, the virus can replicate in and be transmitted by insect vectors, mosquitoes and sandflies, and these insects have been proposed as a reservoir for VSV[188-191].

VSV has been shown to be a zoonotic virus causing mild infections in humans. Upon exposure to VSV, conjunctivitis has been observed as well as acute flu-like illness that is self-limiting and lasts less than a week[184]. Seroprevalance in humans in endemic areas can be as high as 100%, while in non-endemic areas of the US 25% of humans are seropositive[188,192]. While seropositive individuals are found in endemic areas and during epidemics, overall seroprevalence in the general population is quite limited[193].

4.2 VSV life cycle

The receptor that VSV uses to gain entry into a cell has not been identified, but would need to be a ubiquitous molecule due to VSV's broad host

and cellular tropism[194]. Phosphatidylserine has previously been reported as a potential receptor[195], however it has recently been shown that in fact VSV does not use phosphatidylserine as a receptor[196]. Alternatively it has been proposed that VSV binds to cells through non-specific electrostatic interactions rather than utilizing a specific receptor[197].

Once bound to the cell VSV is internalized through endocytosis[185,194]. As the endosome acidifies VSV's glycoprotein fuses with the endocytic membrane leading to release of the virion's contents into the cytosol[185,194,198]. Along with the viral genome, the polymerase is also released into the cytosol since it is packaged in the virion. This is necessary for the transcription of the negative stranded genome upon entry into the cytosol[199].

Once in the cytosol the polymerase begins primary transcription leading to the production of capped mRNA[185]. There is a single entry point for the polymerase at the 3' end of the genome, therefore transcription of viral genes occurs sequentially with the leader transcribed first followed by nucleocapsid, phosphoprotein, matrix protein, glycoprotein and lastly polymerase[200-203]. Each gene is separated by an intergenic region containing signals for poly adenylation and transcriptional start/stop sequences[185,201,204]. Following transcription of the upstream gene the polymerase will either continue reading through to capping and transcribing the next down stream gene or fall off and begin again at the 3' end of the genome[201,204-206]. This leads to a polarity in transcription and there is a

30% reduction in the quantity of mRNA, and therefore protein, of each successive gene, ie. there is 30% more VSV-N than VSV-P[201].

The primary transcription of VSV genes occurs in the absence of protein production, however replication of the genome requires the previous transcription of viral genes[207,208]. Production of both the leader transcript and nucleocapsid protein, as well as fully encapsidated RNA genome, are required for the polymerase to switch from transcriptase to replicase function[185,209]. The switch to replicase also requires the association of a nucleocapsid-phosphoprotein complex with the polymerase, rather than phosphorylated phosphoprotein associated with transcription[210]. Once the polymerase has switched to replicating genomes, it reads through and copies the entire genome into anti-genome (positive stranded) followed by many copies of the negative strand genome which will be packaged into new virions and used as template for secondary transcription[185]. Once enough of the vial proteins are produced, the glycoprotein traffics to the plasma membrane where matrix protein and nucleocapsid coated negative sense genomes assemble along with the polymerase and phosphoprotein followed by budding of new VSV virions from the plasma membrane[185]

4.3 VSV and type I IFN

VSV infection is sensed by both intracellular and extracellular receptors. When VSV enters the cell and begins replicating, dsRNA and ssRNA are

recognized by RIG-I, and TLR-7, respectively(Figure 1)[211-216]. While RIG-I and TLR-7 are required for type I IFN production during VSV infection, RIG-I is a major sensor in fibroblasts while TLR-7 plays a more important role in detection of VSV in pDCs[217]. Survival of mice infected with VSV depends on the intact signaling of both pathways as, MyD88 (TLR-7 pathway[218]) and IPS-1 (RIG-I pathway[215]) knockout mice succumb to VSV infection[219,220]. More recently TLR-4 has been proposed as a VSV-G sensor leading to the induction of type I IFN mRNA in mDCs[221].

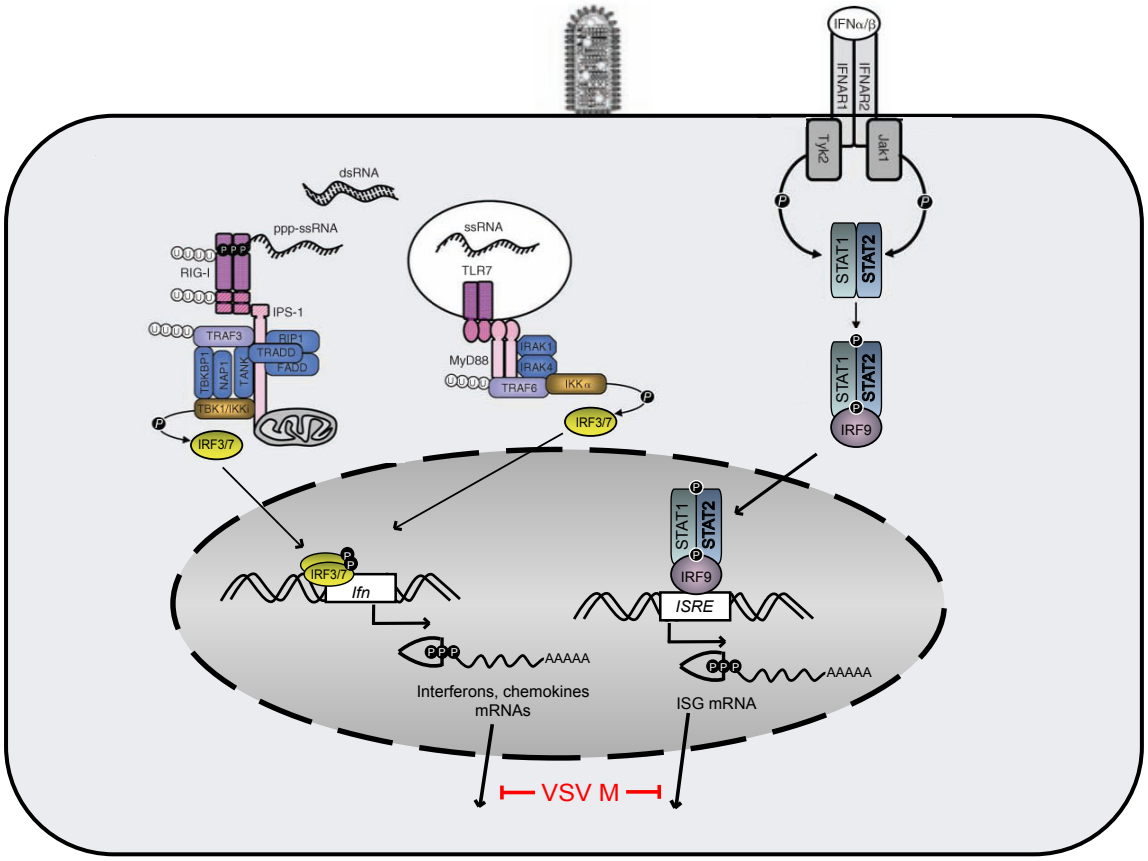


Figure 1: Recognition of VSV infection and VSV control of interferon and ISG production. Signaling pathways initiated following VSV infection leading to production of antiviral genes. VSV blocks these processes through modulation nuclear export of mRNA. Adapted from [216]

VSV is highly sensitive to type I IFN[222] and therefore must have a mechanism to overcome this anti-viral defense. VSV has a very small genome of only 5 genes and 11kb, therefore VSV does not have the ability to encode extra genes to specifically modulate aspects of the immune system. Instead, VSV-M plays an important role in dampening innate anti-viral responses[216].

The matrix protein of VSV impairs anti-viral responses through inhibition of mRNA export from the nucleus[223]. This is accomplished through the interaction of VSV-M with Nup98 and Rae-1 at the nuclear membrane preventing the movement of mRNA into the cytoplasm thereby inhibiting host protein production[223]. While the WT version of VSV-M is able to potently prevent these processes, mutant versions of VSV-M have been identified that are unable to prevent these blockades[223,224].

One such mutant is ΔM51, or the analogous M51R. This mutant does not localize to the nuclear membrane and is unable block the export of mRNA from the nucleus[223] leading to normal host gene expression including type I IFN and other anti-viral genes. Therefore ΔM51 VSV is known to be an interferon-inducing mutant virus that is significantly attenuated *in vivo and in vitro* due to the normal production of IFN during infection[132,225]. Even though mutant VSV is attenuated and unable to effectively replicate in normal tissue, it can replicate to very high titers and kill cells that are unable to respond to type I IFN such as malignant tissue[133].

4.4 VSV as an oncolytic virus

The oncolytic properties of VSV were first described in 2000[25,226]. In these early studies, WT VSV was shown to infect and kill a number of different human tumour cells *in vitro* and *in vivo*[25]. However, in the presence of IFN-α normal cells were not killed by VSV, nor was appreciable virus produced[25]. While WT VSV worked well at controlling tumours in a xenograft mouse model, there was some toxicity associated with the use of WT VSV in athymic mice[25]. Subsequently, VSV variants were identified that induced large amounts of interferon due to a mutation in the matrix protein[132]. These mutant viruses were attenuated *in vivo,* yet retained their oncolytic potential[211].

Although it is clear that VSV infects and directly kills tumour cells, more recently it has been observed that there is also a shut-down in the tumour vasculature following VSV treatment[227,228]. Since VSV delivered intravenously only infects small areas around the rim of the tumour it is likely that the indirect bystander effects of the vasculature shutdown play a major role in the success of VSV treatment. Following infection of a tumour with VSV, neutrophils are recruited to the tumour and there is significant clotting observed in the tumour vasculature, which is dependent on the presence of neutrophils[227,228]. This ultimately prevents blood flow to the core of the tumour. The lack of perfusion causes the death of the core of the tumour[227]. Vasculature shutdown has been observed in numerous tumours and is induced by a variety of oncolytic viruses[147]. As well, this is not just a phenomenon of treating murine tumour models as the

vasculature shutdown of tumours has been observed in patients treated with the poxvirus JX-594[141,170].

5.0 Scope of Thesis Research

VSV treatment of subcutaneous CT26 colon carcinoma tumours leads to regression in all treated tumours, however only 20-40% of mice on average are cured of their subcutaneous tumours. Following treatment anti-tumour immune responses are extremely variable but observed in over half of mice in any given experiment. The immune responses generated are critical for a successful outcome. Treatment of CD-1 Nude mice with VSV leads to a prolonged survival but no durable cures (Figure 2A). As well, if $CD8^+$ T cells are depleted seven days after the start of VSV treatment, a time point at which there is measurable anti-tumour $CD8^+$ T cell responses (data not shown), the tumours begin to grow in all depleted animals at a significantly faster rate than in treated mice with an intact $CD8^+$ T cell compartment (Figure 2B).

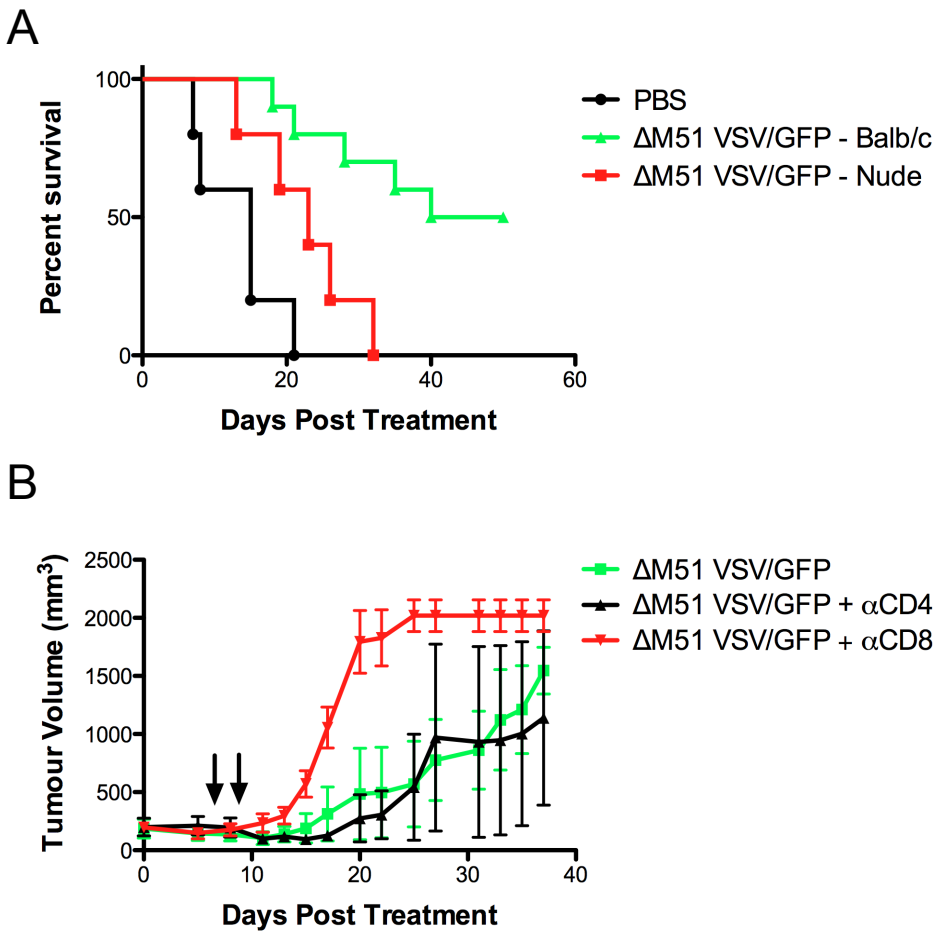


Figure 2 - Requirement for adaptive immune response during VSV therapy. In the absence of adaptive immune responses, specifically $CD8^+$ T cells, VSV oncolytic virotherapy fails. (A) Balb/c and Nude mice were engrafted with $5x10^5$ CT26 subcutaneously. Tumour bearing animals were treated with 3 doses of $5x10^8$ PFU of ΔM51 VSV/GFP every other day once tumours reached 250 mm^3. Survival of animals is presented. (B) Balb/c mice were engrafted with $5x10^5$ CT26 subcutaneously and tumours were allowed to grow to a mean of 250 mm^3. Tumour bearing animals were treated with 2 doses of $5x10^8$ ΔM51 VSV/GFP 48 hours apart. Treated animals were then administered CD4 or CD8 depleting antibody, 200 µg on day 7 and 9, to deplete these cell populations to determine their importance in oncolytic therapy. Tumours were measured and volumes were calculated using the formula $4/3 \times \pi \times (L/2) \times (W/2)^2$.

With less than half of mice cured of their tumours on average following VSV therapy, and a clear requirement for induction of anti-tumour immunity, we set out to improve VSV as an oncolytic virus. The goal of my PhD thesis was to determine ways to improve VSV as an oncolytic virus. **We hypothesized that**

improving the magnitude and consistency of anti-tumour immune responses induced following oncolytic VSV therapy would result in improved therapeutic efficacy. To accomplish this we focussed on improving anti-tumour immune responses following VSV therapy, as we believe that successful oncolytic therapy will require robust, consistent immune responses following oncolytic virus treatment. To accomplish this goal we set out three objectives outlined below.

5.1 Research Objectives

Objective 1 Evaluate whether the expression of cell autonomous transgenes from VSV are able to modify the immunogenicity of tumour cells killed with VSV and if this leads to improved anti-tumour immune responses and VSV efficacy **(Chapter 3)**

Objective 2 Examine the impact expression of soluble hIL-15 in VSV infected cells has on the anti-tumour immune response induced during VSV therapy and whether hIL-15 expression leads to a better therapeutic outcome **(Chapter 4)**. Results related to this objective have been published in the following manuscript:

> Stephenson KB, Barra NG, Davies E, Ashkar AA and Lichty BD. Expressing human interleukin-15 from oncolytic vesicular stomatitis virus improves survival in a murine metastatic colon adenocarcinoma model through enhancement of anti-tumor immunity. *Cancer Gene Ther* (2012)[167].

Objective 3 Investigate the role VSV induced vascular shutdown plays in the induction of anti-tumour immune responses and therapeutic outcomes following VSV oncolytic virotherapy **(Chapter 5)**.

~ Chapter 2 ~

Materials and Methods

Cell lines

Vero, A549, CT26 and L929 were maintained in α-Modified Eagles medium with 10% FBS (Gibco), 2mM L-Glutamine, 100 U/mL penicillin and 100 ug/mL streptomycin. 293T cells were maintained Delbucco's minimal essential medium with 10% FBS (Gibco), 2mM L-Glutamine, 100 U/mL penicillin and 100 ug/mL streptomycin. All cells were cultured at 37 °C with 5% CO_2.

CT26.BCL2 stable cells were created by transfecting N-terminally FLAG-tagged murine BCL2 (accession #: NM_009741.3). BCL-2 was ordered from (Genscript) and PCR amplified using Phusion polymerase (NEB) to add an N-terminal FLAG tag (DYKDDDDK) as well as BamHI and MluI restriction sites to facilitate cloning into pMono (Invivogen). The following primers were used: Forward: CGGATCCGCCACCATGGACTACAAGGACGACGACGACAAGG CGCAAGCCGGGAGAACAGG; Reverse: ACGCGTCGGTCTTCACTTGTGGC. All PCR products and final pMONO-FlagBCL2 were sequenced to verify sequence. pMONO-FlagBCL2 was then transfected into CT26 in 6 well dishes cultured in antibiotic free medium. 4 ug of pMONO-FlagBCL2 plasmid was transfected with Lipofectamine 2000 (Invitrogen) as per the manufacturers protocol. The following day cells were trypsinized and moved into 10cm dishes and allowed to culture 24 hours prior to selection. Transfected CT26 were then selected for Flag-BCL2 expression/incorporation with 13.3 ug/mL Blasticidin (Invivogen). Cells were sub-cultured every 2-3 days supplementing fresh blasticidin. A second round of selection was carried out at passage 13 with

staurosporine (Sigma Aldrich). Blasticidin resistant CT26.BCL2 were treated with 1uM staurosporine overnight. After treatment cells were put back into blasticidin containing medium and cultured as described above.

Cloning of viruses

Transgenes are inserted into the VSV Indiana backbone via XhoI and NheI restriction sites engineered between G and L. All transgenes inserted were PCR amplified using Phusion taq polymerase (NEB) and cloned into pJet cloning vector (Fermentas) sequence and subcloned into pVSV-XN (wild-type) and pVSV-XN Δ51 genome plasmids. See table 3 for primer sequences used to PCR amplify the transgenes to construct FLAG-F1L and GFP-FPV039 expressing viruses, and figure 3 for a graphical representation. Construction of VSV/FAST and ΔM51 VSV/FAST[225], ΔM51 VSV/opt.hIL15[167] ΔM51 VSV/GFP[132] have been previously described.

Recombinant VSV vectors were rescued as described previously[229]. Briefly, A549 were infected with vaccinia virus expressing T7 polymerase and transfected using Lipofectamine 2000 (Invitrogen) 45 min later with 3 μg of the genome plasmid along with the helper plasmids VSV-P, VSV-N and VSV-L (0.75, 1.5, 0.75 μg, respectively). The rescued virus was passaged on Vero cells, then plaque purified twice, amplified and titered on Vero cells.

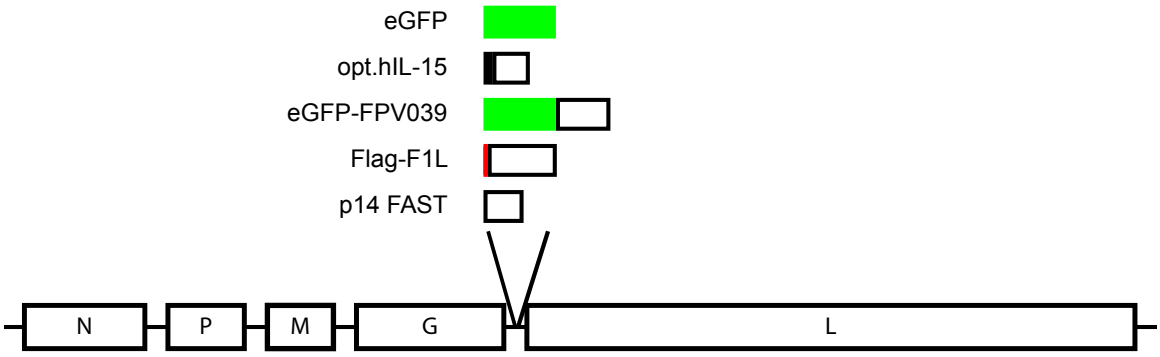


Figure 3 - VSV Genome organization. VSV genome organization and location of transgenes inserted into the genome.

Production of virus for use in animal experiments was performed in HEK293 T cells. Infections were carried out at a multiplicity of infection of 0.01 for 24 h. Supernatants were collected and cell debris was cleared by centrifugation and filtration through a 0.2 μm filter. The virus was then pelleted from the cleared supernatant, resuspended and banded on a continuous 5–40% sucrose gradient made in phosphate-buffered saline. The visible band of virus was then collected from the gradient and dialyzed against phosphate-buffered saline, divided into small aliquots and stored at -80°C.

Table 3 - Primers for construction of anti-apoptotic viruses

Gene	Primer orientation	Restriction site added	Primer Sequence
GFP-FPV039	Forward	SalI	ctgtcaacccggtcgccaccatggtgagcaaggg
	Reverse	XbaI	tatgatcagttatctagatccggtggatcc
FLAG-F1L	Forward	XhoI	ctctcgagctcactatagggagacccaagcttgg
	Reverse	XbaI	gatctagaactggcggccgttactagtggatcc

Western Blotting

Cells were treated with required drugs or viruses for the indicated times. Supernatants and cells were collected and washed with PBS. Cells were lysed in RIPA buffer (1% Triton, 1% sodium deoxycholate, 150 mM NaCl, 50 mM Tris-HCL pH 7.5, 10mM EDTA, 0.1% SDS) on ice for minimum of 30 min. Whole cell lysate was then sonicated for 10 second and chilled on ice and centrifuged at 14000 RPM for 30 min at 4°C. Supernatant was collected and stored at -20°C.

Protein concentrations were determined using the Dc Protein Bioassay (BioRad) and 10 µg of protein was loaded and run on an SDS-PAGE gel at 110V. Protein was then transferred onto nitrocellulose (Santa Cruz) at 400 mA. For small proteins (<20 kDa) the transfer was completed using 0.22 µm nitrocellulose and was transferred for 60-70 minutes. For large proteins including PARP transfers were carried out on 0.45 µm nitrocellulose for 90-100 minutes. Membranes were then blocked in either 5% milk or Licor Odyssey blocking buffer (Licor) diluted 2.5x in PBS. Block was carried out for a maximum of 2 hours prior to probing with primary antibody. See table 2 for antibody's used and blocking hybridization conditions. Following primary antibody membranes were washed with TBS/T (TBS + 0.2% Tween 20). Membranes were then probed with secondary antibodies (see Table 2 for conditions). Following secondary antibody membranes were washed with TBS/T and analyzed on Licor Odyssey (Licor).Quantification was carried out using Odyssey 2.0 software (Licor).

Table 4 - Western blot antibody conditions

Antibody	Company	Block	Hybridization buffer	Dilution	Time and temperature
Actin	Sigma	Odyssey buffer	Odyssey buffer	1:10000	1 hr / RT
PARP	Cell Signalling	Odyssey buffer	Odyssey buffer	1:1000	O/N / 4°C
VSV	N/A	5% Milk	5% Milk	1:2500	1 hr / RT
Polyclonal Flag	Sigma	5% Milk	Odyssey buffer	1:2000	1 hr / RT
Active Caspase-3	Cell Signalling	Odyssey buffer	Odyssey buffer	1:1000	O/N / 4°C
p14 FAST	N/A	5% Milk	5% Milk	1:500	1 hr / RT

Virus growth curves

Growth curves were carried out as part of characterizing all new viruses. Vero's were seeded into 10 cm tissue culture plates and infected at an MOI of 5 for 45 min in minimal medium. At the indicated time points samples were removed from the culture liquid and stored at -80°C. Samples were then thawed, serially diluted and titered by standard plaque assay. Briefly, Vero cells were infected 60 mm tissue culture dishes for 45 min, overlayed with .5% agarose (2x MEM F11 + FBS + agarose) and cultured O/N at 37°C. Plaques were then counted the next day. Data was plotted in Prism 5.0 (Graph Pad) and log transformed before assessing statistics.

Caspase 3/7 apoptosis assay

To assess apoptosis in virally infected and staurosporine treated cells, caspase 3 activation was assayed in triplicate using the Casp-Glo 3/7 Assay (Promega). Following treatment for the required time in a 96 well plate format, 50 µL of media was carefully removed from the wells ensuring no cells were removed, to which 50 µL of Casp-Glo 3/7 reagent was added. The plates were then incubated for 1 hour at room temperature on an orbital shaker. The media with Casp-Glo reagent was then transferred into a white walled 96 well plate and analyzed on a luminometer.

Flow cytometric analysis of apoptosis

To assess cell death by flow cytometry, CT26 were mock infected or infected with ΔM51 VSV/MT or ΔM51 VSV/Flag-F1L for 24 or 42 hours at which time the analysis was performed. Cells were harvested with citric saline to preserve membrane proteins and stained with annexin V and 7-AAD using BD apoptosis detection kit as per the manufactures instructions (BD Biosciences). Briefly, treated cells were washed in cold PBS and resuspended at $1x10^6$ cells/ mL in 1x binding buffer. 100 µL of cell suspension were transferred into a 5 mL polypropylene tube and 5 uL of each PE-AnnexinV and 7-AAD were added. Cells were then vortexed and incubated in the dark at room temperature for 15 min. Cells were topped up with 400 µL of binding buffer and analyzed on CANTO II (BD Biosciences)

Alamar Blue viability assay

CT26 and CT26.Bcl-2 were plated in 96 well plates at a density of $1x10^5$ cells/well. The following day they were infected at MOIs of 1, 0.1, 0.01 and 0.001 in setptuplate or mock treated. 48 hours after infection cell viability was assessed by alamar blue staining. Media was aspirated and 100 µL of PBS containing 5% (v/v) alamar blue was added to the wells. Cells were incubated with alamar blue for 30 min at 37°C and then analyzed on a Safire fluorescence plate reader (excitation = 530nm, emission = 595nm). Data was analyzed and presented as relative viability compared to mock treated samples.

ELISA

The presence and concentration of hIL-15 was determined by enzyme-linked immunosorbent assay (ELISA) using a human IL-15 ELISA kit as per the manufacturer's recommendations (R&D Systems, Minneapolis, MN). For assessment of the ability of ΔM51 VSV/opt.hIL-15 to direct the secretion of hIL-15, Vero cells were infected at an MOI of 5 for 7 h, a time-point where all cells were still viable. Supernatants were collected, centrifuged and analyzed by ELISA. Human IL-15 expression was also assessed in vivo. Balb/c mice bearing subcutaneous CT26 tumors were treated intravenously with $5x10^8$ PFU of ΔM51 VSV/GFP, ΔM51 VSV/opt.hIL-15 or ultraviolet-inactivated VSV. Tumors were removed 72 h after infection, homogenized and hIL-15 was analyzed in the tissue homogenate by ELISA

Animal Studies

Female, 6 to 8 week old BALB/c mice were obtained from Charles River Laboratories (Wilmington, MA). All experiments were conducted with the approval of the McMaster University Animal Research Ethics Board. Mice were anesthetized with 5% induction and 3.5% maintenance of isoflurane for intranasal instillation of 30 µl of virus and allowed to recover under oxygen. Mice were monitored daily and euthanized at indicated time points or upon signs of morbidity.

For tumour studies CT26 tumour cells were cultured to ~75% confluency (around 3-4 $x10^6$ cells/plate). Cells were trypsinzed for 1-2 min, collected and centrifuged at 800 RPM for 8 minutes. Medium was aspirated completely and cells were resuspended in sterile saline and counted for viability with trypan blue. Subcutaneous tumors were established by anesthetizing mice with 5% isoflurane and injecting $5x10^5$ CT26 cells subcutaneously in 100 µl saline on the flank of the mouse at a viability of no <90%. Tumor-bearing mice were then treated with two or three doses of $5x10^8$ PFU of the indicated virus every other day once tumors reached a mean of ~250 mm^3, 10-20mm^3 for the study presented in Chapter 4, figure 20 . Mice were monitored and tumor volumes were measured and calculated using the following formula: $4/3 \times \pi \times L/2 \times (W/2)^2$, where 'L' and 'W' refer to tumor length and width, respectively. For CT26 lung metastases studies, $3x10^5$ CT26 were injected intravenously in 200 µl of saline. At 12 days after tumor

injection, mice were treated with three doses of $5x10^8$ PFU of the indicated virus every other day.

Analysis of vascular shutdown utilizing fluorescent microspheres

To assess vascular shutdown in the tumour, 24 hours after virus treatment mice were injected with 100 µL of 50:50 PBS : 100nm orange fluorescent microspheres(Molecular Probes) i.v. 5 minutes later mice were sacrificed by cervical dislocation, tumours were removed, cross sectioned, frozen in OCT freezing medium and stored at -80°C. Tumours were then sectioned at 10 µm on a cryostat (Leica) and immediately scanned for fluorescence (excitation = 533nm (green laser), emission = 554 (detected with 555 BP 20 filter)) on a Typhoon scanner (GE).

Immunohistochemistry

Tumours were fixed in 10% formalin for a minimum of 72 hours to a maximum of 1 week for immunohistochemical analysis of VSV, fibrinogen (Dako), CD3. Following fixation tissues were processed and embedded in paraffin. For staining, tissues were de-paraffinized in xylene and rehydrated, followed by a methanol/H_2O_2 blocking step to block endogenous peroxidase. For staining with VSV, CD3 and antigen retrieval was carried out by heating tissues in pH 6.0 citrate buffer. For fibrinogen staining, antigen retrieval was achieved by proteinase K treatment of the tissue. Tissues were then blocked with 5% normal

goat serum and probed with the required antibody in Ultra Ab Diluent (Fisher Scientific) at the required dilution (VSV 1:2500, fibrinogen 1:400, CD3 1:50) for 1 hour at RT. Tissues were then washed in PBS and probed with secondary anti-Rabbit Envision detection (DAKO). Tissues were washed and developed in AEC buffer, counterstained with hematoxylin and mounted in 15% gelatin mounting medium.

For detection of VSV and active caspase-3, frozen sections were fixed in 100% acetone, endogenous peroxidase was blocked in 1% methanol/H^2O and then blocked with 5% normal goat serum. Tissues were then probed with VSV (1:2500) or active caspase-3 (1:100) for 1 hour or 2 hours respectively. Tissues were washed and probed with anti-rabbit Envision detection (DAKO), washed and developed in AEC. Tissues were then counterstained with hematoxylin and mounted in 15% gelatin mounting medium.

Viral titers from tissues

Tumours for titering were removed from the animals and immediately snap frozen in 1 mL of sterile PBS on dry ice. The tissue was later thawed, weighed and homogenized for 10 seconds. The tissue was centrifuged for 12 minutes at 1000 RPM at 4°C and the supernatant was transferred to a fresh microfuge tube. The tissue was then vortexed for 30 seconds and again centrifuged at 2000 RPM for 5 minutes. The viral titer in the tumour was determined by standard plaque

assay. Tissue weights and volumes following homogenization were recorded and used to calculate the quantity of virus per gram of tumour.

Analysis of immune responses

At the indicated time-points, blood was collected from the mice and processed by ACK red blood cell lysis (0.15 M NH4Cl, 10 mM KHCO3, 0.1 M Na2EDTA, pH 7.2–7.4). To analyze the tumor- and viral-specific immune responses, peripheral blood mononuclear cells were re-stimulated with peptides ex vivo from VSV-N (N-MPYLIDFGL-C)[230] or CT-26 AH1 (N-SPSYVYHQF-C)[231] (Peprotech) for 6 h at 37°C. At 1.5 h into the stimulation, brefeldin A (BD Biosciences) was added to the cultures. The peripheral blood mononuclear cells were then stained with anti-CD3, -CD8, -CD4 and -IFN-g. All samples were analyzed on a FACSCanto (BD Biosciences, Mississauga, ON, Canada). FlowJo (Tree Star, Ashland, OR) software was used to analyze all FACS data.

IVIS imaging

Animals used for IVIS imaging were treated with firefly luciferase expressing VSV, ΔM51 VSV/SIIN-Luciferase. Animals were imaged daily using IVIS (Caliper Life Sciences) with Living Image 3.2 software (Caliper Life Sciences). For imaging, mice were anesthetized with 4% isoflurane in 1% oxygen and maintained at 2.5% isoflurane until imaging. Mice were injected with 3 mg of

luciferin i.p. and imaged 20 min later with an exposure time of 5 seconds. Data was analyzed using Living Image 3.2 software (Caliper Life Sciences)

Statistical Analyses

All data were analyzed using the GraphPad Prism 5.0 and R Statistics Package. In experiments containing fewer than three groups, a Student's t-test was performed. When more than three groups were compared, a one-way analysis of variance was performed with Bonferonni post-hoc test comparing all groups to the control group. For analysis of tumour growth, a two-way anova was used to assess differences in tumour growth. Normality was assessed in R using Pearson chi-square test. For data not falling under normal distribution either Mann-Whitney T test or Kruskal-Wallis rank sum tests were performed in lieu of Student's T test and one-way ANOVA, respectively. For survival curves, a log-rank test was performed to test for significant differences and a linear regression was performed to assess for correlation between survival times and immune responses. In all experiments, a Grubbs' test was performed to identify outliers and these data points were excluded from the analyses. Power calculations and sample size analyses were performed by Dr. Jemila Hamid (Department of Clinical Epidemiology & Biostatistics). Online power and sample size calculators were also used for some analyses (DSS Research, http://www.dssresearch.com).

~ Chapter 3 ~

Modifying oncolytic VSV through the addition of cell-autonomous transgenes

1.0 Introduction

1.1 Immunogenic cell death

How a cell dies can have profound effects on the resulting immune response. Cells are dying constantly and it is to our benefit for this death to be immunologically "silent" in order to avoid unwanted immune responses directed towards self antigens, leading to autoimmunity. Therefore, we have evolved highly conserved mechanisms to efficiently recognize and clear apoptotic cells quickly[232-234]. When cells die by other means, including necrosis, or if there are too many apoptotic cells that they cannot be cleared efficiently, the immune system can become activated due to the release of DAMPs including HMGB-1 and ATP[232,235,236].

Apoptosis

Apoptosis is a well defined process where cells die in a controlled manner. Cells undergoing apoptosis undergo cell shrinkage, chromatin condensation, nuclear fragmentation and active membrane blebbing, where membrane bound apoptotic bodies are released from the cell[237]. Activation of a family of proteases known as the caspases is also seen in apoptotic cells culminating in the activation of the effector molecule caspase-3, which is involved in the cleavage of numerous substrates, including PARP, mediating the apoptotic program[238-240]. Caspase activation is not completely unique to apoptosis as it has been observed in cells undergoing necrotic cell death[235]. Apoptotic cells were originally thought

to induce immunological tolerance as a method for cells to die without activating the immune system[235,241-244]. This is due to the production of anti-inflammatory cytokines, such as TGFβ, IL-10, and down regulation of IL-12 following the phagocytosis of apoptotic cells[245-247]. More recently the anti-inflammatory properties of apoptotic cells have been challenged and depending on the context, apoptotic cell death can lead to inflammation, activation of the immune system and cross-presentation of antigen to CTLs[48,248,249].

Necrosis / Secondary necrosis

During necrotic cell death the contents of the cell are released in an uncontrolled fashion leading to the presence of cellular components including HMGB-1, uric acid and ATP that induce the production of inflammatory cytokines[236,250-253]. This occurs through the ligation of TLRs and other receptors on phagocytes and generates a very stimulatory environment for the activation of the immune system[251,254,255]. Necrosis occurs when a cell dies suddenly or is severely stressed by toxins or hypoxia[235,236]. Unlike primary necrosis, secondary necrosis occurs when an apoptotic cell is not cleared efficiently and subsequently becomes necrotic[235,256]. It is difficult to detect apoptotic cells *in vivo* because there are highly conserved, efficient mechanisms for clearance by phagocytes through the recognition of phosphatidylserine (PS). However, if this machinery is overwhelmed by a large bolus of cell death, the apoptotic cells will not be cleared,

leading to secondary necrosis[235]. As with primary necrosis the same DAMPs can be released, leading to an inflammatory environment .

1.2 Fusogenic oncolytic viruses

Oncolytic viruses engineered to express fusogenic proteins, including VSV, adenovirus and paramyxovirus, leading to syncytia formation in infected cells have show improved efficacy over their parental non-fusogenic viruses [257-261]. Naturally fusogenic versions of oncolytic HSV are also able to better control tumour growth following treatment[262,263].The formation of syncytia in tumours has been associated with induction of necrotic cell death, increased phagocytosis and better priming of immature dendritic cells compared to similar non-fusogenic treatments[264].

To take advantage of the benefits of syncytia formation, we have created a novel oncolytic VSV vector expressing p14 FAST from a reptilian reovirus[225]. FAST proteins are a family of reoviral proteins involved in cell-cell fusion[265-268]. The FAST family of proteins are non-structural fusogenic proteins that are not incorporated into the virion, but play an important role in viral spread[265]. We have also demonstrated that p14 FAST is a bona fide virulence factor responsible for improved viral dissemination[225] (Appendix 1).

1.3 Apoptosis in VSV infected cells

Cells undergo apoptosis when exposed to a variety of stimuli, including viruses, through intracellular signals (intrinsic pathways) and/or ligation of death receptors on the surface of the cell (extrinsic pathways)[256]. VSV infection leads to the induction of both of these pathways early on in viral replication[269,270]. The apoptotic pathways that are activated during VSV infection depend on the matrix protein and whether it is WT or mutated at methionine 51, the genetic mark associated with the oncolytic version of VSV[271-273].

The differences in apoptosis induction between WT VSV and ΔM51 VSV are partially due to their ability to shut down host gene expression[273]. Cells infected with WT VSV become apoptotic through induction of Bak through the loss of Mcl-1 and BCL-X_L[274]. Pearce *et al.* (2009) showed that due to the short half-life of Mcl-1, it cannot be replenished during WT VSV infection due to the lack of host gene expression, allowing activation of Bak, which is inhibited by only Mcl-1 and BCL-X_L[274]. The loss of Mcl-1, however, was not able to completely explain the induction of apoptosis. Contrary to previous reports, it was shown that Caspase-8 cleavage of tBid was involved in cleavage of Bcl-X_L leading to full activation of Bak[273,274]. ER stress due to VSV-G overloading the ER has also been shown to have a role in apoptosis induction leading to caspase-12 and subsequently caspase-9 and caspase-3 activation[273,275]

Oncolytic versions of VSV do not block host gene expression owing to a mutation in the matrix protein preventing interaction with Nup98[223]. With host

gene expression occurring normally, Mcl-1 depletion is not observed therefore Bak is not activated in ΔM51 VSV infected cells[274]. Instead cells infected with ΔM51 VSV undergo apoptosis through the extrinsic pathway, albeit without Fas/ FasL ligation[276]. This process requires both PKR and Fas leading to the activation of caspase-8 and subsequently caspase-3[276].

1.4 Anti-apoptotic poxviral proteins

Apoptosis is an important process in the fight against viral infections[277]. Because of this, viruses have evolved numerous ways to modulate the apoptotic response to serve the virus' best interest[277]. Poxviruses encode numerous proteins that are able to inhibit apoptosis early in infection, including Vaccinia virus F1L and fowlpox virus FPV039[278]. While both of these proteins impair apoptosis induction, they do so through similar but slightly different mechanisms[279,280].

The F1L protein of vaccinia virus is anchored at the mitochondria and acts to inhibit apoptosis through interaction with Bak[281,282]. The function of F1L is similar to that of Bcl-2 family proteins including Mcl-1[280]. Therefore, F1L can act as an Mcl-1 mimic in the absence of Mcl-1 ensuring that Bak is not activated during vaccinia virus infection[280]. FPV039 binds to and inhibits Bak, but it can also inactivate Bax and inhibit other BH-3 only proteins that are involved in Bax activation[279,283].

1.5 Cell death in cancer therapies

How a cell dies will during cancer therapy plays an important role in the subsequent immunological outcome. The translocation of calreticulin to the cell surface and the release of ATP and HMGB-1 are required for full activation of the immune system following treatment with conventional cancer therapies, and are required for the success of the therapy[250-252,284,285]. The presence of intact TLR and inflammasome signaling are required for these molecules to modulate the induction of anti-tumour immunity by dying tumour cells[251,255]. More recently it has been demonstrated that oncolytic measles virus and coxsackievirus B3 induce an immunogenic form of cell death characterized by HMGB1 and ATP release, and calreticulin surface expression[286,287].

Therefore we **hypothesized that shifting cell death of infected cells away from apoptosis would lead to more immunogenic cell death and improved anti-tumour immune responses**. To move cells away from the typical apoptotic cell death seen in VSV infection we have added p14 FAST and anti-apoptotic proteins F1L and FPV039 to VSV. This chapter will describe the characterization of viruses expressing these proteins and how the viruses performed in a murine colon cancer model, CT26, focussing on the immune responses induced following treatment.

2.0 Results

2.1 Characterization and assessment of the oncolytic potential of ΔM51 VSV/FAST

p14 FAST is expressed from ΔM51 VSV/FAST leading to the formation of large syncytia *in vitro*.

VSV is not a naturally fusogenic virus and spreads through budding of new viral progeny from the cell membrane[288-290]. Therefore, to take advantage of the potential immunological advantages of syncytia formation[264,291,292] we added p14 FAST to VSV, creating a fusogenic VSV vector (VSV/FAST)[225]. Western blot analysis of VSV/FAST infected cells shows that the added p14 FAST transgene is expressed from virally infected cells (Figure 4A Lane 3 and 4). Since p14 FAST is a transmembrane protein [266] and it has been shown that other members of FAST family of proteins traffic to the cell membrane[293] it is possible that p14 FAST could be incorporated into the VSV virion. To assess the presence of FAST in the VSV virion, purified virus was boiled and analyzed by western blot. In figure 4A, lanes 7 and 8, p14 FAST was detected in the purified virus, indicating it is incorporated into the virion. However, due to the small size of p14 FAST compared to that of the VSV glycoprotein, it is unlikely that its presence in the envelope will have any impact on infection or tropism of the virus. The expression of p14 FAST also leads to extensive syncytia formation in VSV/FAST infected monolayers (Figure 4B). The formation of syncytia during VSV infection did not affect viral growth. In a one step growth curve, VSV/FAST has equivalent growth kinetics when compared to the parental VSV/GFP virus infection (Figure 5).

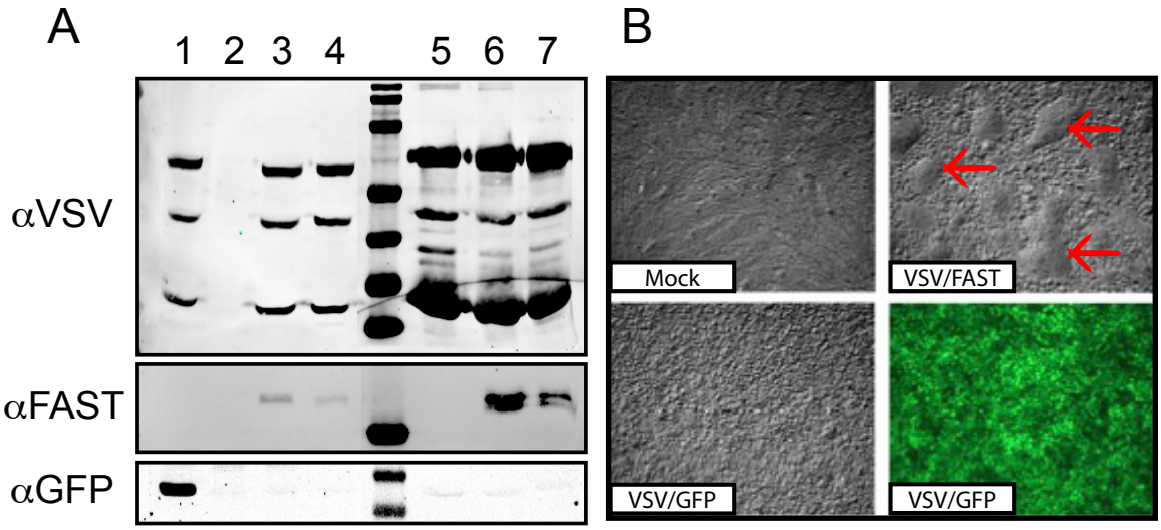


Figure 4 - Characterization of VSV/FAST. (A) Western blot analysis of infected cell lysates and sucrose banded virus reveals that FAST is expressed in VSV/FAST- infected cells and is present in the viral particle. Vero cells were infected with virus overnight, and cellular lysates were run (lanes 1 to 4) or virus was banded on a sucrose gradient and 10^8 PFU were run per lane (lanes 5 to 7). Blots were probed for VSV proteins (upper), FAST protein (middle), or GFP (bottom). Lanes: 1, VSV/GFP; 2, mock; 3, VSV/FAST; 4, ΔM51-VSV/FAST; 5, VSV/GFP; 6, VSV/FAST; 7, ΔM51-VSV/FAST. (B) Confluent Vero cells were infected with the indicated viruses, and photomicrographs taken 24 h later show the large multi-nucleated syncytia induced by the FAST viruses (arrows), which are absent from cells infected with VSV/GFP. Magnification, x8.

ΔM51 VSV/FAST has an increased spread in subcutaneous CT26 tumours.

To determine if the addition of p14 FAST to VSV is able to improve the efficacy of VSV as an oncolytic virus we began by assessing ΔM51 VSV/FAST in a subcutaneous CT26 tumor model. Intravenous treatment of Balb/c mice bearing subcutaneous CT26 with ΔM51 VSV/GFP is known to lead to an infection of the outer rim of the tumor and also induces clotting in the tumour vasculature[227,228].

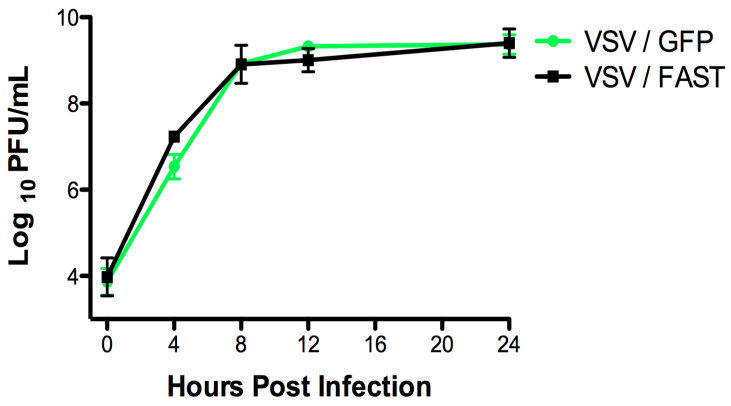


Figure 5 - Replication of VSV is not impaired by the expression of p14 FAST. Vero cells were infected in triplicate with either VSV/GFP or VSV/FAST at a MOI of 5 for 45 min in minimal medium, after which the monolayers were washed three times. Samples were collected at the indicated time points and virus titers were determined by standard plaque assay on Vero cells. Data is presented as mean ± s.e.m.

Therefore we set out to determine if the expression of p14 FAST from VSV modified the vascular shutdown and localization of VSV in the tumor following intravenous delivery of VSV. Twenty-four hours after treatment with ΔM51 VSV/FAST, vascular shutdown is still observed in the tumor (Figure 6A). However when compared to ΔM51 VSV/GFP treated tumors, it is not as complete and there is more perfusion observed towards the center of the tumour. We also observed that compared to ΔM51 VSV/GFP, ΔM51 VSV/FAST was able to infect more areas away from the tumour rim, likely due to its ability to form syncytia, which aided ΔM51 VSV/FAST's spread through the tumour (Figure 6B). The increased spread that is observed does not lead to increased titers in the tumour. Seventy-two hours post-treatment there is over a half log less virus present in ΔM51 VSV/FAST treated tumours (Figure 7).

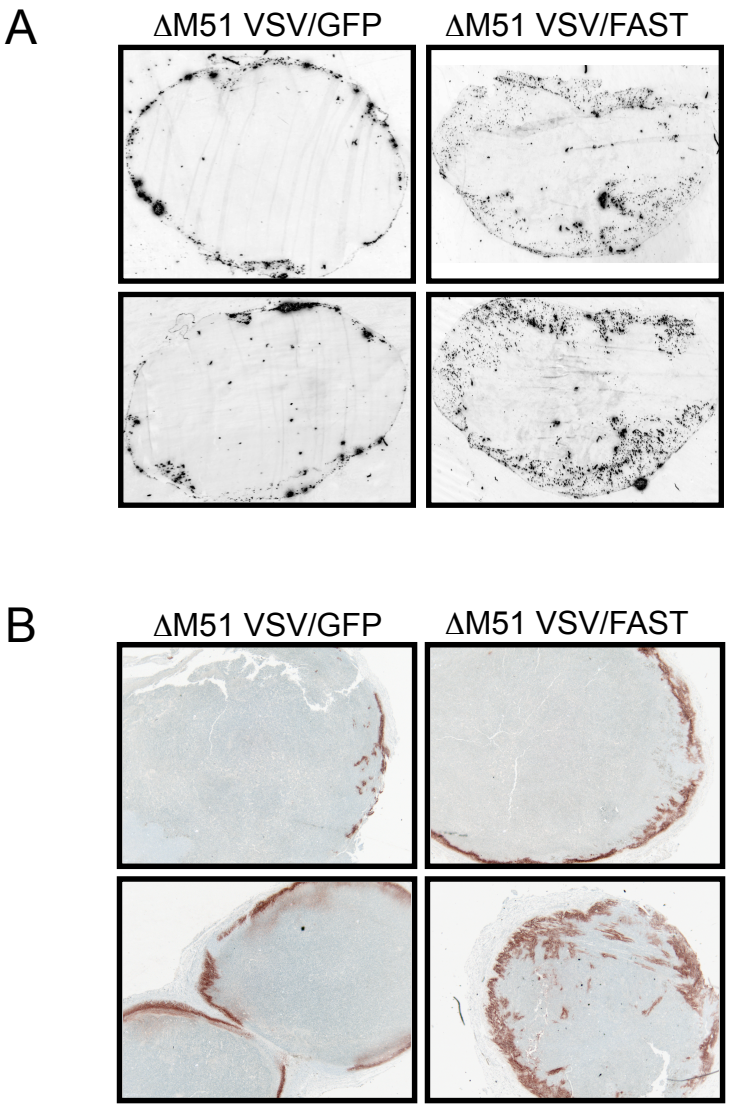


Figure 6 - Vascular perfusion and viral spread in ΔM51 VSV/FAST treated tumours. Balb/c mice bearing ~250 mm^3 tumours were treated with one dose of $5x10^8$ PFU of the indicated virus intravenously. 72 hours after treatment mice were injected with fluorescent microspheres and 5 min later euthanized and the tumours were removed and frozen in OCT freezing media and stored at -80^{O} C. 10 uM frozen sections were cut every 50 uM from the outer edge of the frozen tumours using a cryostat. (A) Sections were scanned for the presence of microspheres indicating the level of perfusion in the tumours using a Typhoon Scanner (GE) (B) Sections were stained for VSV by immunohistochemistry using a pan-VSV polyclonal antibody.

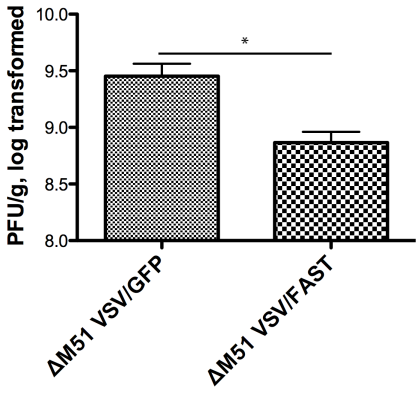


Figure 7 - Titers in ΔM51 VSV/FAST treated tumours is lower than ΔM51 VSV/GFP treated tumours. Balb/c mice bearing CT26 tumors were treated with $5x10^8$ PFU of ΔM51 VSV/GFP (n=2) or ΔM51 VSV/FAST (n=3) intravenously. Tumours were removed 72 hours after treatment, homogenized and analyzed by standard VSV plaque assay. Data presented are mean ± s.e.m.; * *P*=0.0138

ΔM51 VSV/FAST better controls growth of CT26 in CD-1 Nude mice.

To determine if the increased viral spread observed in ΔM51 VSV/FAST treated tumours leads to improved control of tumour growth we first utilized an immunocompromised mouse model. CT26 was engrafted into CD-1 Nude mice, which lack both T and B cells and therefore cannot mount an adaptive immune response. This allows us to address the question of whether increased viral spread in ΔM51 VSV/FAST treated tumours leads to a better outcome than ΔM51 VSV/GFP treated tumours. Since there is no adaptive immune system in these mice the effects that we observed were likely due to the oncolytic viral infection and subsequent destruction of the tumour, however innate responses may have also been involved but were not assessed. As expected, ΔM51 VSV/FAST was shown to better control the CT26 tumours in CD-1 Nude mice stabilizing the tumors for almost two weeks compared to ΔM51 VSV/GFP, which only controlled

tumors for one week (Figure 8B). While ΔM51 VSV/FAST was an improvement of ΔM51 VSV/GFP early on in the study, all tumours eventually grew out and there was no overall difference in the survival of the mice (Figure 8C).

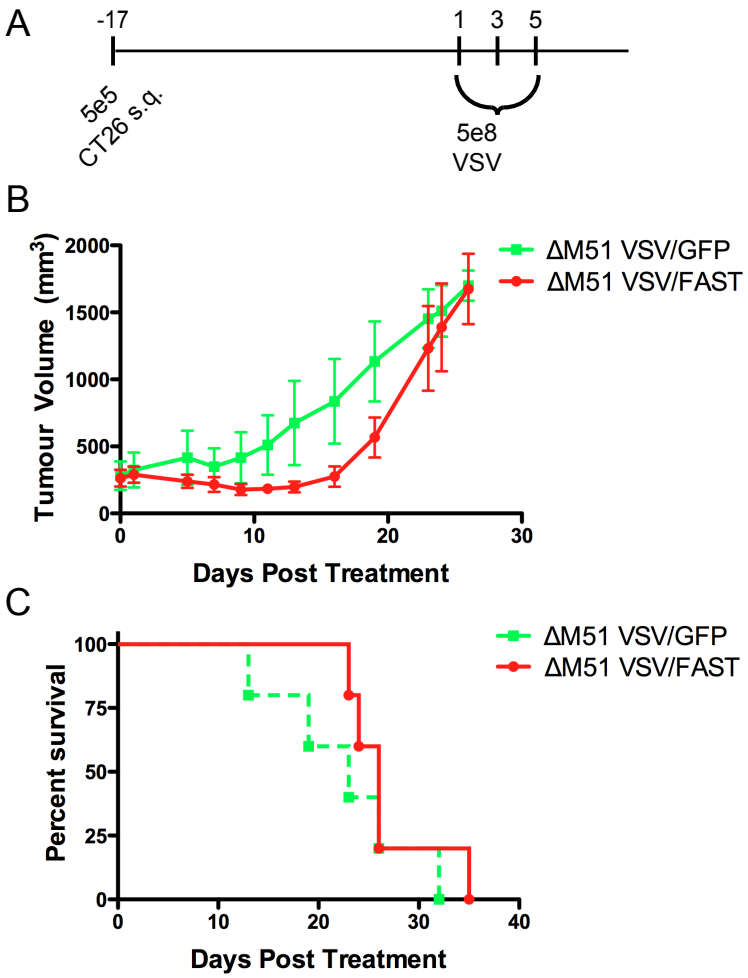


Figure 8 - Δ51 VSV/FAST treatment of CT26 in CD-1 nude mice. CD-1 nude mice were engrafted with CT26 and when the tumours reached ~250 mm^3 they were treated with $5x10^8$ PFU of Δ51 VSV/GFP (n=5) or Δ51 VSV/FAST (n=5)every other day for a total of 3 doses of virus. (A) Experimental outline. (B) Tumour volumes were measured and calculated as an ellipse (where volume = 4/3 x π x L/2 x $((W/2)^2)$), shown as mean ± s.e.m. (C) Survival was monitored and depicted above.

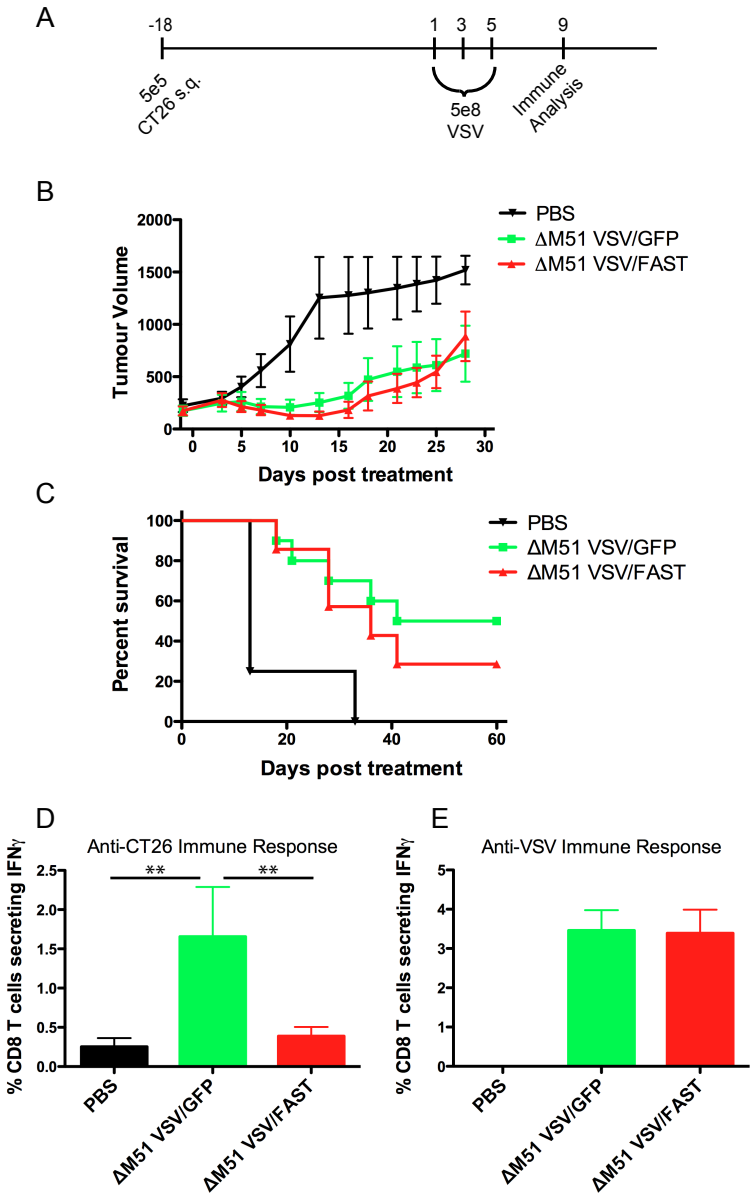


Figure 9 - ΔM51 VSV/FAST treatment of subcutaneous CT26 tumours. Balb/c Mice bearing established subcutaneous CT26 tumours were treated with PBS (n=4), ΔM51 VSV/GFP (n=10) or ΔM51 VSV/FAST (n=10). Once tumours reached ~ 250 mm3, mice were treated with two doses of $5x10^8$ PFU of the indicated virus intravenously 48 hours apart. (A) Experimental outline (B) Tumour volumes were measured and calculated as an ellipse (where volume = 4/3 x π x L/2 x (W/2)^2), shown as mean ± s.e.m. (C) Survival. 10 days after the start of oncolytic virus treatment PBMC were collected to assess the anti-tumour and anti-viral immune responses. PBMCs were stimulated with CT26 (AH1) and VSV peptides and analyzed for tumour or viral specific $CD8^+$ T cells by flow cytometry using ICCS for IFNγ. Anti-tumour and anti-viral immune responses are presented in (D) and (E) respectively. Data are mean ± s.e.m; **P<0.01.

p14 FAST expression from VSV did not improve oncolytic efficacy in immunocompetent Balb/c mice.

With the knowledge that expression of p14 FAST from VSV led to better spread of the virus, decreased vascular shutdown and better control of CT26 in Nude mice, we next moved into testing ΔM51 VSV/FAST in immunocompetent mice. For these studies we engrafted Balb/c mice with subcutaneous CT26 tumours. Tumours were treated with 3 doses of ΔM51 VSV/FAST or the parental ΔM51 VSV/GFP once they reached a mean of 250 mm^3 as outlined in figure 9A. Treatment with ΔM51 VSV/FAST was not an improvement over ΔM51 VSV/GFP considering the final survival and tumour growth outcomes (Figure 9A and B). As with the Nude mouse study in Figure 8, ΔM51 VSV/FAST appeared to initially control the growth of the tumours slightly better, however this did not lead to an improved outcome. As well, when the anti-tumour and anti-viral $CD8^+$ T cell responses were measured it was found that while there was no difference in the anti-viral response, mice treated with ΔM51 VSV/FAST had a significantly decreased anti-tumour response (figure 9D & E). In fact, there was no difference between the anti-tumour immune response in mice that were untreated compared to mice treated with ΔM51 VSV/FAST. Since there was an early difference and the overall survival outcome of both ΔM51 VSV/GFP and ΔM51 VSV/FAST were similar it is possible that there wasn't enough sufficient sample size in the experiment to decipher any small differences. Therefore, the experiment was repeated and the combined survival from the three independent experiments is

presented in figure 10. In the end, the overall survival observed in the three experiments performed was similar to what had been seen in figure 9. Thus, the expression of FAST does not improve the efficacy of VSV in the treatment of subcutaneous CT26.

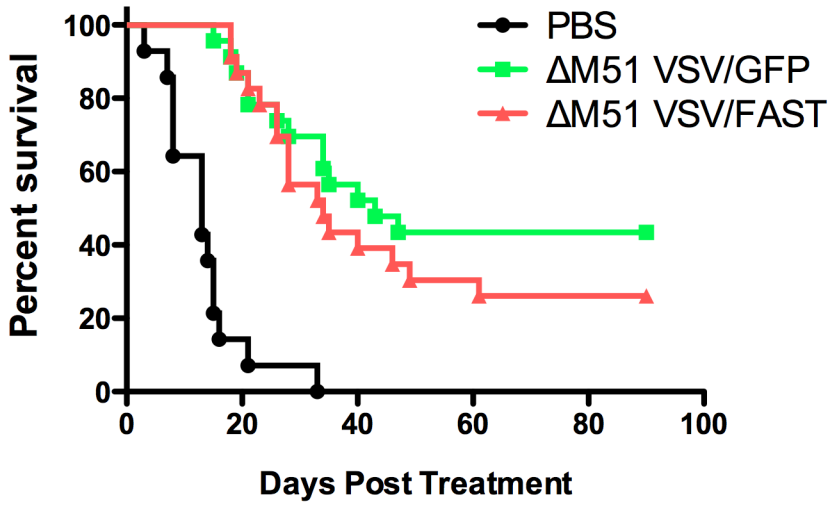


Figure 10 - Expression of FAST from VSV does not improve efficacy. Survival curve for mice treated with PBS (N=14), ΔM51 VSV/GFP (n=23), ΔM51 VSV/FAST (n=23). Mice bearing ~250 mm3 tumours were treated with 2 doses of $5x10^8$ PFU of the indicated virus 48 hours apart. The data presented above is the combined survival from three independent experiments.

ΔM51 VSV/FAST was also unable to outperform ΔM51 VSV/GFP in a CT26 lung metastases model

Although there was no difference between ΔM51 VSV/FAST and ΔM51 VSV/GFP in the subcutaneous CT26 model, this outcome may have been due to an inability to fully overcome the effects of the vasculature shutdown following treatment. Since the vasculature shutdown tends to be less pronounced in

smaller tumours, we decided to test ΔM51 VSV/FAST in a lung metastases model of CT26. Smaller tumours in the lung metastases model also allow ΔM51 VSV/FAST to spread through more tumour nodules, which can be attributed to their size and lack of vasculature shutdown.

Similar to the subcutaneous model in figures 7 and 8, ΔM51 VSV/FAST was not an improvement over ΔM51 VSV/GFP in the lung metastases model (Figure 11A). There was also reduced anti-tumour and anti-viral immune responses (Figure 11C and D), similar to the results observed when treating subcutaneous CT26 tumours.

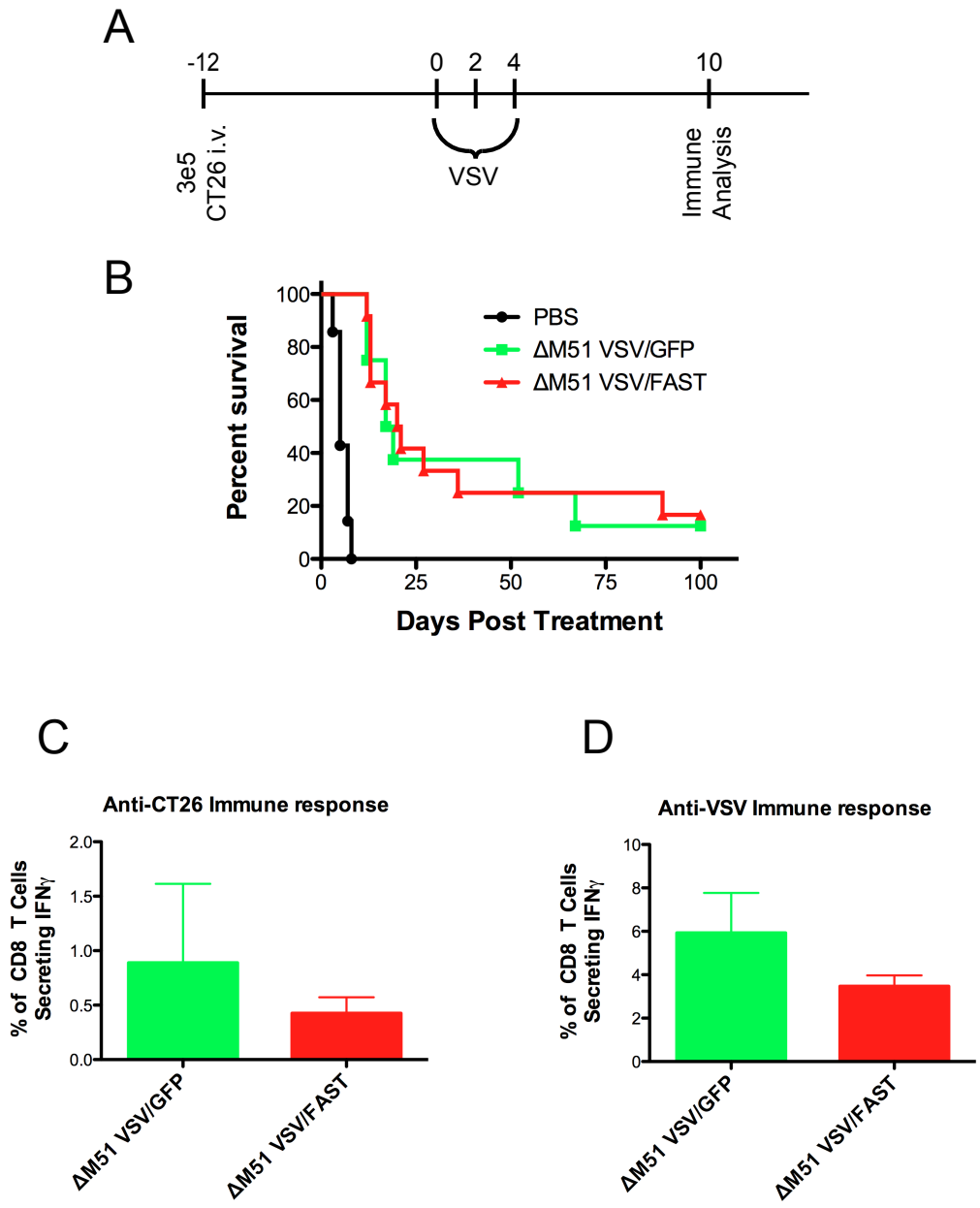


Figure 11 - FAST expression does not improve on VSV oncolytic efficacy in a CT26 lung metastases model. Balb/c mice bearing 12 day old CT26 lung metastases were treated with 3 doses of $5x10^8$ PFU i.v. every other day of either PBS (n = 7), ΔM51 VSV/GFP (n = 8) or ΔM51 VSV/FAST (n = 12). (A) Experimental outline. (B) Mice were monitored for euthanized upon signs of respiratory distress. 10 days after the start of oncolytic virus treatment PBMC were collected to assess the anti-tumour and anti-viral immune responses. PBMCs were stimulated with the CT26 (AH1) and VSV peptides and analyzed for tumour or viral specific $CD8^+$ T cells by flow cytometry using ICCS for IFNγ. Anti-tumour and anti-viral immune responses are presented in (C) and (D) respectively. Data are mean ± s.e.m combined from 2 independent experiments.

2.2 Characterization and assessment of the oncolytic potential of anti-apoptotic VSV vectors ΔM51 VSV/Flag-F1L and ΔM51 VSV/GFP-FPV039

In ΔM51 VSV/FAST treated tumours we were relying on the inefficient clearance of syncytia formed during infection to lead to more immunogenic forms of cell death. However, we do not know whether this was actually what happened or if the innate response was indeed able to deal with the large syncytia formed, and ultimately the expression of p14 FAST from oncolytic VSV did not improve the therapeutic efficacy. Therefore we set out to construct two new viruses expressing anti-apoptotic proteins to directly modify the cell death occurring in the infected cells.

Expression of anti-apoptotic poxviral genes from VSV does not impair viral replication *in vitro*

To construct an anti-apoptotic oncolytic VSV vector, FLAG tagged F1L (FLAG-F1L) and FPV039 GFP fusion protein (GFP-FPV039) were cloned into VSV as outlined in Figure 1. Western blot analysis of cells infected with ΔM51 VSV/Flag-F1L and ΔM51 VSV/GFP-FPV039 shows that the inserted genes were expressed at their expected molecular weights (Figure 12A). Since the expression of these proteins led to changes in the kinetics of cell death, there was a distinct possibility that viral replication would be impacted. Therefore, we performed a one-step growth curve to address this concern. Figure 12B shows that there was in fact no impact on replication by either Flag-F1L or GFP-FPV039 expression.

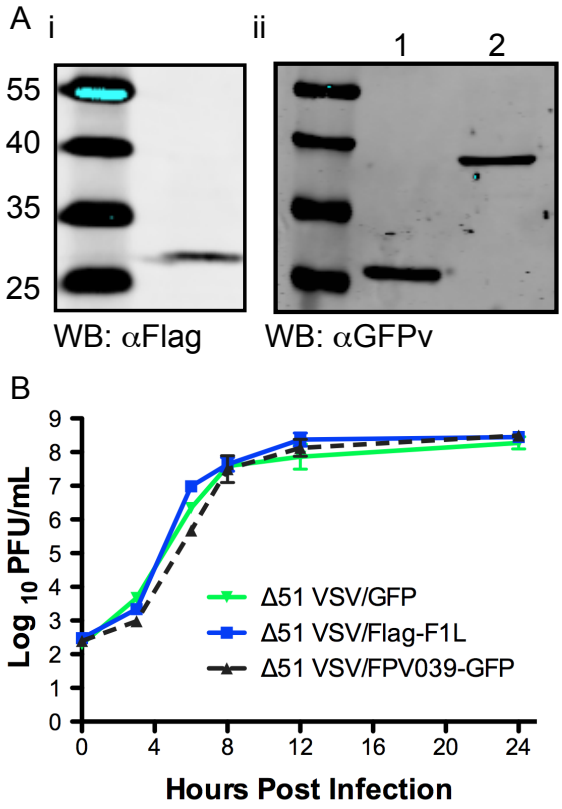


Figure 12 - Characterization of anti-apoptotic VSV. (A) Western blot analysis of infected cell lysates shows that Flag-F1L and GFP-FPV039 were expressed from ΔM51 VSV. (i) Vero cells were infected with ΔM51 VSV/Flag-F1L overnight and 10 µg of whole cell lysates were run and probed for Flag expression. (ii) Vero cells were infected with ΔM51 VSV/GFP (Lane 1) and ΔM51 VSV/GFP-FPV039 (Lane 2) and whole cell lysates were run and probed for GFP expression. (B) The expression of poxviral anti-apoptotic proteins did not impact VSV replication. Vero cells were infected at an MOI of 5, supernatant samples were assayed for VSV at the indicated time points by standard plaque assay. Data presented at mean ± s.e.m.

Expression of Flag-F1L and GFP-FPV039 impairs apoptosis in VSV infected cells.

We next set out to determine if these poxviral proteins were functional and able to modulate apoptosis in VSV infected cells. VSV is known to induce apoptosis through both the intrinsic and extrinsic pathways ultimately leading to caspase-3 activation[274,294]. Active caspase-3 subsequently cleaves poly ADP ribose polymerase (PARP), one of its numerous substrates, which is a hallmark of apoptosis induction[238,295]. Therefore we assessed the activation of caspase-3 and cleavage of PARP in CT26 infected with ΔM51 VSV/Flag-F1L and ΔM51 VSV/ GFP-FPV039. Both ΔM51 VSV/Flag-F1L and ΔM51 VSV/GFP-FPV039 were able to significantly impair activation of caspase-3 compared to ΔM51 VSV/GFP (Figure 13A). As well, ΔM51 VSV/Flag-F1L had a greater impact on caspase-3 activation at later time points compared to ΔM51 VSV/GFP-FPV039 (Figure 13A). This trend was also observed when assessing PARP cleavage. ΔM51 VSV/GFP induced a large amount of cleaved PARP compared to both anti-apoptotic viruses (Figure 13B). In this assay the difference between ΔM51 VSV/Flag-F1L and ΔM51 VSV/GFP-FPV039 was not observed as in the caspase-3 assay (Figure 13A).

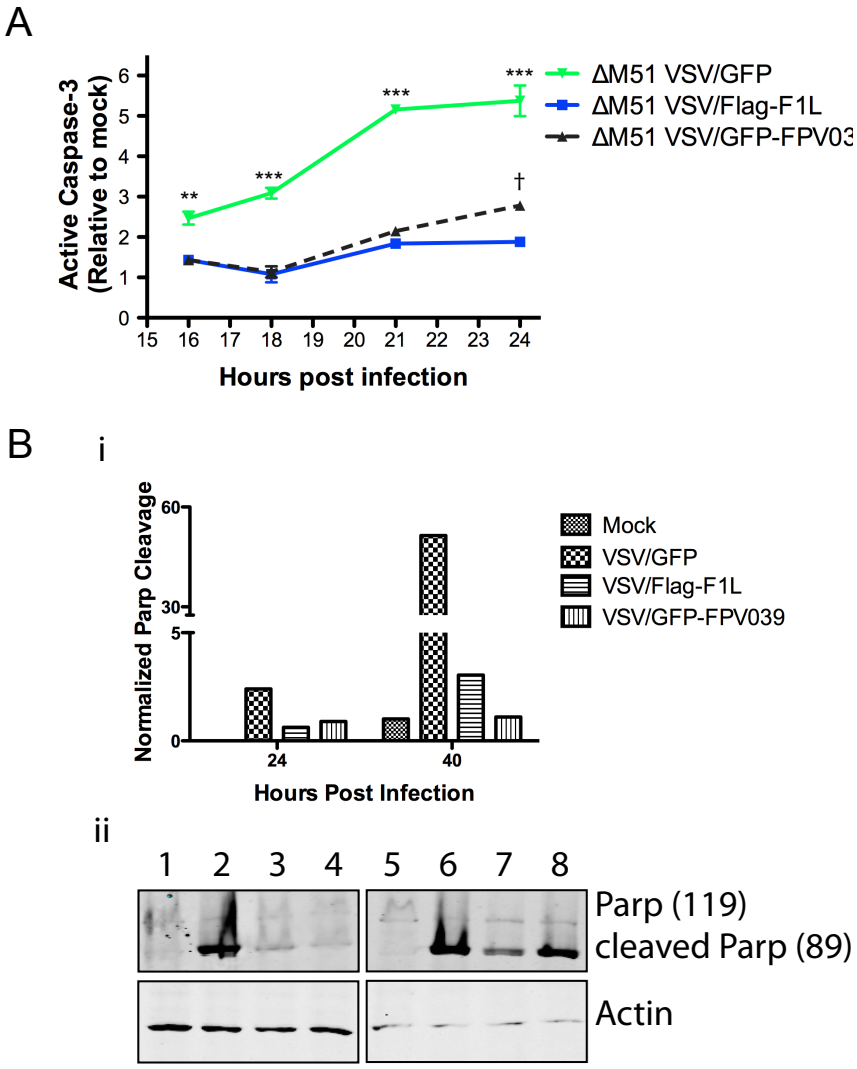


Figure 13 - Apoptosis induction is delayed in Δ51 VSV/Flag-F1L and Δ51 VSV/GFP-FPV039 infected cells. (A) CT26 cells were infected at an MOI of 5 and were assayed at the indicated time points for apoptosis induction using CaspGlo 3/7 assay kit (Promega). Data is presented as mean ± s.e.m.; ΔM51 VSV/GFP vs. ΔM51 VSV/Flag-F1L or ΔM51 VSV/GFP vs. ΔM51 VSV/GFP-FPV039 ** $P < 0.01$, *** $P < 0.001$; ΔM51 VSV/Flag-F1L vs. ΔM51 VSV/GFP-FPV039 † $P < 0.01$. (B) CT26 monolayers were infected with ΔM51 VSV/GFP, ΔM51 VSV/Flag-F1L or ΔM51 VSV/GFP-FPV039 at an MOI of 5 for either 24 or 40 hours. Cells were lysed at the indicated time points and analyzed by western blot for PARP cleavage. (i) Quantification of cleaved PARP is presented normalized to β-Actin. Data are presented as a mean. (ii) Image of the western blot used in the quantification in (i). Lane 1-4 are 24 hours post-infection; Lane 1 - Mock, Lane 2 - ΔM51 VSV/GFP, Lane 3 - ΔM51 VSV/Flag-F1L, Lane 4 - ΔM51 VSV/GFP-FPV039. Lanes 5-8 are 40 hours post-infection; Lane 5 - Mock, Lane 6 - ΔM51 VSV/GFP, Lane7 - ΔM51 VSV/Flag-F1L, Lane 8 - ΔM51 VSV/GFP-FPV039.

Expression of Flag-F1L and GFP-FPV039 also modifies cell death during VSV infection

With apoptosis impaired, we wanted to determine if cell death was delayed or modified by our anti-apoptotic viruses. Both ΔM51 VSV/Flag-F1L and ΔM51 VSV/GFP-FPV039 delayed cell death, however cells infected with these viruses did eventually die as indicated by PI uptake (Figure 16A). Since how cells die can impact on the resulting immune responses generated we utilized AnnexinV and 7-AAD to determine the fate of the infected cells. By using a combination of AnnexinV and 7-AAD positivity it can be determined whether cells are alive (AnnexinV- / 7-AAD-), undergoing necrosis (AnnexinV- / 7-AAD+), apoptosis (AnnexinV+ / 7-AAD-), or secondary necrosis (AnnexinV+ / 7-AAD+). AnnexinV is a peptide that recognizes phosphatidylserine, a marker of apoptosis. During early apoptotic processes phosphatidylserine is externalized to the outer membrane through both caspase dependent and independent processes [238,296-298]. The externalization of phosphatidylserine can be detected utilizing fluorescent labelled AnnexinV. If cells are allowed to continue dying they lose membrane integrity and become 7-AAD positive. Finally cells that only take up 7-AAD, and are unable to be stained with AnnexinV, are necrotic and have not undergone programmed apoptotic cell death.

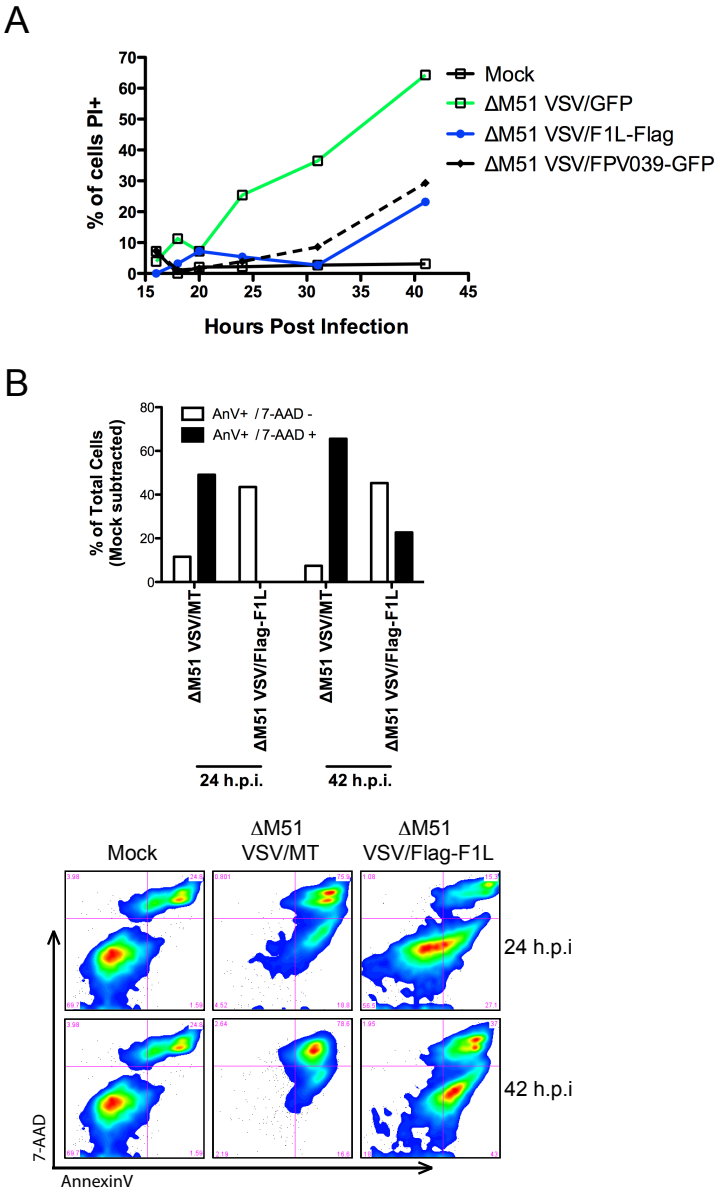


Figure 14 - Infection of CT26 *in vitro* with anti-apoptotic VSV modifies cell death. ΔM51 VSV/Flag-F1L and ΔM51 VSV/GFP-FPV039 infection of CT26 leads to delayed translocation of AnnexinV and cell death compared to parental ΔM51 VSV/MT and ΔM51 VSV/GFP. (A) CT26 cells were infected with the indicated viruses at an MOI of 5 and at the indicated time points the cells were harvested, stained with PI and counted on a hemacytometer. Data is presented as the percentage of cells that incorporated PI as in indication of cell death. (B) CT26 cells were infected with ΔM51 VSV/MT or ΔM51 VSV/Flag-F1L at an MOI of 5 for 24 or 42 hours and stained for AnnexinV and 7-AAD using BD Apoptosis detection Kit to determine the fate of cells following infection.

In figure 14 we assessed the cell death observed in both ΔM51 VSV/GFP and ΔM51 VSV/Flag-F1L infected cells. Similar to the PI uptake in figure 14A, CT26 cells infected with ΔM51 VSV/GFP were found to more quickly move towards late apoptosis. Cells infected with ΔM51 VSV/Flag-F1L were found to become AnV positive and some did take up 7-AAD at the later time point, however not to the level of ΔM51 VSV/MT infected cells (Figure 14B). The AnV/7-AAD assay was only completed with ΔM51 VSV/Flag-F1L due to issues combining the GFP present in ΔM51 VSV/GFP-FPV039 and PE labelled AnV. When these fluorochromes were used in combination it was difficult to compensate the flow cytometry to get reliable data. Therefore only VSV viruses that did not express GFP were utilized including ΔM51 VSV/MT, which does not contain any transgene. Taking the data presented in Figures 11 and 12 together, CT26 cells infected with the anti-apoptotic viruses ΔM51 VSV/Flag-F1L and ΔM51 VSV/GFP-FPV039 have an impaired activation of caspase-3 and therefore delayed cleavage of PARP. Also, while the cells do die if left long enough, death is significantly delayed compared to ΔM51 VSV/GFP or ΔM51 VSV/MT infected cells.

Expression of Flag-F1L and Flag-FPV039 does not modify VSV replication *in vivo*

With the knowledge that the anti-apoptotic transgenes were expressed and functional, we moved into murine models to continue to test these new

oncolytic viruses. Since the initial characterization was carried out in a minimal number of cell lines we wanted to assess replication in an animal model to ensure there were no differences in replication *in vivo*. Therefore we infected Balb/c mice intranasally with wild type VSV expressing either Flag-F1L or GFP-FPV039. Viral replication was assessed in the lungs of infected mice and it was found that expression of anti-apoptotic genes from VSV did not significantly impact viral replication (Figure 15).

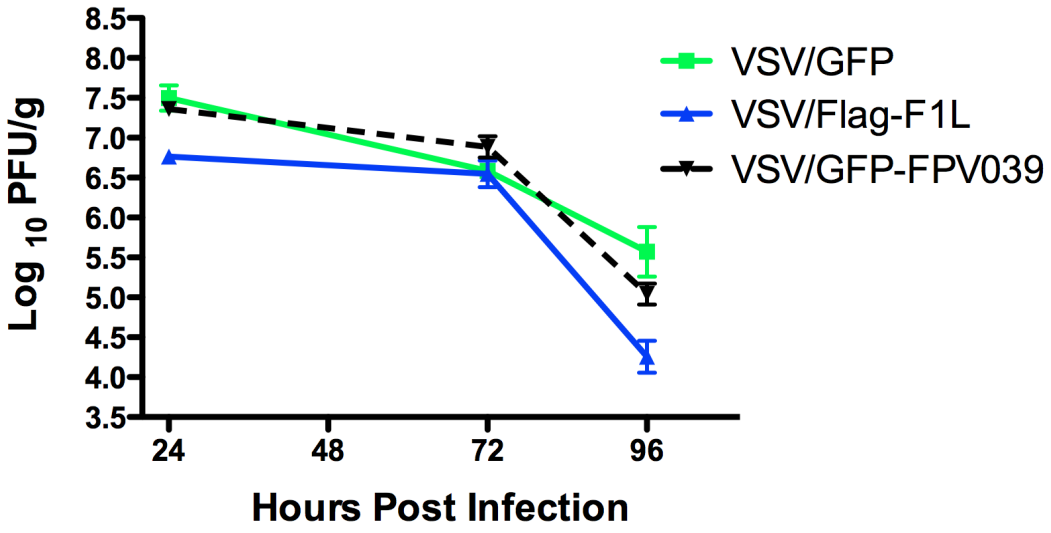


Figure 15 - Replication of anti-apoptotic VSV vectors is not impaired *in vivo*. Balb/c mice were infected i.n. with $5.76X10^8$ PFU in 30 µL to ensure delivery into the lungs of the animals. Lungs were removed at the indicated time points and snap frozen in liquid nitrogen. Lungs were then thawed, homogenized and the viral load was determined in the supernatant by serial dilution and standard plaque assay. Data are presented as mean ± s.e.m.

Impairing apoptosis in VSV infected cells does not improve the outcome following oncolytic therapy in subcutaneous CT26

Infecting CT26 with our anti-apoptotic viruses has been show to modify how cells die during infection *in vitro*. Therefore to determine if this has an impact

on oncolytic virus therapy, we tested these viruses in a subcutaneous CT26 tumour model. Subcutaneous tumours were implanted into Balb/c mice and were treated with either ΔM51 VSV/Flag-F1L, ΔM51 VSV/GFP-FPV039 or the parental control ΔM51 VSV/GFP (Figure 16A). Following treatment, both of the anti-apoptotic viruses had a similar impact on the tumours compated to ΔM51 VSV/GFP early in the therapy (Figure 16B). However, tumours in mice treated with either anti-apoptotic virus began to grow out earlier than those treated with ΔM51 VSV/GFP and ultimately there was no improvement in the efficacy of oncolytic VSV with the added expression of either Flag-F1L or GFP-FPV039 (Figure 16C). Even though there were no significant differences there was a trend towards a decreased efficacy in mice treated with either anti-apoptotic virus, but especially those treated with ΔM51 VSV/GFP-FPV039.

Immune responses were also measured ten days after the start of treatment to determine if modifying how infected cells die modulated the resultant immune response. It was found that mice treated with ΔM51 VSV/GFP-FPV039 had an anti-tumour response equivalent to that of mice treated with ΔM51 VSV/GFP. On the other hand mice treated with ΔM51 VSV/Flag-F1L had almost no detectable anti-tumour response (Figure 17A). These mice did mount an anti-viral immune response (Figure 17B), therefore there were likely no technical issues relating to the lack of anti-tumour response. There was also no significant correlation in these experiments when comparing immune response and overall survival.

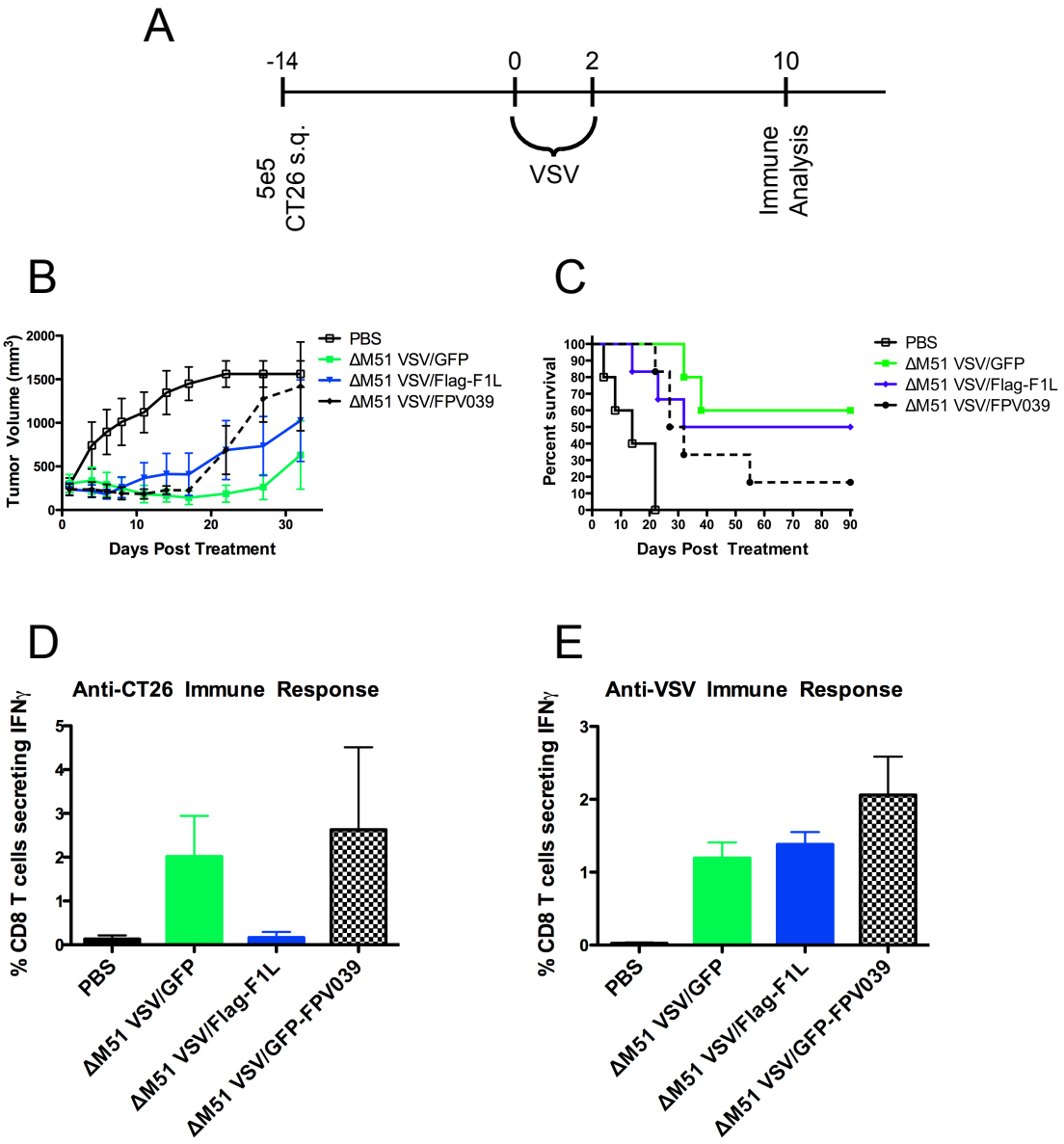


Figure 16 - ΔM51 VSV/Flag-F1L and ΔM51 VSV/GFP-FPV039 treatment of subcutaneous CT26 tumours. Mice bearing established CT26 tumours were treated with PBS (n=5), ΔM51 VSV/GFP (n=5), ΔM51 VSV/Flag-F1L (n=6) or ΔM51 VSV/GFP-FPV039 (n=10). Once tumours reached ~ 250 mm3, mice were treated with two doses of $5x10^8$ PFU of the indicated virus i.v. 48 hours apart. (A) Experimental outline (B) Tumour volumes were measured and calculated as an ellipse (where volume = 4/3 x Pi x L/2 x $((W/2)^2)$), shown as mean ± s.e.m. (C) Survival was monitored and depicted above. 10 days after the start of oncolytic virus treatment PBMC were collected to assess the anti-tumour and anti-viral immune responses. PBMCs were stimulated with the appropriate peptides and analyzed for tumour or viral specific $CD8^+$ T cells by FACS using ICCS for IFNγ. Anti-tumour and anti-viral immune responses are presented in (A) and (B) respectively. Data are mean ± s.e.m.

Expression of Flag-F1L or GFP-FPV039 gave no added benefit to VSV oncolytic treatment of CT26 lung metastases

Similar to testing of the ΔM51 VSV/FAST vector, we assessed both versions of anti-apoptotic vectors in a lung metastases model to determine if they were able to have a larger impact on numerous small tumours. In this model the viruses may be able to impact more tumour outside of the effects of vascular shutdown that is observed following VSV therapies due to the size of tumour nodules at the start of treatment.

Twelve day old CT26 lung metastases were treated with parental ΔM51 VSV/GFP, ΔM51 VSV/Flag-F1L or ΔM51 VSV/GFP-FPV039 intravenously. Even though the survival was atypical for the ΔM51 VSV/GFP parental control (normally >90% of animals are not cured), neither version of the anti-apoptotic viruses was able to improve survival (Figure 17B), even if compared to typical survival observed in control animals (ΔM51 VSV/GFP in Figure 11A). Both the anti-tumour and anti-viral immune responses measured were also lower for the anti-apoptotic viruses (Figure 17C & D). The anti-viral immune response measured in the ΔM51 VSV/GFP treated group was higher than normal (2-5%) possibly pointing to better replication in this experiment and potentially leading to a better outcome.

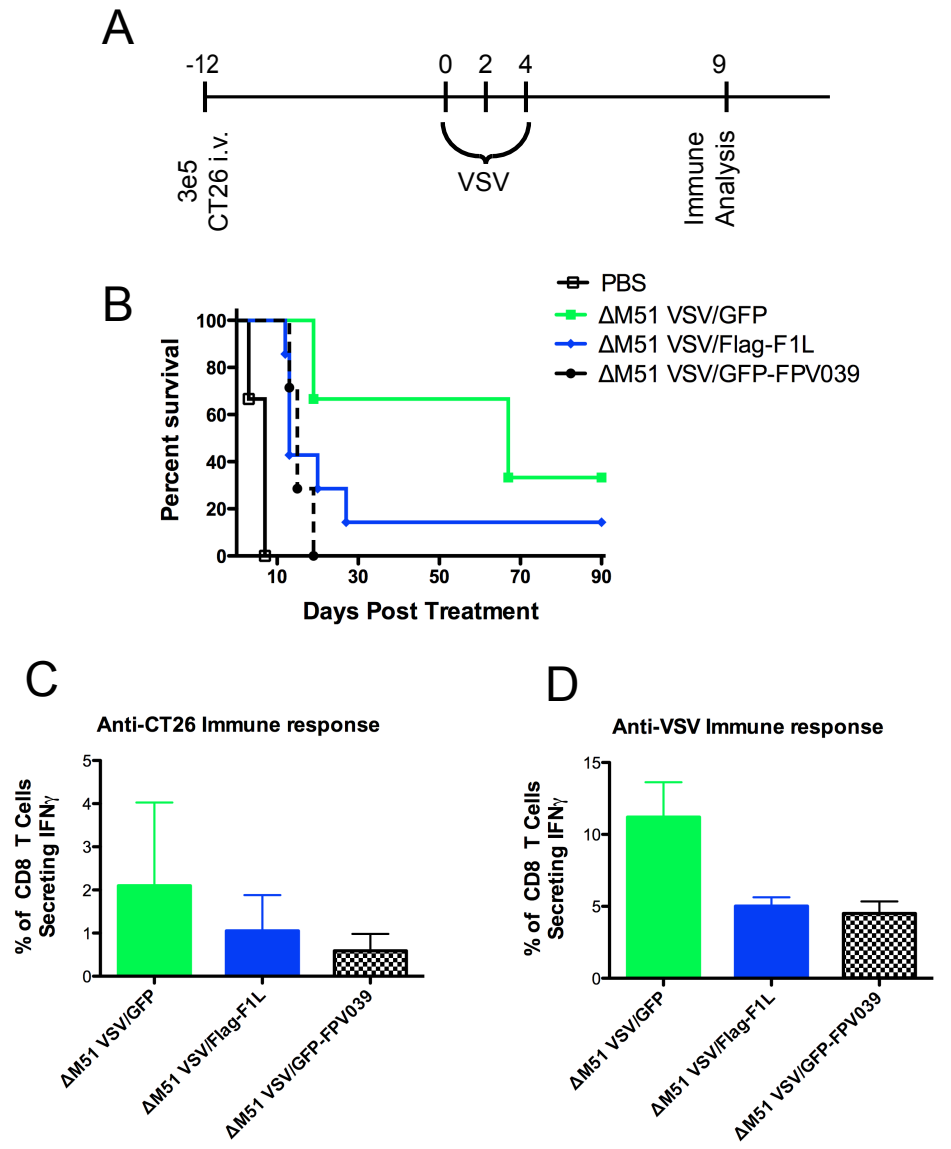


Figure 17 - FAST expression does not improve on VSV oncolytic efficacy in a CT26 lung metastases model. Balb/c mice bearing 12 day old CT26 lung metastases were treated with 3 doses of $5x10^8$ PFU i.v. every other day of either PBS (n = 3), ΔM51 VSV/GFP (n = 3) or ΔM51 VSV/Flag-F1L (n = 7) or ΔM51 VSV/GFP-FPV039 (n = 7). (A) Experimental outline. (B) Mice were monitored for euthanized upon signs of respiratory distress. 10 days after the start of oncolytic virus treatment PBMC were collected to assess the anti-tumour and anti-viral immune responses. PBMCs were stimulated with the appropriate peptides and analyzed for tumour or viral specific $CD8^+$ T cells by flow cytometry using ICCS for IFNγ. Anti-tumour and anti-viral immune responses are presented in (C) and (D) respectively. Data are mean ± s.e.m combined from 2 independent experiments.

3.0 Discussion

The theme of this chapter has been that all three viruses constructed with a transgene to manipulate the infected cells performed as expected *in* vitro. But the changes observed *in vitro* were unable to translate to improvement compared to ΔM51 VSV/GFP *in vivo*. With the current knowledge of indirect bystander effects induced during VSV oncolysis, mainly inhibition of tumour perfusion, it could have been postulated that all of these viruses were destined to fail from the beginning.

With the knowledge that generating an immune response during VSV oncolysis is critical to successful oncolytic therapy with VSV, improving the $CD8^+$ T cell responses should lead to better therapeutic outcomes. Since VSV kills cells predominantly through classical apoptotic mechanisms[273,274,276] and apoptosis is thought to be a largely immunologically silent form of cell death[235,241-244], changing how infected cells die would modify the resulting anti-tumour immune response. One problem is that in the design of these experiments the role that vascular shutdown during oncolysis plays was not fully realized[227,228] and how much of the tumour was actually infected and the location was not fully considered.

First, during the infection of a tumour following i.v. VSV delivery there are two factors to be considered, how long the virus is replicating and where it is located within the tumour. Since the transgenes added to the virus were only expressed in infected cells, these were critical variables that needed to be

considered. VSV replication in CT26 tumours leads to high titers, on the order of 10^9 PFU/g of tissue, however the replication is fairly transient in that it is only detectable for 4-5 days (data not shown). This replication generally occurs in a relatively small area around the rim of the tumours (Figure 6B, top panel). The only exception we have found is in tumours treated with ΔM51 VSV/FAST, there is more spread to other areas of the tumours (Figure 6B, bottom panel). Therefore, the transgenes must have an effect quickly on the cells infected before the infection is extinguished by the immune response. With a relatively small area of the tumour infected, there would have to be a massive effect on the cells infected in this area to have an impact on the outcome of the oncolytic virus therapy. It is unlikely, and this is shown in the outcomes of the experiments presented in this chapter, that the modification of these limited numbers of tumour cells for a short period of time would be able to have enough impact to improve the immunological outcomes. The impact of the cell death in the core of the tumour following the vascular shutdown needed to be considered.

Following oncolytic virus treatment of tumours there is an acute shutdown of the vasculature in the treated tumour mediated by neutrophils and clotting factors[227,228]. This event occurs within the first 24 hours of infection and leads to a large bolus of active caspase-3 positive cells in the core of the tumour[227,228]. It is currently not understood what impact this phenomenon plays on the resulting immune response, however it would be hard to believe that such a large area of the tumour undergoing fairly synchronous cell death would not have a large

impact on the resulting immune response.The area that this core death comprises is much greater than that of the VSV infected and therefore it is likely that modifying virally infected cells would not be able to compete or overcome the effects of this vascular shutdown.

While these VSV induced bystander events in the tumour have a major impact on the outcome of these therapies, there were also potential issues with the cells modified by the transgenes incorporated into the virus. The idea behind adding the p14 FAST transgene to VSV was to have the formation of syncytia in VSV infected cells. The expression of p14 FAST was able to change the pathogenesis of VSV, identifying p14 FAST as a bona fide virulence factor, therefore it is clear that syncytia must be formed *in* vivo by VSV/FAST [225]. Therefore, while there are no images conclusively showing syncytia formed *in vivo* it would be hard to imagine that these syncytia are not formed in the tumour since p14 FAST had such a profound impact on the virulence of VSV *in vivo*.However, the expression of p14 FAST and the syncytia formed were hypothesized to make it more difficult to clear the large multi-nucleated cells therefore modifying how the cells died leading to modified immune responses. Therefore, the presence of syncytia ultimately may not have modified how the cells were cleared and presented by the immune system. In both subcutaneous and lung metastases models the anti-tumour $CD8^+$ T cell responses were found to be lower in mice treated with ΔM51 VSV/FAST. The slight improvements in virus spread may overcome the decreased immune responses in ΔM51 VSV/

FAST treated tumours leading to similar survival rates compared to ΔM51 VSV/GFP. The impact that the formation of syncytia had on tumour cell uptake and antigen presentation was not tested; but it is appears that the presence of syncytia had an unexpected effect that ultimately led to a decreased in the immune responses induced following ΔM51 VSV/FAST treatment.

Similar to the ΔM51 VSV/FAST scenario, there are also some issues surrounding the modification of cell death utilizing Flag-F1L and GFP-FPV039 expression during VSV infection. Although apoptosis was impaired during infection with both ΔM51 VSV/Flag-F1L and ΔM51 VSV/GFP-FPV039, AnV staining by FACS showed that phosphatidylserine was still externalized (Figure 14). PS externalization is known to be important in the clearance of apoptotic cells by phagocytes[299,300]. Therefore, although apoptosis was being impaired at the level of caspase-3 activation and PARP cleavage, the apoptotic cells were likely still cleared efficiently. If they were being cleared then there won't be a chance for them move toward the more immunogenic secondary necrosis. Without a change in cell death there would be no net benefit by adding in an anti-apoptotic gene into VSV oncolytic vectors.

Overall, in the context of VSV oncolytics, the addition of any cell-autonomous transgene is unlikely to improve the therapeutic efficacy. This is mainly due to the temporal and geographical limitations of the infection in the tumour following intravenous delivery. A different strategy was required to improve VSV as an oncolytic and one possible scenario was the addition of

transgenes that are highly secreted and can act within the tumour as well as systemically, again with an eye to improving on the anti-tumour immune response induced.

~ Chapter 4 ~

Expressing human Interleukin-15 from oncolytic VSV improves survival in a murine metastatic colon adenocarcinoma model through the enhancement of anti-tumour immunity

Expressing human interleukin-15 from oncolytic vesicular stomatitis virus improves survival in a murine metastatic colon adenocarcinoma model through the enhancement of anti-tumor immunity

KB Stephenson, NG Barra, E Davies, AA Ashkar and BD Lichty

Department of Pathology and Molecular Medicine, Centre for Gene Therapeutics, McMaster Immunology Research Centre, McMaster University, Hamilton, Ontario, Canada

Published in *Cancer Gene Therapy*
Vol. 19(4), pp 238-246, April 2012
© Nature America, Inc

***Preface*:**
The work presented in this manuscript was conducted throughout my degree, however the majority was conducted between 2006-2008. I designed and conducted all of the experiments presented, with close guidance from my supervisor Dr. Brian Lichty and our collaborator Dr. Ali Ashkar. Prior to my arrival Dr. Lichty's lab the cloning of hIL-15 had been completed by Elizabeth Davies, a former member of Ali Ashkar's laboratory, how*ever I cloned and rescued the hIL-15 expressing virus. As well, Nicole Barra conducted the ELISA presented in Figure 3a. I prepared and wrote the manuscript and addressed reviewer comments with the aid of Dr. Brian Lichty. This work was supervised by Dr. Brian Lichty and guidance was provided by Dr. Ali Ashkar for experiments pertaining to pretreatment of mice with hIL-15/Rα cytokine.*

1.0 Introduction

Oncolytic viruses (OV) have been shown to be a promising new therapeutic in the treatment of cancer and have been found to not only be safe, but have shown good efficacy in both preclinical models and clinical trials[301-303]. Although there are very promising results for several different oncolytic viruses, there is still room for improvement of these therapeutics, including through the modulation of the anti-tumor immune responses induced during oncolytic virus therapy[304].

Vesicular stomatitis virus (VSV) is one such oncolytic virus that has shown promise in pre-clinical models[25,132,303]. VSV is an enveloped negative sense, single stranded RNA virus that is exquisitely sensitive to type I interferon (IFN)[193]. VSV is specifically targeted to replicate in the tumor utilizing its sensitivity to IFN along with the observation that tumors are generally hypo-responsive to type 1 IFN[25]. Our oncolytic VSV vector harbors a deletion of methionine 51 in the matrix protein allowing for type I IFN to be produced from infected cells[132,223]. Therefore, normal cells will be protected from infection but the hypo-responsive tumor cells will still remain susceptible. VSV, when delivered systemically, has been shown to improve survival of mice in various tumor models[305-307]; however, it has been difficult to achieve high proportions of long term survivors with VSV alone. The improvements observed in some cases have been associated with a requirement of adaptive immune responses following oncolytic therapy. Therefore it may be possible to further improve the efficacy of VSV therapeutics by engineering these

viruses to improve on the anti-tumor immune responses induced following OV therapy.

Interleukin-15 (IL-15) is a pleiotropic cytokine that plays a role in numerous innate and adaptive responses to both pathogens and in cancer. IL-15 is a member of the 4-α helix family of cytokines and signals through a receptor complex which includes both the IL-15 specific receptor α chain (IL-15Rα) and the β γ common chain ($\beta\gamma_c$)[308]. IL-15 has been shown to play important roles in numerous immunological processes including natural killer (NK) cell proliferation and activation[309,310], $CD8^+$ T cell activation, in particular, memory cell development[311] and is able to rescue tolerized T cells *ex vivo*[312]. As well, the treatment of established tumors with IL-15 improves survival[313] and pre-association of IL-15 to its receptor α chain further enhances NK and $CD8^+$ T cell activation, proliferation and anti-tumour activity[314,315]. Finally, human (h)IL-15 has also been added to immunotherapeutic[314] and oncolytic vectors[315] in hopes of improving their therapeutic efficacy.

In the current study, expression of a highly secreted form of human IL-15 (opt.hIL-15) from our oncolytic VSV vector was tested in two models of CT26 colon cancer. We have shown that the addition of opt.hIL-15 to VSV improved survival of treated mice compared to controls. This increased survival was found to be significantly correlated to the levels of anti-tumor $CD8^+$ T cell immune responses. The addition of exogenous IL-15 cytokine increased the systemic levels of NK cells, but not $CD8^+$ T cells prior to viral treatment. However this did

not further improve on the efficacy of VSV viral treatment alone. These data indicate that inclusion of an IL15 transgene in an oncolytic virus can enhance anti-tumoural immunity and improve treatment efficacy.

2.0 Results

Recombinant VSV generated to express hIL-15 optimized for enhanced secretion.

Since hIL-15 is poorly secreted in its natural form, we replaced its natural leader sequence with IgK immunoglobulin leader sequence, as previously described[316], to facilitate optimal secretion of hIL-15 from ΔM51 VSV/opt.hIL-15 infected cells**.** This opt.hIL-15 was PCR amplified and cloned into pVSV-XNΔM51 (Figure 18A). Recombinant VSV/opt.hIL-15 was then rescued using standard techniques. The addition of the opt.hIL-15 transgene did not impact viral replication as the replication kinetics of ΔM51 VSV/opt.hIL-15 were similar to ΔM51 VSV/GFP in a one-step growth curve using Vero cells (Fig. 18B). To determine whether hIL-15 was secreted from ΔM51 VSV/opt.hIL-15 infected cells, Vero cells were infected with ΔM51 VSV/opt.hIL-15 or ΔM51 VSV/GFP at an MOI of 5. Seven hours after infection, a time-point when infected cells were still alive, hIL-15 was only present in the supernatants of ΔM51 VSV/opt.hIL-15 infected cells ($p<.001$; Figure 19A). To ensure that hIL-15 was also expressed *in vivo,*

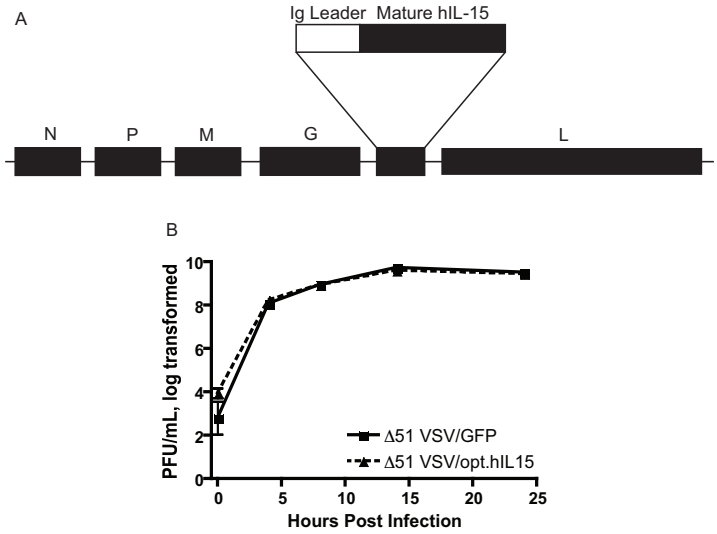


Figure 18 - Construction of ΔM51 VSV/opt.hIL-15. A. Human IL-15 optimized for high level secretion was cloned into the ΔM51 VSV genome between the viral glycoprotein and polymerase. B. To assess viral growth kinetics, Vero monolayers were infected in duplicate with ΔM51 VSV/GFP and ΔM51 VSV/opt.hIL-15 at a multiplicity of infection of 5. Samples were collected at 0, 4, 8, 12 and 24 hours after infection and titered in duplicate on Vero cells using standard plaque assay technique. The mean +/- SEM of log-transformed titers are shown.

mice bearing subcutaneous CT26 tumors were infected with ΔM51 VSV/GFP and ΔM51 VSV/opt.hIL-15 and subsequently tested for hIL-15 levels. Balb/c mice bearing 10-day-old CT26 subcutaneous tumours were treated intravenously with ΔM51 VSV/GFP, ΔM51 VSV/opt.hIL-15 or UV-inactivated ΔM51 VSV/GFP. Forty eight hours after infection tumors were removed and hIL-15 levels were measured in tumor homogenates by ELISA. Only tumors treated with ΔM51 VSV/opt.hIL-15 were found to have high levels of hIL-15 present (Fig. 19B).

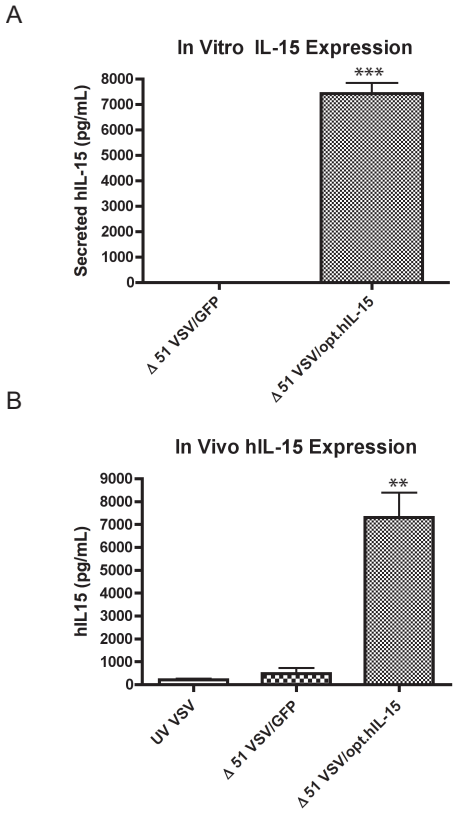


Figure 19 - Expression of hIL-15 from ΔM51 VSV/opt.hIL-15 *in vitro* and *in vivo*. (**A**) Vero cells were infected in duplicate with ΔM51 VSV/GFP or ΔM51 VSV/opt.hIL-15 at an MOI of 5 in minimal media for 45 min followed by another 6.25 h for a total of 7 hours, a time point where all cells are still viable. Supernatants were collected and analyzed by ELISA and hIL-15 was only detected in ΔM51 VSV/opt.hIL-15 infected cells. Data are mean +/- SEM; n = 2; p = .003. (**B**) hIL15 expression was assessed *in vivo* in a subcutaneous CT26 tumor model. Tumor bearing Balb/c mice were treated with $5x10^8$ PFU of UV VSV (n=2), ΔM51 VSV/GFP (n=3) or ΔM51 VSV/opt.hIL-15 (n = 3). 72 hours after treatment tumors were removed and hIL-15 was only detected by ELISA in homogenates from ΔM51 VSV/opt.hIL-15 treated tumors. Data are mean +/- SEM; **P < 0.01.

The addition of hIL-15 to oncolytic VSV did not improve VSV efficacy in a subcutaneous CT26 model.

To determine whether the addition of hIL-15 to our oncolytic VSV vector improved on treatment outcomes we started by testing ΔM51 VSV/opt.hIL-15 in a subcutaneous CT26 colon carcinoma model. Mice were engrafted with CT26 on

the flank and when the mean tumor volumes reached 50 mm^3 they were treated intravenously with ΔM51 VSV/GFP or ΔM51 VSV/opt.hIL-15 given every other day for a total of three treatments. Unfortunately, in this model the parental GFP-expressing virus cured 80% of the mice not allowing us to detect an improvement in outcome when using the ΔM51 VSV/opt.hIL-15 vector, which also cured 80% of the mice (Figure 20).

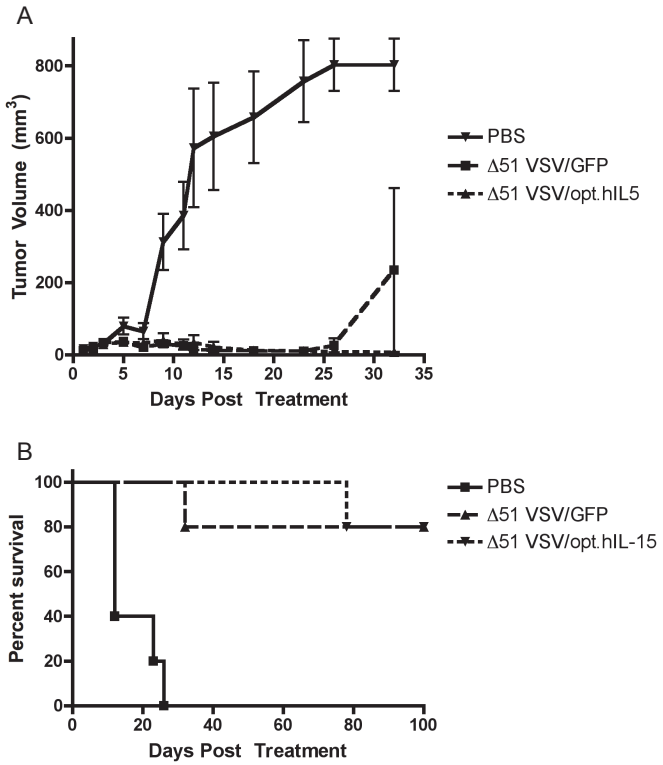


Figure 20 - Treatment of sub-cutaneous CT26 tumors with ΔM51 VSV/opt.hIL-15. Mice bearing established tumors were treated with PBS (n = 5) ΔM51 VSV/GFP (n = 5) or ΔM51 VSV/opt.hIL-15 (n = 5). Once tumors reached a mean of ~10-20 mm3 mice were treated with $5x10^8$ PFU of the indicated virus intra-venously every other day for a total of 3 treatments. (**A**) Tumor volume (calculated as an ellipse where volume = 4/3 x π x L/2 x $(W/2)^2$) is shown as mean +/- SEM and (**B**) Survival were monitored and are depicted above.

ΔM51 VSV/opt.hIL-15 performs better than ΔM51 VSV/GFP in CT26 lung mets model.

Both ΔM51 VSV/GFP and ΔM51 VSV/opt.hIL-15 performed very well in the subcutaneous CT26 model so we moved into the more challenging model of CT26 lung metastases. To this end, Balb/c mice bearing 12-day-old CT26 lung metastases were treated with three doses ΔM51 VSV/GFP or ΔM51 VSV/opt.hIL-15 intravenously every other day (Figure 21A). In this version of the CT26 tumor model we have been unable to cure mice using the parental virus and once again all of the ΔM51 VSV/GFP-treated animals performed better than those treated with PBS (Figure 21B; $p < 0.0001$, Logrank Test), but ultimately succumbed to their tumors. We were however able to cure 50% (5 of 10) of the ΔM51 VSV/opt.hIL-15 treated animals (Figure 21B), a significant improvement over the GFP-expressing parental virus ($p = 0.0022$, Logrank Test). To ensure that the differences observed were not due to variability in tumor engraftment, tumor burden as assessed twelve days post engraftment, which is the time of treatment. We then investigated $CD8^+$ T cell responses versus the tumor (AH1 endogenous MuLV gp70 epitope expressed in CT26 N-SPSYVYHQF-C^{231}) and the oncolytic virus (nucleocapsid epitope N-MPYLIDFGL-C^{230}) nine days post-infection. At this time point, we saw that inclusion of the opt.hIL-15 transgene greatly enhanced anti-tumoural immunity (Figure 21C; $p<0.05$; student's T test) while not modifying the immune response versus the vector (Figure 21D). Thus transient expression of a secreted form of IL-15 from within the infected tumor

enabled the generation of anti-tumoural immunity leading to eradication of CT26 lung mets and long-term survivors.

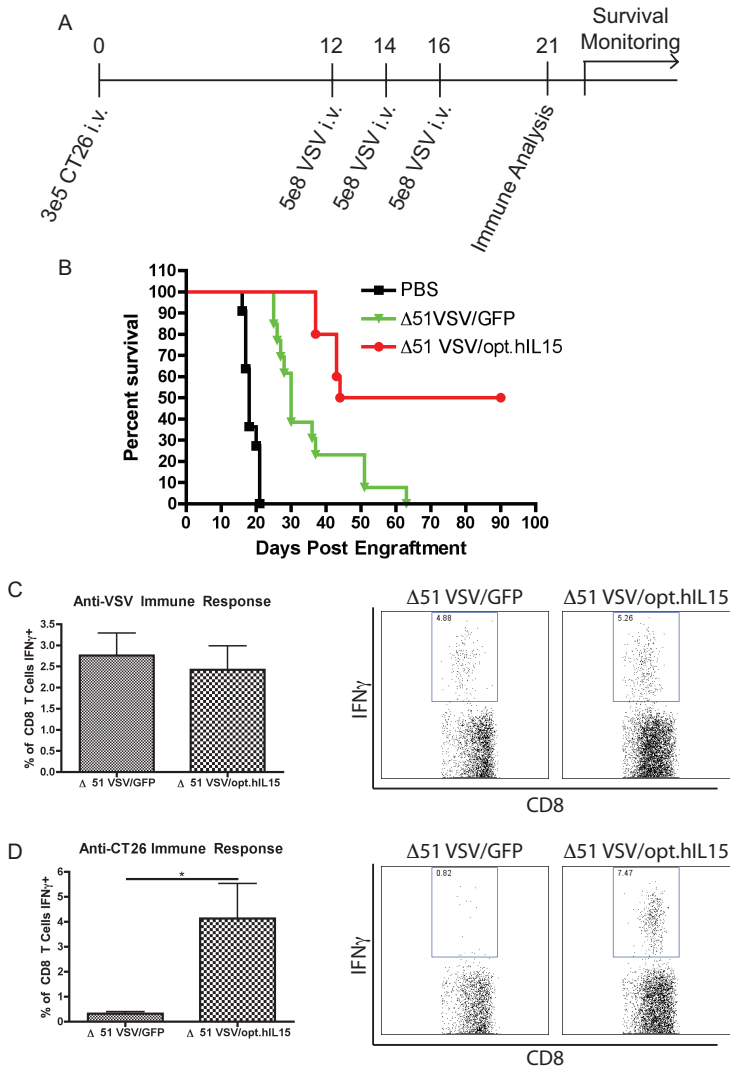


Figure 21 - Expression of human interleukin-15 (hIL-15) from vesicular stomatitis virus (VSV) significantly improves oncolytic virus (OV) therapy. (a) Outline of Experimental design. (b) Survival curve of treated mice; phosphate-buffered saline (PBS), n = 7; ΔM51 VSV/green fluorescent protein (GFP), n = 10; ΔM51 VSV/optimized human interleukin-15 (opt.hIL-15), n = 10; ***P<0.0001. On day 21, 9 days after starting oncolytic virus treatment, blood was collected to assess the anti-tumor and anti-viral immune responses. Peripheral blood mononuclear cells (PBMCs) were stimulated ex vivo with the appropriate peptides and the analyzed for activation by flow cytometry using interferon-g (IFNg). Anti-tumor and anti- viral immune responses are represented in (c) and (d), respectively. Data are mean±s.e.m. combined from 2 to 3 independent experiments; ΔM51 VSV/GFP, n = 13; ΔM51 VSV/opt.hIL-15, n = 10; *P < 0.05.

Pre-treatment with IL-15/Rα increased peripheral NK counts.

We reasoned that since hIL-15 expression by ΔM51 VSV/opt.hIL-15 was very transient only being produced during viral replication, and some effects of IL-15 take as much as a week to manifest [314,317], we decided to pre-treat tumor-bearing animals with recombinant hIL15 + hIL15 receptor α chain (hIL-15/Rα) (Figure 22A). It has been previously demonstrated that the soluble cytokine is more bioavailable and effective *in vivo* when complexed with the soluble receptor α chain[318-320] and that this hIL-15/Rα complex expands NK and CD8 memory T cell numbers[319]. Thus we pre-treated mice with hIL-15/Rα prior to ΔM51 VSV/ opt.hIL-15 or ΔM51 VSV/GFP treatments in an attempt to improve the immune response generated by oncolytic VSV treatment. Mice treated with hIL-15/Rα were assessed prior to viral treatment to determine the effects of hIL-15/Rα on peripheral NK and $CD8^+$ T cells. Mice that received hIL-15/Rα were found to have a significantly higher percentage of peripheral DX5+ NK cells ($p<0.0001$; Figure 22B). However, the hIL-15/Rα did not affect their activation level as assessed by surface expression of the activation marker CD69 (Figure 22C). We did not find any difference in the peripheral $CD8^+$ T cell frequencies in mice treated with hIL-15/Rα (Figure 22d).

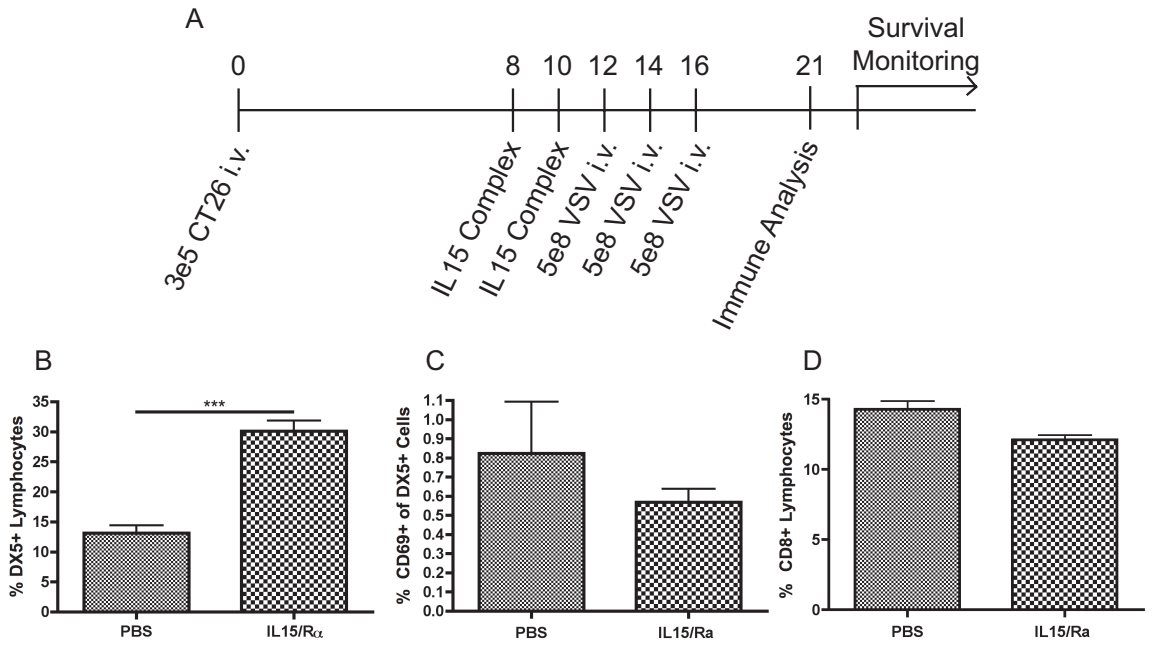


Figure 22 - Pretreatment of CT26 lung metastases with hIL-15/Rα increases peripheral NK cell frequencies. A. Experimental outline for the treatment of mice with hIL-15/Rα prior to oncolytic virus delivery. NK cells (B), activated NK cells (C) and $CD8^+$ T cells (D) were analyzed in PBMCs prior to viral delivery to assess the impact of hIL-15/Rα on the tumor bearing mice. Blood was collected 8 hours prior to viral delivery and analyzed by Flow Cytometry. Data are mean +/- SEM combined from two independent experiments; PBS n=8, hIL-15/Rα n = 33; *** $p < 0.0001$.

Pre-treatment with IL-15Rα failed to enhance anti-tumoural immunity or survival.

The addition of hIL-15/Rα cytokine complex to either VSV therapy did not improve on the anti-tumor immune response elicited by either virus alone (Figure 23A). Although the anti-tumor response in the ΔM51 VSV/GFP + hIL-15/Rα treated mice was increased compared to ΔM51 VSV/GFP alone, this result did not reach significance as assessed by a one-way ANOVA. Surprisingly, the addition of hIL-15/Rα pre-treatment prior to oncolytic viral delivery led to significantly reduced anti-viral $CD8^+$ T cell responses ($p = .0029$, Student's T Test)

(Figure 23Bii). The addition of this soluble cytokine pre-treatment failed to modify the survival outcomes generated by either virus (Figure 23C) indicating, that while the expression of IL-15 from the oncolytic virus is quite transient, local production is more useful in this setting than is systemic pretreatment in enhancing the therapy. Ultimately, there was a significant correlation between the magnitude of anti-tumour $CD8^+$ T cell response and survival (Figure 22) indicating that the enhancement of this response by virally-encoded IL-15 contributed to therapeutic enhancement.

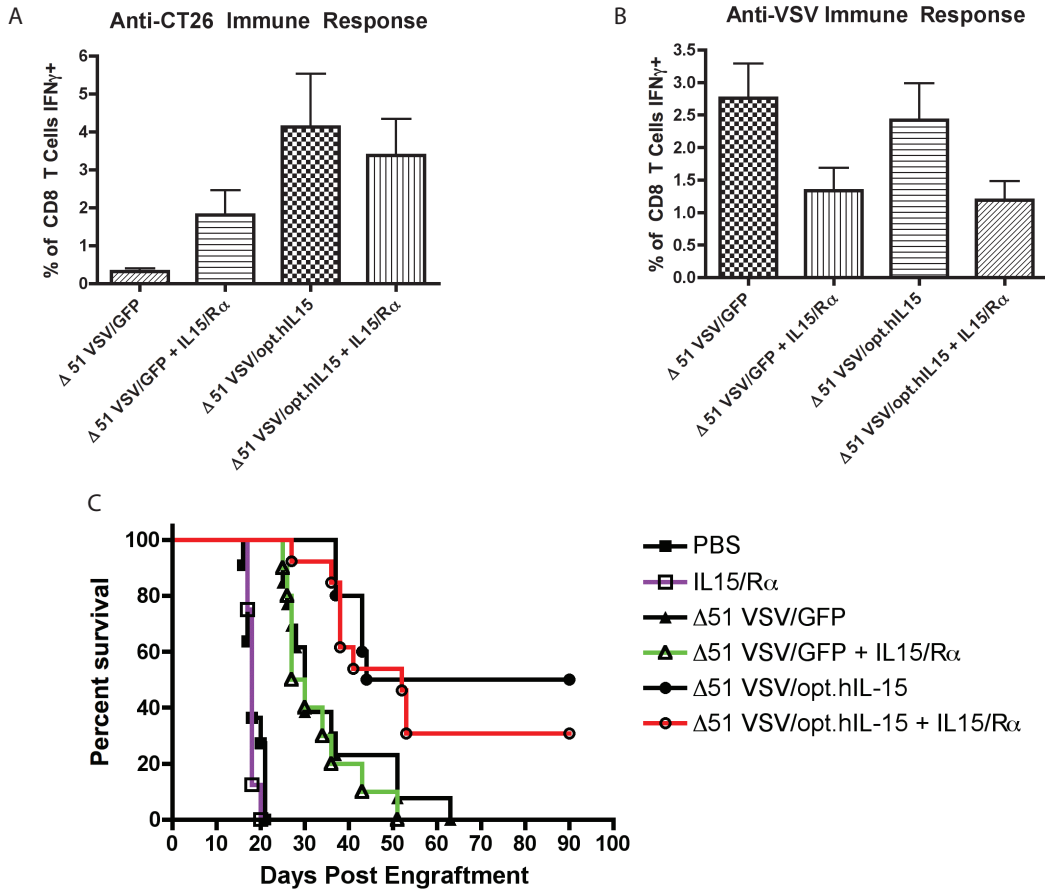


Figure 23 - Pretreatment with hIL-15/Rα does not improve on treatment with either virus alone. A. Blood was collected 9 days after the start of oncolytic virus treatment to assess the anti-tumor and anti-viral immune responses. PBMCs were stimulated ex vivo with the appropriate peptides and the analyzed for activation by flow cytometry using IFNγ. Anti-tumor and anti-viral immune responses are represented in (A) and (B) respectively. Data are mean +/- SEM combined from 2-3 independent experiments; ΔM51 VSV/GFP n=13, ΔM51 VSV/GFP + hIL-15/Rα n=11, ΔM51 VSV/opt.hIL-15 n=10, ΔM51 VSV/opt.hIL-15 + hIL-15/Rα n=13; *P < 0.05. C. Kaplan-Meier survival curve of the indicated treatments. There are three pairs of survival curves (PBS, ΔM51 VSV/GFP and ΔM51 VSV/opt.hIL-15; +/- hIL-15/Rα). Each of the ΔM51 VSV/GFP and ΔM51 VSV/opt.hIL-15 pairs are significantly different from PBS and each other. There was no significant differences between groups within a pairing. (Log-rank test; ΔM51 VSV/opt.hIL-15 vs. PBS P<.0001, ΔM51 VSV/opt.hIL-15 vs. hIL-15/Rα, p<.0001, ΔM51 VSV/opt.hIL-15 vs. ΔM51 VSV/GFP, p=.0017, ΔM51 VSV/opt.hIL-15 vs. ΔM51 VSV/GFP + hIL-15/Rα, p=.0006, ΔM51 VSV/opt.hIL-15 vs. ΔM51 VSV/opt.hIL-15 + hIL-15/Rα, p = ns).

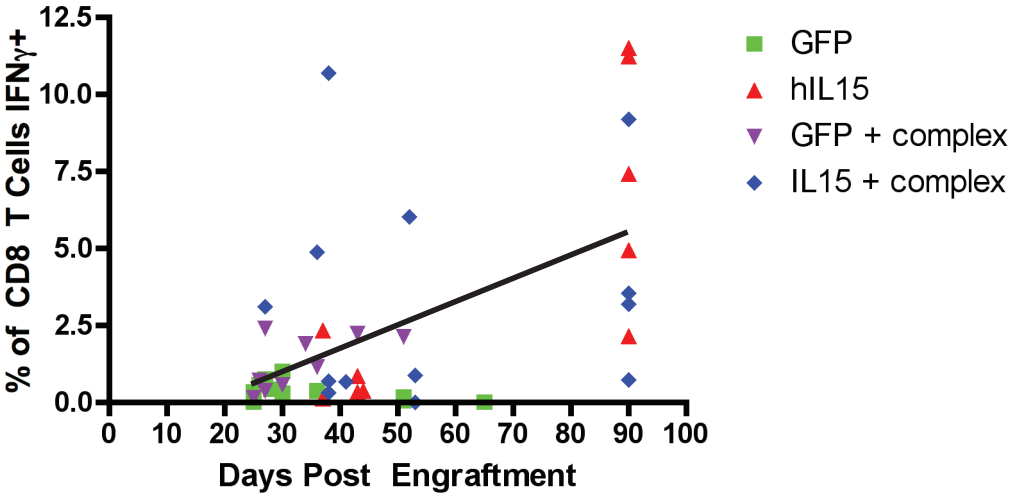


Figure 24 - Survival correlates with anti-tumor immune response. The magnitude of the anti-tumor immune response in peripheral blood 9 days after the start of oncolytic virus treatment was plotted against time to endpoint and is presented above. Data points represent the individual mice that survived to immune analysis. There is a significant correlation between survival and anti-tumor immune response, $p < 0.0001$, $r^2=0.317$.

3.0 Discussion

Oncolytic viral therapy is an emerging strategy for the treatment of cancer. Although the virus infects and kills tumor cells it is unlikely that the virus will be able to destroy entire tumors through viral oncolysis on its own as there are many barriers to viral spread through solid tumors *in vivo*[321]. Therefore, we feel that it would be beneficial to harness the host immune response in an effort to augment the therapeutic effect of oncolytic viruses. Transgenes have been added to oncolytic VSV vectors in an attempt to improve on efficacy through modulation of the immune response, with varying impacts on therapeutic outcome[160,305,322-324]. A number of groups have added cytokines, including IL-4, IL-12, IL-23, into VSV in an effort to polarize the adaptive immune response to improve on anti-tumor

immune responses. While there was some improvement over parental control viruses, the immune responses were either not measured in these studies or showed no, or only very minor increases to immune responses, leaving room for further improvement[160,322-324]. Alternatively, co-stimulatory molecules have been expressed from the oncolytic VSV vector again with no improvement over control viruses in survival or induction of immune responses[305]. To improve on the oncolytic efficacy of VSV we have added a highly secreted form of human IL-15 to our oncolytic VSV vector for its immunostimulatory effects on innate and acquired immunity[308,311,312].

The addition of the hIL-15 transgene did not impair viral replication *in vitro* and led to high levels of hIL-15 secretion of from virally infected cells both *in vit*ro and *in vivo*. We predicted that expression of IL15 from our virus would enhance therapy as it has been shown previously that IL-15 expressed from transfected tumors *in vivo* impacts on tumor growth and subsequent immune responses[313,316,325].

We failed to see an enhancement to therapy when we first tested our viruses in the subcutaneous version of the CT26 model as the parental GFP-expressing virus was already very efficacious in this setting. We suspect that this stems from guaranteed delivery of virus to the one and only tumor target followed by the significant impact on vascular function and massive hypoxic death induced in this setting[227,228]. Therefore we moved into the more challenging model of CT26 lung metastases where we are unable to cure mice of their tumors with

ΔM51 VSV/GFP, possibly due to a failure to infect every tumour nodule by the intravenous route of delivery accompanied by a reduced induction of hypoxia of these smaller tumour nodules in the lung.

As expected mice bearing CT26 lung metastases could not be cured of their disease when treated with ΔM51 VSV/GFP. However high levels of expression of hIL15 during ΔM51 VSV/opt.hIL-15 treatment was able to improve therapy leading to a significant improvement in survival and ultimately leading to 50% of ΔM51 VSV/opt.hIL-15 treated mice being cured. We suspect that the improvement seen in the ΔM51 VSV/opt.hIL-15 treated mice may be due to the enhanced anti-tumor $CD8^+$ T cell responses induced as there was a modest correlation between the magnitude of this response and survival across all groups.

Treatment of the tumour-bearing mice with recombinant IL15/Rα complex led to a systemic increase in NK cell numbers as expected. This failed to directly impact tumour growth as a mono-therapy and also failed to enhance oncolytic viral therapy. However, delivery of IL-15/Rα cytokine complex prior to oncolytic viral therapy led to a reduction in the anti-viral $CD8^+$ T cell response. We speculate that this is indicative of a reduced load of viral antigen in these mice due to an attenuation of viral replication mediated by an enhanced NK cell response. Thus the cytokine pre-treatment may have provided a minor enhancement to anti-tumour responses while also enhancing innate anti-viral responses largely canceling any impact on therapy. Concurrent, or even

subsequent, cytokine administration may provide benefits to the anti-tumour immune response without attenuating viral oncolysis.

In summary the addition of a highly secreted form of IL-15 to an oncolytic VSV vector led to enhanced therapeutic outcomes under circumstances where viral oncolysis alone was unable to mediate durable cures. This enhanced efficacy was correlated with increased anti-tumour immune responses following intravenous viral administration.

~ Chapter 5 ~

Investigating the role of vascular shutdown and apoptotic cell death in the core of VSV treated tumours on induction of anti-tumour immunity and overall therapeutic outcome.

1.0 Introduction

Following intravenous treatment of tumours with VSV, and other oncolytic viruses, there is an observed vascular shutdown mediated by neutrophils and clotting in the tumour vasculature[227,228]. During the first 24 hours after VSV treatment, expression of numerous cytokines and chemokines were increases[227]. These chemokines lead to an influx of neutrophils to the tumour, which is followed by clotting in the vessels leading to a collapse of vasculature in the tumour preventing perfusion through the majority of the tumour[227,228]. Both the recruitment of neutrophils and clotting were shown to be required for the reduction in perfusion observed. When either of these processes were impaired, tumours remain perfused following VSV treatment[227,228].

Despite the fact that there is a better understanding of the early events during VSV oncolysis, how these early events impact the anti-tumour immune responses induced during VSV oncolysis and therapeutic outcome following oncolytic virus therapy is not known. Expressing cell-autonomous transgenes from VSV oncolytic viruses was unsuccessful (Chapter 3) likely due to their inability to modulate the significant bystander killing observed following VSV treatment. Therefore we set out to gain a better understanding of the requirement for vascular shutdown and what aspects are critical for successful therapy using VSV oncolytics. This information will allow us to further improve VSV oncolytic viruses by determining which strategies can be used to act on the whole tumour rather than focussing on modifying only infected cells. **We hypothesized that in**

the absence of vascular shutdown and/or inhibition of cell death in the core of the tumour would impair anti-tumour immunity following oncolytic VSV therapy. To this end we impaired vasculature shutdown utilizing heparin and neutrophil depletion to study the effect of vascular shutdown during VSV therapy. By approaching the shutdown from two angles it allowed us to address whether neutrophils have a role outside of enabling the vasculature shutdown (Table 2).

We also addressed the importance of apoptosis in the core of the tumour utilizing caspase inhibitors. There are numerous cell permeable caspase inhibitors with varying specificity for different caspase molecules. As discussed in Chapter 3 section 1.1, the induction of apoptosis culminates in the activation of caspase-3, an executioner caspase involved in cleavage of numerous substrates, leading to DNA fragmentation and the death of the cell. By inhibiting caspase-3, apoptotic cell death can be avoided. Two such inhibitors are Z-VAD-FMK and Z-DEVD-FMK. Both are irreversible inhibitors of caspase, due to the added fluoromethyl ketone (FMK) group[326], and act on pro-caspases preventing cleavage and therefore activation of the molecules[327]. Z-VAD-FMK is a pan caspase inhibitor with the ability to inhibit most caspases, including caspase-3, while Z-DEVD-FMK is more specific for caspase 3 and 7. Both of these inhibitors have been used *in vivo* and shown to be effective at preventing Fas induced apoptosis in the liver of mice[327,328]. These inhibitors were used to determine if the apoptotic death observed following vascular shutdown is required and what

happens to anti-tumour immune responses if that death is impaired or prevented (Table 4).

Table 5 - Approaches to determine what makes oncolytic VSV successful

	Vascular Shutdown	Neutrophil	Apoptotic Core	Outcome	Anti-Tumour Immune Response
VSV	+	+	+	Cure 20-40%	2-5%
VSV + Z-VAD	+	+	-/ alternative death pathways	?	?
CT26.Bcl-2 Stables	+	+	-	?	?
VSV + Heparin	-	+	-	?	?
VSV + Neutrophil Depletion	-	-	-	?	?

2.0 Results

2.1 Pharmacological inhibition of apoptosis was not achieved using either pan caspase inhibitor or more specific caspase3/7 inhibitor.

To determine what, if any, factors involved in the acute vasculature shutdown observed impact on therapeutic outcome we began by attempting to prevent the apoptotic cell death in the core of the tumour. As discussed previously how a cell dies can have an important role on the immunological outcome. Therefore it is important to determine if the cell death seen in the core of the tumour during oncolysis is important for oncolytic therapy, and if it can be modified making it more immunogenic. The first approach we utilized was preventing global caspase activation in VSV treated CT26 tumour bearing mice utilizing Z-VAD-FMK, a pan caspase inhibitor.

Inhibiting apoptosis with a pan-caspase inhibitor during oncolysis had a significant effect early but did not improve overall outcomes.

To assess caspase inhibition by Z-VAD-FMK, it was combined in the treatment of CT26 with VSV. In figure 25A the experimental design is described with Z-VAD-FMK being administered at 10mg/kg every day for the first three days of the therapy, a dose previously shown to prevent Fas induced apoptosis in mice[329]. It was not continued past the second dose of virus as the vasculature shutdown and core death occur in the first 48 hours. The addition of Z-VAD did not improve on the survival of treated animals, as seen in figure 25C where survival was similar whether or not Z-VAD-FMK was included in the treatment

protocol. While the immune responses measured were relatively low, Z-VAD-FMK had no impact on the resulting tumour or viral immune responses induced (Figures 25D & E). There was however a difference early on in the treatment in mice that were administered Z-VAD-FMK when looking at the tumour volume (Figure 25B). Between days 9 and 15 mice that were treated with ΔM51 VSV/GFP and Z-VAD-FMK had smaller tumours and there was much less variation in these tumours indicating that all of the mice treated had excellent early tumour control (Two-way ANOVA, P = 0.00339, Students T-test at day 10 P = 0.0317). The further inhibition of tumour growth with the addition of Z-VAD could be due to a number of factors including effects on viral replication, maximum titer and duration of replication, or effects on cell death in the core of the tumour following vascular shutdown. To determine what effect Z-VAD was having on the oncolytic therapy we next assessed the tumours shortly after treatment for viral titer and apoptosis in the core of the tumour.

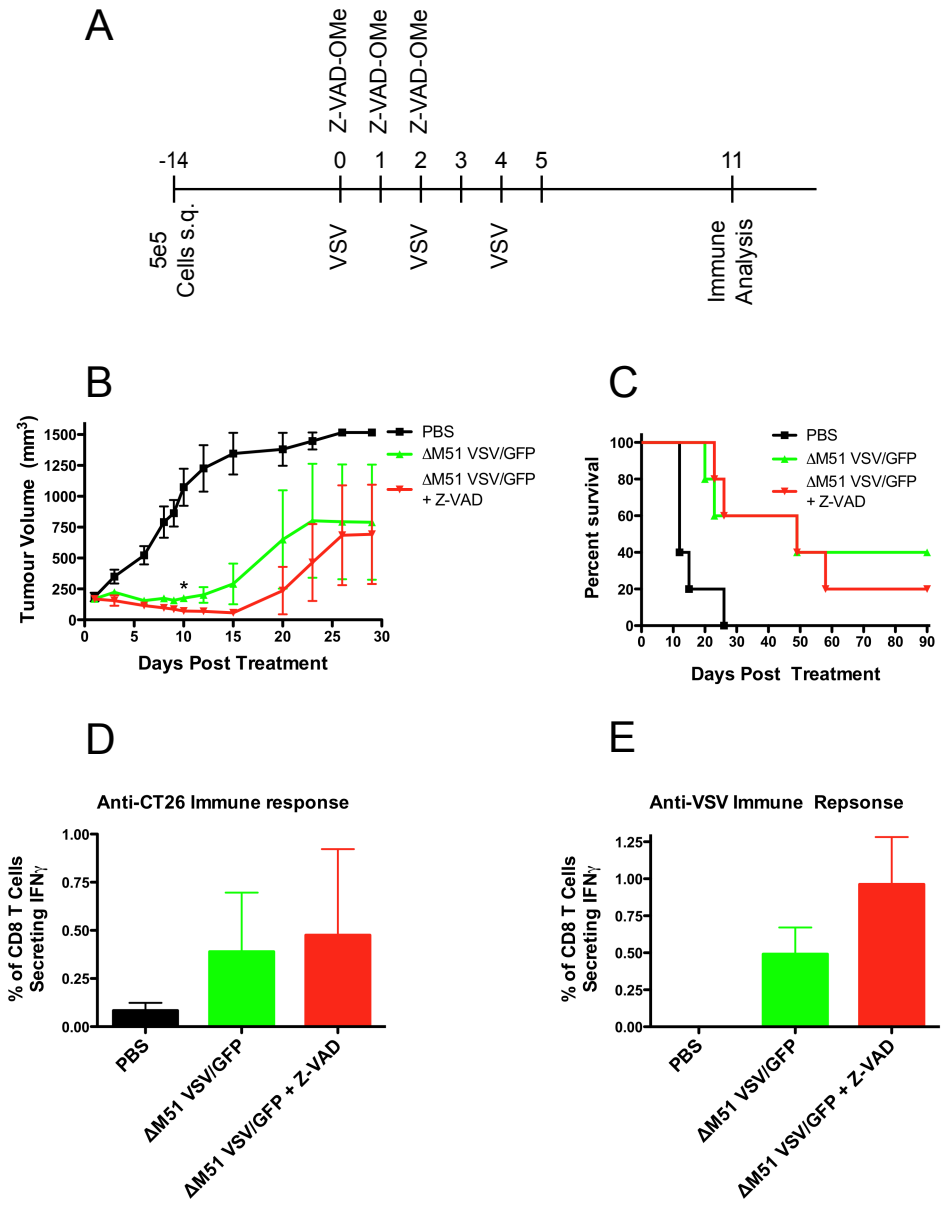


Figure 25 - Inhibiting caspase-3 mediated apoptosis in tumour core did not improve oncolytic VSV therapy. Mice bearing established CT26 tumours were treated with PBS (n=5), ΔM51 VSV/GFP (n=5), ΔM51 VSV/GFP + Z-VAD-FMK (n=5). Once tumours reached ~ 250 mm^3, mice were treated with three doses of $5x10^8$ PFU of ΔM51 VSV/GFP i.v. 48 hours apart. The group treated with ΔM51 VSV/GFP and Z-VAD-FMK were administered 10mg/kg of Z-VAD-FMK i.p. daily for three days beginning with the first dose of ΔM51 VSV/GFP . (A) Experimental outline (B) Tumour volumes were measured and calculated as an ellipse (where volume = 4/3 x π x L/2 x $((W/2)^2)$), shown as mean ± s.e.m; Mann-Whitney T Test at day 10 $P < 0.05$. (C) Survival was monitored and depicted above. 11 days after the start of oncolytic virus treatment PBMC were collected to assess the anti-tumour and anti-viral immune responses. PBMCs were stimulated with the appropriate peptides and analyzed for tumour or viral specific $CD8^+$ T cells by FACS using ICCS for IFNγ. Anti-tumour and anti-viral immune responses are presented in (A) and (B) respectively. Data are mean ± s.e.m.

Z-VAD administration during oncolysis did not modify viral replication or vascular shutdown.

While it appeared that early in treatment the addition of Z-VAD to oncolytic virus protocol had an effect on tumour growth, when we looked in the tumour at virus replication and active caspase-3 staining the addition of Z-VAD had no effect. At all three time points assessed for viral titer, there as no differences observed between ΔM51 VSV/GFP and ΔM51 VSV/GFP + Z-VAD-FMK(Figure 26A). We also assessed the presence of an apoptotic core in the tumour twenty-four hours after VSV delivery. This was an important test to determine if the delivery of Z-VAD-FMK was able to impair apoptosis in the tumour. In all tumours there was still significant levels of active-caspase 3 staining both in the core of the tumour (Figure 26B) and in areas where VSV was replicating (data not shown). Therefore it was clear that administration of Z-VAD-FMK every twenty-four hours was not effective at knocking down apoptotic cell death in the tumour.

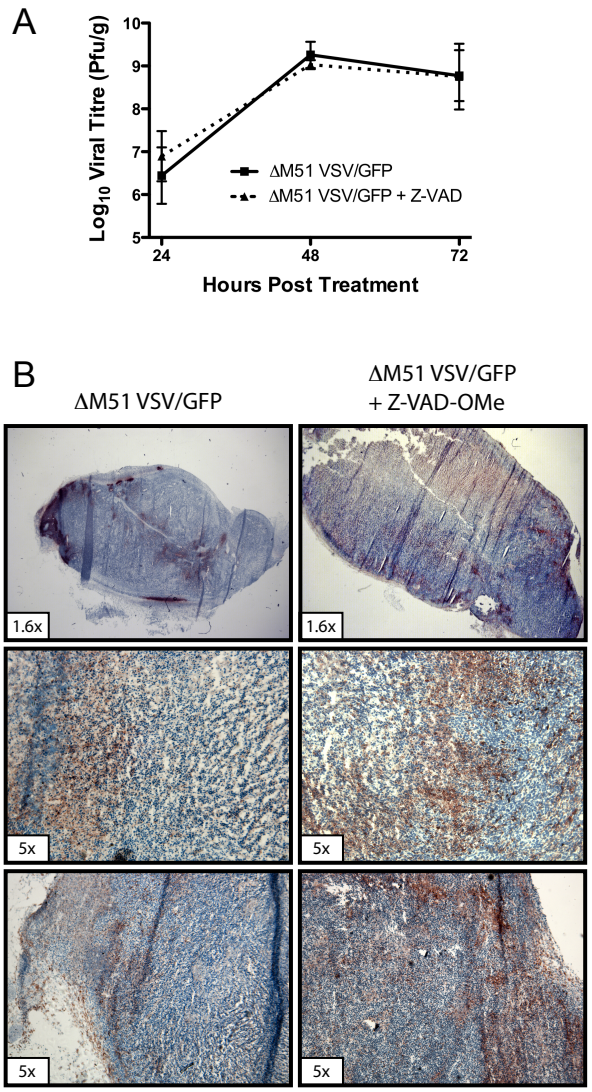


Figure 26 - Z-VAD-FMK does not impair apoptosis in tumours during oncolytic VSV treatment. Mice bearing established CT26 tumours were treated with ΔM51 VSV/GFP +/- Z-VAD-FMK as described in Figure 25. A. Tumours were removed at 24, 48 and 72 hours after VSV treatment began and were snap frozen to assess viral titer. Tumours were thawed and homogenized and viral titer was assessed by standard plaque assay. Data is presented as log transformed mean ± s.e.m. B. Tumours were removed 48 hours after treatment and frozen in OCT. Tumours were sectioned at 10 μm and stained for active caspase-3 by IHC. Photomicrographs were taken with Leica microscope using OpenLab software.

Acute administration of DEVD is unable to impair apoptosis in CT26 during VSV treatment.

The dosing schedule of Z-VAD was likely not condensed enough during the vascular shutdown following VSV treatment to have the desired effects. Since the apoptosis in the core of the tumour is observed beginning around twenty-four hours we chose to concentrate the doses of pharmacological caspase inhibitor to between twenty-four and forty-eight hours post VSV treatment. We also decided to switch to a more specific inhibitor, Z-DEVD-FMK, which is specific for caspase-3 and -7. This would more specifically impair only caspase-3/7 activation while leaving other caspases including caspase-1 activation intact. Caspase-1 activation is an important step activation of the inflammasome, specifically the *NLRP3***,** which has been shown to play an important role in the induction of anti-tumour immune responses[255].

Even though we compressed the doses of DEVD-FMK and gave 4 doses in 24 hours following ΔM51 VSV/GFP treatment, we were still unable to impair the apoptosis in the in ΔM51 VSV/GFP treated tumours (Figure 27). Without impairing apoptosis it is unlikely that the DEVD had the desired effects on the tumour and we therefore did not pursue a survival study combing DEVD-FMK with our oncolytic VSV protocol.

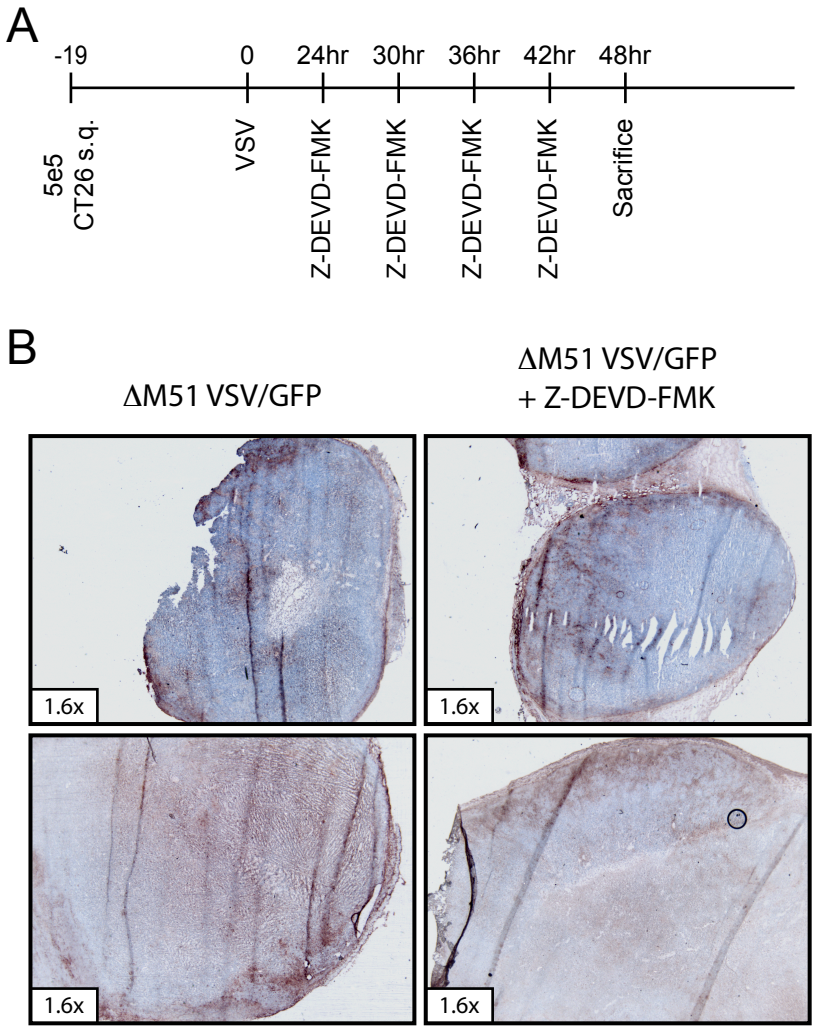


Figure 27 - DEVD treatment is unable to prevent apoptosis in CT26 tumours during VSV oncolysis. Mice bearing established CT26 tumours were treated with ΔM51 VSV/GFP or ΔM51 VSV/GFP + DEVD. When tumours reached ~250 mm^3 mice were treated with $5x10^8$ PFU ΔM51 VSV/GFP. Half of the mice were then treated with four doses of 10 mg/kg DEVD i.p. between 24 and 48 hours. A. experimental outline. B. Tumours were removed 48 hours after ΔM51 VSV/GFP treatment and frozen in OCT freezing medium. Tumours were sectioned at 10 um and stained for active caspase-3 by IHC. Photomicrographs were taken with Leica microscope using OpenLab software.

2.2 Creation of stable CT26 cell line over expressing BCL-2

With both of the pharmacological caspase inhibitors not having the desired effects we moved on to make a CT26 cell line stably expressing Bcl-2, a potent anti-apoptotic protein. To create these cells Bcl-2 was Flag tagged at the N-terminus and cloned into the expression vector pMono. CT26 cells were transfected and selected in blasticidin to generate stable cells. Colonies were then picked, expanded and tested for expression of Flag-Bcl-2 and their apoptotic potential.

Stably over-expressing Bcl-2 in CT26 delayed apoptosis.

The expression of FLAG-Bcl-2 was easily detected in transiently transfected cells, but in the CT26.Bcl-2 cell lines the expression of FLAG-BCL-2 was much lower when assessed by western blot (Figure 28A). This low level expression could be a function of only a few cells expressing the FLAG-Bcl-2 protein, or all cells expressing low levels of the protein. To determine why the expression was detectable but low, CT26.Bcl-2 cell lines were stained for FLAG expression by immunofluorescence. In figure 28B it became clear that there were cells expressing FLAG-Bcl-2, but they only accounted for around 10% of the population of the CT26.Bcl-2 cell lines. We next decided to attempt to further select these cells for FLAG-Bcl-2 expression by exposing the cells to staurosporine, taking advantage of expected differential susceptibility between CT26 and CT26.Bcl-2.

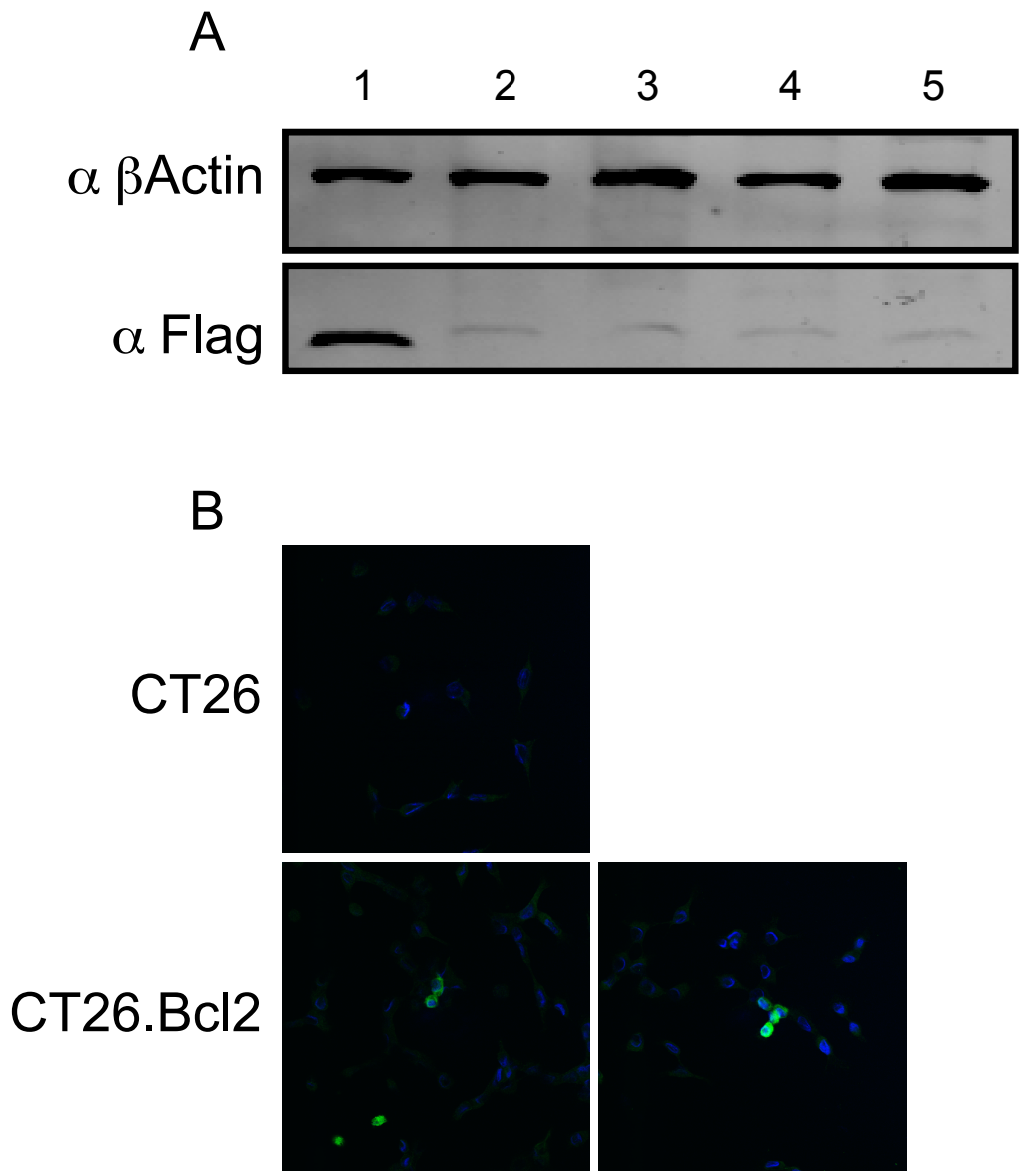


Figure 28 - Testing CT26.Bcl-2 clones for stable expression of Flag-Bcl-2. CT26 transfected with pMono-Flag-Bcl-2 and selected with blasticidin show low level stable expression of Flag-Bcl-2. A. Western blot analysis indicates that there is low level expression of Flag-Bcl-2 in two CT26.Bcl-2 stable cell lines. Whole cell lysates of CT26.Bcl-2 stable cell lines (Lanes 2-5), and CT26 transiently transfected with Flag-Bcl-2 as a positive control (Lane 1), were ran out on a 10% SDS-PAGE gel and blots were probed for Flag-Bcl-2 and β-Actin. Lanes: 1 - CT26 transiently transfected with Flag-Bcl-2; 2 - Cell line 1 ,Passage 1; 3 - Cell line 1, Passage 3; 4 - Cell line 2, Passage 1; Cell line 2, Passage 3. B. CT26 and CT26.BCL2 cell l ine 1 was seeded onto glass coverslips, permeabolized and stained for Flag-Bcl-2 by immunoflourescnce. Photomicrographs were taken on Leica SP5 and analyzed in ImageJ software.

Parental CT26 were efficiently killed by exposure to staurosporine (data not shown). Since the stable CT26.Bcl-2 were over-expressing an anti-apoptotic protein it was thought that by exposing these cells to staurosporine we would be able to further select for stable expression of Flag-Bcl-2. This was indeed the case, and following exposure to staurosporine Flag-Bcl-2 was detected at higher levels by western blot (Figure 29A) and > 90% of cells were expressing Flag-Bcl-2 by immunofluorescence (Figure 29B). A potential issue with making stably expressing cells through selection is that the resulting oligoclonal population, while it expresses FLAG-Bcl-2, may have altered susceptibility to VSV and type I IFN compared to parental CT26. The lack of response to type I IFN in CT26 is critical for VSV to be successful in treating these cells *in vivo.* To determine the IFN responsiveness of the CT26.Bcl-2 stables they were treated O/N with IFN-β and then infected with WT VSV/GFP to assess whether IFN-β was able to protect the cells from infection. Figure 30 shows that indeed the CT26.Bcl-2 stable cell line did not respond to interferon. As well, the CT26.Bcl-2 stables were able to be infected and killed by ΔM51 VSV/GFP (Figure 30B).

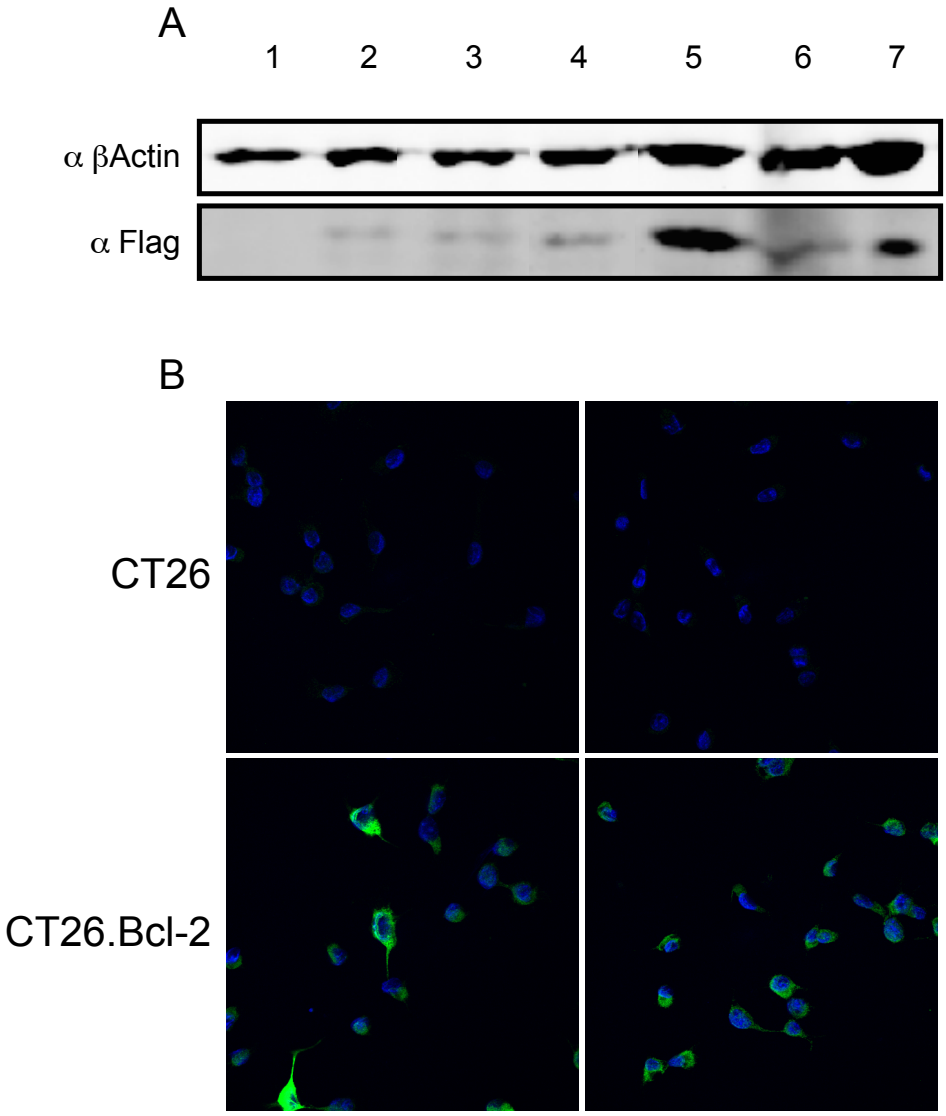
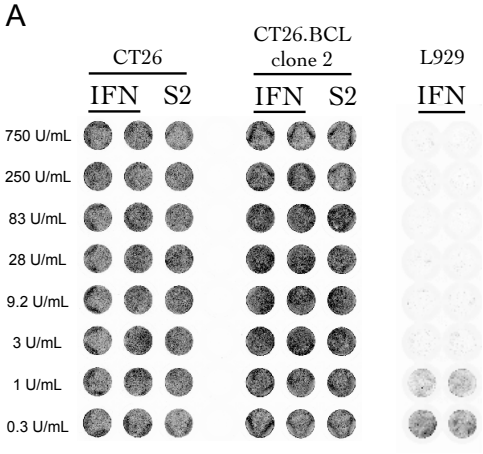


Figure 29 - Staurosporine selection of CT26.Bcl-2 increased the percent of Flag-Bcl-2 positive stable cells. Following a second selection with staurosporine Flag-Bcl-2 expression is increased in CT26.Bcl-2 stable cells. A, Western blot analysis of staurosporine selected CT26.Bcl-2. Whole cell lysates were collected and electrophoresed on a 10% SDS-PAGE gel and blots were probed for Flag-Bcl-2 and β-Actin. Lanes: 1 - CT26; 2 - 4, independent lysates of CT26.Bcl-2 passage 17 (+5 passages from STS selection); 5 - CT26 transiently transfected with Flag-Bcl-2; 6 - CT26.Bcl-2 passage 23 (+ 11 passages from STS selection); 7 - STS selected CT26.Bcl-2 passaged through a mouse.(+ 2 passages). B. CT26 and STS selected CT26.BCL2 was seeded onto glass coverslips, permeabolized and stained for Flag-Bcl-2 by immuno-fluorescence. Photomicrographs were taken on Leica SP5 and analyzed in ImageJ software.

A



B

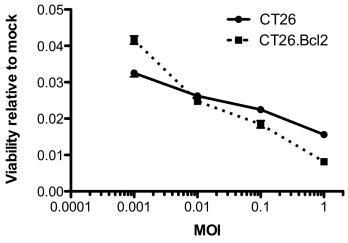


Figure 30 - CT26.Bcl-2 clones have normal response to IFN-β and VSV infection. A. CT26 and CT26.Bcl-2 and L929 were treated with IFN--β or S2 control supernatant overnight at the indicated concentrations. Cells were then infected with $5x10^5$ PFU WT VSV/GFP overnight. Plates were then scanned on Typhoon (GE) for GFP fluorescence. B. CT26 and CT26.Bcl-2 were infected at the indicated MOIs with ΔM51 VSV/GFP for 48 hours in septuplate. An alamar blue assay was then performed to assess cell viability. Data is presented as mean relative to mock.

Since the CT26-Bcl-2 expressing cells were designed to investigate the role of apoptotic cell death in the tumour following VSV oncolysis, they were tested for their ability to undergo apoptosis when infected with VSV and treated with staurosporine. In both cases apoptosis was impaired early when assessed by a luminescent caspase-3 cleavage assay (Promega). Following staurosporine treatment the CT26.Bcl-2 cell line showed a delayed PARP cleavage (data not shown) which correlated to caspase-3 cleavage (Figure 31A). Due to some technical difficulties the PARP assay did not yield useful data in VSV infected cells to compare the cleavage of PARP between the CT26.Bcl-2 stables and parental CT26. Even though caspase-3 cleavage is delayed (Figure 31B) in the

CT26.Bcl-2 cell line, the cells were killed with similar kinetics to parental CT26 (Figure 30B) when infected with VSV. This indicates that while the CT26.Bcl-2 cells are killed by VSV, they die in a different manner and may potentially be more immunogenic.

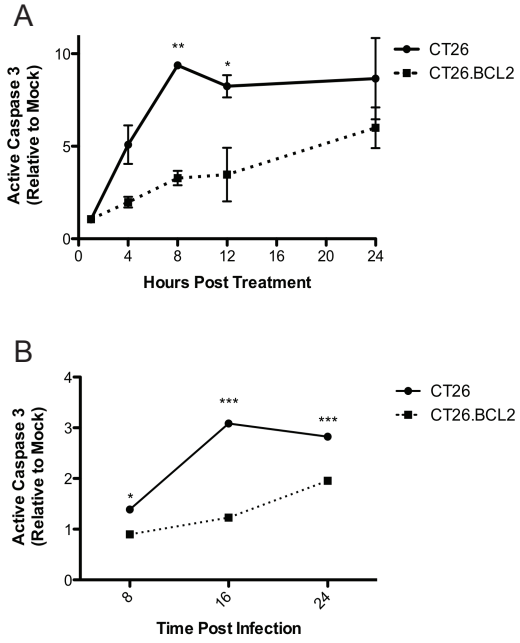


FIgure 31 - Stable Bcl-2 expression delays onset of apoptosis. Caspase-3 activation is delayed in CT6.Bcl-2 stable cells following VSV infection and STS treatment. A. CT26 and CT26.Bcl-2 were treated with 1 μM STS and analyzed at the indicated time points in triplicate using the CaspGlo3/7 assay (Promega) as per the manufacturers instructions. Data are presented as mean ± s.e.m. from two independent experiments; * $P < 0.05$, ** $P < 0.01$. B. CT26 and CT26.Bcl-2 were infected with ΔM51 VSV/GFP at an MOI of 5 and analyzed at the indicated time points and analyzed in triplicate using CaspGlo3/7 assay (Promega) as per the manufacturers instructions. Data are presented as a mean of the triplicates. * $P < 0.05$, *** $P < 0.001$.

Over-expression of Bcl-2 in CT26 *in vivo* did not change the therapeutic outcome following oncolytic VSV treatment

With the CT26.Bcl-2 cell line having the expected apoptotic properties *in vitro*, we moved onto testing *in vivo* to determine the role of apoptotic death in the tumour following oncolytic VSV therapy. Balb/c mice were engrafted with CT26 or CT26.Bcl-2 and treated as per our normal oncolytic VSV protocol. For this study ΔM51 VSV/SIIN-Luciferase was used to treat CT26 tumour bearing animals to allow tracking of viral replication daily by IVIS during the survival study without having to euthanize the animals to assess viral titer (Figure 32A). The IVIS imaging in figure 32B shows that replication of ΔM51 VSV is not altered in CT26.Bcl-2 tumours. Therefore any differences in response to VSV therapy between CT26 and CT26.Bcl-2 would not be a function of differences in VSV replication.

However there were no differences observed in either tumour growth or survival when comparing the two cell lines. Both CT26 and CT26.Bcl-2 had identical tumour growth curves and survival (Figures 33A and B). When the anti-tumour (Figure 33C) and anti-viral (Figure 33D) immune responses were assessed there were also no differences observed. And in this study only two animals mounted an anti-tumour immune response, which is the cause of the large error bars observed in figure 33C. These animals, one in each of CT26 and CT26.Bcl-2 had responses of >10% $CD8^+$ T cells expressing IFNγ, were also the only two survivors following treatment. Again corroborating the importance of

mounting an anti-tumour immune response for the success of oncolytic VSV therapeutics.

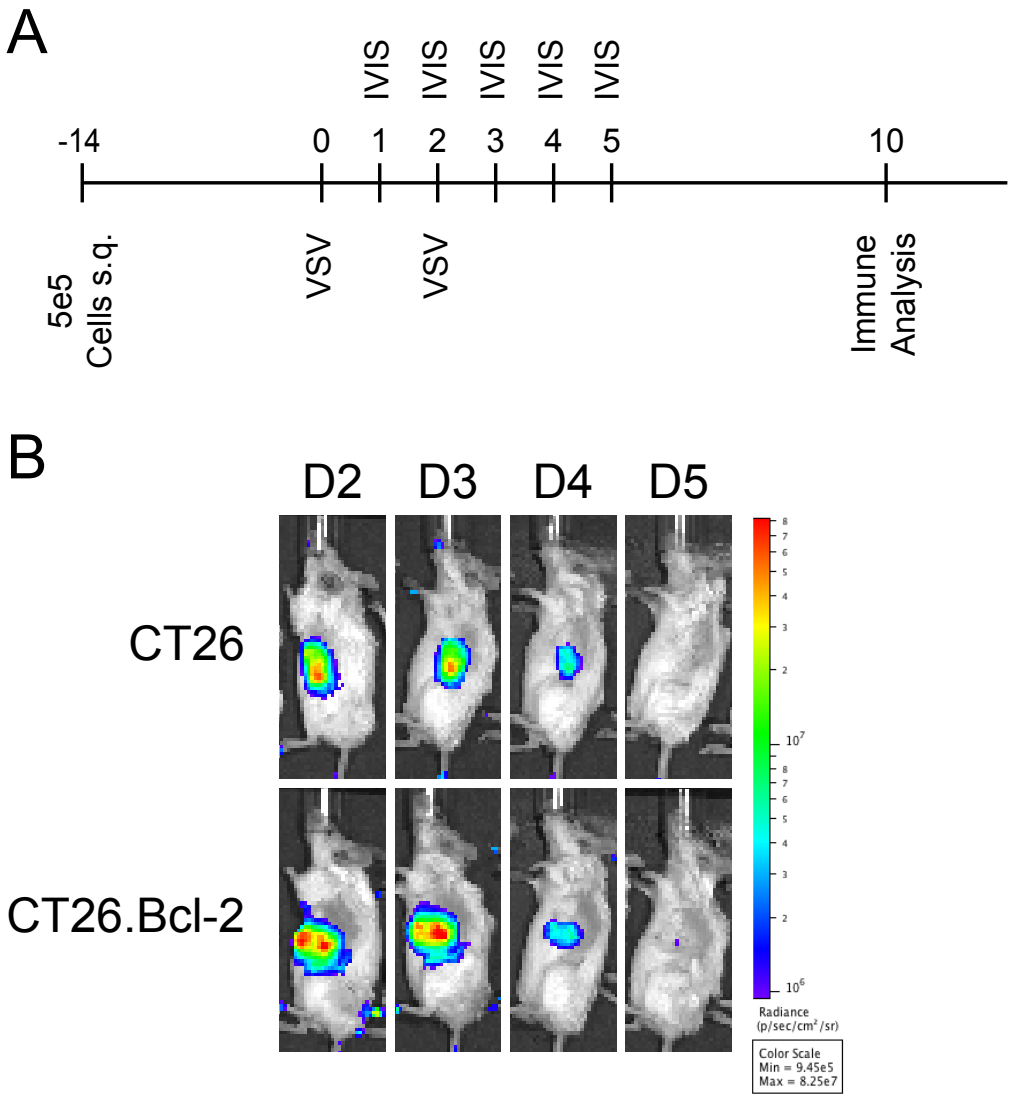


Figure 32 - VSV replication is not modified in CT26.Bcl-2 *in vivo*. Balb/c mice bearing CT26 or CT26.Bcl-2 tumours were treated with ΔM51 VSV/SIIN-Luciferase when tumours reached ~250 mm^3. Mice were treated with two doses of $5x10^8$ PFU ΔM51 VSV/SIIN-Luciferase forty-eight hours apart. IVIS imaging was carried out daily for five days after the initiation of treatment. A. Experimental outline. B. Mice were anesthetized and injected daily with 3 mg of luciferin i.p. and imaged 20 min later with a five second exposure using Xenogen IVIS-200 imaging system (Caliper Life Sciences) and analyzed using Living Image 3.2 software (Caliper Life Sciences)

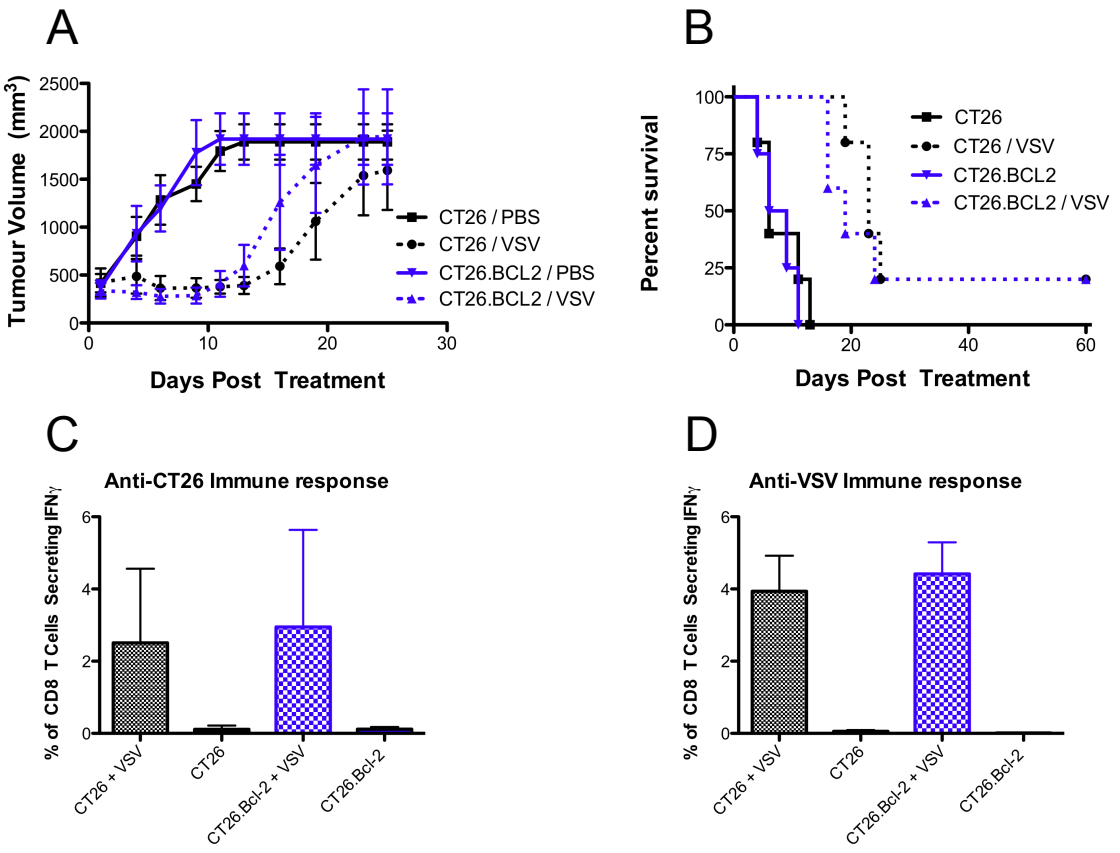


Figure 33 - Mice bearing established CT26 tumours were treated with PBS (n=5), ΔM51 VSV/GFP (n=5), ΔM51 VSV/Flag-F1L (n=6) or ΔM51 VSV/GFP-FPV039 (n=10). Once tumours reached ~ 250 mm^3, mice were treated with two doses of $5x10^8$ PFU of the indicated virus i.v. 48 hours apart. (A) Experimental outline (B) Tumour volumes were measured and calculated as an ellipse (where volume = 4/3 x Pi x L/2 x $((W/2)^2)$), shown as mean ± s.e.m. (C) Survival was monitored and depicted above. 10 days after the start of oncolytic virus treatment PBMC were collected to assess the anti-tumour and anti-viral immune responses. PBMCs were stimulated with the appropriate peptides and analyzed for tumour or viral specific $CD8^+$ T cells by FACS using ICCS for IFNγ. Anti-tumour and anti-viral immune responses are presented in (A) and (B) respectively. Data are mean ± s.e.m.

2.3 Heparin treatment during VSV oncolysis proved unable to prevent vascular shut-down.

Moving away from cell death in the tumour following VSV treatment we next investigated the events that lead to that cell death and determine the importance of neutrophils and clotting on the induction of anti-tumour immunity

and success of VSV as a therapeutic. We first set out to test our ability to prevent the clotting in the vasculature and therefore perfusion of the tumour using heparin. Balb/c mice were engrafted with CT26 and treated with VSV along with four doses of heparin over the first 24 hours of infection (Figure 34A), a treatment regimen previously shown to prevent clotting in the tumour vasculature and prevent the vascular shutdown observed following VSV treatment[228].

Unfortunately, in our hands, we were unable to completely prevent vascular shutdown in the CT26 tumours when heparin was used in combination with VSV. There were some tumours that were completely perfused, yet others were not perfused, or partially perfused (Figure 34). Knowing that vascular shutdown was not impaired equally in all tumours, interpreting any survival studies would be difficult. Some tumours would still have an intact vascular shutdown, and we would not know which tumours these were as it can only be assessed by sacrificing the animals. Therefore we did not move forward assessing the impact of clotting following VSV treatment of CT26 has on the resulting immune response and survival following VSV therapy. Further optimization of heparin dosing schedules would be required to ensure that all tumours have an equal effect before pursing any survival or immunological studies.

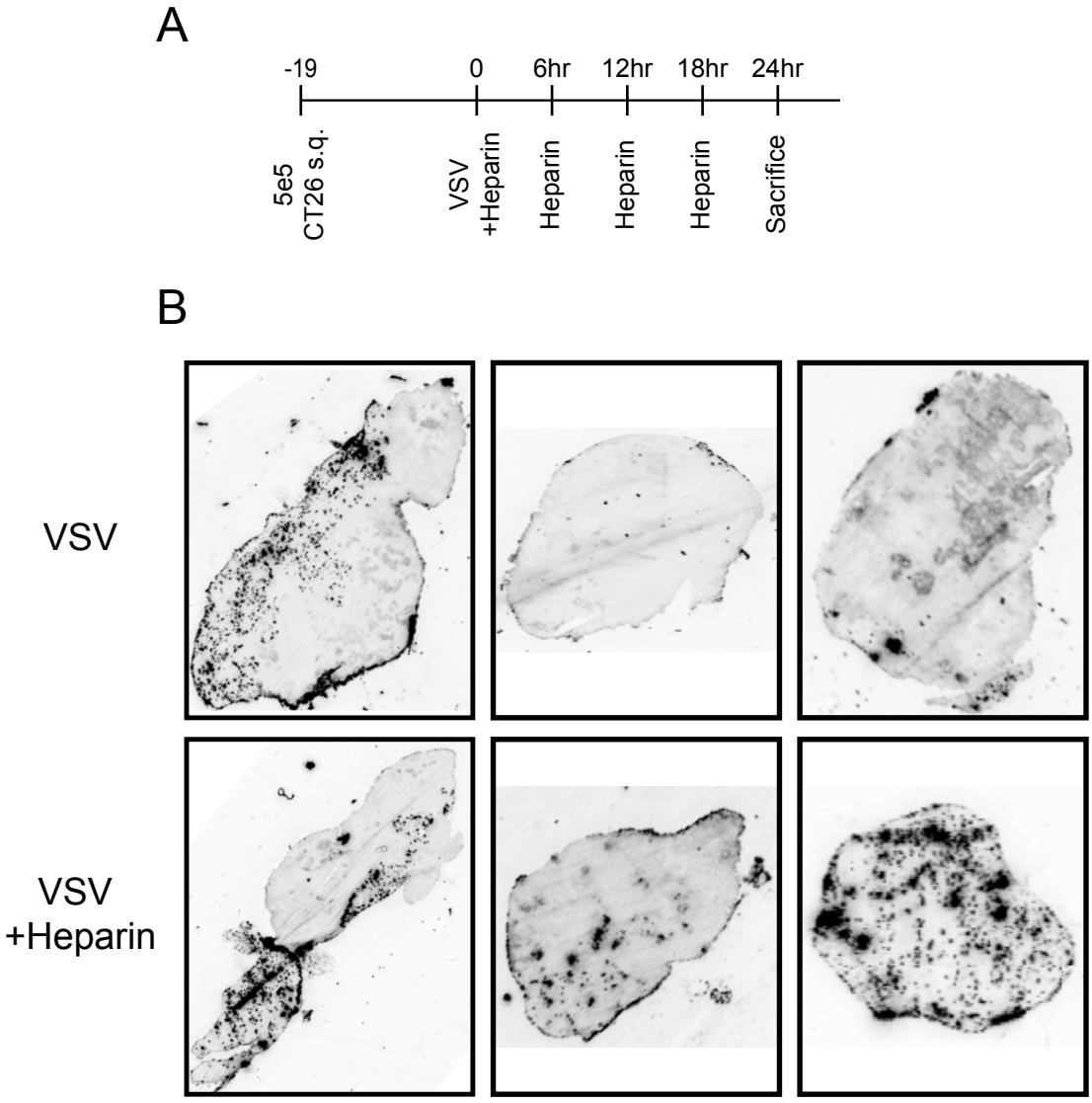


Figure 34 - Heparin treatment during VSV oncolysis does not completely prevent vascular shutdown. Balb/c mice bearing CT26 tumours were treated with ΔM51 VSV/GFP ± heparin to prevent clotting in the tumour during VSV oncolysis. Following ΔM51 VSV/GFP treatment, four doses of heparin were given over 22 hours and tumours were removed twenty-four hours after VSV treatment to assess tumour perfusion. A. Experimental outline. B. Mice were injected with fluorescent microspheres 5 min before sacrifice. Tumours were then removed, frozen in OCT and sectioned at 10 μm. Immediately following sectioning, tissues were scanned for fluorescence on Typhoon Scanner (GE).

2.4 Depletion of neutrophils impairs vascular shutdown

While heparin was unable to adequately inhibit VSV induced vascular shutdown, we could still address the question of what impact the vascular shutdown had on anti-tumour immunity and survival following VSV treatment by depleting neutrophils[227,228]. VSV infection of CT26 tumours leads to expression of numerous chemokines, including those involved in neutrophil trafficking[227]. Within 24 hours of infection, neutrophils are be observed in treated CT26 tumours ([227], and data not shown) and these neutrophils mediate events leading to vascular shutdown within the tumour, as in the absence of neutrophils tumours remain perfused[227]. However, the role of neutrophils and vascular shutdown in anti-tumour immune induction and survival is not known.

Before completing the full survival/immune study with neutrophil depletion during VSV treatment, we first assessed our neutrophil depletion and perfusion of tumours treated with VSV in neutrophil depleted animals. To this end, Balb/c mice bearing subcutaneous CT26 were treated with two doses of α-neutrophil antibody (α-Ly6G/C; clone RB6-8C5), every forty-eight hours beginning two days before the first dose of VSV (Figure 35A). Following ΔM51 VSV/GFP treatment the mice were sacrificed at the indicated time points (Figure 35A) and assessed for tumour perfusion, fibrinogen deposition, VSV infection and the presence of apoptosis in the core of the tumour (Figure 36). At the time of VSV treatment neutrophil depletion was >95% as assessed by CD11b and Gr-1 staining of PBMCs (Figure 35B). Unlike the heparin treatment, depletion of neutrophils was able to block the

vascular shutdown observed following VSV therapy (Figure 36; perfusion), indicating that we were able to recapitulate previously reported effects that neutrophils have on vascular shutdown in the tumour[227]. Neutrophil depletion ahead of VSV treatment was also found to decrease hemorrhage and clotting in the tumours (Figure 36; Fibrinogen) but had less of an impact on active caspase-3 staining. Even with the tumour fully perfused, VSV was still only found at the rim of the tumours in neutrophil depleted animals with some local foci of infection around what appear to be vessels in the centers of the tumours, but there was no difference in VSV infection between depleted and un-depleted animals (Figure 36; VSV). Since we were able to achieve the desired effects of neutrophil depletion we could now move into a larger survival study to assess the impact neutrophil mediated vascular shutdown has on survival and the resulting anti-tumour immune responses.

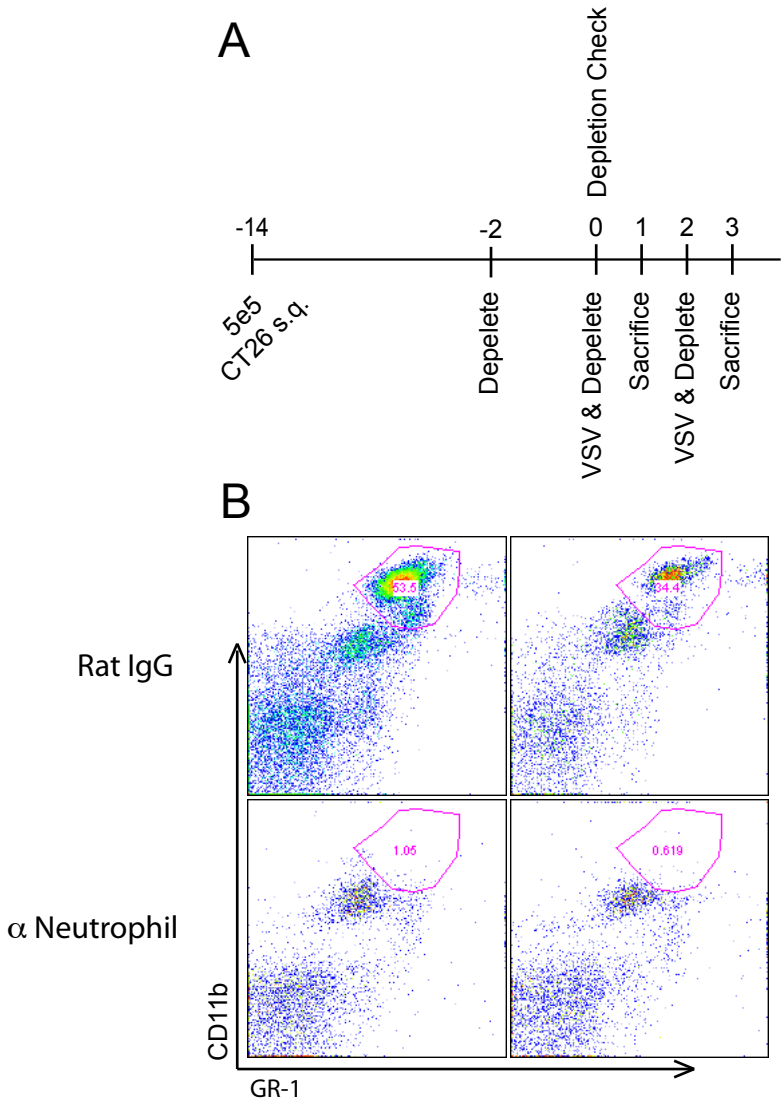


Figure 35 - Neutrophil depletion led to >95% reduction in neutrophils. Balb/c mice bearing subcutaneous CT26 tumours were depleted of neutrophils (150 µg of αGr-1 or Rat IgG) beginning two days before ΔM51 VSV/GFP treatment and subsequent doses were administered with VSV to maintain depletion. Mice were sacrificed on the indicated days to assess tumour perfusion and clotting, apoptosis and VSV spread by IHC on the indicated days. Neutrophil depletion was assessed in the blood prior to the beginning of treatment with ΔM51 VSV/GFP. A. Experimental outline. B. PBMCs were isolated and stained with CD11b and Gr-1 to assess neutrophil depletion. Samples were captured using FACS DIVA on a Canto II (BD Biosciences) and were analyzed using FlowJo (Treestar). Gated population indicates neutrophils that are $CD11b^{+}$ and $Gr\text{-}1^{hi}$. Neutrophils were reduced by 98% in depleted animals compared to IgG controls.

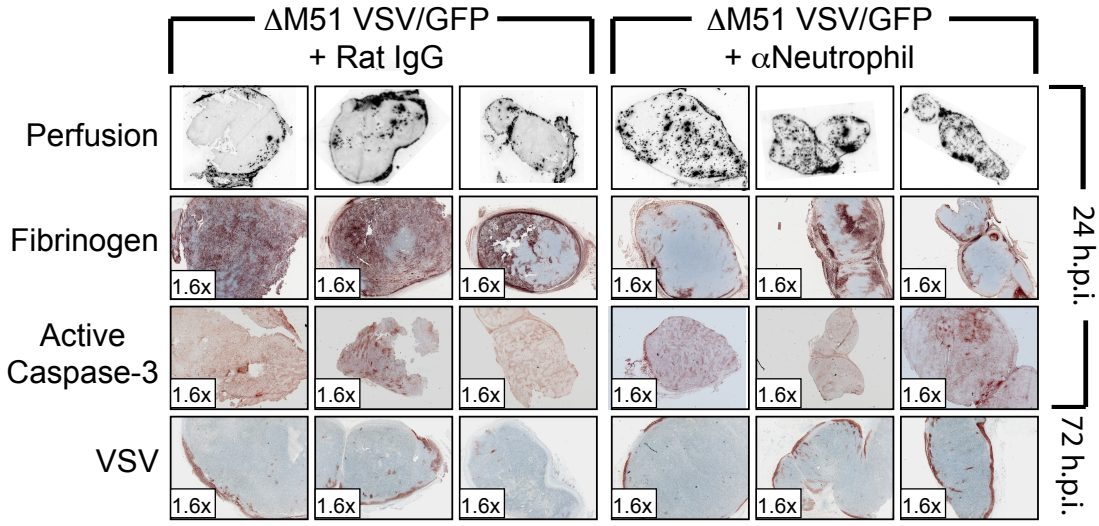


Figure 36 - Immunohistochemistry following neutrophil depletion during VSV treatment. Balb/c mice bearing subcutaneous CT26 were treated with ΔM51 VSV/GFP + α-neutrophil (n = 5) or ΔM51 VSV/GFP + rat IgG (n=5) as outlined in figure 35A. 24 hours after the first dose of ΔM51 VSV/GFP mice were injected with fluorescent microspheres for 5 min and then sacrificed. Tumours were removed. cross sectioned and half was frozen in OCT freezing medium while the other half was fixed in 10% formalin and then paraffin embedded. Frozen tissue was sectioned at 10 μm and scanned for perfusion with fluorescent microspheres and stained for active caspase-3 by IHC. Paraffin embedded sections were stained for fibrinogen by IHC. 72 hours following the first dose of VSV tumours were removed and fixed in 10% formalin. 4 μm sections were stained for VSV antigen to assess spread within the tumour.

Neutrophil depletion extends viral replication in CT26

The role of neutrophils in the control of viral infections is not completely understood, however it has been proposed that they play a role in control of some viral infections[330]. Depletion of neutrophils during VSV oncolysis has been shown to prolong replication of VSV when tumours were treated with a single dose of virus[227]. We therefore utilized a luciferase expressing oncolytic VSV to investigate whether in the context of a full treatment regimen, two doses of VSV forty-eight hours apart (Figure 37A), VSV replication is modified by the lack of

neutrophils. We assessed both the amount and duration of replication and found that there was a trend toward heightened VSV replication (Figure 37B). Detection of VSV replication was also extended from five days to seven days in the mice depleted of neutrophils (Figure 37B).

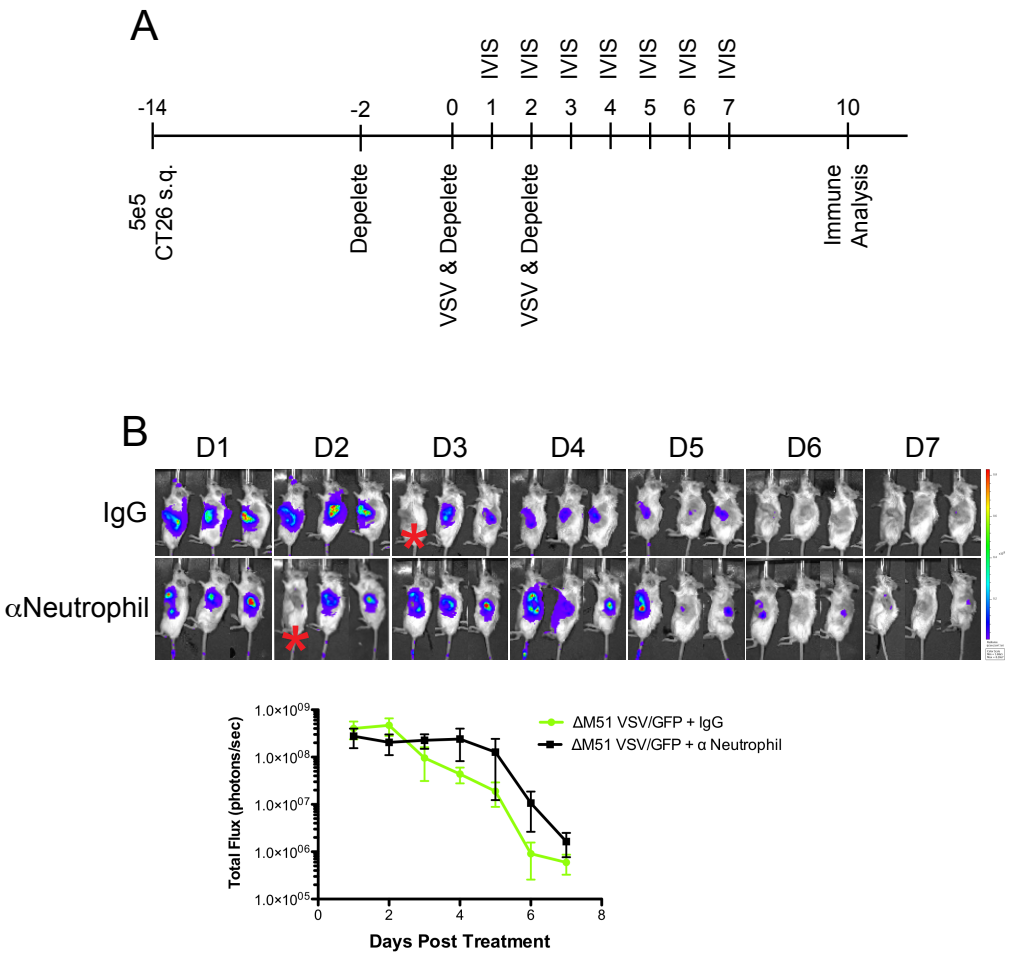


Figure 37 - Neutrophil depletion increases and extends VSV replication in CT26. Balb/c mice bearing CT26 tumours were administered α-neutrophil antibody (n = 5) or rat IgG (n = 5) and treated with ΔM51 VSV/SIIN-Luciferase to assess replication of VSV in tumours where vascular shutdown has been impaired in living animals by IVIS imaging. A. Experimental design. B. Daily images of animals taken using Xenogen IVIS-200 (Caliper Life Sciences). 20 minutes prior to image capture animals were injected with 3 mg of luciferin i.p. Total luminescence was calculated using Living Image 3.2 software (Caliper Life Sciences). Mice denoted with a red star indicate mice that there was an issue with capturing luminescence due to an issue with luciferin injection. These mice were not included in subsequent quantification. Data is presented as mean ± s.e.m.

Modification of tumour perfusion and viral replication with neutrophil depletion did not lead to an overall survival advantage

We next designed a set of experiments to assess the importance of vascular shutdown in induction of anti-tumour immune responses and overall survival when treating CT26 with ΔM51 VSV/GFP. The depletion and viral treatment schedule was the same as in figure 37A. Two independent experiments were conducted and are presented in figure 38A and B. In the first attempt, depicted in figure 38A, the depletion of neutrophils had no added benefit on tumour regression through the first two weeks of treatment. As the experiment progressed, differences in tumour growth began to emerge. The lower mean tumour volumes of animals treated with ΔM51 VSV/GFP and α-neutrophil antibody was a result of more tumours regressing in this group leading to a survival advantage, with 66.67% of animals surviving compared to only 20% of animals treated with ΔM51 VSV/GFP and a control rat IgG antibody. The differences in tumour growth were significantly different (two-way ANOVA; treatment $P = 0.0072$). When the survival curve for this individual replicate was analyzed (data not shown) there was no difference by Log-Rank test. With such a large difference in the survival percentages of the two groups a Chi-square test was ran on the final survival proportions. While this analysis did not lead to a significant difference, there was a trend towards significance with P value of 0.09. A power calculation was performed and it was found that with the group sizes in this experiment there was a 50% chance of rejecting a false null hypothesis, that

there is no difference between the survival curves (DSS Research Statistical Power Calculator, http://www.dssresearch.com/KnowledgeCenter/toolkitcalculators/statisticalpowercalculators.aspx). In order to get a proper assessment of whether there was a true significant difference (at an α level of 0.05) in survival of animals depleted of neutrophils it was determined that both depleted and non-depleted groups need to contain a minimum of 13 animals to reach a power of 80%, meaning there is only a 20% chance that a false null hypothesis would fail to be rejected (DSS Research Statistical Sample Size Calculator, http://www.dssresearch.com/KnowledgeCenter/toolkitcalculators/samplesizecalculators.aspx).

To increase our statistical power mice were again treated as in figure 37A (except no IVIS was carried out) with ΔM51 VSV/GFP and neutrophil depletion with n=10 per group. Unlike the first attempt, in this second experiment there was no difference in either the tumour growth curve (Figure 38B) or survival (data not shown). And when the survival of each experiment was combined (Figure 38C) there was no difference in the survival curves by log rank, and the overall survival proportions were not significantly different (Chi-square P = 0.1258, Power = 89%).

Neutrophil depletion impairs vascular shutdown and subsequently how the tumour dies during oncolysis, therefore we assessed the immune responses to determine if anti-tumour immune responses differ in the absence of neutrophils and vascular shutdown. Combining the data from two independent experiments

(survival of combined experiments is presented in Figure 38C) there was a significant improvement in the anti-tumour immune response in animals where vascular shutdown was impaired by neutrophil depletion (Figure 39A). When the data was assessed more closely it was determined that depletion with the α-neutrophil antibody clone we used also depleted a portion of the $CD8^+$ T cells as measured in the blood (Figure 40A). After the immune analysis was completed, it was discovered that the antibody clone used to deplete neutrophils in this experiment has been shown to deplete a population of $CD44^{hi}$ $CD62L^{hi}$ memory $CD8^+$ T cells[331]. With such a large difference in the numbers of circulating $CD8^+$ T cells, this could be an explanation for the observed increase of anti-CT26 $CD8^+$ T cells in mice depleted of neutrophils (Figure 39A). Therefore, the immune data from the survival study presented in FIgure 38B was analyzed to determine absolute numbers of CT26 and VSV specific $CD8^+$ T cells circulating in the blood. When the absolute numbers were compared, there was only a slight increase in neutrophil depleted mice that was not statistically significant (Figure 40C). Therefore the significant improvement in anti-tumour $CD8^+$ T cell response presented in figure 39A is a function of the differences in CD8 numbers rather than a true impact of vascular shutdown impairment on the anti-tumour immune response induced by oncolytic treatment.

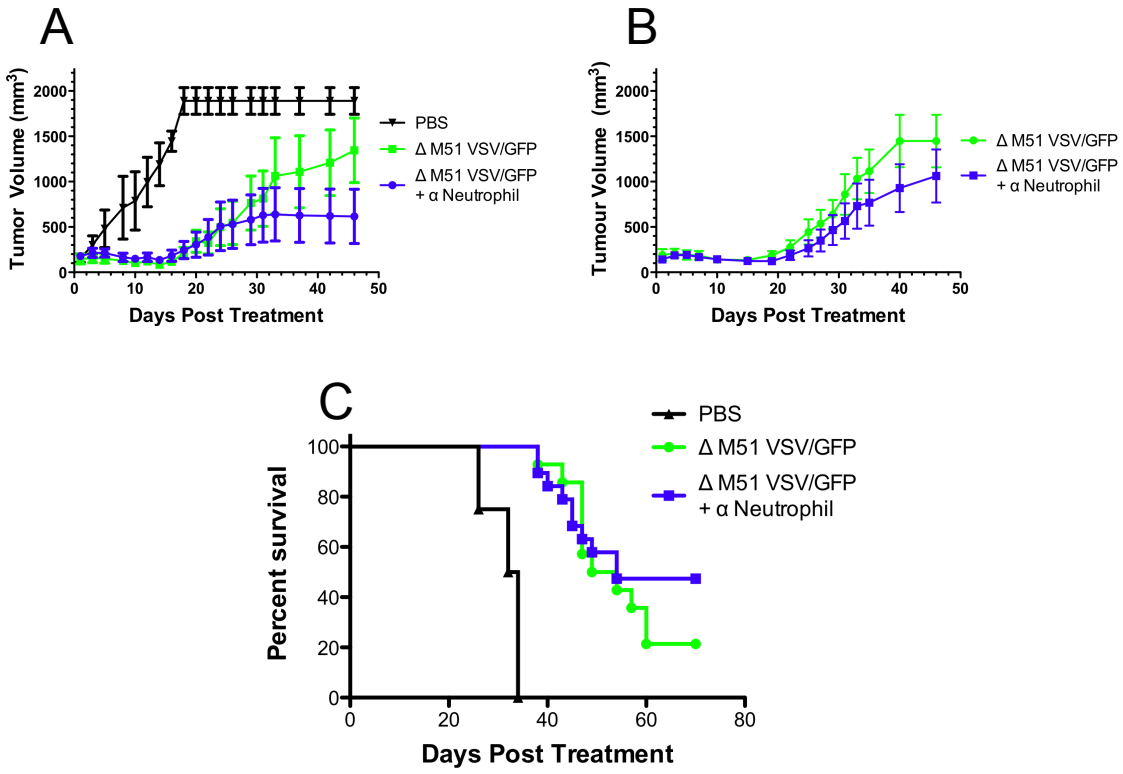


Figure 38 - Depletion of neutrophils during VSV oncolysis has no significant treatment effect. A. Mice bearing established CT26 tumours were treated with PBS (n=5), ΔM51 VSV/GFP + rat IgG (n=5), ΔM51 VSV/GFP + α-neutrophil (n=9). Once tumours reached ~ 250 mm^3, mice were treated with two doses of $5x10^8$ PFU of the indicated virus i.v. 48 hours apart and α-neutrophil or rat IgG (see figure 35A for experimental outline). B. A. Mice bearing established CT26 tumours were treated with ΔM51 VSV/GFP + rat IgG (n=10), ΔM51 VSV/GFP + α-neutrophil (n=10). Once tumours reached ~ 250 mm^3, mice were treated with two doses of $5x10^8$ PFU of the indicated virus i.v. 48 hours apart and α-neutrophil or rat IgG (see figure 35A for experimental outline) Tumour volumes were measured and calculated as an ellipse (where volume = 4/3 x Pi x L/2 x $((W/2)^2)$), shown as mean ± s.e.m. A and B show two independent experiments C. Survival was monitored and depicted above. Data is combined from two independent studies presented in A and B; PBS (n=5), ΔM51 VSV/GFP + rat IgG (n=15) and ΔM51 VSV/GFP + α-neutrophil (N=19).

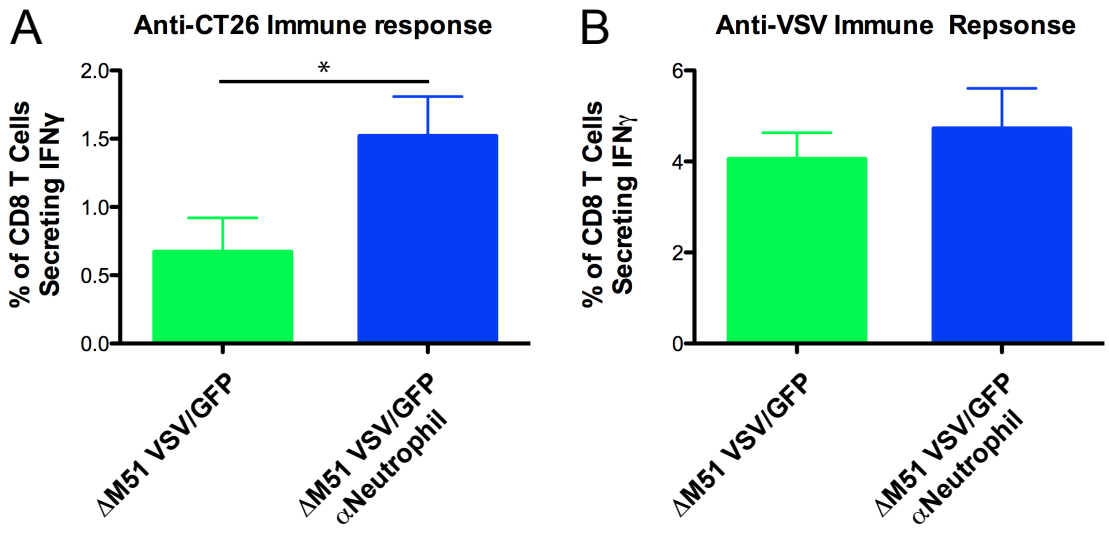


Figure 39 - Inhibiting vasculature shutdown through neutrophil depletion significantly improves the percentage of anti-tumour CD8$^+$ T cells. 10 days after the first dose of ΔM51 VSV/GFP PBMCs were stimulated *ex vivo* with to determine the impact of impairing vascular shutdown on anti-tumour and anti-viral immune responses in A and B respectively. Data is combined from two independent experiments presented in figure 38 and presented as mean ± s.e.m.; * P = 0.0188)

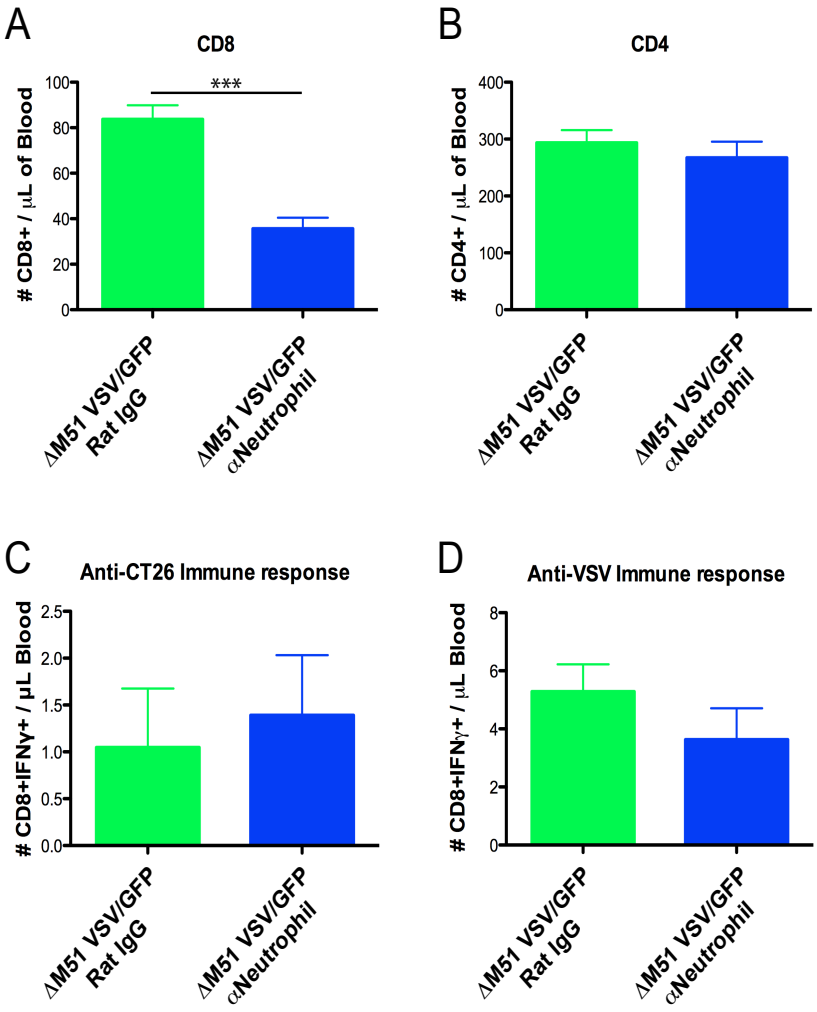


Figure 40 - Neutrophil depletion also depletes CD8$^+$ T cells. Cell counts in PBMCs of CD8$^+$ and CD4$^+$ T cells, A and B respectively. With such a discrepancy in the numbers of circulating CD8$^+$ T cells in depleted animals, the absolute numbers of tumour and VSV specific CD8$^+$ T cells were calculated and are presented in C and D respectively. Data are from experiment presented in figure 38B and are shown as mean ± s.e.m.

3.0 Discussion

Oncolytic VSV works well in CT26 curing upwards of half of animals treated, therefore there is still room for improvement. There are a number of possible ways to improve VSV including expression of transgenes, discussed earlier, or through the use of pharmacological compounds modifying cell death, clotting or acting directly on immune cells. In order to determine which path will lead to the best therapeutic protocol, we need to gain a better understanding of what impact events following infection of the tumour with oncolytic VSV have on therapeutic outcomes. This is especially important when addressing the impact on the immune responses generated. It is clear that inducing a robust anti-tumour immune response following oncolytic therapy is required for a successful outcome following VSV treatment, therefore the impact of vascular shutdown, neutrophils and clotting were assessed for their role in generating anti-tumour immune responses and ultimately survival.

Along with viral replication and direct oncolysis, which is required, there are indirect processes during oncolytic VSV treatment leading to vascular shutdown and apoptosis throughout the core of the treated tumour[227,228]. It is not known what contribution these indirect events have on immune induction and overall survival. Therefore we set out to assess which processes were critical for the induction of anti-tumour immunity and therefore successful oncolytic therapy. To accomplish this goal we designed three sets of experiments to separate out the vasculature shutdown, apoptosis and role of neutrophils in oncolytic therapy.

First, we attempted to prevent apoptosis during oncolysis to determine the role apoptosis in the core of the tumour plays in anti-tumour immune response induction. Second, the role of vasculature shutdown during oncolysis was assessed by inhibiting fibrinogen deposition or depleting neutrophils. Utilizing two separate strategies to impair vascular shutdown we were also able to address the role of neutrophils in the absence of vascular shutdown. By separating these events we hoped to gain knowledge about which aspects of VSV oncolysis are critical and should be manipulated to improve VSV oncolytic therapies.

We began by investigating cell death in the core of the tumours attempting to prevent apoptotic cell death through the use of Z-VAD-FMK and DEVD-FMK. We unfortunately ran into a number of technical issues in the use of these inhibitors. We began by going straight into a survival study using Z-VAD in combination with oncolytic VSV (Figure 25). In this study, Z-VAD-FMK was found to aid in better control of tumours early on but ultimately there were no differences observed in either survival or immune responses. Unfortunately when we further investigated Z-VAD-FMK and its effect on viral replication (FIgure 26) in the tumour we found that Z-VAD-FMK was unable to prevent apoptosis in the tumour and therefore could not be pursued further since the desired effect was not achieved.

The reason that Z-VAD-FMK was unable to prevent caspase-3 activation in the tumour is likely due to issues around dose and timing of doses. Caspase-3 activation in the core of the tumour appears early on in the therapy. While Z-VAD-

FMK is an irreversible pan-caspase inhibitor, it is likely that the effects of Z-VAD-FMK lasted less than 24 hours, which was the timing between doses, allowing the cells to undergo caspase-3 activation once they were able to make new substrates. The timing of the Z-VAD-FMK doses was poorly designed. The cell death we were trying to prevent occurs very early following VSV treatment. It is usually detectable between 24-48 hours (Figure 26B). Therefore with only one dose of Z-VAD-FMK prior to 24 hours after treatment we were likely set up for failure. In an attempt to improve the inhibition we set up a new pilot study utilizing a more specific caspase inhibitor, DEVD-FMK, which specifically inhibits caspase-3/7. As well we concentrated the doses between 24 and 48 hours after treatment attempting to prevent caspase-3 activation early to have a maximal impact on preventing apoptosis following VSV treatment (Figure 27). Compressing the number of doses to every 6 hours between 24 and 48 hours still failed to prevent caspase-3 activation. It is not clear why this dosing schedule was unable to impact caspase activation. This failure is likely related to non-optimized route of delivery, dose and timing leading sub-optimal concentrations in the tumour at the time of caspase-3 activation. Without a working inhibitor we next moved onto making a stable CT26 cell line that would be resistant to apoptosis to assess the importance of indirect apoptosis in the core of tumours following oncolytic Virus treatment.

To construct a stable cell line that resists apoptosis we chose to use Bcl-2 as it is not expressed in CT26[332] and in the literature it has been shown to impair

apoptosis in a number of cell lines[333-335]. While the cell line expressed Flag-Bcl-2 (Figures 26 & 29) and performed as expected *in vitro* (Figures 30 & 31), when subcutaneous CT26.Bcl-2 tumours were treated *in vivo* with ΔM51 VSV/SIIN-Luciferase they responded similarly to CT26 parental tumours with respect to replication (Figure 32), immune responses and overall survival (Figure 33). Immunohistochemistry was attempted on endpoint tumours in this study to ensure FLAG-Bcl-2 was expressed for the duration of the experiment. The FLAG antibodies that we currently use have some background when used on mouse cells, which can be seen by both western blot and immunofluorescence(data not shown). This background ended up causing problems with the immunohistochemistry and a protocol was not able to be optimized to minimize the background observed, preventing assessment of the expression of FLAG-Bcl-2 in the stable cell line *in vivo*. Alternatively, the tumour sections should have been stained with an anti-Bcl-2 antibody to assess Bcl-2 levels in both CT26 and CT26.Bcl-2 tumours. Although it is not clear in this experiment whether expression was stable in the mice, in a previous test, FLAG-Bcl-2 expression was detected from a CT26.Bcl-2 explanted tumour that was put into culture in the presence of blasticidin (Figure 29A Lane 7). Therefore it is probable that FLAG-Bcl-2 was expressed in the survival study presented in figure 33, however it still remains a possible explanation for the lack of any differences between the stable and parental cell lines. To fully assess what occurred in this study we would need to repeat the experiment assessing acute effects in the tumour, focusing on

caspase-3 activation and determine if cell death in the core of the tumour still occurred following VSV treatment.

Treating the CT26.Bcl-2 tumours with VSV still leads to vascular shutdown and subsequently cell death in the core of the tumour. Since CT26.Bcl-2 tumours express BCL-2, they should not be able to initiate apoptosis via the intrinsic apoptotic pathway, however pathways not inhibited by Bcl-2 will still be active, including the extrinsic apoptosis pathway[336]. With treatment outcomes similar between parental and stable CT26 tumours, it is likely that the cells in the tumour died in a similar fashion, albeit possibly through different pathways. The signals leading to the induction of caspase-3 cleavage in the core of the tumour following VSV treatment are not currently known. While Bcl-2 expression in the tumour will impair apoptosis originating from intrinsic pathways mediating mitochondrial membrane permeability and subsequent caspase-3 activation; Bcl-2 will have less impact on apoptotic programs that go through other pathways including death receptors. Since caspase-3 activation is the culmination of a number of pathways, it is not known if CT26 and CT26.BCL-2 go through the same upstream signaling cascade. Therefore it is possible that the ultimate outcome in CT26 and CT26.Bcl-2 in terms of core cell death are equivalent, even though the manner in which they become active caspase-3 positive may be different.

With vascular shutdown of tumours intact, both CT26 and CT26.Bcl-2 tumours underwent similar infarcts leading to cell death in the tumour core. Attempting to block the resulting apoptotic cell death would push cells toward a

necrotic type of cell death. However, this modification might not have ultimately led to differences in the cell death between CT26 and CT26.Bcl-2 tumours. As cells die by apoptosis the innate immune cells attempt to clear them quietly, without immune activation. However this system can become overwhelmed leading to inefficient clearance of apoptotic cells[235]. These cells therefore continue through apoptosis to secondary necrosis due to the lack of clearance by innate phagocytes[235]. Therefore, while attempting to inhibit apoptosis in CT26.Bcl-2, the cells may have been directed to the same outcome that is likely to occur naturally following oncolytic VSV treatment.

Taken together, it is potentially difficult, if not improbable, that any intervention will be able to significantly modify the cell death in the core away from what naturally occurs during ΔM51 VSV treatment. This is especially true without knowing exactly what signal leads to the cell death that occurs and focussing on the correct pathway rather than attempting a general inhibition of apoptosis. These data lead to the conclusion that events upstream of the core cell death, neutrophil recruitment and clotting, are likely more important in the overall effects observed during oncolytic VSV treatment.

There are two known ways to prevent vascular shutdown following oncolytic VSV treatment of CT26, through depletion of neutrophils and preventing clotting of the blood vessels allowing tumours to remain perfused[227,228]. While both affect vascular shutdown, by using two different methods we can also ask the question of what impact neutrophils have, at least in the absence of vascular

shutdown. Learning from the experiences with Z-VAD and DEVD, we wanted to first ensure that we could accomplish the desired effects of combining heparin with VSV prior to taking on larger studies. Unfortunately the previously reported[228] effects of heparin treatment during VSV oncolysis could not be replicated. While there was a partial impairment in some tumours, it was not complete or consistent enough to continue on with heparin. Therefore we focussed our efforts on neutrophil depletion to determine the role that vascular shutdown has on VSV oncolytic therapy, specifically on the induction of anti-tumour immune responses.

Neutrophil depletion worked well to impair vascular shutdown leaving tumours well perfused compared to mice treated with IgG controls (Figure 36). There was also a reduction in fibrinogen staining in these depleted tumours indicating there was less clotting and hemorrhage in the depleted tumours (Figure 36). This replicated well previously reported data on neutrophil depletion[227]. VSV replication has also been shown to be impacted by the lack of neutrophils, prolonging replication[227]. In this report only one dose of virus was used to assess replication, which does not completely recapitulate the typical treatment regimen used with oncolytic VSV. However, it was confirmed here that with two doses there was an increased luciferase signal in tumours of neutrophil depleted animals, and this signal lasted longer, to almost 7 days of viral replication (Figure 37). Even with these effects on the tumours during oncolysis, and a small survival advantage in the neutrophil depleted group (47% vs 21% in

controls) in the end there was no significant difference in overall survival (Figure 38C) or change in the resulting anti-tumour immune response observed (Figure 39C).

One significant complication with interpreting the immunological data when depleting neutrophils was that the α-neutrophil antibody clone (RB6-8C5) that was utilized also depleted a significant number of $CD8^+$ T cells (Figure 40A). Upon further investigation, the RB6-8C5 has been shown to not only deplete neutrophils but also subsets of $CD8^+$ T cells ($CD44^{hi}$ $CD62L^{hi}$ central memory T cells) and monocytes[331,337]. This is due to RB6-8C5 binding to both Ly-6G and Ly-6C. An alternative approach to deplete neutrophils would be to use clone 1A8 which only binds Ly-6G leading to a more specific depletion of neutrophils, however possibly to a lesser extent than RB6-8C5[337].

Even with the depletion of some $CD8^+$ T cells, we were still able to detect a robust anti-tumour immune response indicating that these T cells were left intact. Initially it appeared that in the absence of neutrophils there was a significant increase in the anti-tumour immune response generated when viewed as a percentage of $CT8^+$ T cells (Figure 39A). Further analysis revealed that these numbers were skewed due to the fact that there is a much lower number of $CD8^+$ T cells in the periphery (Figure 40A). When the absolute numbers of tumour specific T cells were quantitated there was no difference between those mice depleted of neutrophils and those treated with control IgG. It is difficult to interpret this data with the knowledge that the neutrophil depletion would have also

depleted monocytes and T cells[331,337]. Following infection monoctyes are recruited and play an important role in the initiation of adaptive responses[338]. If the monocyte population is impacted by the depletion the resulting ability to properly mount an adaptive response could be impaired. This can be seen by a partial, although not significant, reduction in the anti-viral immune response in neutrophil depleted animals (Figure 40D). Therefore to fully assess the impact of neutrophil mediated vascular shutdown on the induction of anti-tumour immune responses these studies will need to be repeated utilizing a different clone, 1A8, which more specifically deplete neutrophils.

It was hypothesized that in the absence of neutrophils, VSV treatment of tumours would not be as successful. It was thought that without shutdown and the large bolus of core cell death observed that immune responses would be impaired and survival would actually be decreased in depleted animals. In the end this was not the case and in fact there was a slight survival advantage, although not statistically significant, in neutrophil depleted animals. One effect of the depletion is an increase in the duration of viral replication. This increased replication could make up for some of the tumour growth control that was lost from the lack of vascular shutdown. A caveat that needs to be considered is that the increased replication may be due to a loss of monocytes in addition to the neutrophils during the depletion. Monoctyes have been shown to play an important role in the control of viral infections[339-341] and if their numbers are decreased, viral control can be compromised leading to the increased duration of

replication. This is yet another reason that these studies would need to be repeated with a more specific depletion. The depletion of neutrophils also impacts on the immunological cell populations present in the tumours. The loss of neutrophils, and possibly other immune populations due to the depletion of Ly-6G and Ly-6C, may be compensated for by other immune cell types. This was not assessed but would need to be in the future in order to determine the makeup of cell types in a VSV treated tumour in the absence of neutrophils. This will help in determining the compensatory roles that a change in immune cell make up plays in relation to preventing vascular shutdown.

On the surface it appears that manipulating the indirect effects that occur following VSV treatment of tumours did not lead to any significant changes in the ultimate outcome of the therapy (Table 5). There were however some issues and oversights associated with some aspects of the work presented in this chapter. These issues will need to be addressed before a definitive conclusion can be made as to the true impact of vascular shutdown on the immunological and survival outcomes following VSV therapy. Any time a biological system is perturbed by means of depleting a cell type or modifying apoptotic pathways, compensatory mechanisms will likely be activated and need to be considered carefully when interpreting the data obtained.

Table 6 - Survival and immunological outcomes from interventions presented in Chapter 5.

	Vascular Shutdown	Neutrophil	Apoptotic Core	Outcome (cured animals)	Mean Anti-Tumour Immune Response
VSV	+	+	+	Cure 20-50%	2-5%
VSV + Z-VAD	+	+	-/ alternative death pathways	20%	0.5-1%[a]
CT26.Bcl-2 Stables	+	+	-/ alternative death pathways	20%	2-2.5%[b]
VSV + Heparin	-	+	-	NC	NC
VSV + Neutrophil Depletion	-	-	-	50%	1.5%[c]

NC: Not completed

[a] While relatively low, this mean anti-tumour response was equivalent to ΔM51 VSV/GFP treated controls

[b] Only one mouse had a significant response in this group leading to the mean, four mice had no response

[c] Neutrophil depletion led to a reduction in CD8 as well, therefore the percentage of tumour reactive cells is not completely accurate.

~ Chapter 6 ~

Summary and Conclusions

The data herein describes the work conducted on VSV oncolytic viruses during my PhD. The studies described were designed to gain further understanding of VSV oncolytic therapy in an attempt to improve VSV as an oncolytic virus through the manipulation of anti-tumour immune responses following VSV therapy.

1.0 Summary of findings

In **Chapters 3 and 4** we spent a considerable amount of time and effort on improving VSV through the addition of transgenes that were hypothesized to improve on the anti-tumour immune responses generated during VSV treatment. There are a number of examples of adding transgenes to oncolytic viruses (Introduction, section 3.3) showing improvements in anti-tumour immunity following oncolytic virus treatment and improving therapeutic outcome. The addition of transgenes to VSV was approached from two directions; engineering the VSV vectors to express either cell-autonomous transgenes or a highly secreted immunomodulatory cytokine.

What was realized is that of all the transgenes added (p14 FAST, F1L, FPV039 and hIL-15) the only successful iteration was the expression of a highly secreted version of IL-15. We were able to show that the expression of hIL-15 from VSV led to significantly improved anti-tumour immune responses leading to improved survival following oncolytic therapy[167]. The simple explanation for the differences in the success of ΔM51 VSV/opt.hIL15 and viruses expressing cell-

autonomous transgenes is that when treating tumours, especially subcutaneous tumours, VSV infused intravenously only infects a small area of the tumour. As discussed previously, this relatively small infection leads to large indirect effects of vascular shutdown and cell death in the tumour core[227,228]. It is unlikely that modification of a limited number of infected cells had significant effects compared to the more dominant effect of tumour core cell death. The cell death in the core of the tumour is so vast that it is unlikely that it was be cleaned up “quietly”, leading to more immunogenic secondary necrotic cell death[235].

Another issue with expressing a cell-autonomous transgene from VSV is the limited duration of replication, and therefore limited temporal expression of the transgene. As with many RNA viruses, VSV replicates quickly to maximize viral spread before innate viral responses are mounted in an effort to limit replication. Therefore a cell-autonomous transgene must have a rapid and significant impact on the desired processes within the infected cell as the infected cell dies shortly after infection. In contrast, a soluble transgene such as hIL-15 is going to be secreted throughout replication and have local and systemic effects on the immune system, specifically NK and $CD8^+$ T cells.

The use of any transgene to modify an oncolytic virus needs to be thought out critically taking into account the characteristics of the oncolytic virus being used, especially replication. Based on the data presented in Chapters 3 and 4 it would not be recommended to add cell-autonomous transgenes to VSV, or any

other RNA virus that replicates quickly and shows limited foci of replication in treated tumours.

In order to further improve VSV we need a better understanding of which events are required and critical for the induction of anti-tumour immunity and survival of treated animals. We know that virus replication is required (data not shown) and induction of anti-tumour immune responses is needed to keep the tumour in check (Figure 2), leading to durable cures. However the impact of other indirect events during VSV oncolysis, mainly vascular shutdown and cell death in the core of the tumour, on therapeutic outcome is currently not understood. In **Chapter 5** we have attempted to dissect these events to determine if any or all were required for successful VSV therapy. With a better understanding of the importance of each event, we will be able to design better oncolytic viruses, alone or in combination with other therapeutic agents, by manipulating critical components of oncolytic VSV therapy.

In attempting to blunt vascular shutdown and tumour cell death we encountered a variety of technical hurdles. Neither pharmacological inhibition of caspase activation nor heparin were able to achieve the desired outcome and were unable to be pursued further. Therefore we continued the studies with a cell line, which *in vitro* was found to resist apoptosis to VSV and staurosporine, and neutrophil depletion. In the end there were no statistically significant differences observed by impairing apoptotic cell death or neutrophil mediated vascular

shutdown, however there were some technical issues that made interpretation of these results somewhat difficult, as previously discussed.

While the data surrounding the impact of apoptotic cell death in the core of tumours following VSV therapy may be somewhat inconclusive, I believe that with such a large amount of death occurring due to vascular shutdown, that it will be sufficiently immunogenic due to lack of efficient clearance[235]. Therefore the upstream effects, mainly VSV replication and vascular shutdown, were likely the critical events driving therapeutic efficacy. Future studies will need to more carefully address the impact of vascular shutdown, and whether it is a useful pathway to target. In the current studies, inhibiting vascular shutdown through neutrophil depletion led to a slight increase in overall survival, however there were two significant problems with this study. First, the power of the study is quite low. Assuming the data obtained represent the true outcome, then the power associated with the study is 0.57. This indicates that there is a greater than 40% chance that a false null hypothesis (there is no difference between the overall survival of depleted and undepleted animals) was rejected. In other words, there is a reasonable probability that this outcome may be a false negative. At the survival rates in figure 38C, to be sufficiently powered (power of 80%) we would require a balanced sample size of 72 mice per group, which is not a feasible number to attempt to repeat the experiment as presented. The second issue with the experiment is neutrophil depletion with the antibody clone used (RB6-8C5) also depleted some $CD8^+$ T cells (Figure 40A) and likely some monoctyes[337].

Therefore it is possible that the induction of immune responses may be partially impaired. To truly assess the impact of vascular shutdown on the induction of anti-tumour immune responses, a more specific depletion with a different more neutrophil specific clone (1A8) will be required. As well, it would be interesting to inhibit vascular shutdown while keeping neutrophils intact to determine their role in oncolytic VSV therapy.

The research presented as part of my PhD thesis has made contributions to the field of oncolytic virotherapy through gaining an improved understanding of how to modify VSV oncolytics, and potentially any RNA based oncolytic virus, through the addition of transgenes. We have also begun to gain further knowledge on the impact of indirect processes involved in VSV oncolytic virotherapy.

2.0 Considerations for future VSV oncolytic studies.

Although the CT26.Bcl-2 cell line appeared to die differently from parental CT26 *in vitro*, there was no impact of Bcl-2 expression on VSV therapy. It would have been interesting to further assess the impact of modified cell death on the immunogenicity of the infected CT26.Bcl-2 cell line. When treating tumours *in vivo* it is difficult to control infection and cell death, but the level of infection and cell death can be easily controlled during *in vitro* infections. The use of an infected cell vaccine (ICV) approach would have allowed us to assess the immunogenicity of CT26.Bcl-2 in comparison to CT26. The application of ICV

approaches, where tumour cells are infected *in vitro* and then administered to animals to generate anti-tumour immune responses, have been shown to be successful in a prophylactic and therapeutic settings[342]. Therefore to assess the immunogenicity of dying CT26.Bcl-2, VSV infected CT26.Bcl-2 and parental CT26 could be used to vaccinate tumour bearing and tumour free animals followed by assessment of anti-CT26 immune responses and rejection of existing tumours or subsequent tumour challenge. The advantage of this approach is that infected tumour cells can also be assessed for infection and cell death using flow cytometry at the time they are injected.

While it would be hypothesized that the immune response generated to infected CT26.Bcl-2 would be enhanced due to modified cell death, it is plausible that there would be no difference between the two cell lines. While typically apoptotic cell death is seen as tolerogenic, more recently it has been shown that apoptosis can be inflammatory and able to lead to immune induction (see Chapter 3, section 1.1). Therefore, while VSV infection induces apoptosis, in the context of the viral infection and associated PAMPs the apoptosis generated may be sufficiently immunogenic. Either way, it would have also been interesting to test the ability to boost anti-tumour immunity induced following oncolytic therapy. An ICV could be administered between 10 and 14 days following VSV treatment while treated tumours are still being held in check to determine if this strategy would be able to further enhance anti-tumour immune responses and survival of treated animals.

Moving forward, there is still room to improve VSV as an oncolytic virus. Treatment of subcutaneous tumours with ΔM51 VSV/GFP extends survival, but only cures 1/3 of animals, and the added benefit from expression of IL-15 was only able to cure 1/2 of mice in a lung metastases model[167]. However, in the design of future studies further consideration needs to be afforded to the control virus used (ie. GFP expression) and to the power of the experiment being performed.

In the experiments presented, ΔM51 VSV/GFP was used as the control virus for consistency as it was the virus used early on in my studies. Although GFP is thought to be innocuous, the use of GFP as a control transgene may not be the ideal choice as it has been found to impact on cellular signaling[343]. In experiments assessing the impact of immunogenic transgenes, the more appropriate control would be a functionally inactive version of the same transgene. Alternatively, a control virus lacking a transgene could be used. This transgene-less virus would need to be compared to GFP for both replication differences and *in vivo* to ensure there are no differences in oncolytic efficacy. With that being said, the likelihood of a cell-autonomous transgene, such as GFP, having an impact on the outcome of therapy is unlikely. However it would be useful to assess the impact of GFP.

A potentially more important consideration is the power associated with any experimental design. In the majority of experiments 5 mice were used to initially test a new therapeutic regimen. However, for an experiment this size to

be sufficiently powered, effectively every animal would have to be cured assuming a survival rate of 30% in control animals (Table 6). In order to be able to accurately assess smaller difference 10-15 animals would be required to reach appropriate power of >80% (Table 6). Therefore I would argue that initial pilot studies were generally under powered, and small but significant differences may be overlooked or missed. A second consideration is that an unbalanced experimental design has the potential to reduce the power of experiments, therefore experimental designs should take this into consideration, ensuring equal numbers of animals in all groups (Personal communication with Dr. Jamila Hamid).

Table 7 - Power associated with group numbers and overall survival assuming 30% survival of control animals. N1 and P1 represent number of animals and proportion of animals surviving after treatment 1, respectively. N2 and P2 represent number and proportion of control animals surviving, respectively. D represents difference in survival. (Analysis performed in PASS statistical software with the help of Dr. Jamila Hamid)

Power	N1	N2	P1	P2	D	Nominal α	Actual α
0.8036	72	72	0.5	0.3	0.2	0.05	0.0523
0.8122	33	33	0.6	0.3	0.3	0.05	0.0518
0.8074	17	17	0.7	0.3	0.4	0.05	0.0598
0.8103	12	12	0.75	0.3	0.45	0.05	0.0615
0.8404	11	11	0.8	0.3	0.5	0.05	0.0554
0.8224	7	7	0.85	0.3	0.55	0.05	0.0964
0.8325	6	6	0.9	0.3	0.6	0.05	0.0933
0.8613	5	5	0.95	0.3	0.65	0.05	0.0914

3.0 Concluding remarks

With phase III clinical trials beginning and backing from the pharmaceutical industry increasing[344], oncolytic viruses are gaining momentum as a valuable new treatment modality in the fight against cancer. Not only has the safety of oncolytic viruses been excellent, there are numerous clinical trials that have shown they are also efficacious in a number of patients and cancer etiologies (Table 1). With that being said there is definitely room to improve these viruses, and we believe that harnessing the immune system is the best way to improve on current oncolytic virus platforms.

In light of mounting evidence in both mice and humans indicating that the immune system is critical in control of growing malignancies and successful therapeutics, it is important for future research and clinical trial design to address the anti-tumour immune response. When considering how to improve immunity following oncolytic virus treatment of cancer, aiming for an increased magnitude of response is likely not the only way to improve oncolytic therapeutics. We have observed a highly variable ability to induce anti-tumour immune responses, ranging from no detectable response to greater than 5% anti-CT26 $CD8^+$ T cells. Therefore, moving forward it will be important to determine methods to more consistently induce anti-tumour immunity, which will lead to improved overall therapeutic outcomes. To this end we have shown that the addition of a cytokine, IL-15, to VSV leads to improved immune responses and therapeutic outcome.

Oncolytic viruses have historically been proposed mainly as a stand-alone therapy. While there is potential for the oncolytic virus to be successful on its own there are many barriers that must be overcome for the virus to be successful[321,345]. Because of this, work has begun using oncolytic viruses in combination with other treatment modalities, including chemotherapeutics and other biological therapies. Indeed, the combination of chemotherapy and oncolytic viruses has been shown to be safe with good efficacy in early phase clinical trials[153-155], and this combination is moving into phase II/III clinical trials (Table 2). Oncolytic viruses have also been proposed as a potential way to induce inflammation, overcoming the immunosuppressive tumour microenvironment. This inflammation has been shown assist in the success of DC based vaccination strategies[346,347]. Finally, oncolytic viruses have been shown to be excellent vectors for both priming anti-tumour immunity[348] and boosting immune responses in the context of an adenovirus prime leading to potent anti-tumour immunity[349,350]. The latter strategy is able to take advantage of some of the cytolytic properties of the virus, but also boost an adenovirus primed anti-tumour immune response leading to extremely robust anti-tumour immunity[349,350].

With the safety profiles and efficacy observed in recent clinical trials, oncolytic viruses have a bright future. Whether used as a stand alone monotherapy, or in combination with other therapeutic interventions, oncolytic viruses have the potential to change the face of cancer therapy.

References

1.The World Health Organization. Cancer. *The World Health Organization* (2012). at <http://www.who.int/mediacentre/factsheets/fs297/en/index.html>

2.Futreal, P. A. *et al.* BRCA1 mutations in primary breast and ovarian carcinomas. *Science* **266,** 120–122 (1994).

3.Miki, Y. *et al.* A strong candidate for the breast and ovarian cancer susceptibility gene BRCA1. *Science* **266,** 66–71 (1994).

4.Wooster, R. *et al.* Identification of the breast cancer susceptibility gene BRCA2. *Nature* **378,** 789–792 (1995).

5.Papadopoulos, N. *et al.* Mutation of a mutL homolog in hereditary colon cancer. *Science* **263,** 1625–1629 (1994).

6.Peltomäki, P. *et al.* Genetic mapping of a locus predisposing to human colorectal cancer. *Science* **260,** 810–812 (1993).

7.Couraud, S., Zalcman, G., Milleron, B., Morin, F. & Souquet, P.-J. Lung cancer in never smokers--a review. *Eur. J. Cancer* **48,** 1299–1311 (2012).

8.Letašiová, S. *et al.* Bladder cancer, a review of the environmental risk factors. *Environmental Health* **11,** S11 (2012).

9.Carrillo-Infante, C., Abbadessa, G., Bagella, L. & Giordano, A. Viral infections as a cause of cancer (review). *Int J Oncol* **30,** 1521–1528 (2007).

10.Hanahan, D. & Weinberg, R. A. The hallmarks of cancer. *Cell* **100,** 57–70 (2000).

11.Hanahan, D. & Weinberg, R. A. Hallmarks of Cancer: The Next Generation. *Cell* **144,** 646–674 (2011).

12.Knudson, A. G. Mutation and cancer: statistical study of retinoblastoma. *Proc Natl Acad Sci USA* **68,** 820–823 (1971).

13.Naik, S. & Russell, S. J. Engineering oncolytic viruses to exploit tumor specific defects in innate immune signaling pathways. *Expert Opin. Biol. Ther.* **9,** 1163–1176 (2009).

14.Sgorbissa, A. & Brancolini, C. IFNs, ISGylation and cancer: Cui prodest? *Cytokine Growth Factor Rev* 1–8 (2012). doi:10.1016/j.cytogfr.2012.07.003

15.Grandér, D. & Einhorn, S. Interferon and malignant disease--how does it work and why doesn't it always? *Acta Oncol* **37,** 331–338 (1998).

16.Colamonici, O. R., Domanski, P., Platanias, L. C. & Diaz, M. O. Correlation between interferon (IFN) alpha resistance and deletion of the IFN alpha/beta genes in acute leukemia cell lines suggests selection against the IFN system. *Blood* **80,** 744–749 (1992).

17.Takaoka, A. & Yanai, H. Interferon signalling network in innate defence. *Cell Microbiol* **8,** 907–922 (2006).

18.Zhang, K.-X. *et al.* Down-regulation of type I interferon receptor sensitizes bladder cancer cells to vesicular stomatitis virus-induced cell death. *Int J Cancer* **127,** 830–838 (2010).

19.Xu, B., Grandér, D., Sangfelt, O. & Einhorn, S. Primary leukemia cells resistant to alpha-interferon in vitro are defective in the activation of the DNA-binding factor interferon-stimulated gene factor 3. *Blood* **84,** 1942–1949 (1994).

20.Krishnamurthy, S., Takimoto, T., Scroggs, R. A. & Portner, A. Differentially regulated interferon response determines the outcome of Newcastle disease virus infection in normal and tumor cell lines. *J Virol* **80,** 5145–5155 (2006).

21.Abril, E. *et al.* Characterization of a gastric tumor cell line defective in MHC class I inducibility by both alpha- and gamma-interferon. *Tissue Antigens* **47,** 391–398 (1996).

22.Sun, W. H. *et al.* Interferon-alpha resistance in a cutaneous T-cell lymphoma cell line is associated with lack of STAT1 expression. *Blood* **91,** 570–576 (1998).

23.Wong, L. H. *et al.* Interferon-resistant human melanoma cells are deficient in ISGF3 components, STAT1, STAT2, and p48-ISGF3gamma. *J Biol Chem* **272,** 28779–28785 (1997).

24.Kolla, V., Lindner, D. J., Xiao, W., Borden, E. C. & Kalvakolanu, D. V. Modulation of interferon (IFN)-inducible gene expression by retinoic acid. Up-regulation of STAT1 protein in IFN-unresponsive cells. *J Biol Chem* **271,** 10508–10514 (1996).

25.Stojdl, D. *et al.* Exploiting tumor-specific defects in the interferon pathway with a previously unknown oncolytic virus. *Nat Med* **6,** 821–825 (2000).

26.Bremers, A. J., Rutgers, E. J. & van de Velde, C. J. Cancer surgery: the last 25 years. *Cancer Treat. Rev.* **25,** 333–353 (1999).

27.Braun, M. S. & Seymour, M. T. Balancing the efficacy and toxicity of chemotherapy in colorectal cancer. *Ther Adv Med Oncol* **3,** 43–52 (2011).

28.Malhotra, V. & Perry, M. C. Classical chemotherapy: mechanisms, toxicities and the therapeutic window. *Cancer Biol Ther* **2,** S2–4 (2003).

29.Baguley, B. C. Multiple Drug Resistance Mechanisms in Cancer. *Mol Biotechnol* **46,** 308–316 (2010).

30.Jorgensen, T. J. Enhancing radiosensitivity: targeting the DNA repair pathways. *Cancer Biol Ther* **8,** 665–670 (2009).

31.Stea, B., Hazard, L. J., Gonzalez, V. J. & Hamilton, R. The role of radiation therapy in the control of locoregional and metastatic cancer. *J Surg Oncol* **103,** 627–638 (2011).

32.Kavanagh, B. D. & Timmerman, R. D. Stereotactic radiosurgery and stereotactic body radiation therapy: an overview of technical considerations and clinical applications. *Hematol. Oncol. Clin. North Am.* **20,** 87–95 (2006).

33.Janeway, C. A. & Medzhitov, R. Innate immune recognition. *Annu Rev Immunol* **20,** 197–216 (2002).

34.Chaplin, D. D. 1. Overview of the human immune response. *J. Allergy Clin. Immunol.* **117,** S430–5 (2006).
35.Bonilla, F. A. & Oettgen, H. C. Adaptive immunity. *J. Allergy Clin. Immunol.* **125,** S33–40 (2010).
36.Ghosh, S., May, M. J. & Kopp, E. B. NF-kappa B and Rel proteins: evolutionarily conserved mediators of immune responses. *Annu Rev Immunol* **16,** 225–260 (1998).
37.Banchereau, J. & Steinman, R. M. Dendritic cells and the control of immunity. *Nature* **392,** 245–252 (1998).
38.Steinman, R. M. & Hemmi, H. Dendritic cells: translating innate to adaptive immunity. *Curr Top Microbiol Immunol* **311,** 17–58 (2006).
39.Kleijmeer, M. J. *et al.* MHC class II compartments and the kinetics of antigen presentation in activated mouse spleen dendritic cells. *J Immunol* **154,** 5715–5724 (1995).
40.Pierre, P. *et al.* Developmental regulation of MHC class II transport in mouse dendritic cells. *Nature* **388,** 787–792 (1997).
41.Cresswell, P. Invariant chain structure and MHC class II function. *Cell* **84,** 505–507 (1996).
42.Winzler, C. *et al.* Maturation stages of mouse dendritic cells in growth factor-dependent long-term cultures. *J Exp Med* **185,** 317–328 (1997).
43.Cella, M., Engering, A., Pinet, V., Pieters, J. & Lanzavecchia, A. Inflammatory stimuli induce accumulation of MHC class II complexes on dendritic cells. *Nature* **388,** 782–787 (1997).
44.Banchereau, J. *et al.* Immunobiology of dendritic cells. *Annu Rev Immunol* **18,** 767–811 (2000).
45.Joffre, O. P., Segura, E., Savina, A. & Amigorena, S. Cross-presentation by dendritic cells. *Nat Rev Immunol* **12,** 557–569 (2012).
46.Albert, M. L. *et al.* Immature dendritic cells phagocytose apoptotic cells via alphavbeta5 and CD36, and cross-present antigens to cytotoxic T lymphocytes. *J Exp Med* **188,** 1359–1368 (1998).
47.Norbury, C. C., Chambers, B. J., Prescott, A. R., Ljunggren, H. G. & Watts, C. Constitutive macropinocytosis allows TAP-dependent major histocompatibility complex class I presentation of exogenous soluble antigen by bone marrow-derived dendritic cells. *Eur J Immunol* **27,** 280–288 (1997).
48.Albert, M. L., Sauter, B. & Bhardwaj, N. Dendritic cells acquire antigen from apoptotic cells and induce class I-restricted CTLs. *Nature* **392,** 86–89 (1998).
49.Sigal, L. J., Crotty, S., Andino, R. & Rock, K. L. Cytotoxic T-cell immunity to virus-infected non-haematopoietic cells requires presentation of exogenous antigen. *Nature* **398,** 77–80 (1999).

50.Zitvogel, L. *et al.* Eradication of established murine tumors using a novel cell-free vaccine: dendritic cell-derived exosomes. *Nat Med* **4,** 594–600 (1998).
51.Regnault, A. *et al.* Fcgamma receptor-mediated induction of dendritic cell maturation and major histocompatibility complex class I-restricted antigen presentation after immune complex internalization. *J Exp Med* **189,** 371–380 (1999).
52.Villadangos, J. A. & Schnorrer, P. Intrinsic and cooperative antigen-presenting functions of dendritic-cell subsets in vivo. *Nat Rev Immunol* **7,** 543–555 (2007).
53.Pohl, C., Shishkova, J. & Schneider-Schaulies, S. Viruses and dendritic cells: enemy mine. *Cell Microbiol* **9,** 279–289 (2007).
54.Ridge, J. P., Di Rosa, F. & Matzinger, P. A conditioned dendritic cell can be a temporal bridge between a CD4+ T-helper and a T-killer cell. *Nature* **393,** 474–478 (1998).
55.Bennett, S. R. *et al.* Help for cytotoxic-T-cell responses is mediated by CD40 signalling. *Nature* **393,** 478–480 (1998).
56.Schoenberger, S. P., Toes, R. E., van der Voort, E. I., Offringa, R. & Melief, C. J. T-cell help for cytotoxic T lymphocytes is mediated by CD40-CD40L interactions. *Nature* **393,** 480–483 (1998).
57.Hou, S., Mo, X. Y., Hyland, L. & Doherty, P. C. Host response to Sendai virus in mice lacking class II major histocompatibility complex glycoproteins. *J Virol* **69,** 1429–1434 (1995).
58.Buller, R. M., Holmes, K. L., Hügin, A., Frederickson, T. N. & Morse, H. C. Induction of cytotoxic T-cell responses in vivo in the absence of CD4 helper cells. *Nature* **328,** 77–79 (1987).
59.Heath, W. R. & Carbone, F. R. Cross-presentation in viral immunity and self-tolerance. *Nat Rev Immunol* **1,** 126–134 (2001).
60.Dustin, M. L. & Long, E. O. Cytotoxic immunological synapses. *Immunol. Rev.* **235,** 24–34 (2010).
61.Lieberman, J. Anatomy of a murder: how cytotoxic T cells and NK cells are activated, develop, and eliminate their targets. *Immunol. Rev.* **235,** 5–9 (2010).
62.Russell, J. H. & Ley, T. J. Lymphocyte-mediated cytotoxicity. *Annu Rev Immunol* **20,** 323–370 (2002).
63.Barry, M. & Bleackley, R. C. Cytotoxic T lymphocytes: all roads lead to death. *Nat Rev Immunol* **2,** 401–409 (2002).
64.Keefe, D. *et al.* Perforin triggers a plasma membrane-repair response that facilitates CTL induction of apoptosis. *Immunity* **23,** 249–262 (2005).
65.Browne, K. A. *et al.* Cytosolic delivery of granzyme B by bacterial toxins: evidence that endosomal disruption, in addition to transmembrane pore formation, is an important function of perforin. *Mol Cell Biol* **19,** 8604–8615 (1999).

66.Thiery, J. *et al.* Perforin activates clathrin- and dynamin-dependent endocytosis, which is required for plasma membrane repair and delivery of granzyme B for granzyme-mediated apoptosis. *Blood* **115,** 1582–1593 (2010).

67.Ostergaard, H. L., Kane, K. P., Mescher, M. F. & Clark, W. R. Cytotoxic T lymphocyte mediated lysis without release of serine esterase. *Nature* **330,** 71–72 (1987).

68.Li, J. H. *et al.* The regulation of CD95 ligand expression and function in CTL. *J Immunol* **161,** 3943–3949 (1998).

69.Waring, P. & Müllbacher, A. Cell death induced by the Fas/Fas ligand pathway and its role in pathology. *Immunol Cell Biol* **77,** 312–317 (1999).

70.Kimura, M. *et al.* TNF combined with IFN-alpha accelerates NF-kappaB-mediated apoptosis through enhancement of Fas expression in colon cancer cells. *Cell Death Differ* **10,** 718–728 (2003).

71.Moulian, N., Bidault, J., Planché, C. & Berrih-Aknin, S. Two signaling pathways can increase fas expression in human thymocytes. *Blood* **92,** 1297–1307 (1998).

72.Peshes-Yaloz, N., Rosen, D., Sondel, P. M., Krammer, P. H. & Berke, G. Up-regulation of Fas (CD95) expression in tumour cells in vivo. *Immunology* **120,** 502–511 (2007).

73.Schreiber, R. D., Old, L. J. & Smyth, M. J. Cancer immunoediting: integrating immunity's roles in cancer suppression and promotion. *Science* **331,** 1565–1570 (2011).

74.Vesely, M. D., Kershaw, M. H., Schreiber, R. D. & Smyth, M. J. Natural innate and adaptive immunity to cancer. *Annu Rev Immunol* **29,** 235–271 (2011).

75.Mlecnik, B., Bindea, G., Pagès, F. & Galon, J. Tumor immunosurveillance in human cancers. *Cancer Metastasis Rev.* **30,** 5–12 (2011).

76.Shankaran, V. *et al.* IFNgamma and lymphocytes prevent primary tumour development and shape tumour immunogenicity. *Nature* **410,** 1107–1111 (2001).

77.Svane, I. M. *et al.* Chemically induced sarcomas from nude mice are more immunogenic than similar sarcomas from congenic normal mice. *Eur J Immunol* **26,** 1844–1850 (1996).

78.Engel, A. M., Svane, I. M., Rygaard, J. & Werdelin, O. MCA sarcomas induced in scid mice are more immunogenic than MCA sarcomas induced in congenic, immunocompetent mice. *Scand. J. Immunol.* **45,** 463–470 (1997).

79.Dunn, G. P., Bruce, A. T., Ikeda, H., Old, L. J. & Schreiber, R. D. Cancer immunoediting: from immunosurveillance to tumor escape. *Nat Immunol* **3,** 991–998 (2002).

80.Chow, M. T., Möller, A. & Smyth, M. J. Inflammation and immune surveillance in cancer. *Semin Cancer Biol* **22,** 23–32 (2012).

81.Penn, I. Malignant melanoma in organ allograft recipients. *Transplantation* **61,** 274–278 (1996).
82.Gatti, R. A. & Good, R. A. Occurrence of malignancy in immunodeficiency diseases. A literature review. *Cancer* **28,** 89–98 (1971).
83.Sheil, A. G. Cancer after transplantation. *World J Surg* **10,** 389–396 (1986).
84.Zorn, E. & Hercend, T. A natural cytotoxic T cell response in a spontaneously regressing human melanoma targets a neoantigen resulting from a somatic point mutation. *Eur J Immunol* **29,** 592–601 (1999).
85.Aguirre-Ghiso, J. A. Models, mechanisms and clinical evidence for cancer dormancy. *Nat Rev Cancer* **7,** 834–846 (2007).
86.Koebel, C. M. *et al.* Adaptive immunity maintains occult cancer in an equilibrium state. *Nature* **450,** 903–907 (2007).
87.Restifo, N. P. *et al.* Loss of functional beta 2-microglobulin in metastatic melanomas from five patients receiving immunotherapy. *J Natl Cancer Inst* **88,** 100–108 (1996).
88.Khong, H. T., Wang, Q. J. & Rosenberg, S. A. Identification of multiple antigens recognized by tumor-infiltrating lymphocytes from a single patient: tumor escape by antigen loss and loss of MHC expression. *J Immunother* **27,** 184–190 (2004).
89.Jager, E. *et al.* Inverse relationship of melanocyte differentiation antigen expression in melanoma tissues and CD8+ cytotoxic-T-cell responses: evidence for immunoselection of antigen-loss variants in vivo. *Int J Cancer* **66,** 470–476 (1996).
90.Töpfer, K. *et al.* Tumor Evasion from T Cell Surveillance. *Journal of Biomedicine and Biotechnology* **2011,** 1–19 (2011).
91.Zou, W. & Chen, L. Inhibitory B7-family molecules in the tumour microenvironment. *Nat Rev Immunol* **8,** 467–477 (2008).
92.Freeman, G. J. *et al.* Engagement of the PD-1 immunoinhibitory receptor by a novel B7 family member leads to negative regulation of lymphocyte activation. *J Exp Med* **192,** 1027–1034 (2000).
93.Dong, H. *et al.* Tumor-associated B7-H1 promotes T-cell apoptosis: a potential mechanism of immune evasion. *Nat Med* **8,** 793–800 (2002).
94.Shin, M. S. *et al.* Mutations of tumor necrosis factor-related apoptosis-inducing ligand receptor 1 (TRAIL-R1) and receptor 2 (TRAIL-R2) genes in metastatic breast cancers. *Cancer Res* **61,** 4942–4946 (2001).
95.Takahashi, H. *et al.* FAS death domain deletions and cellular FADD-like interleukin 1beta converting enzyme inhibitory protein (long) overexpression: alternative mechanisms for deregulating the extrinsic apoptotic pathway in diffuse large B-cell lymphoma subtypes. *Clin Cancer Res* **12,** 3265–3271 (2006).

96.Kataoka, T. *et al.* FLIP prevents apoptosis induced by death receptors but not by perforin/granzyme B, chemotherapeutic drugs, and gamma irradiation. *J Immunol* **161,** 3936–3942 (1998).
97.Hinz, S. *et al.* Bcl-XL protects pancreatic adenocarcinoma cells against CD95- and TRAIL-receptor-mediated apoptosis. *Oncogene* **19,** 5477–5486 (2000).
98.Groh, V., Wu, J., Yee, C. & Spies, T. Tumour-derived soluble MIC ligands impair expression of NKG2D and T-cell activation. *Nature* **419,** 734–738 (2002).
99.Villablanca, E. J. *et al.* Tumor-mediated liver X receptor-alpha activation inhibits CC chemokine receptor-7 expression on dendritic cells and dampens antitumor responses. *Nat Med* **16,** 98–105 (2010).
100.Herber, D. L. *et al.* Lipid accumulation and dendritic cell dysfunction in cancer. *Nat Med* **16,** 880–886 (2010).
101.Terabe, M. & Berzofsky, J. A. Immunoregulatory T cells in tumor immunity. *Curr Opin Immunol* **16,** 157–162 (2004).
102.Sakaguchi, S., Wing, K., Onishi, Y., Prieto-Martin, P. & Yamaguchi, T. Regulatory T cells: how do they suppress immune responses? *Int Immunol* **21,** 1105–1111 (2009).
103.Gabrilovich, D. I. & Nagaraj, S. Myeloid-derived suppressor cells as regulators of the immune system. *Nat Rev Immunol* **9,** 162–174 (2009).
104.Li, H., Han, Y., Guo, Q., Zhang, M. & Cao, X. Cancer-expanded myeloid-derived suppressor cells induce anergy of NK cells through membrane-bound TGF-beta 1. *J Immunol* **182,** 240–249 (2009).
105.Dock, G. The Influence of Complicating Diseases Upon Leukaemia.*. *The American Journal of the Medical Sciences* **127,** 563 (1904).
106.Taylor, A. W. Effects of glandular fever infection in acute leukaemia. *Br Med J* **1,** 589–593 (1953).
107.Pelner, L., Fowler, G. A. & NAUTS, H. C. EFFECT OF CONCURRENT INFECTIONS AND THEIR TOXINS ON THE COURSE OF LEUKEMIA. *Acta Medica Scandinavica* (1958).
108.Pasquinucci, G. Possible effect of measles on leukaemia. *Lancet* **1,** 136 (1971).
109.Gross, S. Measles and leukaemia. *Lancet* **1,** 397–398 (1971).
110.Zygiert, Z. Hodgkin's disease: remissions after measles. *Lancet* **1,** 593 (1971).
111.Bluming, A. Z. & Ziegler, J. L. Regression of Burkitt's lymphoma in association with measles infection. *Lancet* **2,** 105–106 (1971).
112.Taqi, A. M., Abdurrahman, M. B., Yakubu, A. M. & Fleming, A. F. Regression of Hodgkin's disease after measles. *Lancet* **1,** 1112 (1981).
113.Kelly, E. & Russell, S. J. History of oncolytic viruses: genesis to genetic engineering. *Mol Ther* **15,** 651–659 (2007).

114.Asada, T. Treatment of human cancer with mumps virus. *Cancer* **34,** 1907–1928 (1974).
115.Huebner, R. J., Rowe, W. P., Schatten, W. E., Smith, E. & Thomas, L. B. Studies on the use of viruses in the treatment of carcinoma of the cervix. *Cancer* **9,** 1211–1218 (1956).
116.Cassel, W. A., Murray, D. R. & Phillips, H. S. A phase II study on the postsurgical management of Stage II malignant melanoma with a Newcastle disease virus oncolysate. *Cancer* **52,** 856–860 (1983).
117.Cassel, W. A. & Murray, D. R. A ten-year follow-up on stage II malignant melanoma patients treated postsurgically with Newcastle disease virus oncolysate. *Med Oncol Tumor Pharmacother* **9,** 169–171 (1992).
118.Batliwalla, F. M. *et al.* A 15-year follow-up of AJCC stage III malignant melanoma patients treated postsurgically with Newcastle disease virus (NDV) oncolysate and determination of alterations in the CD8 T cell repertoire. *Mol. Med.* **4,** 783–794 (1998).
119.Wildner, O. Oncolytic viruses as therapeutic agents. *Ann. Med.* **33,** 291–304 (2001).
120.Vähä-Koskela, M. J. V., Heikkilä, J. E. & Hinkkanen, A. E. Oncolytic viruses in cancer therapy. *Cancer Lett.* **254,** 178–216 (2007).
121.Aghi, M. & Martuza, R. L. Oncolytic viral therapies - the clinical experience. *Oncogene* **24,** 7802–7816 (2005).
122.Park, M.-S., García-Sastre, A., Cros, J. F., Basler, C. F. & Palese, P. Newcastle disease virus V protein is a determinant of host range restriction. *J Virol* **77,** 9522–9532 (2003).
123.Yap, T. A., Brunetto, A. B., Pandha, H., Harrington, K. & de Bono, J. S. Reovirus therapy in cancer: has the orphan virus found a home? *Expert Opin. Investig. Drugs* **17,** 1925–1935 (2008).
124.Strong, J. E., Coffey, M. C., Tang, D., Sabinin, P. & Lee, P. W. The molecular basis of viral oncolysis: usurpation of the Ras signaling pathway by reovirus. *EMBO J* **17,** 3351–3362 (1998).
125.Stanford, M. M. & McFadden, G. Myxoma virus and oncolytic virotherapy: a new biologic weapon in the war against cancer. *Expert Opin. Biol. Ther.* **7,** 1415–1425 (2007).
126.Lun, X. Myxoma Virus Is a Novel Oncolytic Virus with Significant Antitumor Activity against Experimental Human Gliomas. *Cancer Res* **65,** 9982–9990 (2005).
127.Rintoul, J. L. *et al.* ORFV: a novel oncolytic and immune stimulating parapoxvirus therapeutic. *Molecular Therapy* **20,** 1148–1157 (2012).
128.Mineta, T., Rabkin, S. D., Yazaki, T., Hunter, W. D. & Martuza, R. L. Attenuated multi-mutated herpes simplex virus-1 for the treatment of malignant gliomas. *Nat Med* **1,** 938–943 (1995).

129.Hummel, J., Safroneeva, E. & Mossman, K. The role of ICP0-Null HSV-1 and interferon signaling defects in the effective treatment of breast adenocarcinoma. *Molecular Therapy* **12,** 1101–1110 (2005).
130.Kim, J. H. *et al.* Systemic armed oncolytic and immunologic therapy for cancer with JX-594, a targeted poxvirus expressing GM-CSF. *Mol Ther* **14,** 361–370 (2006).
131.Mastrangelo, M. J. *et al.* Intratumoral recombinant GM-CSF-encoding virus as gene therapy in patients with cutaneous melanoma. *Cancer Gene Ther* **6,** 409–422 (1999).
132.Stojdl, D. F. *et al.* VSV strains with defects in their ability to shutdown innate immunity are potent systemic anti-cancer agents. *Cancer Cell* **4,** 263–275 (2003).
133.Barber, G. N. VSV-tumor selective replication and protein translation. *Oncogene* **24,** 7710–7719 (2005).
134.Gromeier, M., Lachmann, S., Rosenfeld, M. R., Gutin, P. H. & Wimmer, E. Intergeneric poliovirus recombinants for the treatment of malignant glioma. *Proc Natl Acad Sci USA* **97,** 6803–6808 (2000).
135.Ren, R. B., Costantini, F., Gorgacz, E. J., Lee, J. J. & Racaniello, V. R. Transgenic mice expressing a human poliovirus receptor: a new model for poliomyelitis. *Cell* **63,** 353–362 (1990).
136.Nakamura, T. *et al.* Rescue and propagation of fully retargeted oncolytic measles viruses. *Nat Biotechnol* **23,** 209–214 (2005).
137.Russell, S. J., Peng, K.-W. & Bell, J. C. Oncolytic virotherapy. *Nat Biotechnol* **30,** 658–670 (2012).
138.Rowan, K. Oncolytic viruses move forward in clinical trials. *J Natl Cancer Inst* **102,** 590–595 (2010).
139.Liu, T.-C., Galanis, E. & Kirn, D. Clinical trial results with oncolytic virotherapy: a century of promise, a decade of progress. *Nat Clin Pract Oncol* **4,** 101–117 (2007).
140.Liu, T.-C. & Kirn, D. Gene therapy progress and prospects cancer: oncolytic viruses. *Gene Ther* **15,** 877–884 (2008).
141.Park, B.-H. *et al.* Use of a targeted oncolytic poxvirus, JX-594, in patients with refractory primary or metastatic liver cancer: a phase I trial. *Lancet Oncol.* **9,** 533–542 (2008).
142.Hu, J. C. C. *et al.* A phase I study of OncoVEXGM-CSF, a second-generation oncolytic herpes simplex virus expressing granulocyte macrophage colony-stimulating factor. *Clin Cancer Res* **12,** 6737–6747 (2006).
143.Senzer, N. N. *et al.* Phase II clinical trial of a granulocyte-macrophage colony-stimulating factor-encoding, second-generation oncolytic herpesvirus in patients with unresectable metastatic melanoma. *J Clin Oncol* **27,** 5763–5771 (2009).

144.Kaufman, H. L. *et al.* Local and distant immunity induced by intralesional vaccination with an oncolytic herpes virus encoding GM-CSF in patients with stage IIIc and IV melanoma. *Ann Surg Oncol* **17,** 718–730 (2010).

145.Kaufman, H. L. & Bines, S. D. OPTIM trial: a Phase III trial of an oncolytic herpes virus encoding GM-CSF for unresectable stage III or IV melanoma. *Future Oncol* **6,** 941–949 (2010).

146.Hwang, T.-H. *et al.* A mechanistic proof-of-concept clinical trial with JX-594, a targeted multi-mechanistic oncolytic poxvirus, in patients with metastatic melanoma. *Mol Ther* **19,** 1913–1922 (2011).

147.Breitbach, C. J. *et al.* Intravenous delivery of a multi-mechanistic cancer-targeted oncolytic poxvirus in humans. *Nature* **477,** 99–102 (2011).

148.Forsyth, P. *et al.* A phase I trial of intratumoral administration of reovirus in patients with histologically confirmed recurrent malignant gliomas. *Mol Ther* **16,** 627–632 (2008).

149.Vidal, L. *et al.* A phase I study of intravenous oncolytic reovirus type 3 Dearing in patients with advanced cancer. *Clin Cancer Res* **14,** 7127–7137 (2008).

150.Soefje, S. A. *et al.* A phase II study of intravenous reolysin (wild-type reovirus) in the treatment of patients with bone and soft tissue sarcomas metastatic to the lung. *J Clin Oncol* **26,** abstr 10568 (2008).

151.Gollamudi, R. *et al.* Intravenous administration of Reolysin, a live replication competent RNA virus is safe in patients with advanced solid tumors. *Invest New Drugs* **28,** 641–649 (2010).

152.Galanis, E. *et al.* Phase II Trial of Intravenous Administration of Reolysin(®) (Reovirus Serotype-3-dearing Strain) in Patients with Metastatic Melanoma. *Mol Ther* (2012). doi:10.1038/mt.2012.146

153.Heo, J. *et al.* Sequential therapy with JX-594, a targeted oncolytic poxvirus, followed by sorafenib in hepatocellular carcinoma: preclinical and clinical demonstration of combination efficacy. *Mol Ther* **19,** 1170–1179 (2011).

154.Lolkema, M. P. *et al.* A phase I study of the combination of intravenous reovirus type 3 Dearing and gemcitabine in patients with advanced cancer. *Clin Cancer Res* **17,** 581–588 (2011).

155.Comins, C. *et al.* REO-10: a phase I study of intravenous reovirus and docetaxel in patients with advanced cancer. *Clin Cancer Res* **16,** 5564–5572 (2010).

156.Reschner, A., Hubert, P., Delvenne, P., Boniver, J. & Jacobs, N. Innate lymphocyte and dendritic cell cross-talk: a key factor in the regulation of the immune response. *Clin Exp Immunol* **152,** 219–226 (2008).

157.Tan, J. & O'Neill, H. Maturation requirements for dendritic cells in T cell stimulation leading to tolerance versus immunity. *J Leukoc Biol* **78,** 319–324 (2005).

158.Choi, K. *et al.* Concurrent delivery of GM-CSF and B7-1 using an oncolytic adenovirus elicits potent antitumor effect. *Gene Ther* **13,** 1010–1020 (2006).

159.Fukuhara, H., Ino, Y., Kuroda, T., Martuza, R. & Todo, T. Triple gene-deleted oncolytic herpes simplex virus vector double-armed with interleukin 18 and soluble B7-1 constructed by bacterial artificial chromosome-mediated system. *Cancer Res* **65,** 10663–10668 (2005).

160.Shin, E. *et al.* Interleukin-12 expression enhances vesicular stomatitis virus oncolytic therapy in murine squamous cell carcinoma. *Laryngoscope* **117,** 210–214 (2007).

161.Su, C. *et al.* Immune gene-viral therapy with triplex efficacy mediated by oncolytic adenovirus carrying an interferon-gamma gene yields efficient antitumor activity in immunodeficient and immunocompetent mice. *Mol Ther* **13,** 918–927 (2006).

162.Varghese, S. *et al.* Enhanced therapeutic efficacy of IL-12, but not GM-CSF, expressing oncolytic herpes simplex virus for transgenic mouse derived prostate cancers. *Cancer Gene Ther* **13,** 253–265 (2006).

163.Vigil, A. *et al.* Use of reverse genetics to enhance the oncolytic properties of Newcastle disease virus. *Cancer Res* **67,** 8285–8292 (2007).

164.Zhao, H., Janke, M., Fournier, P. & Schirrmacher, V. Recombinant Newcastle disease virus expressing human interleukin-2 serves as a potential candidate for tumor therapy. *Virus Res* **136,** 75–80 (2008).

165.Carew, J. F. *et al.* A novel approach to cancer therapy using an oncolytic herpes virus to package amplicons containing cytokine genes. *Mol Ther* **4,** 250–256 (2001).

166.Dasgupta, S., Bhattacharya-Chatterjee, M., O'Malley, B. & Chatterjee, S. Recombinant vaccinia virus expressing interleukin-2 invokes anti-tumor cellular immunity in an orthotopic murine model of head and neck squamous cell carcinoma. *Mol Ther* **13,** 183–193 (2006).

167.Stephenson, K. B., Barra, N. G., Davies, E., Ashkar, A. A. & Lichty, B. D. Expressing human interleukin-15 from oncolytic vesicular stomatitis virus improves survival in a murine metastatic colon adenocarcinoma model through the enhancement of anti-tumor immunity. *Cancer Gene Ther* **19,** 238–246 (2012).

168.van Rikxoort, M. *et al.* Oncolytic Effects of a Novel Influenza A Virus Expressing Interleukin-15 from the NS Reading Frame. *PLoS One* **7,** e36506 (2012).

169.Diaconu, I. *et al.* Immune Response Is an Important Aspect of the Antitumor Effect Produced by a CD40L-Encoding Oncolytic Adenovirus. *Cancer Res* **72,** 2327–2338 (2012).

170.Liu, T.-C., Hwang, T., Park, B.-H., Bell, J. & Kirn, D. H. The targeted oncolytic poxvirus JX-594 demonstrates antitumoral, antivascular, and anti-HBV

activities in patients with hepatocellular carcinoma. *Mol Ther* **16,** 1637–1642 (2008).

171.Pesonen, S. *et al.* Oncolytic Immunotherapy of Advanced Solid Tumors with a CD40L-Expressing Replicating Adenovirus: Assessment of Safety and Immunologic Responses in Patients. *Cancer Res* **72,** 1621–1631 (2012).

172.Lapteva, N. *et al.* Targeting the intratumoral dendritic cells by the oncolytic adenoviral vaccine expressing RANTES elicits potent antitumor immunity. *J Immunother* **32,** 145–156 (2009).

173.Liu, B. *et al.* ICP34.5 deleted herpes simplex virus with enhanced oncolytic, immune stimulating, and anti-tumour properties. *Gene Ther* **10,** 292–303 (2003).

174.Todo, T., Martuza, R., Dallman, M. & Rabkin, S. In situ expression of soluble B7-1 in the context of oncolytic herpes simplex virus induces potent antitumor immunity. *Cancer Res* **61,** 153–161 (2001).

175.Mueller, D., Jenkins, M. & Schwartz, R. Clonal expansion versus functional clonal inactivation: a costimulatory signalling pathway determines the outcome of T cell antigen receptor occupancy. *Annu Rev Immunol* **7,** 445–480 (1989).

176.Ino, Y., Saeki, Y., Fukuhara, H. & Todo, T. Triple combination of oncolytic herpes simplex virus-1 vectors armed with interleukin-12, interleukin-18, or soluble B7-1 results in enhanced antitumor efficacy. *Clin Cancer Res* **12,** 643–652 (2006).

177.Trinchieri, G., Pflanz, S. & Kastelein, R. The IL-12 family of heterodimeric cytokines: new players in the regulation of T cell responses. *Immunity* **19,** 641–644 (2003).

178.de Jong, E., Smits, H. & Kapsenberg, M. Dendritic cell-mediated T cell polarization. *Springer Semin Immunopathol* **26,** 289–307 (2005).

179.Lui, V., He, Y., Falo, L. & Huang, L. Systemic administration of naked DNA encoding interleukin 12 for the treatment of human papillomavirus DNA-positive tumor. *Hum Gene Ther* **13,** 177–185 (2002).

180.Leonard, J. *et al.* Effects of single-dose interleukin-12 exposure on interleukin-12-associated toxicity and interferon-gamma production. *Blood* **90,** 2541–2548 (1997).

181.Wong, R. *et al.* Angiogenesis inhibition by an oncolytic herpes virus expressing interleukin 12. *Clin Cancer Res* **10,** 4509–4516 (2004).

182.Lee, Y. *et al.* Enhanced antitumor effect of oncolytic adenovirus expressing interleukin-12 and B7-1 in an immunocompetent murine model. *Clin Cancer Res* **12,** 5859–5868 (2006).

183.Rodríguez, L. L. Emergence and re-emergence of vesicular stomatitis in the United States. *Virus Res* **85,** 211–219 (2002).

184.Letchworth, G. J., Rodriguez, L. L. & Del cbarrera, J. Vesicular stomatitis. *Vet. J.* **157,** 239–260 (1999).

185.Lyles, D. S. & Rupprecht, C. E. in *Fields Virology, Fifth Edition* (Knipe, D. M. & Howley, P. M.) 1364–1408 (Lippincott Williams & Wilkins, 2006).

186.Cotton, W. E. Vesicular stomatitis. *Veterinary Medicine* **22,** 169–175 (1927).

187.Cotton, W. E. Vesicular stomatitis and its relation to the diagnosis of foot-and-mouth disease.

. *J. Am. Vet. Med. Assoc.* **69,** 313–332 (1926).

188.Johnson, K. M., Tesh, R. B. & Peralta, P. H. Epidemiology of vesicular stomatitis virus: some new data and a hypothesis for transmission of the Indian serotype. *J. Am. Vet. Med. Assoc.* **155,** 2133–2140 (1969).

189.Sudia, W. D., Fields, B. N. & Calisher, C. H. The isolation of vesiculay stomatitis virus (Indiana strain) and other viruses from mosquitoes in New Mexico, 1965. *Am. J. Epidemiol.* **86,** 598–602 (1967).

190.Tesh, R. B., Chaniotis, B. N. & Johnson, K. M. Vesicular stomatitis virus (Indiana serotype): transovarial transmission by phlebotomine sandlies. *Science* **175,** 1477–1479 (1972).

191.Tesh, R. B., Chaniotis, B. N. & Johnson, K. M. Vesicular stomatitis virus, Indiana serotype: multiplication in and transmission by experimentally infected phlebotomine sandflies (Lutzomyia trapidoi). *Am. J. Epidemiol.* **93,** 491–495 (1971).

192.Karstad, L. & Hanson, R. P. Primary isolation and comparative titrations of five field strains of vesicular stomatitis virus in chicken embryos, hogs and mice. *Am. J. Vet. Res.* **19,** 233–236 (1958).

193.Lichty, B. D., Power, A. T., Stojdl, D. F. & Bell, J. C. Vesicular stomatitis virus: re-inventing the bullet. *Trends Mol Med* **10,** 210–216 (2004).

194.Albertini, A. A. V., Baquero, E., Ferlin, A. & Gaudin, Y. Molecular and Cellular Aspects of Rhabdovirus Entry. *Viruses* **4,** 117–139 (2012).

195.Schlegel, R., Tralka, T. S., Willingham, M. C. & Pastan, I. Inhibition of VSV binding and infectivity by phosphatidylserine: is phosphatidylserine a VSV-binding site? *Cell* **32,** 639–646 (1983).

196.Coil, D. A. & Miller, A. D. Phosphatidylserine is not the cell surface receptor for vesicular stomatitis virus. *J Virol* **78,** 10920–10926 (2004).

197.Bailey, C. A., Miller, D. K. & Lenard, J. Effects of DEAE-dextran on infection and hemolysis by VSV. Evidence that nonspecific electrostatic interactions mediate effective binding of VSV to cells. *Virology* **133,** 111–118 (1984).

198.Florkiewicz, R. Z. & Rose, J. K. A cell line expressing vesicular stomatitis virus glycoprotein fuses at low pH. *Science* **225,** 721–723 (1984).

199.Baltimore, D., Huang, A. S. & Stampfer, M. Ribonucleic acid synthesis of vesicular stomatitis virus, II. An RNA polymerase in the virion. *Proc Natl Acad Sci USA* **66,** 572–576 (1970).

200.Banerjee, A. K. & Barik, S. Gene expression of vesicular stomatitis virus genome RNA. *Virology* **188,** 417–428 (1992).

201.Iverson, L. E. & Rose, J. K. Localized attenuation and discontinuous synthesis during vesicular stomatitis virus transcription. *Cell* **23,** 477–484 (1981).
202.Emerson, S. U. Reconstitution studies detect a single polymerase entry site on the vesicular stomatitis virus genome. *Cell* **31,** 635–642 (1982).
203.Abraham, G. & Banerjee, A. K. Sequential transcription of the genes of vesicular stomatitis virus. *Proc Natl Acad Sci USA* **73,** 1504–1508 (1976).
204.Rose, J. K. Complete intergenic and flanking gene sequences from the genome of vesicular stomatitis virus. *Cell* **19,** 415–421 (1980).
205.Iverson, L. E. & Rose, J. K. Sequential synthesis of 5'-proximal vesicular stomatitis virus mRNA sequences. *J Virol* **44,** 356–365 (1982).
206.Abraham, G., Rhodes, D. P. & Banerjee, A. K. The 5' terminal structure of the methylated mRNA synthesized in vitro by vesicular stomatitis virus. *Cell* **5,** 51–58 (1975).
207.Wertz, G. W. & Levine, M. RNA synthesis by vesicular stomatitis virus and a small plaque mutant: effects of cycloheximide. *J Virol* **12,** 253–264 (1973).
208.Patton, J. T., Davis, N. L. & Wertz, G. W. N protein alone satisfies the requirement for protein synthesis during RNA replication of vesicular stomatitis virus. *J Virol* **49,** 303–309 (1984).
209.Blumberg, B. M., Leppert, M. & Kolakofsky, D. Interaction of VSV leader RNA and nucleocapsid protein may control VSV genome replication. *Cell* **23,** 837–845 (1981).
210.Gupta, A. K., Shaji, D. & Banerjee, A. K. Identification of a novel tripartite complex involved in replication of vesicular stomatitis virus genome RNA. *J Virol* **77,** 732–738 (2003).
211.Stojdl, D. F. *et al.* The murine double-stranded RNA-dependent protein kinase PKR is required for resistance to vesicular stomatitis virus. *J Virol* **74,** 9580–9585 (2000).
212.Kato, H. *et al.* Differential roles of MDA5 and RIG-I helicases in the recognition of RNA viruses. *Nature* **441,** 101–105 (2006).
213.Lund, J. M. *et al.* Recognition of single-stranded RNA viruses by Toll-like receptor 7. *Proc Natl Acad Sci USA* **101,** 5598–5603 (2004).
214.Yoneyama, M. & Fujita, T. Function of RIG-I-like Receptors in Antiviral Innate Immunity. *jvi.asm.org.libaccess.lib.mcmaster.ca* **282,** 15315–15318 (2007).
215.Kawai, T. *et al.* IPS-1, an adaptor triggering RIG-I- and Mda5-mediated type I interferon induction. *Nat Immunol* **6,** 981–988 (2005).
216.Rieder, M. & Conzelmann, K.-K. Rhabdovirus evasion of the interferon system. *J. Interferon Cytokine Res.* **29,** 499–509 (2009).
217.Yoneyama, Y. *et al.* Development of immunostimulatory virotherapy using non-transmissible Sendai virus-activated dendritic cells. *Biochem Biophys Res Commun* **355,** 129–135 (2007).

218.Takeuchi, O. & Akira, S. Innate immunity to virus infection. *Immunol. Rev.* **227,** 75–86 (2009).
219.Zhou, S. *et al.* Role of MyD88 in route-dependent susceptibility to vesicular stomatitis virus infection. *J Immunol* **178,** 5173–5181 (2007).
220.Kumar, H. *et al.* Essential role of IPS-1 in innate immune responses against RNA viruses. *J Exp Med* **203,** 1795–1803 (2006).
221.Georgel, P. *et al.* Vesicular stomatitis virus glycoprotein G activates a specific antiviral Toll-like receptor 4-dependent pathway. *Virology* **362,** 304–313 (2007).
222.Kramer, M. J. *et al.* Cell and virus sensitivity studies with recombinant human alpha interferons. *J Interferon Res* **3,** 425–435 (1983).
223.Kobbe, von, C. *et al.* Vesicular stomatitis virus matrix protein inhibits host cell gene expression by targeting the nucleoporin Nup98. *Mol Cell* **6,** 1243–1252 (2000).
224.Ahmed, M. *et al.* Ability of the matrix protein of vesicular stomatitis virus to suppress beta interferon gene expression is genetically correlated with the inhibition of host RNA and protein synthesis. *J Virol* **77,** 4646–4657 (2003).
225.Brown, C. W. *et al.* The p14 FAST protein of reptilian reovirus increases vesicular stomatitis virus neuropathogenesis. *J Virol* **83,** 552–561 (2009).
226.Balachandran, S. & Barber, G. N. Vesicular stomatitis virus (VSV) therapy of tumors. *IUBMB Life* **50,** 135–138 (2000).
227.Breitbach, C. J. *et al.* Targeted Inflammation During Oncolytic Virus Therapy Severely Compromises Tumor Blood Flow. *Mol Ther* **15,** 1686–1693 (2007).
228.Breitbach, C. J. *et al.* Targeting tumor vasculature with an oncolytic virus. *Mol Ther* **19,** 886–894 (2011).
229.Lawson, N. D., Stillman, E. A., Whitt, M. A. & Rose, J. K. Recombinant vesicular stomatitis viruses from DNA. *Proc Natl Acad Sci USA* **92,** 4477–4481 (1995).
230.Ramsburg, E. A., Publicover, J. M., Coppock, D. & Rose, J. K. Requirement for CD4 T cell help in maintenance of memory CD8 T cell responses is epitope dependent. *J Immunol* **178,** 6350–6358 (2007).
231.Casares, N. *et al.* Immunization with a tumor-associated CTL epitope plus a tumor-related or unrelated Th1 helper peptide elicits protective CTL immunity. *Eur J Immunol* **31,** 1780–1789 (2001).
232.Krysko, D. V., D'Herde, K. & Vandenabeele, P. Clearance of apoptotic and necrotic cells and its immunological consequences. *Apoptosis* **11,** 1709–1726 (2006).
233.Zitvogel, L. *et al.* Immune response against dying tumor cells. *Adv Immunol* **84,** 131–179 (2004).
234.Lemke, G. & Rothlin, C. V. Immunobiology of the TAM receptors. *Nat Rev Immunol* **8,** 327–336 (2008).

235.Savill, J., Dransfield, I., Gregory, C. & Haslett, C. A blast from the past: clearance of apoptotic cells regulates immune responses. *Nat Rev Immunol* **2,** 965–975 (2002).

236.Green, D. R., Ferguson, T., Zitvogel, L. & Kroemer, G. Immunogenic and tolerogenic cell death. *Nat Rev Immunol* **9,** 353–363 (2009).

237.Kerr, J. F., Wyllie, A. H. & Currie, A. R. Apoptosis: a basic biological phenomenon with wide-ranging implications in tissue kinetics. *Br J Cancer* **26,** 239–257 (1972).

238.Tewari, M. *et al.* Yama/CPP32 beta, a mammalian homolog of CED-3, is a CrmA-inhibitable protease that cleaves the death substrate poly(ADP-ribose) polymerase. *Cell* **81,** 801–809 (1995).

239.Fernandes-Alnemri, T., Litwack, G. & Alnemri, E. S. CPP32, a novel human apoptotic protein with homology to Caenorhabditis elegans cell death protein Ced-3 and mammalian interleukin-1 beta-converting enzyme. *J Biol Chem* **269,** 30761–30764 (1994).

240.Coelho, D. *et al.* Caspase-3-like activity determines the type of cell death following ionizing radiation in MOLT-4 human leukaemia cells. *Br J Cancer* **83,** 642–649 (2000).

241.Savill, J., Fadok, V., Henson, P. & Haslett, C. Phagocyte recognition of cells undergoing apoptosis. *Immunol Today* **14,** 131–136 (1993).

242.Albert, M. L., Jegathesan, M. & Darnell, R. B. Dendritic cell maturation is required for the cross-tolerization of CD8+ T cells. *Nat Immunol* **2,** 1010–1017 (2001).

243.Steinman, R. M., Turley, S., Mellman, I. & Inaba, K. The induction of tolerance by dendritic cells that have captured apoptotic cells. *J Exp Med* **191,** 411–416 (2000).

244.Sauter, B. *et al.* Consequences of Cell Death: Exposure to Necrotic Tumor Cells, but Not Primary Tissue Cells or Apoptotic Cells, Induces the Maturation of Immunostimulatory Dendritic Cells. *J Exp Med* **191,** 423–434 (2000).

245.Kim, S., Elkon, K. B. & Ma, X. Transcriptional suppression of interleukin-12 gene expression following phagocytosis of apoptotic cells. *Immunity* **21,** 643–653 (2004).

246.Fadok, V. A. *et al.* Macrophages that have ingested apoptotic cells in vitro inhibit proinflammatory cytokine production through autocrine/paracrine mechanisms involving TGF-beta, PGE2, and PAF. *J Clin Invest* **101,** 890–898 (1998).

247.Voll, R. E. *et al.* Immunosuppressive effects of apoptotic cells. *Nature* **390,** 350–351 (1997).

248.Lorimore, S. A., Coates, P. J., Scobie, G. E., Milne, G. & Wright, E. G. Inflammatory-type responses after exposure to ionizing radiation in vivo: a

mechanism for radiation-induced bystander effects? *Oncogene* **20,** 7085–7095 (2001).

249. Restifo, N. P. Building better vaccines: how apoptotic cell death can induce inflammation and activate innate and adaptive immunity. *Curr Opin Immunol* **12,** 597–603 (2000).
250. Scaffidi, P., Misteli, T. & Bianchi, M. E. Release of chromatin protein HMGB1 by necrotic cells triggers inflammation. *Nature* **418,** 191–195 (2002).
251. Apetoh, L. *et al.* Toll-like receptor 4-dependent contribution of the immune system to anticancer chemotherapy and radiotherapy. *Nat Med* **13,** 1050–1059 (2007).
252. Shi, Y., Evans, J. E. & Rock, K. L. Molecular identification of a danger signal that alerts the immune system to dying cells. *Nature* **425,** 516–521 (2003).
253. Hanley, P. J. *et al.* Extracellular ATP induces oscillations of intracellular Ca2+ and membrane potential and promotes transcription of IL-6 in macrophages. *Proc Natl Acad Sci USA* **101,** 9479–9484 (2004).
254. Amaravadi, R. K. & Thompson, C. B. The roles of therapy-induced autophagy and necrosis in cancer treatment. *Clin Cancer Res* **13,** 7271–7279 (2007).
255. Ghiringhelli, F. *et al.* Activation of the NLRP3 inflammasome in dendritic cells induces IL-1beta-dependent adaptive immunity against tumors. *Nat Med* **15,** 1170–1178 (2009).
256. Kepp, O. *et al.* Immunogenic cell death modalities and their impact on cancer treatment. *Apoptosis* **14,** 364–375 (2009).
257. Ebert, O. Syncytia Induction Enhances the Oncolytic Potential of Vesicular Stomatitis Virus in Virotherapy for Cancer. *Cancer Res* **64,** 3265–3270 (2004).
258. Chang, G. *et al.* Enhanced oncolytic activity of vesicular stomatitis virus encoding SV5-F protein against prostate cancer. *J. Urol.* **183,** 1611–1618 (2010).
259. Shin, E. J. *et al.* Fusogenic vesicular stomatitis virus for the treatment of head and neck squamous carcinomas. **136,** 811–817 (2007).
260. Guedan, S. *et al.* GALV expression enhances the therapeutic efficacy of an oncolytic adenovirus by inducing cell fusion and enhancing virus distribution. *Gene Ther* (2011). doi:10.1038/gt.2011.184
261. Gainey, M. D., Manuse, M. J. & Parks, G. D. A hyperfusogenic F protein enhances the oncolytic potency of a paramyxovirus simian virus 5 P/V mutant without compromising sensitivity to type I interferon. *J Virol* **82,** 9369–9380 (2008).
262. Fu, X. & Zhang, X. Potent systemic antitumor activity from an oncolytic herpes simplex virus of syncytial phenotype. *Cancer Res* **62,** 2306–2312 (2002).

263.Takaoka, H. *et al.* A novel fusogenic herpes simplex virus for oncolytic virotherapy of squamous cell carcinoma. *Virol J* **8,** 294 (2011).

264.Bateman, A. *et al.* Fusogenic membrane glycoproteins as a novel class of genes for the local and immune-mediated control of tumor growth. **60,** 1492–1497 (2000).

265.Duncan, R., Chen, Z., Walsh, S. & Wu, S. Avian reovirus-induced syncytium formation is independent of infectious progeny virus production and enhances the rate, but is not essential, for virus-induced cytopathology and virus egress. *Virology* **224,** 453–464 (1996).

266.Corcoran, J. A. & Duncan, R. Reptilian reovirus utilizes a small type III protein with an external myristylated amino terminus to mediate cell-cell fusion. *J Virol* **78,** 4342–4351 (2004).

267.Salsman, J., Top, D., Boutilier, J. & Duncan, R. Extensive syncytium formation mediated by the reovirus FAST proteins triggers apoptosis-induced membrane instability. *J Virol* **79,** 8090–8100 (2005).

268.Corcoran, J. A. *et al.* The p14 Fusion-associated Small Transmembrane (FAST) Protein Effects Membrane Fusion from a Subset of Membrane Microdomains. *Journal of Biological Chemistry* **281,** 31778–31789 (2006).

269.Koyama, A. H. Induction of apoptotic DNA fragmentation by the infection of vesicular stomatitis virus. *Virus Res* **37,** 285–290 (1995).

270.Gadaleta, P., Vacotto, M. & Coulombié, F. Vesicular stomatitis virus induces apoptosis at early stages in the viral cycle and does not depend on virus replication. *Virus Res* **86,** 87–92 (2002).

271.Kopecky, S. A., Willingham, M. C. & Lyles, D. S. Matrix protein and another viral component contribute to induction of apoptosis in cells infected with vesicular stomatitis virus. *J Virol* **75,** 12169–12181 (2001).

272.Kopecky, S. A. & Lyles, D. S. Contrasting effects of matrix protein on apoptosis in HeLa and BHK cells infected with vesicular stomatitis virus are due to inhibition of host gene expression. *J Virol* **77,** 4658–4669 (2003).

273.Gaddy, D. F. & Lyles, D. S. Vesicular stomatitis viruses expressing wild-type or mutant M proteins activate apoptosis through distinct pathways. *J Virol* **79,** 4170–4179 (2005).

274.Pearce, A. F. & Lyles, D. S. Vesicular stomatitis virus induces apoptosis primarily through Bak rather than Bax by inactivating Mcl-1 and Bcl-XL. *J Virol* **83,** 9102–9112 (2009).

275.Baltzis, D. *et al.* Resistance to vesicular stomatitis virus infection requires a functional cross talk between the eukaryotic translation initiation factor 2alpha kinases PERK and PKR. *J Virol* **78,** 12747–12761 (2004).

276.Gaddy, D. F. & Lyles, D. S. Oncolytic vesicular stomatitis virus induces apoptosis via signaling through PKR, Fas, and Daxx. *J Virol* **81,** 2792–2804 (2007).

277.Galluzzi, L. *et al.* Viral strategies for the evasion of immunogenic cell death. *Journal of Internal Medicine* **267,** 526–542 (2010).
278.Taylor, J. M. & Barry, M. Near death experiences: poxvirus regulation of apoptotic death. *Virology* **344,** 139–150 (2006).
279.Banadyga, L., Gerig, J., Stewart, T. & Barry, M. Fowlpox virus encodes a Bcl-2 homologue that protects cells from apoptotic death through interaction with the proapoptotic protein Bak. *J Virol* **81,** 11032–11045 (2007).
280.Campbell, S., Hazes, B., Kvansakul, M., Colman, P. & Barry, M. Vaccinia Virus F1L Interacts with Bak Using Highly Divergent Bcl-2 Homology Domains and Replaces the Function of Mcl-1. *Journal of Biological Chemistry* **285,** 4695–4708 (2010).
281.Stewart, T. L., Wasilenko, S. T. & Barry, M. Vaccinia virus F1L protein is a tail-anchored protein that functions at the mitochondria to inhibit apoptosis. *J Virol* **79,** 1084–1098 (2005).
282.Wasilenko, S. T., Banadyga, L., Bond, D. & Barry, M. The vaccinia virus F1L protein interacts with the proapoptotic protein Bak and inhibits Bak activation. *J Virol* **79,** 14031–14043 (2005).
283.Banadyga, L., Veugelers, K., Campbell, S. & Barry, M. The fowlpox virus BCL-2 homologue, FPV039, interacts with activated Bax and a discrete subset of BH3-only proteins to inhibit apoptosis. *J Virol* **83,** 7085–7098 (2009).
284.Obeid, M. *et al.* Calreticulin exposure dictates the immunogenicity of cancer cell death. *Nat Med* **13,** 54–61 (2007).
285.Aymeric, L. *et al.* Tumor cell death and ATP release prime dendritic cells and efficient anticancer immunity. *Cancer Res* **70,** 855–858 (2010).
286.Donnelly, O. G. *et al.* Measles virus causes immunogenic cell death in human melanoma. *Gene Ther* (2011). doi:10.1038/gt.2011.205
287.Miyamoto, S. *et al.* Coxsackievirus B3 is an oncolytic virus with immunostimulatory properties that is active against lung adenocarcinoma. *Cancer Res* **72,** 2609–2621 (2012).
288.Rolls, M. M., Webster, P., Balba, N. H. & Rose, J. K. Novel infectious particles generated by expression of the vesicular stomatitis virus glycoprotein from a self-replicating RNA. *Cell* **79,** 497–506 (1994).
289.Knipe, D. M., Baltimore, D. & Lodish, H. F. Maturation of viral proteins in cells infected with temperature-sensitive mutants of vesicular stomatitis virus. *J Virol* **21,** 1149–1158 (1977).
290.Metsikkö, K. & Simons, K. The budding mechanism of spikeless vesicular stomatitis virus particles. *EMBO J* **5,** 1913–1920 (1986).
291.Bateman, A. R. *et al.* Viral fusogenic membrane glycoproteins kill solid tumor cells by nonapoptotic mechanisms that promote cross presentation of tumor antigens by dendritic cells. *Cancer Res* **62,** 6566–6578 (2002).

292.Linardakis, E. *et al.* Enhancing the efficacy of a weak allogeneic melanoma vaccine by viral fusogenic membrane glycoprotein-mediated tumor cell-tumor cell fusion. **62,** 5495–5504 (2002).

293.Shmulevitz, M., Corcoran, J., Salsman, J. & Duncan, R. Cell-cell fusion induced by the avian reovirus membrane fusion protein is regulated by protein degradation. *J Virol* **78,** 5996–6004 (2004).

294.Sharif-Askari, E. *et al.* Bax-dependent mitochondrial membrane permeabilization enhances IRF3-mediated innate immune response during VSV infection. *Virology* **365,** 20–33 (2007).

295.Nicholson, D. W. *et al.* Identification and inhibition of the ICE/CED-3 protease necessary for mammalian apoptosis. *Nature* **376,** 37–43 (1995).

296.Martin, S. J., Finucane, D. M., Amarante-Mendes, G. P., O'Brien, G. A. & Green, D. R. Phosphatidylserine externalization during CD95-induced apoptosis of cells and cytoplasts requires ICE/CED-3 protease activity. *J Biol Chem* **271,** 28753–28756 (1996).

297.Ferraro-Peyret, C., Quemeneur, L., Flacher, M., Revillard, J.-P. & Genestier, L. Caspase-independent phosphatidylserine exposure during apoptosis of primary T lymphocytes. *J Immunol* **169,** 4805–4810 (2002).

298.Vanags, D. M., Pörn-Ares, M. I., Coppola, S., Burgess, D. H. & Orrenius, S. Protease involvement in fodrin cleavage and phosphatidylserine exposure in apoptosis. *J Biol Chem* **271,** 31075–31085 (1996).

299.Fadeel, B. Programmed cell clearance. *Cell Mol Life Sci* **60,** 2575–2585 (2003).

300.Fadok, V. A., de Cathelineau A, Daleke, D. L., Henson, P. M. & Bratton, D. L. Loss of phospholipid asymmetry and surface exposure of phosphatidylserine is required for phagocytosis of apoptotic cells by macrophages and fibroblasts. *J Biol Chem* **276,** 1071–1077 (2001).

301.Cattaneo, R., Miest, T., Shashkova, E. V. & Barry, M. A. Reprogrammed viruses as cancer therapeutics: targeted, armed and shielded. *Nat Rev Microbiol* **6,** 529–540 (2008).

302.Breitbach, C. J., Reid, T., Burke, J., Bell, J. C. & Kirn, D. H. Navigating the clinical development landscape for oncolytic viruses and other cancer therapeutics: no shortcuts on the road to approval. *Cytokine Growth Factor Rev* **21,** 85–89 (2010).

303.Parato, K. A., Senger, D., Forsyth, P. A. J. & Bell, J. C. Recent progress in the battle between oncolytic viruses and tumours. *Nat Rev Cancer* **5,** 965–976 (2005).

304.Prestwich, R. J. *et al.* Oncolytic viruses: a novel form of immunotherapy. *Expert Rev Anticancer Ther* **8,** 1581–1588 (2008).

305.Galivo, F. *et al.* Interference of CD40L-mediated tumor immunotherapy by oncolytic vesicular stomatitis virus. *Hum Gene Ther* **21,** 439–450 (2010).

306.Lun, X. *et al.* Effects of intravenously administered recombinant vesicular stomatitis virus (VSV(deltaM51)) on multifocal and invasive gliomas. *J Natl Cancer Inst* **98,** 1546–1557 (2006).

307.Ebert, O., Harbaran, S., Shinozaki, K. & Woo, S. Systemic therapy of experimental breast cancer metastases by mutant vesicular stomatitis virus in immune-competent mice. *Cancer Gene Ther* **12,** 350–358 (2005).

308.Waldmann, T. A. & Tagaya, Y. The multifaceted regulation of interleukin-15 expression and the role of this cytokine in NK cell differentiation and host response to intracellular pathogens. *Annu Rev Immunol* **17,** 19–49 (1999).

309.Carson, W. E. *et al.* Interleukin (IL) 15 is a novel cytokine that activates human natural killer cells via components of the IL-2 receptor. *J Exp Med* **180,** 1395–1403 (1994).

310.Ohteki, T. Critical role for IL-15 in innate immunity. *Curr Mol Med* **2,** 371–380 (2002).

311.Kokaji, A. I., Hockley, D. L. & Kane, K. P. IL-15 transpresentation augments CD8+ T cell activation and is required for optimal recall responses by central memory CD8+ T cells. *J Immunol* **180,** 4391–4401 (2008).

312.Teague, R. M. *et al.* Interleukin-15 rescues tolerant CD8+ T cells for use in adoptive immunotherapy of established tumors. *Nat Med* **12,** 335–341 (2006).

313.Ugen, K. E. *et al.* Regression of subcutaneous B16 melanoma tumors after intratumoral delivery of an IL-15-expressing plasmid followed by in vivo electroporation. *Cancer Gene Ther* **13,** 969–974 (2006).

314.Yiang, G.-T. *et al.* Immunotherapy: rAAV2 expressing interleukin-15 inhibits HeLa cell tumor growth in mice. *J Biomed Sci* **16,** 47 (2009).

315.Liu, J. *et al.* Myxoma virus expressing interleukin-15 fails to cause lethal myxomatosis in European rabbits. *J Virol* **83,** 5933–5938 (2009).

316.Araki, A. *et al.* Tumor secreting high levels of IL-15 induces specific immunity to low immunogenic colon adenocarcinoma via CD8+ T cells. *Int J Mol Med* **14,** 571–576 (2004).

317.Bessard, A., Solé, V., Bouchaud, G., Quéméner, A. & Jacques, Y. High antitumor activity of RLI, an interleukin-15 (IL-15)-IL-15 receptor alpha fusion protein, in metastatic melanoma and colorectal cancer. *Molecular Cancer Therapeutics* **8,** 2736–2745 (2009).

318.Stoklasek, T. A., Schluns, K. S. & Lefrançois, L. Combined IL-15/IL-15Ralpha immunotherapy maximizes IL-15 activity in vivo. *J Immunol* **177,** 6072–6080 (2006).

319.Dubois, S., Patel, H. J., Zhang, M., Waldmann, T. A. & Müller, J. R. Preassociation of IL-15 with IL-15R alpha-IgG1-Fc enhances its activity on proliferation of NK and CD8+/CD44high T cells and its antitumor action. *J Immunol* **180,** 2099–2106 (2008).

320.Rubinstein, M. P. *et al.* Converting IL-15 to a superagonist by binding to soluble IL-15R{alpha}. *Proc Natl Acad Sci USA* **103,** 9166–9171 (2006).

321.Smith, E., Breznik, J. & Lichty, B. Strategies to Enhance Viral Penetration of Solid Tumors. *Hum Gene Ther* (2011). doi:10.1089/hum.2010.227

322.Miller, J. M., Bidula, S. M., Jensen, T. M. & Reiss, C. S. Vesicular stomatitis virus modified with single chain IL-23 exhibits oncolytic activity against tumor cells in vitro and in vivo. *Int J Infereron Cytokine Mediator Res* **2010,** 63–72 (2010).

323.Fernandez, M., Porosnicu, M., Markovic, D. & Barber, G. N. Genetically engineered vesicular stomatitis virus in gene therapy: application for treatment of malignant disease. *J Virol* **76,** 895–904 (2002).

324.Willmon, C. L. *et al.* Expression of IFN-beta enhances both efficacy and safety of oncolytic vesicular stomatitis virus for therapy of mesothelioma. *Cancer Res* **69,** 7713–7720 (2009).

325.Tasaki, K. *et al.* Transduction of murine colon carcinoma cells with interleukin-15 gene induces antitumor effects in immunocompetent and immunocompromised hosts. *Cancer Gene Ther* **7,** 255–261 (2000).

326.Villa, P., Kaufmann, S. H. & Earnshaw, W. C. Caspases and caspase inhibitors. *Trends Biochem. Sci.* **22,** 388–393 (1997).

327.Slee, E. A. *et al.* Benzyloxycarbonyl-Val-Ala-Asp (OMe) fluoromethylketone (Z-VAD.FMK) inhibits apoptosis by blocking the processing of CPP32. *Biochem. J.* **315 (Pt 1),** 21–24 (1996).

328.Leifeld, L. *et al.* Anti-Apoptotic Function of Gelsolin in Fas Antibody-Induced Liver Failure in Vivo. *The American Journal of Pathology* **168,** 778–785 (2006).

329.Künstle, G. *et al.* ICE-protease inhibitors block murine liver injury and apoptosis caused by CD95 or by TNF-alpha. *Immunol Lett* **55,** 5–10 (1997).

330.Guidotti, L. G. & Chisari, F. V. Noncytolytic control of viral infections by the innate and adaptive immune response. *Annu Rev Immunol* **19,** 65–91 (2001).

331.Matsuzaki, J. *et al.* Successful elimination of memory-type CD8+ T cell subsets by the administration of anti-Gr-1 monoclonal antibody in vivo. *Cell Immunol* **224,** 98–105 (2003).

332.Choi, K.-H. *et al.* Transcriptional regulation of TNF family receptors and Bcl-2 family by chemotherapeutic agents in murine CT26 cells. *J. Cell. Biochem.* **91,** 410–422 (2004).

333.Borner, C. *et al.* The protein bcl-2 alpha does not require membrane attachment, but two conserved domains to suppress apoptosis. *J Cell Biol* **126,** 1059–1068 (1994).

334.Liao, C. L. *et al.* Effect of enforced expression of human bcl-2 on Japanese encephalitis virus-induced apoptosis in cultured cells. *J Virol* **71,** 5963–5971 (1997).

335.Fernandez, A. *et al.* Angiogenic potential of prostate carcinoma cells overexpressing bcl-2. *J Natl Cancer Inst* **93,** 208–213 (2001).

336.Chipuk, J. E., Moldoveanu, T., Llambi, F., Parsons, M. J. & Green, D. R. The BCL-2 Family Reunion. *Molecular Cell* **37,** 299–310 (2010).

337.Daley, J. M., Thomay, A. A., Connolly, M. D., Reichner, J. S. & Albina, J. E. Use of Ly6G-specific monoclonal antibody to deplete neutrophils in mice. *Journal of Leukocyte Biology* **83,** 64–70 (2007).

338.Shi, C. & Pamer, E. G. Monocyte recruitment during infection and inflammation. *Nat Rev Immunol* **11,** 762–774 (2011).

339.Lim, J. K. *et al.* Chemokine receptor Ccr2 is critical for monocyte accumulation and survival in West Nile virus encephalitis. *J Immunol* **186,** 471–478 (2011).

340.Aldridge, J. R. *et al.* TNF/iNOS-producing dendritic cells are the necessary evil of lethal influenza virus infection. *Proc Natl Acad Sci U S A* **106,** 5306–5311 (2009).

341.Herold, S. *et al.* Alveolar epithelial cells direct monocyte transepithelial migration upon influenza virus infection: impact of chemokines and adhesion molecules. *J Immunol* **177,** 1817–1824 (2006).

342.Lemay, C. G. *et al.* Harnessing oncolytic virus-mediated antitumor immunity in an infected cell vaccine. *Molecular Therapy* **20,** 1791–1799 (2012).

343.Baens, M. *et al.* The Dark Side of EGFP: Defective Polyubiquitination. *PLoS One* **1,** e54 (2006).

344.Deal watch: Amgen buys oncolytic virus company. *Nat Rev Drug Discov* **10,** 166 (2011).

345.Ferguson, M. S., Lemoine, N. R. & Wang, Y. Systemic Delivery of Oncolytic Viruses: Hopes and Hurdles. *Advances in Virology* **2012,** 1–14 (2012).

346.Woller, N. *et al.* Virus-induced tumor inflammation facilitates effective DC cancer immunotherapy in a Treg-dependent manner in mice. *J Clin Invest* **121,** 2570–2582 (2011).

347.Woller, N., Kühnel, F. & Kubicka, S. Virus infections in tumors pave the way for tumor-directed dc-vaccines. *oncoimmunology* **1,** 208–210 (2012).

348.Kottke, T. *et al.* Broad antigenic coverage induced by vaccination with virus-based cDNA libraries cures established tumors. *Nat Med* **17,** 854–859 (2011).

349.Bridle, B. W. *et al.* Potentiating cancer immunotherapy using an oncolytic virus. *Mol Ther* **18,** 1430–1439 (2010).

350.Bridle, B. W. *et al.* Vesicular stomatitis virus as a novel cancer vaccine vector to prime antitumor immunity amenable to rapid boosting with adenovirus. *Mol Ther* **17,** 1814–1821 (2009).

Appendix 1
The p14 FAST Protein of Reptilian Reovirus Increases VSV Neuropathogensis

Christopher W. Brown,[1,2]† Kyle B. Stephenson,[3]† Stephen Hanson,[3] Michael Kucharczyk[3], Roy Duncan[4], John C. Bell[2], and Brian D. Lichty[3]*

[1] Ottawa Health Research Institute, Department of Microbiology and Immunology
University of Ottawa, Ontario, Canada
[2] Department of Orthopaedic Surgery
University of Ottawa, Ontario, Canada
[3] Department of Medical Sciences
McMaster University, Hamilton, Ontario Canada
[4] Departments of Microbiology and Immunology and Paediatrics
Dalhousie University, Halifax, Nova Scotia, Canada

Published in *Journal of Virology*
Vol. 83(2), pp 552-561, January 2009
© American Society for Microbiology

Preface:

This research presented in this manuscript was a collaborative effort between myself and Christopher Brown in Dr. John Bell's laboratory at the OHRI, and took place between 2006 and 2008. The p14 FAST expressing viruses were rescued by Christopher Brown, while the remaining work was shared between Christopher Brown and myself. Specifically, i conducted research that led to the western blots presented in FIgure 1B, Figure 2, histological examination of brains from infected mice presented in figures 3 and 4, figure 5, and the immune analyses presented in figure 6 and 7. I also contributed to the survival data making up Table 1. Dr. Brian Lichty wrote the manuscript with input from Christopher Brown, Dr. John Bell and myself. The work was supervised by Drs. Brian Lichty and John Bell. Dr. Roy Duncan provided the p14 FAST gene and antibodies and also contributed significantly to revisions of the manuscript prior to re-submission.

ABSTRACT

The fusogenic orthoreoviruses express nonstructural fusion-associated small transmembrane (FAST) proteins that induce cell-cell fusion and syncytium formation. It has been speculated that the FAST proteins may serve as virulence factors by promoting virus dissemination and increased or altered cytopathology. To directly test this hypothesis, the gene encoding the p14 FAST protein of reptilian reovirus was inserted into the genome of a heterologous virus that does not naturally form syncytia, vesicular stomatitis virus (VSV). Expression of the p14 FAST protein by the VSV/FAST recombinant gave the virus a highly fusogenic phenotype in cell culture. The growth of this recombinant fusogenic VSV strain was unaltered in vitro but was significantly enhanced in vivo. The VSV/FAST recombinant consistently generated higher titers of virus in the brains of BALB/c mice after intranasal or intravenous infection compared to the parental VSV/green fluorescent protein (GFP) strain that expresses GFP in place of p14. The VSV/FAST recombinant also resulted in an increased incidence of hind-limb paralysis, it infected a larger volume of brain tissue, and it induced more extensive neuropathology, thus leading to a lower maximum tolerable dose than that for the VSV/GFP parental virus. In contrast, an interferon-inducing mutant of VSV expressing p14 was still attenuated, indicating that this interferon-inducing phenotype is dominant to the fusogenic properties conveyed by the FAST protein. Based on this evidence, we conclude that the reovirus p14 FAST protein can function as a bona fide virulence factor.

INTRODUCTION

The genus Orthoreovirus is one of 12 accepted genera within the family Reoviridae, a family of icosahedral nonenveloped viruses containing a double-stranded RNA (dsRNA) genome comprised of 10 to 12 genome segments (23). Reoviruses have been isolated from a broad range of mammalian, avian, and reptilian hosts and are currently classified into five recognized species (4). Four of these five orthoreovirus species have the unusual ability to induce syncytium formation, both in infected cell cultures and in the tissues of infected animals (7, 11, 14, 34). While syncytium formation is a common cytopathic effect associated with numerous enveloped viruses, such as paramyxoviruses, herpesviruses, and retroviruses, the fusogenic reoviruses comprise the majority of examples of nonenveloped viruses with this phenotype. Relatively little is known about the role of syncytium formation in the replication cycle of the fusogenic reoviruses.

A series of recent studies have revealed the basis for the syncytium-inducing property of the fusogenic reoviruses (5, 6, 31). The four fusogenic orthoreovirus species contain an open reading frame not present in the genomes of the nonfusogenic mammalian reovirus subgroup. This open reading frame, contained

within a polycistronic genome segment, encodes a small, single-pass membrane protein, and ectopic expression of this protein by itself in transfected cells results in syncytium formation (6, 31). Collectively, these different reovirus fusion

associated small transmembrane (FAST) proteins define a new family of viral membrane fusion proteins.

There are currently four members of the FAST protein family: the p10 proteins of avian reovirus and Nelson Bay reovirus, the p14 protein of reptilian reovirus, and the p15 protein of baboon reovirus, all named according to their predicted molecular mass (5, 6, 31). The p10 proteins share clear amino acid identities and an identical arrangement of structural motifs, while the p14 and p15 proteins lack sequence similarity to each other or to the p10 proteins, and each has its own unique arrangement of structural motifs. The FAST proteins do, however, share some defining structural and biological features (29). As nonstructural viral proteins, the FAST proteins play no role in reovirus entry into cells. Instead, following their expression inside virus-infected or transfected cells, the FAST proteins are trafficked to the plasma membrane in a $N_{exoplasmic}/C_{cytoplasmic}$ topology, where they induce fusion of virus-infected cells with neighboring uninfected cells. The FAST proteins are also promiscuous fusogens, fusing a wide range of different cell types. Why a nonenveloped virus would encode a dedicated, promiscuous cell-cell fusogen remains unclear.

Recent studies suggest syncytium formation may serve a dual role in the fusogenic reovirus replication cycle (29). Initially, cell-cell fusion would allow rapid localized dissemination of the infection while subsequent extensive syncytium formation triggers apoptosis-induced cell lysis, resulting in a burst of progeny virus release and enhanced systemic infection. This enhanced dissemination

model suggests the FAST proteins could function as virulence factors, and circumstantial evidence supports this hypothesis. While the nonfusogenic mammalian reoviruses are relatively benign, the fusogenic reoviruses are pathogenic following natural infections and induce a variety of clinical symptoms. These symptoms include fatal proliferative interstitial pneumonia, subacute tracheitis, acute or fatal hepatic necrosis, and enteritis (2, 15, 17). Furthermore, there is a correlation between the extent of syncytium formation in cell culture and the pathogenicity of two natural isolates of avian reovirus (8). At present, a reverse genetics system has not been developed for the fusogenic reoviruses; therefore, it has not been possible to directly test whether the FAST proteins contribute to pathogenesis.

To further test the hypothesis that the FAST proteins can function as virulence factors, we sought to develop a recombinant virus expressing the 125-residue p14 FAST protein of reptilian reovirus (5). As a recipient virus we chose vesicular stomatitis virus (VSV), a prototypical member of the *Rhabdoviridae* family, since the pathogenesis of this virus is well characterized in mice. VSV is an enveloped negative-stranded RNA virus that buds from the plasma membrane of the infected cell and does not cause the formation of syncytia (19). VSV is spread by biting insects in subtropical regions, where it causes a relatively mild disease in farm animals characterized by lesions on the oral mucosa. When used to infect laboratory mice in experimental models, however, VSV displays a strong neurotropism and neurovirulence and can lead to lethal encephalitis, especially

after intranasal administration, a characteristic not seen in cows, horses, or pigs (reviewed in reference 19). The transit of VSV into the central nervous systems (CNS) of mice has been extensively studied and has been used as a model for CNS infection, pathogenesis, and immunology (3, 13, 33). We now show that the VSV/FAST recombinant displayed normal replication in vitro but enhanced spread and neurovirulence in vivo, consistently replicating to higher titers in the brains of infected mice and mediating extensive tissue damage. The p14 FAST protein of reptilian reovirus is therefore a bona fide virulence factor that enhances viral spread in vivo.

MATERIALS AND METHODS

Generation of VSV/FAST. PCR was performed on a plasmid containing the p14 FAST cDNA using the primers CGCTCGAGACCACCATGGGGAGTGG ACCCTCTAATTTC and CGGCTAGCCTAAATGGCTGAGACATTAT CGAT in order to add an upstream XhoI site and a downstream NheI site. The resulting PCR product was cloned into the XhoI/NheI sites of pVSV-XN and pVSV-XN M51. After sequencing, the genome plasmids were used to rescue infectious virus. The procedure for rescuing infectious recombinant VSV was similar to that previously described (16). Briefly, BHK cells expressing the T7 RNA polymerase (BHK-T7) were grown to ca. 85% confluence in sterile polystyrene 24-well microtiter plates (Costar catalog no. 3526). BHK-T7 cells were transfected by using Lipofectamine 2000 (Invitrogen) according to the manufacturer's protocol,

with 0.5 g of the genome plasmid and 0.5 g of the support plasmids containing the elements of the viral ribonucleoprotein (125 ng of pBS-VSV N, 313 ng of pBS-VSV P, and 63 ng of pBS-VSV L). Rescued VSV/FAST was plaque purified three times, amplified, and titrated on Vero cells.

Viruses and cells. Vero and HEK 293T cells were obtained from the American Type Culture Collection. Cells were propagated in Dulbecco modified Eaglemedium (HyClone) supplemented with 10% fetal calf serum (Cansera). BHK-T7 cells (a gift from Karl-Klaus Conzelmann) were grown in the presence of G418 (Invitrogen) at a final concentration of 0.2 mg/ml and used for virus rescues. For production of virus used in animal experiments HEK 293T cells were infected at a multiplicity of infection of 0.01. Culture supernatants were collected 24 h later and cleared by centrifugation and filtration through a 0.2-m-pore-size filter. Virus was pelleted and then banded on a continuous 5 to 40% sucrose gradient made in phosphate-buffered saline (PBS). Approximately 1/12 the volume of the gradient containing a visible virus band was collected and extensively dialyzed against PBS, divided into aliquots, and stored at 80°C. Stock titers were determined on Vero cells. The G VSV/RFP/FAST virus was rescued as described above except that a VSV-G expression plasmid was included in the rescue transfection. This virus was propagated on VSV-G-expressing 293 cells to provide VSV-G in *trans* and titers were determined on Vero cells by visualizing red syncytia under a fluorescence microscope.

Western blotting. Infected cells or banded virus were lysed directly in sodium dodecyl sulfate loading buffer and run on polyacrylamide gels, transferred to nitrocellulose, and blocked overnight. Blots were probed with polyclonal rabbit antibodies against VSV (a gift from Earl Brown), green fluorescent protein (GFP; Abcam), or FAST protein (5). After the blots were washed, they were probed with an Alexa Fluor 680-conjugated chicken anti-rabbit secondary antibody (Invitrogen), and the blots were then scanned on a LiCor Odyssey apparatus.

Mouse experiments. Female, 8- to 10-week-old BALB/c mice were obtained from Charles River Laboratories (Wilmington, MA). All experiments were conducted with the approval of the University of Ottawa or McMaster University Animal Care and Veterinary Services. Mice were anesthetized with 3% induction and 2% maintenance of isoflurane for intranasal instillation of 10 l of virus and allowed to recover under oxygen. Intravenous administration of 100 l of virus was performed through the tail vein. Mice were monitored daily and euthanized at indicated time points or upon signs of morbidity by carbon dioxide narcosis. Tissues were collected from euthanized mice and immediately placed at minus 80°C. For the in vivo biodistribution assay, single organs were halved before freezing; otherwise, only one bilateral organ was used for virus titration. The viral content of homogenized tissues was determined by plaque assay on Vero cells. All tissues had undergone only one freeze-thaw cycle, and the tissue weight was measured after homogenization.

Immunohistochemistry. Tissues were harvested as described, placed in OCT mounting media (Tissue-Tek; Sakura Finetek), and sectioned in 4-m sections with a microtome cryostat. Sectioned tissues were fixed in 4% paraformaldehyde for 20 min and used for hematoxylin and eosin staining or immunochemistry (IHC). IHC was performed using reagents from a Vectastain ABC kit for rabbit primary antibodies (Vector Labs) according to instructions provided. Primary antibodies used were polyclonal rabbit antibodies against VSV. Briefly, endogenous peroxidase activity was blocked by incubating with 3% H2O2, followed by blocking of nonspecific epitopes with 1.5% normal goat serum and then blocking with avidin and biotin. PBS washes were performed between all blocking and incubating steps. Sections were incubated with anti-VSV antibody (1:5,000, 30 min), followed by anti-rabbit biotinylated secondary antibody. The avidin-biotinylated enzyme complex was added, and the antigen was localized by incubation with 3,3-diaminobenzidine. Sections were counterstained with hematoxylin. Slides were scanned on a Nikon Coolscan.

Detection of anti-VSV T cells. BALB/c mice were infected with 1e7 PFU of either VSV/GFP or VSV/FAST intravenously. Blood samples were taken 5 and 7 days post-infection, and spleens were removed at 7 days post-infection. PBMC and splenocytes were stimulated for 6 h with the N-MPYLIDFGL-C peptide (Biomer Technology), a CD8 epitope of VSV-N (25). Golgi plug (BD Bioscience) was added 2 h into the stimulation medium. Cells were then fixed; permeabilized; stained with antibodies to CD3, CD8, and gamma interferon (IFN-γ); and

analyzed by flow cytometry on a FACSCanto instrument. The data were analyzed by using FlowJo software.

Determination of neutralizing antibody titers. BALB/c mice were infected with 107 PFU of either VSV/GFP or VSV/FAST intravenously. Blood was collected from a terminal bleed into heparin-treated Hanks balanced salt solution and centrifuged. The resulting plasma was collected, and complement was inactivated by incubating the samples at 56°C for 30 min. Each sample was then serially diluted in duplicate and incubated with 10^4 PFU of VSV/GFP for 30 min at 37°C. These neutralized samples were then transferred onto confluent Vero cells. GFP expression was analyzed on a GE Typhoon scanner 24 h later.

RESULTS

Recombinant VSV expressing the p14 protein induces syncytium formation at neutral pH with no adverse effects on VSV replication.

The p14 open reading frame was PCR amplified with flanking XhoI and NheI sites, and the resulting PCR product was subcloned into the corresponding sites of pVSV-XN and pVSV-XNM51 (Fig. 1A). The recombinant VSV/FAST and dM51VSV/FAST viruses were rescued by using standard procedures. Since recombinant VSV strains are known to be attenuated relative to parental, nonrecombinant virus (26) and insertion of additional genes into the VSV genome results altered the transcription profiles from the extended negative-strand template we therefore created the VSV/GFP recombinant to serve as the parental control, which contains the gene encoding EGFP inserted into the same location

in the VSV genome as the p14 gene in VSV/FAST recombinants (Fig. 1A). The gene encoding the VSV G protein, responsible for virus attachment and virus-cell fusion during the virus entry process, was also deleted from the VSV/FAST genome and replaced with the gene encoding the red fluorescent protein (RFP) to generate the recombinant deltaG/ RFP/FAST virus (Fig. 1A). These recombinant viruses were used to infect Vero cells, and cell lysates were analyzed by Western blotting. Along with the normal repertoire of VSV proteins, the p14 protein was also expressed in cells infected with the recombinant VSV/ FAST virus (Fig. 1B). Interestingly, when progeny virions from these infected cells were isolated by sucrose density gradient centrifugation, Western blotting detected the p14 protein in the same fraction containing VSV virions (Fig. 1B, top and middle panels). This was not the case for the soluble GFP protein expressed in cells infected with the VSV/GFP recombinant virus (Fig. 1B, bottom panel). The presence of p14 in the sucrose fractions containing VSV virions suggested the p14 protein might be pseudotyped onto VSV virions. Since the p14 protein possesses no receptor-binding activity and relies on cellular adhesion proteins to mediate cell binding and close membrane apposition prior to cell-cell membrane fusion (28), any p14 protein pseudotyped onto VSV virions is unlikely to affect VSV entry. This contention was supported by examining the infectivity of progeny virions released from dGVSV/RFP/FAST-infected cells. Since viruses with the G protein deleted bud from cells (22, 27, 30), progeny virions released from the dGVSV/RFP/FAST-infected cells would be lacking the VSV-G protein but might

be pseudotyped with p14. These virions, however, were noninfectious, as indicated by a lack of RFP expression or syncytium formation in the recipient cultures (data not shown). Any p14 protein pseudotyped onto VSV virions is therefore unlikely to affect VSV entry. The ability of the p14 protein expressed from the recombinant viruses to induce cell-cell fusion was confirmed by microscopy, following infection of Vero cells with the VSV/FAST virus (Fig. 1C). Efficient infection by the VSV/GFP virus, confirmed by fluorescence microscopy to detect GFP expression, resulted in no syncytia since the fusion activity of the VSV G protein is dependent on low pH activation. In contrast, the potent fusion activity of the p14 FAST protein at neutral pH was evident by light microscopy from the presence of numerous large syncytia in cells infected with either the VSV/FAST or the dG/RFP/FAST recombinants (Fig. 1C). Fluorescence microscopy confirmed infection by the dG/RFP/FAST recombinant. Similar results were obtained with HEK 293T, CT26, and BHK-T7 cells (not shown), confirming the promiscuous cell-cell fusion activity of the FAST proteins and the successful production of recombinant VSV expressing p14. Since the recombinant VSV expressing p14 rapidly induced the formation of large syncytia in infected monolayers, and the FAST proteins have been demonstrated to induce apoptosis after cell-cell fusion (29), p14-mediated syncytium formation could impair VSV replication in vitro. This was not the case, however, since the growth kinetics of the VSV/FAST and VSV/GFP in a one-step growth curve on Vero cells were identical (Fig. 2). These results indicated that recombinant VSV containing the

gene for the p14 FAST protein can be grown to high titers and that the recombinant virus possesses the cell-cell fusion activity of the fusogenic reoviruses. These recombinant viruses were used to examine the role of the p14 protein as a virulence determinant in vivo.

The p14 FAST protein increases the clinical signs of VSV neuropathogenesis.

To investigate the impact of the p14 protein on VSV spread and replication in vivo, groups of five BALB/c mice were infected intranasally with a range of doses of the attenuated parental VSV/GFP or VSV/FAST recombinants. Animals were monitored for signs of hind-limb paralysis as an indicator of neuropathogenesis and euthanized at the first clear signs of paralysis. Mice developed hind-limb paralysis at day 7 post-infection with VSV/FAST at doses of $1X10^7$ PFU (one of five) and $5X10^7$ PFU (three of five), while at a dose of $5X10^8$ three of four mice had hind-limb paralysis at day 5, and the remaining mouse developed paralysis at day 7 (Table 1). Mice receiving $1X10^7$ or $5X10^7$ PFU of VSV/GFP intranasally failed to develop any clinical signs of hind-limb paralysis and survived treatment. Only one of five mice receiving the highest dose of VSV/GFP developed hind-limb paralysis at 7 days post-infection. IFN-inducing mutants of VSV with a mutation in the matrix protein (M51) have been shown to be highly attenuated in vivo. These viruses have mutations in the matrix protein, making them unable to block the production of IFN by infected cells (10, 32, 35). Intranasal administration of up to 10^9 PFU of a recombinant VSV carrying the p14 gene in

the dM51 background (dM51VSV/FAST) resulted in no toxicity (Table 1), a dose well above the lethal dose for wild-type VSV/FAST. Thus, the fusogenic phenotype does not overcome the severe attenuation associated with IFN induction.

The p14 FAST protein increases the histopathological signs of VSV neuropathogenesis.

It should be noted that in the previous experiment mice surviving infection with VSV/GFP showed no overt sequelae, while the two mice that did not develop hind-limb paralysis after infection with $5X10^7$ PFU of wild-type VSV/FAST (Table 1) did not appear to recover fully. These mice both displayed weight loss, hunched posture, ruffled fur, sunken/shut eyes, erratic movement, and isolation. To further characterize the mice that survived this dose (two from VSV/FAST 9group and all five from the VSV/GFP group), the animals were euthanized at day 21 post-infection, and their brains were processed for histology. Histological examination of brain tissue revealed focal regions of hemorrhage and necrosis (Fig. 3). Both mice that had received VSV/FAST displayed extensive zones of cell loss extending through greater than 400 μm of tissue adjacent to the third ventricle. Immunohistochemical staining of sections adjacent to those showing histopathology detected residual VSV antigens in scatteredcells within these lesions (Fig. 3). There was no evidence of cell loss or damage in any of the VSV/GFP-infected brains (Fig. 3), nor were residual VSV antigens detected in brain sections from mice infected with VSV/GFP stained at the same time post-

infection (data not shown). Therefore, based on both clinical symptoms and preliminary histopathology, the VSV/FAST recombinant appeared to be more neuropathogenic than the corresponding parental virus not expressing the FAST protein. To obtain further histopathological evidence that the p14 protein increases the neurovirulence of VSV, groups of five BALB/c mice were infected intranasally with $5X10^8$ PFU of either the parental VSV/GFP or the VSV/FAST viruses. This dose of virus was previously shown to induce hind-limb paralysis by 5 to 7 days post-infection in 100% of the mice infected with VSV/FAST, while inducing little, if any, paralysis in mice infected with VSV/GFP (Table 1). The brains of infected animals were harvested 4 to 5 days post-infection, and serial sections were processed by immunohistochemistry using a pan-VSV antiserum to determine the extent of infection. At both time points, the extent of the zones of infection and the intensity of staining in these zones was greater in VSV/FAST-infected brains (Fig. 4). At day 4 post-infection, virus was primarily confined to the olfactory bulb in the brains of mice infected with either virus, although some sections also showed staining at distal sites (Fig. 4A and B). By day 5 post-infection, there were notable differences observed in the immunohistochemical staining of brain tissues from animals infected with the two viruses. The staining pattern within the brains of mice infected with VSV/GFP remained largely the same as that observed at the earlier time point, with small regions of staining in the olfactory bulbs and at or near ventricles that did not extend beyond a 200-μm-thick zone (Fig. 4C, arrows in the third section). In contrast, extensive staining

was seen in the middle of the brains of animals infected with the p14-expressing VSV/FAST recombinant, especially around the third ventricle (Fig. 4D). Not only was the intensity of staining stronger than that observed in VSV/GFP infected brain tissue, but the individual foci of infection extended beyond 1,000 μm in diameter (i.e., spanning the five tissue sections examined). This enhanced intensity and greater extent of staining was seen in all VSV/FAST-infected brains. Thus, the VSV/FAST recombinant virus infected a much greater volume of brain tissue than the parental VSV/GFP virus. The immunohistochemistry results therefore provided clear evidence that the p14 FAST protein increases the ability of an attenuated strain of VSV to spread through brain tissue following intranasal infection.

The p14 FAST protein enhances the replication of VSV in the brain.

Further support that the VSV/FAST recombinant is more neuropathogenic was obtained by examining the titers of infectious virus present in the brain. Groups of five BALB/c mice were infected intranasally with $5X10^7$ PFU of either VSV/GFP, M51VSV/GFP, or VSV/FAST. On day 6 the mice were euthanized, brains were collected, and the infectious virus loads were measured by plaque assay. As expected, the IFN inducing ΔM51VSV/GFP recombinant virus failed to replicate in the brain, whereas viral replication was clearly detected in the brains of animals infected with either of the recombinant viruses containing a wild-type VSV backbone (Fig. 5). The parental VSV/GFP virus yielded highly variable virus titers

at this time point, a feature we frequently observe when using this virus to infect mice (unpublished results). In contrast, all five mice infected with the VSV/FAST virus yielded consistently high titers of virus in the brain (Fig. 5), and virus isolated from the VSV/FAST-infected brains retained the syncytial phenotype in cell culture (data not shown). Although the mean tissuetiters were not significantly different, the VSV/FAST-infected brains showed significantly less variation in titer since this virus consistently generated high titers after intranasal infection. The increased clinical and histopathological evidence of neuropathogenesis (Table 1 and Fig. 3 and 4) and consistently high virus titers in brain tissue (Fig. 5) all indicate that expression of the p14 FAST protein by recombinant VSV increases the neurovirulence of the virus.

The p14 FAST protein increases VSV replication in the brain following intravenous infection.

To determine whether the presence of the p14 protein in VSV-infected cells could alter viral pathogenesis after infection via different routes, we examined virus biodistribution after intravenous infection with the VSV/FAST or parental VSV/GFP recombinants. In two independent experiments, groups of three mice were injected intravenously with $2X10^8$ PFU of the recombinant viruses, and the in vivo biodistribution was assessed by using a plaque assay to determine the viral load in various tissues after systemic infection. Although VSV titers increased over time in brains (Fig. 6), they declined and became undetectable by 96 h in all other tissues examined (lung, liver, spleen, heart, kidney, colon, muscle, and

blood; Fig. 6 and data not shown). Although modest, the titers of VSV/FAST in tissues other than the lung were slightly elevated relative to the levels of VSV/GFP between 24 and 48 h post-infection, indicating that the VSV/FAST recombinant infects and replicates to equivalent, or slightly higher, levels compared to the parental VSV/GFP virus in numerous tissues after intravenous administration. This was not the case in lung tissue, where the titers of VSV/GFP were 3 logs higher than the titers of VSV/FAST at 24 h post-infection, declining to near-equivalent titers by 48 h post-infection (Fig. 6). It is currently unclear why expression of the p14 FAST protein in lung tissues might transiently compromise VSV replication. In contrast to the virus yield data in these tissues, infectious virus present in the brains of animals infected with both VSV/FAST and VSV/GFP progressively increased, rather than decreased, from 24 to 96 h post-infection (Fig. 6). These results highlight the neurotropic nature of VSV. More importantly, the analysis of infectious viral yield clearly indicated a more extensive infection of the brain after the intravenous administration of VSV/FAST. At all time points tested, infectious VSV/FAST present in brain tissue was increased by 1 to 4 logs between 24 and 96 h post-infection relative to the titers obtained in animals infected with VSV/GFP (Fig. 6). In addition, hind-limb paralysis was noted in one of the three animals infected with VSV/FAST at the 96-h time point, whereas none of the VSV/GFP-infected animals demonstrated any signs of neurotoxicity by this time. Therefore, expression of the p14 FAST protein

increases the neurovirulence of recombinant VSV viruses when administered via the mucosal or hematogenous routes.

Expression of the p14 protein has little, if any, effect on the immune response to VSV.

Since VSV/FAST was able to cause hind-limb paralysis at lower doses than VSV/GFP in immunocompetent hosts, we sought to determine whether VSV/FAST might alter the acquired immune response to the VSV recombinants. To this end, the $CD8^+$ T-cell responses and neutralizing antibody titers induced after infection with either VSV/GFP or VSV/FAST were examined. After a single, sublethal intravenous dose of 107 PFU, peripheral blood was collected at 5 days post-infection, and both blood and spleens were collected at day 7 post-infection. The percentage of $CD3^+$ $CD8^+$ T cells displaying IFN-γ expression after exposure to the MPYLIDFGL nucleocapsid peptide was similar in each case (Fig. 7). The VSV/FAST-infected mice displayed approximately half the neutralizing antibody titer induced by VSV/GFP at day 7 post-infection (Fig. 8), although the titer was really only different in two of five VSV/FAST-infected mice. Thus, the recombinant VSV expressing the p14 FAST protein appears to induce a similar magnitude of T-cell response after infection and a slightly lower neutralizing antibody response.

DISCUSSION

Several enveloped viruses, such as respiratory syncytial virus, measles virus, human immunodeficiency virus, and henipaviruses, induce syncytium

formation in vivo. Since the viral proteins responsible for syncytium formation are also required for virus entry, it is difficult to examine the role of the syncytial phenotype in pathogenesis while excluding possible alterations in viral entry. By adding this fusogenic function to VSV, we have made a virus that does not require the syncytial phenotype for entry but utilizes this ability to enhance its spread in vivo.

In the present study we set out to determine whether or not the reoviral p14 FAST fusogenic protein can serve as a virulence factor when transferred to another, unrelated virus. To this end, we generated several recombinant strains of VSV expressing p14, in a wild-type VSV background, in an IFN inducing mutant VSV background, and in a version with the G protein deleted. All of these viruses induced significant syncytium formation in monolayers of cultured cells in vitro. We wondered whether the rapid formation of large syncytia may lead to premature cell death and negatively impact on VSV replication; however, one-step growth curves show that VSV/FAST grows at a similar rate and to similar titers as VSV/GFP. Thus, the replication of VSV is sufficiently rapid to reach plateau prior to extensive killing of infected cells through syncytium formation.

After intranasal delivery, VSV/FAST induced hind-limb paralysis at lower doses than VSV/GFP and generated high titers of virus in the brains of these mice more consistently. We also detected enhanced replication in the CNS after intravenous administration of VSV/FAST, especially at the 48-h time point and observed hind-limb paralysis within 4 days by this route. This enhanced spread of

the virus and more efficient and rapid entry into the CNS by VSV/FAST establishes the FAST fusogenic protein as a virulence factor. We do not know why the VSV/FAST virus consistently produced lower lung titers at 24 h post-infection, although one might speculate that this is the one tissue where cell death induced by syncytium formation acutely reduced VSV replication. It should also be noted that the high titers seen in brains after delivery of $5X10^7$ VSV/GFP did not necessarily lead to hind-limb paralysis, while this dose of VSV/FAST usually did, despite a similar viral load in the brain. The greater brain tissue damage and clinical signs in mice that survived this dose of VSV/FAST would imply that not only does this virus enter the CNS more readily, it also does more damage once it arrives, thereby demonstrating the role of FAST as a virulence factor.

We consistently detected, after intranasal infection, VSV staining beyond the olfactory bulb at day 4 in VSV/GFP-infected brains, but we rarely detected this in VSV/FAST-infected brains (Fig. 4 and data not shown). Although the VSV/FAST virus appeared to travel into the brain more slowly by the intranasal route, the infected volume of brain and the intensity of immunohistochemical staining was always greater. After intravenous delivery, however, VSV/FAST clearly entered the brain more efficiently (Fig. 5). The formation of syncytia by this virus in the brains of mice likely leads to the greater extent of histopathology and in turn results in the increased incidence of hind-limb paralysis compared to VSV/GFP at doses that yield comparable brain tissue titers.

VSV-G is known to confer a very broad tropism; as such, it is difficult to ascertain whether the viral tropism of VSV/FAST is altered. We have observed that acid neutralization of VSV-G renders the VSV/FAST virus noninfectious but does not inhibit FAST-mediated cell-to-cell fusion (data not shown), indicating that the FAST protein retains its function in these conditions but is unable to mediate viral entry. In the absence of the VSV-G protein, the RFP/FAST virus was able to spread via cell-to-cell fusion; however, infectious progeny could not be propagated when filtered supernatants were passaged onto independent cell cultures, thereby supporting the notion that the FAST protein is unable to mediate viral binding and entry in the absence of G function. Furthermore, since the p14 protein possesses no receptor-binding activity and relies on cellular adhesion proteins to mediate cell binding and close membrane apposition prior to cell-cell membrane fusion (28), any p14 protein pseudotyped onto VSV virions is unlikely to affect VSV entry.

We did not detect any differences in the T-cell responses and only minor reductions in serum neutralizing antibodies after VSV/FAST infection. Based on these data, we feel that it is unlikely that the FAST protein gives this virus any significant immunoevasive properties. The infections investigated here were all of an acute nature, and in some cases the mice were reaching the endpoint prior to day 7, when a full-blown adaptive immune response would come to bear. Thus, it is unlikely that alterations in immunogenicity could explain the differences in neuropathogenesis seen between VSV/GFP and VSV/FAST.

Although it is not clear why enhanced tissue damage might benefit the reovirus from which the FAST protein is derived, this enhanced spread from the bloodstream in the infected host could help these viruses disseminate more rapidly prior to the development of an effective immune response. Alternatively, the enhanced IHC staining we observed in VSV/FAST infected tissues may indicate that by fusing together the cytoplasm of multiple cells these viruses may have an enhanced ability to commandeer protein translation machinery. This may allow fusogenic viruses to generate more viral protein, leading to enhanced replication, especially for a virus such as reovirus that does not need to bud, since syncytia would have a reduced plasma membrane/cytoplasmic volume ratio.

The IFN-inducing mutation in the ΔM51-VSV/FAST virus attenuates toxicity in vivo and thus these fusogenic properties are not able to make VSV IFN resistant in any manner. Based on other work with this IFN-inducing mutant of VSV (1, 9, 21, 32, 36), we would predict that M51-VSV/FAST will display good tumor targeting but enhanced spread in permissive tumor cells and may prove to be a superior oncolytic virus. Fusogenic viruses have also been demonstrated to have an enhanced ability to induce anti-tumoral immunity following oncolysis in mouse models of cancer (12, 18, 20, 24). We are currently testing our novel fusogenic VSV vector as an oncolytic therapeutic.

REFERENCES

1. **Ahmed, M., S. D. Cramer, and D. S. Lyles.** 2004. Sensitivity of prostate tumors to wild-type and M protein mutant vesicular stomatitis viruses. Virology **330**:34–49.
2. **Benavente, J., and J. Martinez-Costas.** 2007. Avian reovirus: structure and biology. Virus Res. **123**:105–119.
3. **Browning, M., C. S. Reiss, and A. S. Huang.** 1990. The soluble viral glycoprotein of vesicular stomatitis virus efficiently sensitizes target cells for lysis by CD4+T Lymphocytes. J. Of Virology **64:**3810-3816.
4. **Chappell, J. D., R. Duncan, P. P. C. Mertens, and T. S. Dermody.** 2005. *In* C. M. Fauquet, M. A. Mayo, J. Maniloff, U. Desselberger, and L. A. Ball (ed.), Virus taxonomy. Eighth report of the International Committee on Taxonomy of Viruses. Elsevier Academic, San Diego, CA.
5. **Corcoran, J. A., and R. Duncan.** 2004. Reptilian reovirus utilizes a small type III protein with an external myristylated amino terminus to mediate cell-cell fusion. J. Virol. **78**:4342–4351.
6. **Dawe, S., and R. Duncan. 2002.** The S4 genome segment of baboon reovirus is bicistronic and encodes a novel fusion-associated small transmembrane protein. J. Virol. **76**:2131–2140.
7. **Duncan, R., F. A. Murphy, and R. R. Mirkovic.** 1995. Characterization of a novel syncytium-inducing baboon reovirus. Virology **212**:752–756.
8. **Duncan, R., and K. Sullivan.** 1998. Characterization of two avian reoviruses that exhibit strain-specific quantitative differences in their syncytium-inducing and pathogenic capabilities. Virology **250**:263–272.
9. **Ebert, O., S. Harbaran, K. Shinozaki, and S. L. Woo.** 2005. Systemic therapy of experimental breast cancer metastases by mutant vesicular stomatitis virus in immune-competent mice. Cancer Gene Ther. **12**:350–358.
10. **Faria, P. A., P. Chakraborty, A. Levay, G. N. Barber, H. J. Ezelle, J. Enninga, C. Arana, J. van Deursen, and B. M. Fontoura.** 2005. VSV disrupts the Rae1/mrnp41 mRNA nuclear export pathway. Mol. Cell **17**:93–102.
11. **Gard, G., and R. W. Compans.** 1970. Structure and cytopathic effects of Nelson Bay virus. J. Virol. **6**:100–106.
12. **Hoffmann, D., W. Bayer, and O. Wildner.** 2007. Therapeutic immune response induced by intratumoral expression of the fusogenic membrane protein of vesicular stomatitis virus and cytokines encoded by adenoviral vectors. Int. J. Mol. Med. **20**:673–681.
13. **Huneycutt, B. S., I. V. Plakhov, Z. Shusterman, S. M. Bartido, A. Huang, C. S. Reiss, and C. Aoki**. 1994. Distribution of vesicular stomatitis virus proteins in the brains of BALB/c mice following intranasal inoculation: an immunohistochemical analysis. Brain Res. **635**:81–95.

14. **Kibenge, F. S., and A. S. Dhillon.** 1987. A comparison of the pathogenicity of four avian reoviruses in chickens. Avian Dis. **31**:39–42.
15. **Lamirande, E. W., D. K. Nichols, J. W. Owens, J. M. Gaskin, and E. R. Jacobson.** 1999. Isolation and experimental transmission of a reovirus pathogenic in ratsnakes (Elaphe species). Virus Res. **63**:135–141.
16. **Lawson, N. D., E. A. Stillman, M. A. Whitt, and J. K. Rose.** 1995. Recombinant vesicular stomatitis viruses from DNA. Proc. Natl. Acad. Sci. USA **92**:4477–4481.
17. **Leland, M. M., G. B. Hubbard, H. T. Sentmore III, K. F. Soike, and J. K. Hilliard.** 2000. Outbreak of orthoreovirus-induced meningoencephalomye -litsin baboons. Comp. Med. **50**:199–205.
18. **Li, H., A. Dutuor, X. Fu, and X. Zhang. 2007.** Induction of strong antitumor immunity by an HSV-2-based oncolytic virus in a murine mammary tumor model. J. Gene Med. **9**:161–169.
19. **Lichty, B. D., A. T. Power, D. F. Stojdl, and J. C. Bell.** 2004. Vesicular stomatitis virus: re-inventing the bullet. Trends Mol. Med. 10:210–216.
20 **Linardakis, E., A. Bateman, V. Phan, A. Ahmed, M. Gough, K. Olivier, R. Kennedy, F. Errington, K. J. Harrington, A. Melcher, and R. Vile.** 2002. Enhancing the efficacy of a weak allogeneic melanoma vaccine by viral fusogenic membrane glycoprotein-mediated tumor cell-tumor cell fusion. Cancer Res. **62:**5495–5504.
21. **Lun, X., D. L. Senger, T. Alain, A. Oprea, K. Parato, D. Stojdl, B. Lichty, A. Power, R. N. Johnston, M. Hamilton, I. Parney, J. C. Bell, and P. A. Forsyth.** 2006. Effects of intravenously administered recombinant vesicular stomatitis virus (VSV(M51)) on multifocal and invasive gliomas. J. Natl. Cancer Inst. **98:1546–1557.**
22. **Mebatsion, T., M. Konig, and K. K. Conzelmann.** 1996. Budding of rabies virus particles in the absence of the spike glycoprotein. Cell **84:941–951.**
23. **Mertens, P. P. C., R. Duncan, H. Attoui, and T. S. Dermody.** 2005. Reoviridae. *In* C. M. Fauquet, M. A. Mayo, J. Maniloff, U. Desselberger, and L. A. Ball (ed.), Virus taxonomy. Eighth report of the International Committee on Taxonomy of Viruses. Elsevier/Academic Press, London, England.
24. **Nakamori, M., X. Fu, R. Rousseau, S. Y. Chen, and X. Zhang.** 2004. Destruction of nonimmunogenic mammary tumor cells by a fusogenic oncolytic herpes simplex virus induces potent antitumor immunity. Mol. Ther. **9**:658–665.
25. **Ramsburg, E. A., J. M. Publicover, D. Coppock, and J. K. Rose.** 2007. Requirement for CD4 T-cell help in maintenance of memory CD8 T-cell responses is epitope dependent. J. Immunol. **178:**6350–6358.
26. **Roberts, A., E. Kretzschmar, A. S. Perkins, J. Forman, R. Price, L. Buonocore, Y. Kawaoka, and J. K. Rose. 1998.** Vaccination with a

recombinant vesicular stomatitis virus expressing an influenza virus hemagglutinin provides complete protection from influenza virus challenge. J. Virol. **72:**4704–4711.

27. **Robison, C. S., and M. A. Whitt.** 2000. The membrane-proximal stem region of vesicular stomatitis virus G protein confers efficient virus assembly. J. Virol. **74:**2239–2246.
28. **Salsman, J., D. Top, C. Barry, and R. Duncan.** 2008. A virus-encoded **c**ell-cell fusion machine dependent on surrogate adhesins. PLoS Pathog**. 4**:e1000016.
29. **Salsman, J., D. Top, J. Boutilier, and R. Duncan.** 2005. Extensive syncytium formation mediated by the reovirus FAST proteins triggers apoptosis-induced membrane instability. J. Virol. **79**:8090–8100.
30. **Schnell, M. J., J. E. Johnson, L. Buonocore, and J. K. Rose.** 1997. Construction of a novel virus that targets HIV-1-infected cells and controls HIV-1 infection. Cell **90**:849–857.
31. **Shmulevitz, M., and R. Duncan.** 2000. A new class of fusion-associated small transmembrane (FAST) proteins encoded by the non-enveloped fusogenic reoviruses. EMBO J. **19:**902–912.
32. **Stojdl, D. F., B. D. Lichty, B. R. tenOever, J. M. Paterson, A. T. Power, S. Knowles, R. Marius, J. Reynard, L. Poliquin, H. Atkins, E. G. Brown, R. K. Durbin, J. E. Durbin, J. Hiscott, and J. C. Bell.** 2003. VSV strains with defects in their ability to shutdown innate immunity are potent systemic anti-cancer agents. Cancer Cell **4**:263–275.
33. **Trottier, M. D., D. S. Lyles, and C. S. Reiss.** 2007. Peripheral, but not central nervous system, type I interferon expression in mice in response to intranasal vesicular stomatitis virus infection. J. Neurovirol. **13**:433–445.
34. **Vieler, E., W. Baumgartner, W. Herbst, and G. Kohler.** 1994. Characterization of a reovirus isolate from a rattle snake, *Crotalus viridis*, with neurological dysfunction. Arch. Virol. **138**:341–344.
35. **von Kobbe, C., J. M. van Deursen, J. P. Rodrigues, D. Sitterlin, A. Bachi, X. Wu, M. Wilm, M. Carmo-Fonseca, and E. Izaurralde.** 2000. Vesicular stomatitis virus matrix protein inhibits host cell gene expression by targeting the nucleoporin Nup98. Mol. Cell **6**:1243–1252.
36. **Wu, Y., X. Lun, H. Zhou, L. Wang, B. Sun, J. C. Bell, J. W. Barrett, G. McFadden, J. A. Biegel, D. L. Senger, and P. A. Forsyth.** 2008. Oncolytic efficacy of recombinant vesicular stomatitis virus and myxoma virus in experimental models of rhabdoid tumors. Clin. Cancer Res. **14**:1218–1227.

FIGURE LEGENDS

Figure 1. Generation of VSV-FAST. (A) The p14 FAST gene from a fusogenic reptilian reovirus was subcloned into the pVSV-XN genome plasmid between the glycoprotein (G) and polymerase (L) as EGFP had been inserted previously. The G-deleted version was then made by replacing G with RFP. (B) Western blot analysis of infected cell lysates and sucrose banded virus reveals that FAST is expressed in VSV/FAST infected cells and is present in the viral particle. Vero cells were infected with virus overnight, and cellular lysates were run (lanes 1 to 4) or virus was banded on a sucrose gradient and 108 PFU were run per lane (lanes 5 to 7). Blots were probed for VSV proteins (upper), FAST protein (middle), or GFP (bottom). Lanes: 1, VSV/GFP; 2, mock; 3, VSV/FAST; 4, M51-VSV/FAST; 5, VSV/GFP; 6, VSV/FAST; 7, M51-VSV/FAST. (C) Confluent Vero cells were infected with the indicated viruses, and photomicrographs taken 24 h later show the large multinucleated syncytia induced by the FAST viruses (arrows). Magnification, 8.

Figure 2. Growth of VSV/FAST *in vitro*. Confluent monolayers of Vero cells were infected in triplicate with either VSV/GFP or VSV/FAST at a multiplicity of infection of 5.0 for 45 min in minimal medium, after which the monolayers were washed three times. Samples were collected at 0, 4, 8, 12, and 24 h post-

infection, and virus titers were determined in duplicate by plaque assay on Vero cells using standard techniques. The mean of the log-transformed titers are shown the standard error of the mean (SEM).

Figure 3. VSV in the brain following intranasal administration. Of the five mice receiving $5X10^7$ PFU of VSV/FAST intranasally, two failed to develop hind-limb paralysis but continued to display clinical signs (piloerection, hunched posture, etc.). These mice were euthanized on day 21 post-infection, and the brains were subjected to histological and immunohistological analysis. Sections were either stained with hematoxylin and eosin or stained with a pan-VSV polyclonal antibody. Both VSV/FAST-infected mice had large zones of damaged and inflamed tissue. Mouse 2 displayed two zones of clear damage (red circles), one of which showed a few VSV-antigen positive cells (left panel). Mouse 3 displayed one zone of clear damage that showed occasional VSV-antigen positive cells (right panel, arrows). The VSV/GFP-infected mice were also examined, and a representative section is shown, demonstrating that this obvious damage is only caused by the VSV/FAST virus. VSV antigen was undetectable in this mouse (data not shown).

Figure 4. Distribution of VSV/GFP and VSV/FAST in the brain after intranasal administration. BALB/c mice were infected intranasally with $5X10^8$ PFU of either the parental wild-type VSV/GFP or wild-type VSV/FAST. The brains

were collected for immunohistochemical staining on days 4 and 5 post-infection and stained with a pan-VSV polyclonal antibody. At day 4 post-infection virus was detected within the olfactory bulb (lower arrow, middle section, panel A), as well as in the middle of the brain (upper arrow, middle section, panel A), in brains infected with VSV/GFP, whereas the VSV/FAST virus was primarily confined to the olfactory bulb at this time point (arrow, middle section, panel B), although some brains showed staining at distal sites even at this earlier time point (arrow, rightmost section near the hippocampal sulcus, panel B). At day 5 post-infection small regions of staining were seen in olfactory bulbs at or near ventricles within the brains of mice infected with VSV/GFP (arrows, third section, panel C), while extensive staining was seen in the middle of brains, especially around the third ventricle, in mice infected with VSV/FAST (first five sections, panel D). The intensity and extent of staining observed was consistently greater in VSV/FAST-infected brains; representative brains are shown. The horizontal or axial sections shown for each brain are 200 μm apart proceeding from the bottom to the top of the brain left to right (A and B) or top to bottom (C and D).

Figure 5. VSV titers in the brain following intranasal administration. Three groups of five BALB/c mice were infected intranasally with $5X10^7$ PFU VSV/GFP, ΔM51-VSV/GFP, or VSV/FAST. On day 6 brains were collected, and tissue titers were determined by duplicate plaque assays. The VSV/GFP-infected brains showed highly variable tissue titers with two brains near the limit of detection and

one falling below this limit. The VSV/FAST-infected brains all showed similar, high tissue titers. Although the mean titer for the M51-VSV-infected brains was significantly different than the other groups (one-way analysis of variance, P 0.05), the mean titers for the VSV/GFP- and VSV/FAST-infected brains were not significantly different at this time point (one-way analysis of variance, P = 0.05). However, these two groups showed significantly different variances (P = 0.0092).

Figure 6. Biodistribution of viruses. VSV/FAST enters the brains of mice more rapidly after intravenous infection. In two independent experiments mice were injected intravenously with $2X10^8$ PFU of either VSV/GFP or VSV/FAST, and tissues from three animals were analyzed for each time point. Although in most tissues the titers measured were similar between these two viruses (i.e., the spleen shown here and data not shown), the VSV/FAST virus generated higher titers in brains and thyroid/cervical lymph nodes at the 48 h time point while showing lower titers in the lung at 24 h. At the 96-h time point virus was only detectable in brains for both viruses. Mean titers the SEM are shown. An asterisk (*) indicates a statistically significant difference (P < 0.05, two-tailed t test).

Figure 7. CD8 T cell responses after VSV infection. Groups of five BALB/c mice were infected intravenously with 107 PFU of either VSV/GFP or VSV/FAST. (A) Five days post-infection peripheral blood was collected, and VSV-responsive CD8 T cells were enumerated by intracellular staining for IFN-γ production in

response to the MPY peptide derived from the nucleocapsid of VSV Indiana. (B) At 7 days post-infection peripheral blood and splenocytes were collected, and VSV-responsive CD8 T cells were again enumerated. The percentages of CD3 $CD8^+$ T cells that were IFN-γ after peptide stimulation ex vivo are displayed. The data shown represent the mean ± the SEM. No significant differences were detected.

Figure 8. VSV/FAST induces slightly lower antibody titers. Two groups of five BALB/c mice infected intravenously with 107 PFU of virus each. After 7 days, blood was collected into heparin-treated Hanks buffer, followed by centrifugation. The resulting plasma was collected, and complement was inactivated by incubating the samples at 56°C for 30 min. Each sample was then serially diluted in duplicate and incubated with 10^4 PFU of VSV/GFP for 30 min at 37°C. These neutralized samples were then transferred onto confluent Vero cells in 96-well plates. (A) These plates were scanned on a Typhoon scanner 24 h later to detect GFP expression (shown as black). (B) Quantification of the fluorescence intensity across each row demonstrated increased GFP intensity across the 1:135 and 1:405 dilution rows. The mean fluorescence intensity the SEM are shown; a statistically significant difference was detected at the 1:405 dilution (two-tailed *t* test).

FIGURES

FIgure 1

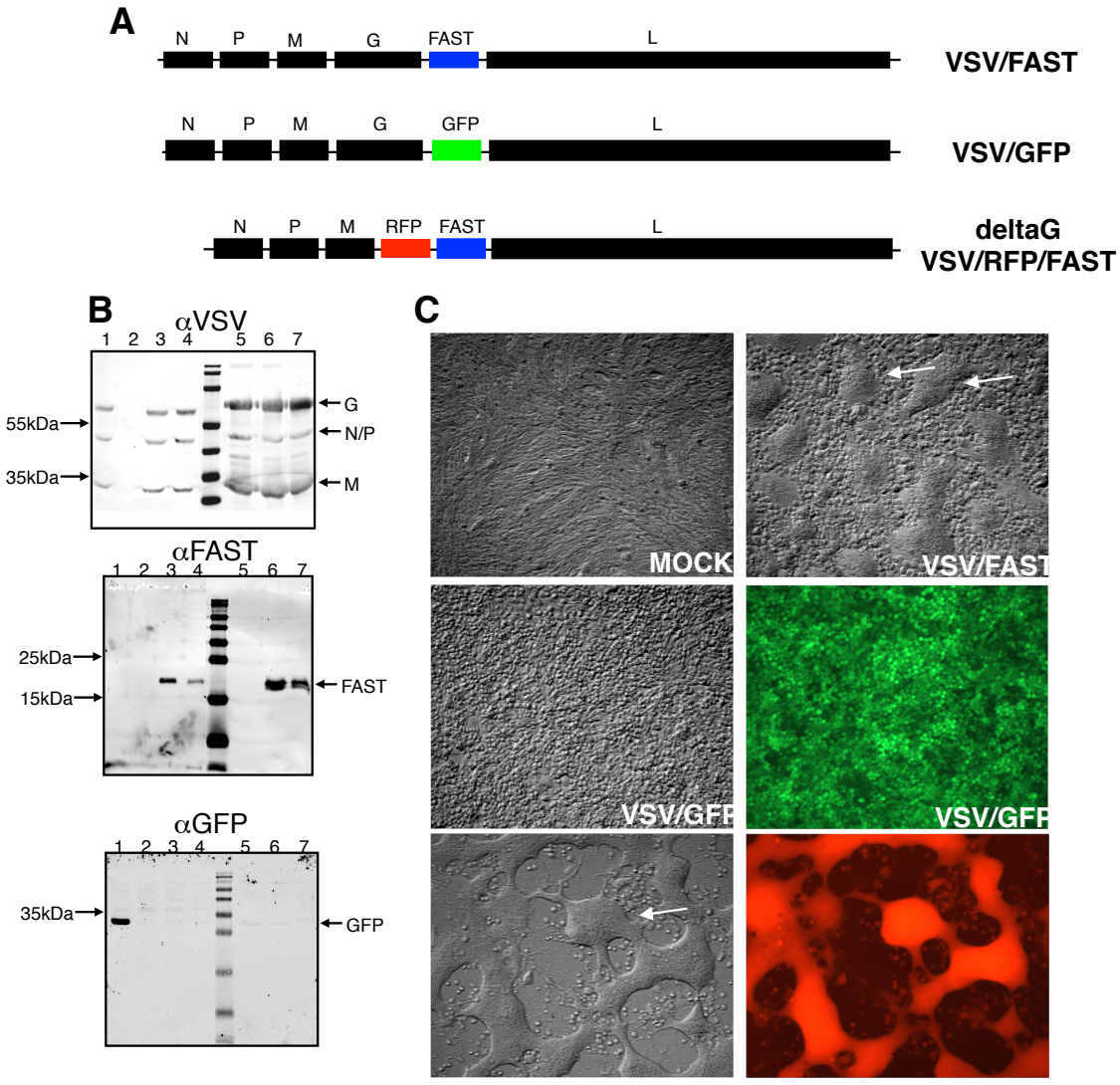


Figure 2

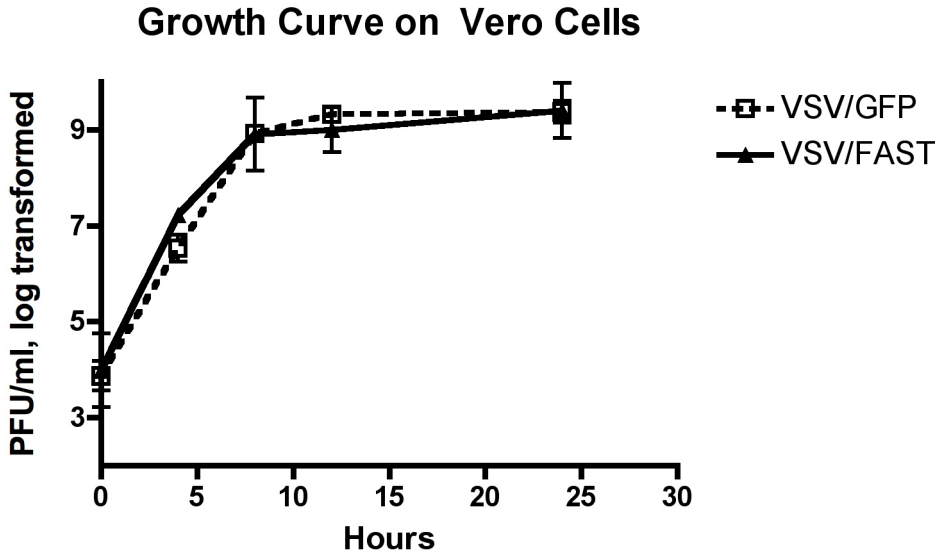

Growth Curve on Vero Cells
PFU/ml, log transformed
9
7
5
3
0
5
10
15
20
25
30
Hours
VSV/GFP
VSV/FAST

Figure 3

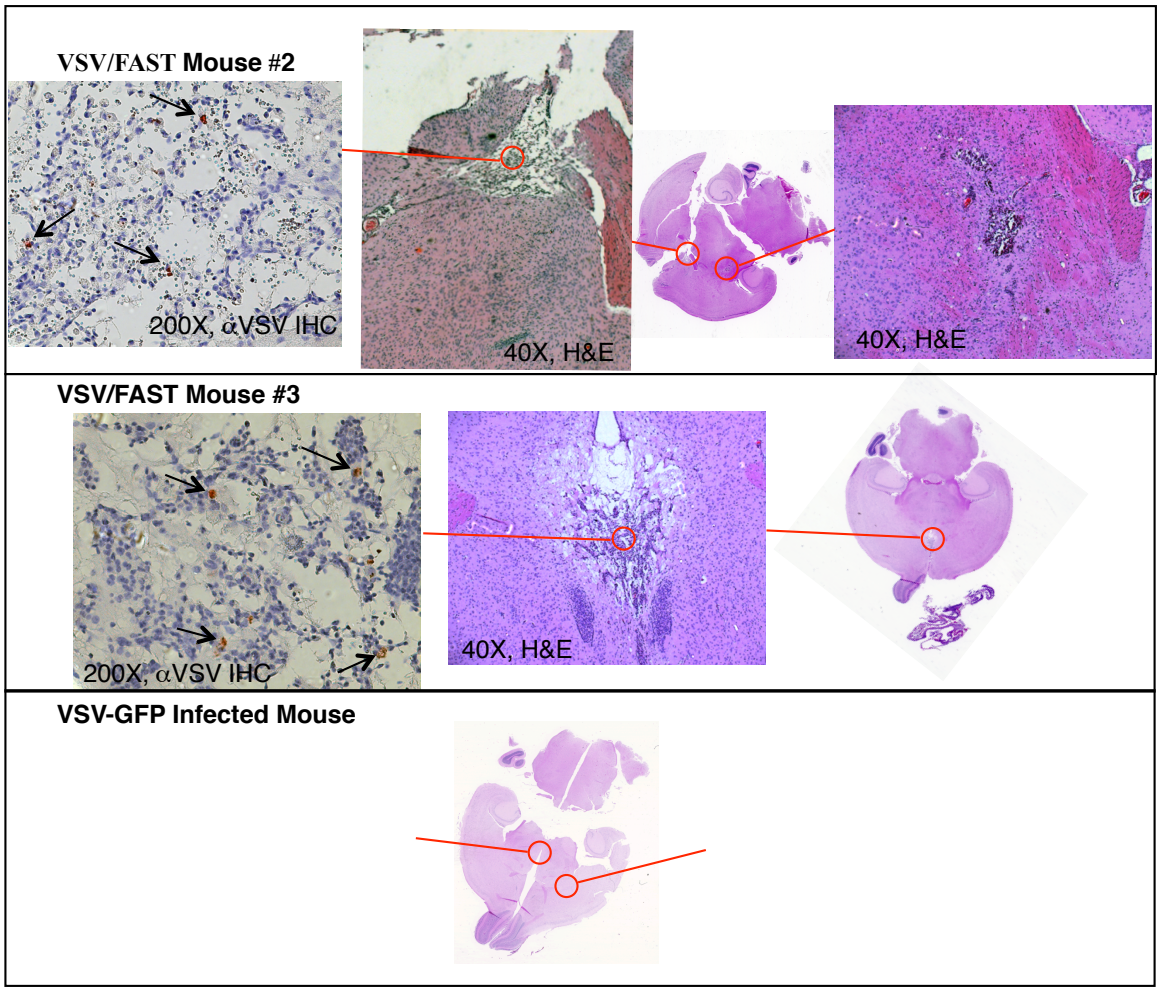

VSV/FAST Mouse #2
200X, αVSV IHC
40X, H&E
40X, H&E
VSV/FAST Mouse #3
200X, αVSV IHC
40X, H&E
VSV-GFP Infected Mouse

Figure 4

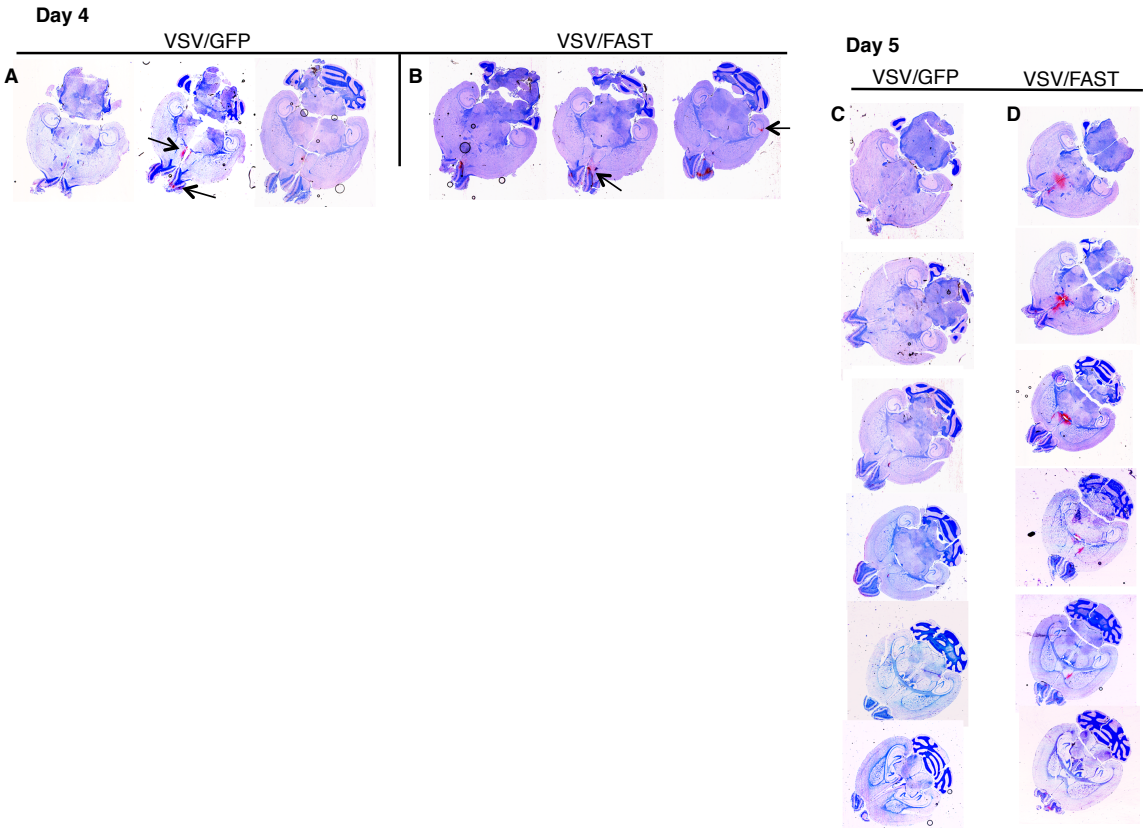


Figure 5

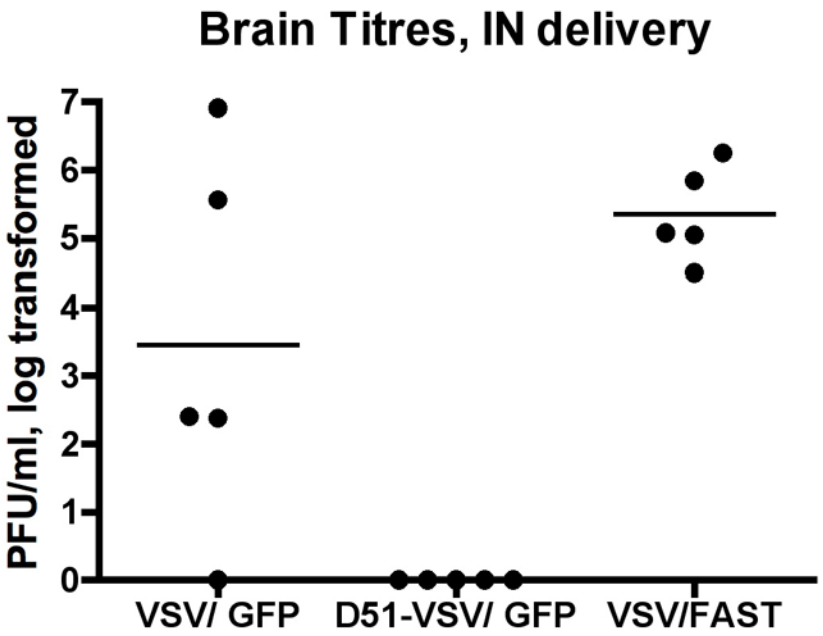

Brain Titres, IN delivery
PFU/ml, log transformed
0
1
2
3
4
5
6
7
VSV/ GFP
D51-VSV/ GFP
VSV/FAST

Figure 6

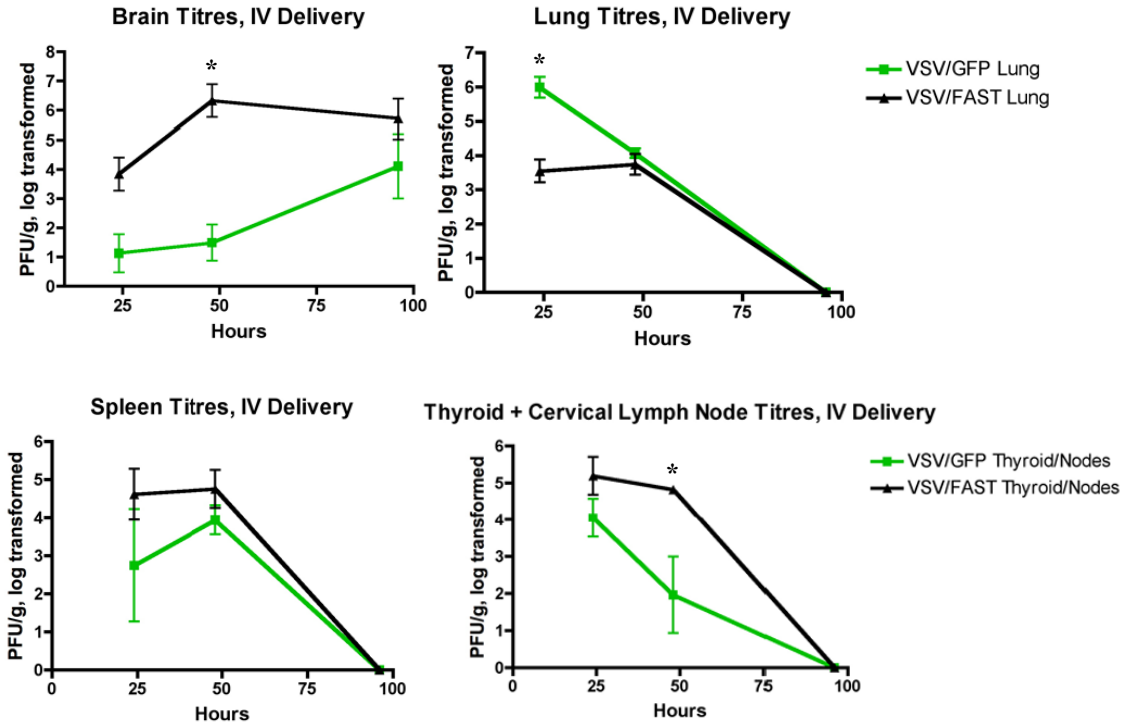

Brain Titres, IV Delivery
PFU/g, log transformed
Hours
*
Lung Titres, IV Delivery
PFU/g, log transformed
Hours
*
VSV/GFP Lung
VSV/FAST Lung
Spleen Titres, IV Delivery
PFU/g, log transformed
Hours
Thyroid + Cervical Lymph Node Titres, IV Delivery
PFU/g, log transformed
Hours
*
VSV/GFP Thyroid/Nodes
VSV/FAST Thyroid/Nodes

Figure 7

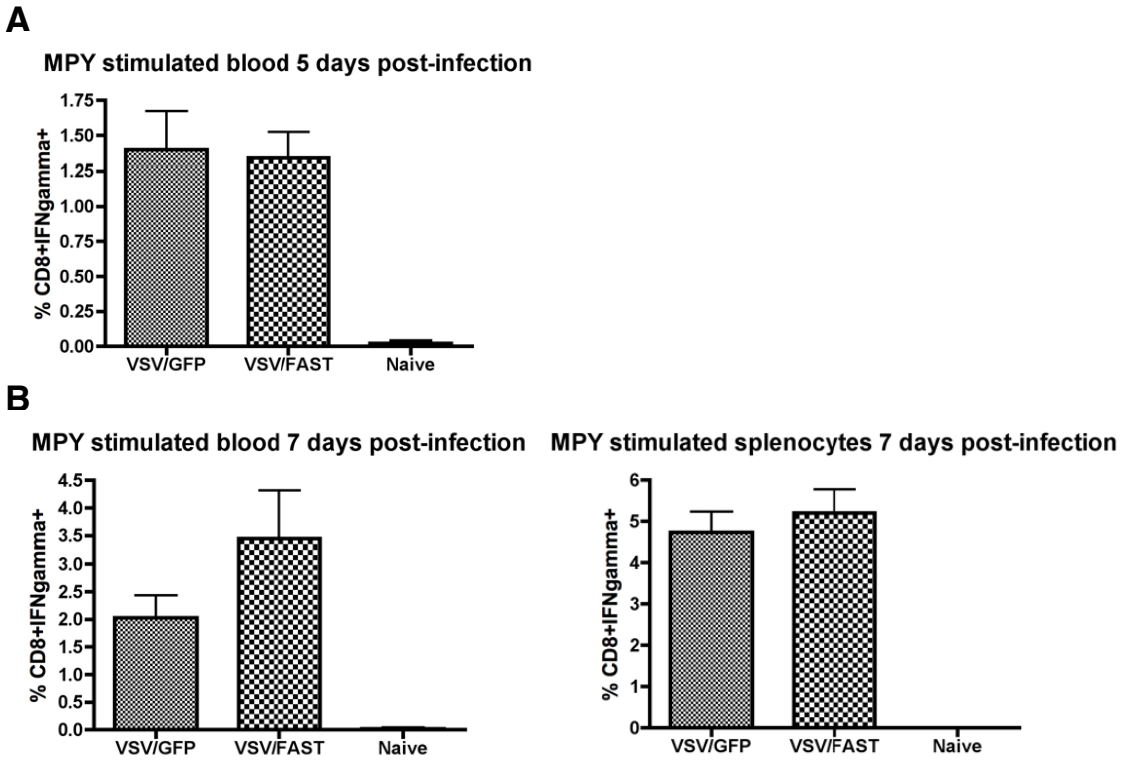

A
MPY stimulated blood 5 days post-infection
% CD8+IFNgamma+
1.75
1.50
1.25
1.00
0.75
0.50
0.25
0.00
VSV/GFP
VSV/FAST
Naive
B
MPY stimulated blood 7 days post-infection
% CD8+IFNgamma+
4.5
4.0
3.5
3.0
2.5
2.0
1.5
1.0
0.5
0.0
VSV/GFP
VSV/FAST
Naive
MPY stimulated splenocytes 7 days post-infection
% CD8+IFNgamma+
6
5
4
3
2
1
0
VSV/GFP
VSV/FAST
Naive

Figure 8

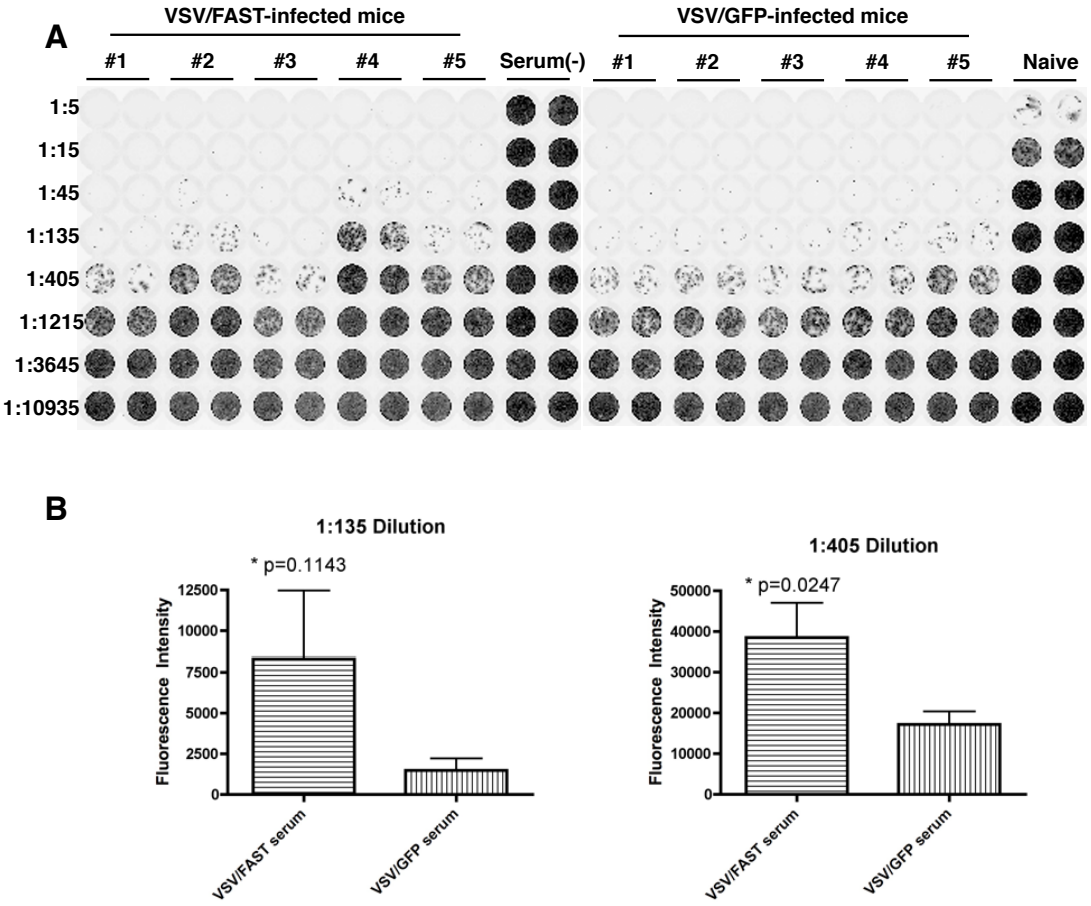

A
VSV/FAST-infected mice
VSV/GFP-infected mice
#1
#2
#3
#4
#5
Serum(-)
#1
#2
#3
#4
#5
Naive
1:5
1:15
1:45
1:135
1:405
1:1215
1:3645
1:10935
B
1:135 Dilution
* p=0.1143
Fluorescence Intensity
12500
10000
7500
5000
2500
0
VSV/FAST serum
VSV/GFP serum
1:405 Dilution
* p=0.0247
Fluorescence Intensity
50000
40000
30000
20000
10000
0
VSV/FAST serum
VSV/GFP serum

TABLE LEGENDS

TABLE 1. Development of hind-limb paralysis after intranasal infection

[a]Values are expressed as the number of animals developing paralysis/total number of animals tested. *, Hind-leg paralysis appeared on day 7 post-infection; †, hind-leg paralysis appeared on day 5 in three cases and on day 7 in the fourth case. ND, not determined.

TABLES

Table 1

Table 1: Development of Hind-limb Paralysis Following Intranasal Infection.

	Virus		
Intranasal Dose	WT-VSV/GFP	WT-VSV/FAST	DM51-VSV/FAST
$5x10^6$	0/4	0/4	ND
$1x10^7$	0/5	1/5*	ND
$5x10^7$	0/5	3/5*	ND
$5x10^8$	1/5*	4/4^	0/5
$5x10^9$	ND	ND	0/5

* HLP appeared on day 7 post-infection

^ HLP appeared on day 5 in three cases and day 7 in the fourth case

Appendix 2

Permission to reprint published manuscripts

Cancer Gene Therapy (Chapter 4):

Permission requests

On this page

Nature Publishing Group grants permission for authors, readers and third parties to reproduce material from its journals and online products as part of another publication or entity. This includes, for example, the use of a figure in a presentation, the posting of an abstract on a web site, or the reproduction of a full article within another journal. Certain permissions can be granted free of charge; others incur a fee.

For answers to frequently asked questions **click here**

- **Type of permission request**
- **Permission request options**

Types of permission request

Permission can be obtained for re-use of portions of material - ranging from a single figure to a whole paper - in books, journals/magazines, newsletters, theses/dissertations, classroom materials/academic course packs, academic conference materials, training materials (including continuing medical education), promotional materials, and web sites. Some permission requests can be granted free of charge, others carry a fee.

Nature Publishing Group rarely grants free permission for PDFs of full papers to be reproduced online, however e-print PDFs can be **purchased as commercial reprints**. If you wish to purchase multiple stand-alone copies of a Nature Publishing Group paper, which is then printed and shipped to you, please go to **commercial reprints**.

Permission request options

Permission requests from authors

The authors of articles published by Nature Publishing Group, or the authors' designated agents, do not usually need to seek permission for re-use of their material as long as the journal is credited with initial publication. For further information about the terms of re-use for authors please see below.

Author Requests

If you are the author of this content (or his/her designated agent) please read the following. Since 2003, ownership of copyright in in original research articles remains with the Authors*, and provided that, when reproducing the Contribution or extracts from it, the Authors acknowledge first and reference publication in the Journal, the Authors retain the following non-exclusive rights:

a. To reproduce the Contribution in whole or in part in any printed volume (book or thesis) of which they are the author(s).
b. They and any academic institution where they work at the time may reproduce the Contribution for the purpose of course teaching.
c. To reuse figures or tables created by them and contained in the Contribution in other works created by them.
d. To post a copy of the Contribution as accepted for publication after peer review (in Word or Tex format) on the Author's own web site, or the Author's institutional repository, or the Author's funding body's archive, six months after publication of the printed or online edition of the Journal, provided that they also link to the Journal article on NPG's web site (eg through the DOI).

NPG encourages the self-archiving of the accepted version of your manuscript in your funding agency's or institution's repository, six months after publication. This policy complements the recently announced policies of

Journal of Virology (Appendix 1):

Rightslink® by Copyright Clearance Center https://s100.copyright.com/AppDispatchServlet#formTop

Copyright Clearance Center RightsLink®

Home Create Account Help

AMERICAN SOCIETY FOR MICROBIOLOGY

Title: The p14 FAST Protein of Reptilian Reovirus Increases Vesicular Stomatitis Virus Neuropathogenesis

Author: Christopher W. Brown, Kyle B. Stephenson, Stephen Hanson, Michael Kucharczyk, Roy Duncan, John C. Bell, Brian D. Lichty

Publication: Journal of Virology

Publisher: American Society for Microbiology

Date: Jan 15, 2009

Copyright © 2009, American Society for Microbiology

User ID

Password

Enable Auto Login

LOGIN

Forgot Password/User ID?

If you're a copyright.com user, you can login to RightsLink using your copyright.com credentials. Already **a RightsLink user** or want to learn more?

Permissions Request

Authors in ASM journals retain the right to republish discrete portions of his/her article in any other publication (including print, CD-ROM, and other electronic formats) of which he or she is author or editor, provided that proper credit is given to the original ASM publication. ASM authors also retain the right to reuse the full article in his/her dissertation or thesis. For a full list of author rights, please see: http://journals.asm.org/site/misc/ASM_Author_Statement.xhtml

BACK CLOSE WINDOW

Copyright © 2012 Copyright Clearance Center, Inc. All Rights Reserved. Privacy statement.
Comments? We would like to hear from you. E-mail us at customercare@copyright.com

Springer; Experimental and Applied Immunotherapy (Introduction section 3.4):

Springer
the language of science

Springer Science+Business Media B.V.
Van Godewijckstraat 30
3311 GX Dordrecht
The Netherlands
tel +31 (0)78 / 65 76 - 000
fax +31 (0)78 / 65 76 - 254
www.springer.com

Springer Science+Business Media | P.O. Box 17 | 3300 AA Dordrecht | The Netherlands

Kyle Stephenson
Department of Pathology and Molecular Medicine
1280 Main Street West Hamilton
ON L8S 4K1
USA

Dordrecht, 01-10-2012

Mr. Frank Koorevaar
Rights Sales
Van Godewijckstraat 30
3311 GX Dordrecht
Netherlands
Frank.Koorevaar@springer.com

Dear Sir,

With reference to your request (Stephenson, K. B., Bell, J., & Lichty, B. (2011). Combining Oncolytic Viruses with Cancer Immunotherapy. In J. Medin & D. Fowler (Eds.), Experimental and Applied Immunotherapy. New York: Humana Press.) to reprint material on which Springer Science and Business Media control the copyright, our permission is granted, free of charge, for the use indicated in your enquiry.

This permission

- allows you non-exclusive reproduction rights throughout the World.
- excludes use in an electronic form. Should you have a specific project in mind, please reapply for permission.
- requires a full credit (Springer book/journal title, volume, year of publication, page, chapter/article title, name(s) of author(s), figure number(s), original copyright notice) to the publication in which the material was originally published, by adding: with kind permission of Springer Science and Business Media.
- Material may not be republished until at least one year after our publication date.
- The material can only be used for the purpose of defending your dissertation, and with a maximum of 30 extra copies in paper.

Permission free of charge on this occasion does not prejudice any rights we might have to charge for reproduction of our copyrighted material in the future.

Please do not hesitate contacting me if you have any questions regarding this mail.

Springer Science+Business Media B.V., Dordrecht | Chamber of Commerce Rotterdam, Nr.: 230.510.97 | VAT Nr.: NL 0043.61.337.B01
The Royal Bank of Scotland, Nr.: 59.62.47.524 | IBAN: NL22 RBOS 0596 2475 24 | BIC Code: RBOSNL2A
Managing Directors: Derk Haank, Martin Mos, Dr. Ulrich Vest, Peter Hendriks

Kind regards,

Frank Koorevaar
Springer
Rights and Permissions

Van Godewijckstraat 30
3311 GX
Dordrecht
The Netherlands

frank.koorevaar@springer.com
+31 (0) 78 657 6630
www.springer.com